

UNIVERSITY OF OKLAHOMA

GRADUATE COLLEGE

SOIL TRACE METALS CONCENTRATIONS IN A MINING IMPACTED AGRICULTURAL
WATERSHED: COMPARISON OF ANALYTICAL METHODS, GEOSPATIAL DISTRIBUTION,
AND EVALUATION OF RISK

A THESIS

SUBMITTED TO THE GRADUATE FACULTY

In partial fulfilment of the requirements for the

Degree of

MASTER OF SCIENCE IN ENVIRONMENTAL ENGINEERING

By

AMY LYNNE SIKORA
Norman, Oklahoma
2018

SOIL TRACE METALS CONCENTRATIONS IN A MINING IMPACTED AGRICULTURAL
WATERSHED: COMPARISON OF ANALYTICAL METHODS, GEOSPATIAL DISTRIBUTION,
AND EVALUATION OF RISK

A THESIS APPROVED FOR THE
SCHOOL OF CIVIL ENGINEERING AND ENVIRONMENTAL SCIENCE

BY

Dr. Robert W. Nairn, Chair

Dr. Elizabeth C. Butler

Dr. Gerald A. Miller

©Copyright by AMY LYNNE SIKORA 2018
All Rights Reserved.

To Reggie

(the hedgie)

Acknowledgements

This project was funded by the GRDA grant #1053733. I would like to personally thank Aaron Roper from GRDA for his assistance. Thank you to everyone on the CREW research team who spent long days out in the field collecting soil samples with me (which involved trekking through creeks, fields of thorn bushes, getting eaten by mosquitos, and covered in mud, on both freezing and blazing hot days) and special thanks to Darren Shepherd for providing the ATVs that allowed for much more efficient field work. I am especially grateful for my undergraduate research assistant, Lane Maguire, for her help with laboratory work and data reduction on the organic content portion of this study. To all my friends who let me exploit their personal emails to get free software trials, I am indebted to you and very sorry for the number of emails you've probably been spammed with since signing up. In addition, I would like to express the deepest appreciation for my committee chair and advisor, Dr. Robert Nairn, for his support, expertise, advice, and dad jokes during this project.

Finally, I want to give special thanks to my family- especially my parents, Tina and Ron Sikora, and siblings, Nate, Kara, and Luke, who provided love and encouragement during my graduate program.

Table of Contents

Acknowledgements	iv
Table of Contents	v
List of Tables	ix
List of Figures	xii
Abstract	xvii
Chapter I: Project Introduction	1
1.1 Introduction	1
1.1.1 Source of Contamination	2
1.2 Purpose and Scope of Project.....	6
1.3 Site Description.....	7
1.4 Hypotheses	11
1.5 Objectives	12
Chapter II: A Comparison of Methods for Analyses of Soil Trace Metals in A Mining Impacted Agricultural Watershed	13
2.1 Introduction	13
2.1.1 XRF Technology	14
2.1.2 XRF and ICP-OES Method Comparison.....	15
2.2 Methods.....	17
2.2.1 Site Description	17
2.2.2 <i>In Situ</i> Soil Sample Analysis and Collection	18
2.2.3 Laboratory Sample Analysis	20
2.2.4 Quality Assurance / Quality Control.....	23
2.2.5 Statistical Analysis	23

2.3 Results and Discussion	24
2.3.1 Comparison of XRFS <i>In Situ</i> and XRFS Laboratory Concentration Readings ..	24
2.3.2 Moisture Content Effect on XRFS Readings	29
2.3.3 Organic Content Effect and XRFS Readings	37
2.3.4 Comparison of ICP-OES and Laboratory XRFS Concentration Readings	41
2.3.5 Prediction of Cadmium Concentrations from Zinc Concentrations.....	47
2.4 Conclusions	50
Chapter III: Geospatial Distribution of Trace Metals in Soils of a Mining Impacted Agricultural Watershed	53
3.1 Introduction	53
3.1.1 Determination of Soil Metals Concentrations	54
3.1.2 Trace Metals in Soils and Sediments.....	55
3.1.3 Spatial Distribution of Trace Metals.....	57
3.1.4 Contaminants of Primary Concern.....	59
3.2 Methods.....	60
3.2.1 Site Description	60
3.2.2 Determination of Minimum Sample Size.....	63
3.2.3 Sampling Locations.....	65
3.2.4 Soil Sample Collection	67
3.2.5 Laboratory Sample Analysis	68
3.2.6 Estimation of Cadmium.....	71
3.2.7 Statistical Analysis	71
3.2.8 Geospatial Analysis	72
3.3 Results and Discussion	75

3.3.1 Elm Creek Riparian Concentration Distribution	75
3.3.2 Uplands Concentration Distribution	88
3.3.3 Analysis of the Creek and Uplands.....	105
3.4 Conclusions	110
Chapter IV: Analysis of Potential Ingestion and Uptake of Lead, Zinc, and Cadmium by White-tailed Deer (<i>Odocoileus virginianus</i>) and Associated Human Health Risk in the Elm Creek Watershed.....	113
4.1 Introduction	113
4.1.1 Estimating Exposure of Trace Metals Intake into White-tailed Deer	115
4.1.2 Human Health Effects Associated with Consumption of Lead, Zinc, and Cadmium	116
4.2 Methods.....	122
4.2.1 Site Description	122
4.2.2 Estimation of Lead, Zinc, and Cadmium Ingestion and Uptake by White-Tailed Deer	124
4.2.3 Evaluation of Risk to Humans from Consumption of White-Tailed Deer	133
4.3 Results and Discussion	137
4.3.1 Determination of Possible Adverse Effects to White-tailed Deer	137
4.3.2 Estimation of Tissue Concentration in White-tailed Deer	138
4.3.3 Evaluation of Human Health Risk.....	147
4.4 Conclusions	149
Chapter V: Conclusions and Future Work	152
5.1 Conclusions	152
5.1.1 Comparison of Methods	152
5.1.2 Distribution of Trace Metals in Elm Creek	154

5.1.3 Distribution of Trace Metals in Uplands	154
5.1.4 Estimation of Trace Metals Uptake in White-Tailed Deer	155
5.1.5 Human Health Risk Evaluation	155
5.1.6 Final Comments.....	156
References	157
Appendix A.....	173

List of Tables

Table 1.1: Comparison of lead, zinc, and cadmium metals concentrations of uncontaminated soils, TSMD background concentrations, Ottawa County Remedial Goals, Tar Creek residential yards, and maximum concentrations in chat	5
Table 1.2: Sediment quality guidelines for freshwater ecosystems (i.e., concentrations above given values are likely to have harmful effects observed)	6
Table 2.1: Laboratory analysis and corresponding methods	21
Table 2.2: Descriptive statistics for field and laboratory XRFS readings for lead and zinc	25
Table 2.3: Wilcoxon signed ranks test distribution and p-value for the comparison of laboratory XRFS and field XRFS readings for lead and zinc	25
Table 2.4: Descriptive statistics for field and laboratory XRFS readings for lead and zinc split into less than 10% moisture content, less than 20% moisture content, and greater than 20% moisture content	30
Table 2.5: Wilcoxon signed ranks test distribution and p-value for the comparison of laboratory XRFS and field XRFS readings for lead and zinc in different moisture content ranges	31
Table 2.6: Descriptive statistics for laboratory XRFS readings and ICP values for lead and zinc split into less than 10% organic content and greater than 10% organic content for soils passing the #60 sieve fraction	39
Table 2.7: Wilcoxon signed ranks test distribution and p-value for the comparison of laboratory XRFS readings and ICP values for lead and zinc in less than 10% organic content and greater than 10% organic content for soils passing the #60 sieve fraction	39
Table 2.8: Descriptive statistics for laboratory XRFS readings and ICP results for lead and zinc	41
Table 2.9: Wilcoxon signed ranks test distribution and p-value for the comparison of laboratory XRFS readings and ICP results for lead and zinc	42
Table 3.1: Summary statistics for Elm Creek riparian area soil lead, zinc, and cadmium concentrations (mg/kg) from Nairn (2014b)	64

Table 3.2: Summary statistics for Elm Creek upland soil lead, zinc, and cadmium concentrations (mg/kg) from Nairn (2014b)	64
Table 3.3: Lead and zinc concentrations reported by XRFS and estimated cadmium concentrations with the corresponding ICP values for each Elm Creek terrace location within the GRDA properties that exceeded SQGs.	82
Table 3.4: The descriptive statistics and p-value (Friedman test) for lead, zinc, and estimated cadmium concentrations in the top, primary or lower terraces of the east branch and main stem of Elm Creek.	83
Table 3.5: The descriptive statistics and p-value (for Mann-Whitney U-test) for lead, zinc, and predicted cadmium in the east and west branches of Elm Creek	87
Table 3.6: Zinc and cadmium concentrations determined by XRFS and ICP analysis for soil samples in the uplands with XRFS values exceeding the RG	91
Table 3.7: Average background soil concentrations for lead, zinc, and cadmium found in the Oklahoma, Kansas, and Missouri portions of the TSMD	106
Table 3.8: The distance from the headwaters, ending distance, and total distance for Groups 1-6	107
Table 3.9: The descriptive statistics for lead, zinc, and cadmium concentrations within Groups 1-6 and the corresponding p-value when concentrations are compared to TSMD background concentrations	108
Table 3.10: Descriptive statistics for lead, zinc, and cadmium in the uplands and creek terrace locations and the test p-value for each metal	109
Table 4.1: The common and scientific names for each plant used to determine forage trace metals concentrations from White (2006), Garvin et al., (2017), and Andrews (2011)	127
Table 4.2: Median concentrations of lead, zinc, and cadmium in potential forage for white-tailed deer in the Elm Creek Watershed	128
Table 4.3: Summary statistics of lead, zinc, and cadmium concentrations in soil samples collected in the Elm Creek watershed upland environment.	129
Table 4.4: Summary statistics of unfiltered lead, zinc, and cadmium concentrations in water samples collected by CREW at the east Elm Creek County Road E30 road crossing, Ottawa County, OK, 2005-2008	130

Table 4.5: Daily food and water consumption values for a 68 kg white-tailed deer	131
Table 4.6: Input parameters to determine the average daily dose for lead, zinc, and cadmium for humans consuming white-tailed deer within the Elm Creek Watershed	135
Table 4.7: The daily ingestion of lead, zinc, and cadmium for plant matter, soil, and water and corresponding NOAELs and LOAELS for the consumption of lead, zinc, and cadmium for white-tailed deer determined by Opresko et al. (1996) [all units in mg/kg/day]	137
Table 4.8: Estimated ingestion rates for a 68 kg white-tailed deer in the Elm Creek watershed	138
Table 4.9: The breakdown of all four white-tailed deer genders, ages, and approximate weights from CH2M (2017)	140
Table 4.10: The tissue concentrations for the heart, liver, meat, and total weighted average for white-tailed deer determined by CH2M (2017) along with the estimated tissue concentrations from this study	141
Table 4.11: Estimated transfer coefficients for lead, zinc, and cadmium into the heart, liver, and meat of a white-tailed deer living in the around the Elm Creek Watershed	143
Table 4.12: Mean metals concentrations of meat, liver, kidneys, and other tissues in white-tailed deer from studies conducted in the State of Oklahoma	145
Table 4.13: The oral RfD for each trace metal and ADD for each tissue from white-tailed deer hunted in the Elm Creek watershed	147
Table 4.14: The HQ for lead, zinc, and cadmium and corresponding HI for each tissue type in white-tailed deer hunted in the Elm Creek Watershed	147

List of Figures

Figure 1.1: A pecan orchard (a), open farmland (b), bottomland hardwood forest wetland ecosystem (c), riverine ecosystem (Elm Creek) (d), and oxbow lake (e) present within the Neosho Bottoms	8
Figure 1.2: The locations of the Tar Creek Superfund Site, Elm Creek, Elm Creek watershed, the Neosho River, and the GRDA-owned properties with respect to each other	10
Figure 2.1: The locations of the Tar Creek Superfund Site, Elm Creek, the Neosho River, and the GRDA-owned properties with respect to each other	18
Figure 2.2: The field portable Thermo-Fisher Scientific Niton XL3t GOLDD+ XRFs being operated <i>in situ</i> on a soil surface with all debris removed	20
Figure 2.3: Packed circular XRFs soil sample cups lined with polypropylene X-ray film for analysis	22
Figure 2.4: (a) Thermo Scientific Field Mate test stand is used to lock in the Thermo-Fisher Scientific Niton XL3t GOLDD+ XRFs with the nose of the device pointing towards the sample cup; (b) The Field Mate holds the circular sample cup within the base	22
Figure 2.5: Regression of field XRFs measurements against laboratory XRFs measurements for zinc. The estimated relationship (dashed line) and 100% recovery (solid red) are provided.	27
Figure 2.6: Regression of field XRFs measurements against laboratory XRFs measurements for zinc. The estimated relationship (dashed line) and 100% recovery (solid red) are provided.	28
Figure 2.7: Upland XRFs data with field XRFs measurements against laboratory XRFs measurements for lead separated into moisture content ranges. The trendlines for each range (dashed line) and 100% recovery (solid red) are presented.	34
Figure 2.8: Creek XRFs data with field XRFs measurements against laboratory XRFs measurements for lead separated into moisture content ranges. The trendlines for each range (dashed line) and 100% recovery (solid red) are presented	34
Figure 2.9: Upland XRFs data with field XRFs measurements against laboratory XRFs measurements for zinc separated into moisture content ranges. The	35

trendlines for each range (dashed line) and 100% recovery (solid red) are presented.

Figure 2.10: Creek XRFs data with field XRFs measurements against laboratory XRFs measurements for zinc separated into moisture content ranges. The trendlines for each range (dashed line) and 100% recovery (solid red) are presented. 35

Figure 2.11: Regression for laboratory XRFs measurements against ICP for K, Ca, Cr, Fe, Cu, Zn, and Pb. The deeming relationship (dashed line) and 100% recovery (solid red) are shown in each plot 44

Figure 2.12: Regression of lead laboratory XRFs measurements plotted against ICP-OES. Upper and lower confidence limits are presented in the plot. 46

Figure 2.13: Regression of zinc laboratory XRFs measurements plotted against ICP-OES. Upper and lower confidence limits are presented in the plot. 46

Figure 2.14: Regression of zinc and cadmium concentrations determined by ICP-OES. Upper and lower confidence limits are presented in the plot. 48

Figure 2.15: Estimated cadmium and ICP cadmium values 50

Figure 3.1: The GRDA-owned properties (highlighted in green) proximity to the Neosho River, Elm Creek and The Tar Creek Superfund Site 63

Figure 3.2: Image of Elm Creek, located in Ottawa County, Oklahoma, in October 2016 with the stream terraces clearly identified 65

Figure 3.3: Elm Creek riparian zone sampling sites 66

Figure 3.4: Developed upland transect locations within the GRDA-owned properties 68

Figure 3.5: Packed circular XRFs soil sample cups lined with polypropylene X-ray film for analysis 70

Figure 3.6: (a) Thermo Scientific Field Mate test stand is used to lock in the Thermo-Fisher Scientific Niton XL3t GOLDD+ XRFs with the nose of the device pointing towards the sample cup; (b) The Field Mate holds the circular sample cup within the base 70

Figure 3.7: Elm Creek sampling locations marked with distances (in kilometers) from creek headwaters 76

Figure 3.8: Elm Creek lead concentrations on the left bank for each sampling location starting closest to the headwaters and continuing downstream. Concentrations for the top of bank, primary terrace, and lower terrace are presented with the SQG for lead indicated in red. 77

Figure 3.9: Elm Creek lead concentrations on the right bank for each sampling location starting closest to the headwaters and continuing downstream. Concentrations for the top of bank, primary terrace, and lower terrace are presented with the SQG for lead indicated in red. 77

Figure 3.10: Elm Creek zinc concentrations on the left bank for each sampling location starting closest to the headwaters and continuing downstream. Concentrations for the top of bank, primary terrace, and lower terrace are presented with the SQG for zinc indicated in red. 78

Figure 3.11: Elm Creek zinc concentrations on the right bank for each sampling location starting closest to the headwaters and continuing downstream. Concentrations for the top of bank, primary terrace, and lower terrace are presented with the SQG for zinc indicated in red. 78

Figure 3.12: Elm Creek estimated cadmium concentrations on the left bank for each sampling location starting closest to the headwaters and continuing downstream. Concentrations for the top of bank, primary terrace, and lower terrace are presented with the SQG for cadmium indicated in red. 79

Figure 3.13: Elm Creek estimated cadmium concentrations on the right bank for each sampling location starting closest to the headwaters and continuing downstream. Concentrations for the top of bank, primary terrace, and lower terrace are presented with the SQG for cadmium indicated in red. 79

Figure 3.14: Elm Creek sampling locations on the east and west branches at the E30, E40, and E50 County Road crossings. 85

Figure 3.15: Elm Creek east and west branch lead concentrations. Each branch presents concentrations for the top of bank, primary terrace, and lower terrace for the left and right banks at each road crossing. The SQG is marked in red. 86

Figure 3.16: Elm Creek east and west branch zinc concentrations. Each branch presents concentrations for the top of bank, primary terrace, and lower terrace for the left and right banks at each road crossing. The SQG is marked in red. 86

Figure 3.17: Elm Creek east and west branch estimated cadmium concentrations. Each branch presents concentrations for the top of bank, primary terrace, and lower terrace for the left and right banks at each road crossing. The SQG is marked in red.	87
Figure 3.18: The 278 sampling locations for all soil samples in the GRDA Properties.	89
Figure 3.19: The frequency distributions for lead, zinc, and cadmium concentrations in upland soils.	90
Figure 3.20: Locations where samples exceed the RG's for zinc and cadmium	91
Figure 3.21: The (a) IDW geospatial interpretation and (b) ordinary kriging maps for lead in the uplands	93
Figure 3.22: The (a) IDW geospatial interpretation and (b) ordinary kriging maps for zinc in the uplands	94
Figure 3.23: The (a) IDW geospatial interpretation and (b) ordinary kriging maps for estimated cadmium in the uplands	95
Figure 3.24: The spatial distribution map of significant hotspot clusters and cold spot clusters using the (a) local Moran's I spatial statistic for identification of clusters and (b) the Geris-Ord G_i^* spatial statistic for identification of hot and cold spots for lead concentrations in the uplands. An inverse distance band of 300 m was used for both methods. Points are overlain on IDW interpolation map	97
Figure 3.25: The spatial distribution map of significant hotspot clusters and cold spot clusters using the (a) local Moran's I spatial statistic for identification of clusters and (b) the Geris-Ord G_i^* spatial statistic for identification of hot and cold spots for zinc concentrations in the uplands. An inverse distance band of 300 m was used for both methods. Points are overlain on IDW interpolation map	98
Figure 3.26: The spatial distribution map of significant hotspot clusters and cold spot clusters using the (a) local Moran's I spatial statistic for identification of clusters and (b) the Geris-Ord G_i^* spatial statistic for identification of hot and cold spots for estimated cadmium concentrations in the uplands. An inverse distance band of 300 m was used for both methods. Points are overlain on IDW interpolation map	99

Figure 3.27: Reference map for the identification of areas A, B, and C	101
Figure 3.28: Elevation contours within the GRDA properties with the Elm Creek Watershed outlined in grey	103
Figure 3.29: USGS discharge rates for Elm Creek gauge station at the #65 road crossing from January to October 2017. Data from USGS, 2018	104
Figure 3.30: USGS water surface elevation at the #65 road crossing at the Elm Creek gauge station from January to October 2017. Data from USGS, 2018	104
Figure 3.31: The locations of each tested group with Elm Creek terrace sampling locations and upland sampling locations marked within each boundary. All upland samples fell within a 100 m radius of Elm Creek	107
Figure 4.1: The Elm Creek watershed, Elm Creek, and Tar Creek Superfund Site locations and areas, Ottawa County, Oklahoma (Google Earth, 2018)	123
Figure 4.2: Two white-tailed deer grazing in the GRDA-owned properties in the Elm Creek Watershed on August 5, 2017. Photo provided by Aaron Roper of GRDA	124
Figure 4.3: The locations of the Tar Creek Superfund Site, Elm Creek, Elm Creek watershed, the water quality data location, and the soil trace metal concentration area, located in Ottawa County, OK (Google Earth, 2018)	130
Figure 4.4: The locations of the Tar Creek Superfund Site, Elm Creek and corresponding watershed, the water quality data location, and the soil trace metal concentration area with respect to where the white-tailed deer were hunted, Ottawa County, OK	140

Abstract

This study investigated four aspects surrounding lead, zinc, and cadmium soil trace metals concentrations within a mining impacted watershed: (1) a comparison of three soil trace metal quantification methods relating measurements from field portable X-ray fluorescence spectroscopy (XRFS) in *in situ* and laboratory environments, and inductively coupled plasma-optical emission spectrometry (ICP-OES), (2) distribution of soil trace metals in riparian terraces of a creek, (3) distribution of soil trace metals in an upland environment, (4) analysis of trace metals uptake into white-tailed deer (*Odocoileus virginianus*) and the human health risk associated with consuming said deer. This study was conducted within the Elm Creek watershed, located in Ottawa County in northeastern Oklahoma, and situated to the west and south of the Tar Creek Superfund Site, part of the historic Tri-State Lead-Zinc Mining District (TSMD). Trace metals contamination has been documented in Elm Creek, however, questions remain about broader impacts in the Elm Creek watershed. Elm Creek watershed properties purchased by the Grand River Dam Authority (GRDA), a public power provider, are designated to be used as offsite mitigation for fish and wildlife impacts under the Pensacola Dam Hydropower License under the Federal Energy Regulatory Commission. This study found: (1) *In situ* XRFS analysis on soils with less than 10% moisture content yielded statistical similarities to laboratory XRFS concentrations for lead and zinc when the samples were homogenized, dried and sieved, while samples with moisture contents exceeding 20% showed no similarities. Organic contents greater than 10% caused underreporting of lead XRFS values when compared to ICP

concentrations and ICP and laboratory XRF concentrations were not statistically different for lead but were for zinc ($p < 0.05$). The XRF overreported zinc concentrations when compared to ICP values. (2) The creek branch with headwaters originating within the Tar Creek Superfund Site had the most influence on downstream soils concentrations and concentrations of trace metals within creek terraces decreased with increasing distances from the headwaters. (3) Areas with elevated trace metals concentrations within upland environments were located closest to the stream at lower elevations suggesting that the creek is depositing contaminated material during flood events. Creek terraces and upland soils within 100 m of the creek reflected background soil concentrations 11.5 km downstream from the headwaters of the branch originating within the Tar Creek Superfund Site. (4) Uptake of trace metals into white-tailed deer tissues were accurate for lead and cadmium, and conservative estimates of risk to humans from consumption of white-tailed deer found no associated human health risk ($HI < 1$). This study highlights the differences in trace metals detection methods and impacts of trace metals within a mining impacted agricultural watershed. The results of this study will influence long-term land use in the watershed.

Chapter I: Project Introduction

1.1 Introduction

Metals concentrations in soil vary widely depending on the geochemical environment from which the soils originate. Metals occur naturally in soils and can be essential for healthy soil function (Kabata-Pendias and Mukherjee, 2007; Tchounwou et al., 2012; Alloway, 2012). Elevated levels of ecotoxic trace metals in soils, often due to anthropogenic activities, may present undue risk to affected ecosystems as they are both persistent and non-biodegradable which enables metals to remain bioavailable over extended periods of time (Alloway, 2012; Kabata-Pendias and Pendias, 2001; Lewin and Macklin, 1987; Li, 2014; Monitha et al., 2012; Qi et al., 2016; Smith and Huyck, 1999; Qin et al., 2012; Tchounwou et al., 2012; Lee et al., 2016). Elevated levels of lead, zinc, and cadmium pose a risk to human health from direct exposure or from accumulation up the food chain (Dames and Moore, 1993; Chaney, 2010; Zota et al., 2011; Lee et al., 2016). The toxic effects from elevated trace metals on ecosystems negatively impacts the health of animals, biodiversity of species, crop and other plant growth, and soil quality (Alloway, 2012; Sileo and Beyer, 1985; French and Mateo, 2005; Cheng et al., 2007; Phelps and Mcbee, 2009; Lee et al., 2016). Many anthropogenic sources of trace metal contamination, such as mining operations, have harmful effects on local human populations and ecosystems for decades to centuries after the contamination is first introduced (Cheng et al., 2007; Lee et al., 2016).

The determination of trace metals concentrations in soils often involve the use of atomic spectrophotometry or X-ray spectroscopy technologies. Each of these techniques works by measuring the electromagnetic radiation either absorbed or emitted by specific atoms after excited valence electrons undergo transitions from different energy levels (Kalnicky and Singhvi, 2001). Because each element has its own unique characteristic wavelength, the intensity of light either absorbed or emitted can be used to determine the concentration of the element in focus (Alloway, 2012). Field portable X-ray fluorescence spectroscopy (XRF) techniques provide an effective approach to screening on-site soils due to their non-destructive and rapid analysis capabilities. Although the data determined using this method in the field are commonly used in scientific papers, questions regarding the accuracy of calculated values exist due to possible interactions between the XRF technique and field conditions, such as elevated moisture and organic matter (Pyle and Nocerino, 1996; Lin, 2009; Melquiades and Appoloni, 2004). Established technologies, like atomic absorption and inductively coupled plasma spectroscopy include preparation and digestion procedures to address these issues (USEPA, 2007a; 2007b).

1.1.1 Source of Contamination

Historic mining activities in the Tri State Lead and Zinc Mining District (TSMD), that spans portions of Oklahoma, Kansas, and Missouri began in the mid-1800s to produce lead and zinc ore (USEPA, 1997; USEPA, 2008; USFWS, 2013). The Tar Creek Superfund Site, the portion of the TSMD in the state of Oklahoma, was added to the National Priorities List by the Comprehensive Environmental Response, Compensation,

and Liability Act (CERCLA) in 1983 (USEPA, 1997). Extensive mining operations for lead and zinc in Oklahoma began in the 1890s and continued until the 1970s and left extensive trace metal contamination on the surface which remains exposed to this day (USEPA, 1997; Datin and Cates, 2002; White, 2006; USEPA, 2008; Andrews, 2011; USFWS, 2013). The solid mining waste, locally known as “chat”, consists of “chert (microcrystalline quartz), calcite, dolomite, marcasite, pyrite, sphalerite (ZnS), galena (PbS), and hemimorphite (Zn silicate)” (Schaidler et al., 2014) and contains residual amounts of trace metals (USEPA, 1997; Carroll et al., 1998; O’Day et al., 1998; Datin and Cates, 2002; Schaidler et al., 2014). Dispersion of the chat was caused by both natural processes and humans (Juracek and Drake, 2016). Chat ranges from 16 mm (5/8 inch) to below the 200-mesh size (<75 µm) and the smallest size fraction is known to contain the greatest concentrations of trace metals (Horowitz, 1985; Datin and Cates, 2002). The small particles are easily transported downstream by rainfall and erosion events and are subsequently deposited in the streambed, within riparian zones, and in upland areas after flooding cycles (Datin and Cates, 2002; Alloway, 2012; Juracek and Drake, 2016). This gravel like material was also previously used in rural roads and driveways (USEPA, 2008; Juracek and Drake, 2016).

These residuals pose potential human health and ecological risks and elevated concentrations of lead, zinc, and cadmium in these mining wastes have been identified as Contaminants of Primary Concern (COPC) by the United States Environmental Protection Agency (USEPA) (Żukowska and Biziuk, 2008; Kabata-Pendias and Mukherjee, 2007; USEPA, 2008; Zota et al., 2011). The USEPA defines COPC within the Tar Creek

Superfund Site as “chemical substances found at the site that the EPA has determined pose an unacceptable risk to human health or the environment” (USEPA, 2017a). The USEPA determined enforceable remedial goals for transition soil metals concentrations within the areas of Ottawa County impacted by mining wastes under Operable Unit 4 (USEPA, 2008; ATSDR 2008). These goals were selected with the intent to decrease human exposure to COPCs from soil through the ingestion of plants and meat products that were grown or fed near the source area (USEPA, 2008). The USEPA selected remedial goals for transition zone soil and soil under the source material for lead, zinc, and cadmium of 500 mg/kg, 1,100 mg/kg, and 10 mg/kg, respectively (USEPA, 2008). If the soil trace metal contains concentrations exceed the values listed above, the USEPA Record of Decision calls for the excavation of the contaminated soil down to native soils (USEPA, 2008). Table 1.1 lists lead, zinc, and cadmium trace metals concentrations of uncontaminated soils, TSMD background values, Tar Creek residential yards, Tar Creek RGs, and maximum concentrations in chat.

Table 1.1: Comparison of lead, zinc, and cadmium metals concentrations of uncontaminated soils, TSMD background concentrations, Ottawa County Remedial Goals, Tar Creek residential yards, and maximum concentrations in chat

	All concentrations in mg/kg			Source
	Lead	Zinc	Cadmium	
Uncontaminated soils concentrations (National averages)	<40	<88	<1.1	Alloway, 2012; Kabata-Pendias and Pendias, 2001
Concentration ranges for TSMD background levels	17-91	44-433	0.4-4.1	Dames and Moore, 1993; USEPA, 2008
Remedial Goals for Ottawa, County, OK	500	1,100	10.0	USEPA, 2008
Concentration ranges in residential yard soil within the Tar Creek Superfund Site	0.05-14,400	1-10,700	0.5-53.8	USEPA, 2008
Concentration ranges of chat within the Tar Creek Superfund Site	260-2,200	11,100-34,400	16-96	Datin and Cates, 2002

Ingersoll et al. (2009) determined probable effect concentrations (PECs) for lead, zinc, and cadmium in sediments within Grand Lake of the Cherokees into which TSMD waters eventually flow. Concentrations exceeding the PECs represent values in which adverse health effects (survival or growth) will occur frequently (MacDonald et al., 2000). MacDonald et al. (2000) determined freshwater Sediment Quality Guidelines (SQGs) for lead, zinc and cadmium where concentrations exceeding the SQGs will have observable harmful effects on organisms. These guidelines have been used to identify areas of concern and to aid in remediation by presenting remediation goals (MacDonald et al., 2000). They have also been used to conduct remedial investigations and assess ecological risk (MacDonald et al., 2000). The national and TSMD SQGs for metals in freshwater sediments determined by MacDonald et al., (2000) reflect the PECs developed by Ingersoll et al. (2009) and are summarized in Table 1.2.

Table 1.2: Sediment quality guidelines for freshwater ecosystems (i.e., concentrations above given values are likely to have harmful effects observed)

	All concentrations in mg/kg			Source
	Lead	Zinc	Cadmium	
National SQGs	128	459	4.98	MacDonald et al., 2000
TSMD-specific SQGs	150	2,100	11.1	Ingersoll et al., 2009; MacDonald et al., 2000

1.2 Purpose and Scope of Project

The purpose of this study is three-fold: 1) assess if trace metals concentrations determined by three different analytical techniques (*in situ* field XRFs, laboratory XRFs, and hot acid digestion/inductively coupled plasma-optical emission spectroscopy (ICP-

OES)) are adequately comparable for environmental assessments; 2) evaluate trace metals concentrations (with a focus on lead, zinc, and cadmium) in stream terraces and upland environments in a mining impacted watershed; and 3) estimate and quantify potential ingestion and uptake of lead, zinc, and cadmium by white-tailed deer and to evaluate the human health risk associated with the consumption of white-tailed deer tissue harvested from a lead and zinc mining impacted watershed.

1.3 Site Description

The Oklahoma Department of Wildlife Conservation, U.S. Department of Agriculture Natural Resources Conservation Service, and the Oklahoma Forestry Service have identified the Neosho River and Elm Creek watersheds as an area in need of conservation (Brabander et al., 1985; Ducks Unlimited, 2012). The Grand River Dam Authority (GRDA) obtained approximately 7.2 square kilometer area of land within the Neosho Bottoms area, including portions of the Elm Creek watershed, to evaluate land restoration potential. These properties known collectively as the “Neosho Bottoms”, have the potential to be used as offsite mitigation for impacts under the Pensacola Dam hydropower license to fulfill the requirements for the *Fish and Waterfowl Habitat Management Plan* under the Federal Energy Regulatory Commission (FERC) (Ducks Unlimited, 2012). These properties currently consist of a mix of pasture, open farmland, pecan orchards, and a variety of different wetland types ranging from scrub-shrub wetlands to bottomland hardwood forest wetland ecosystems (Figure 1.1).

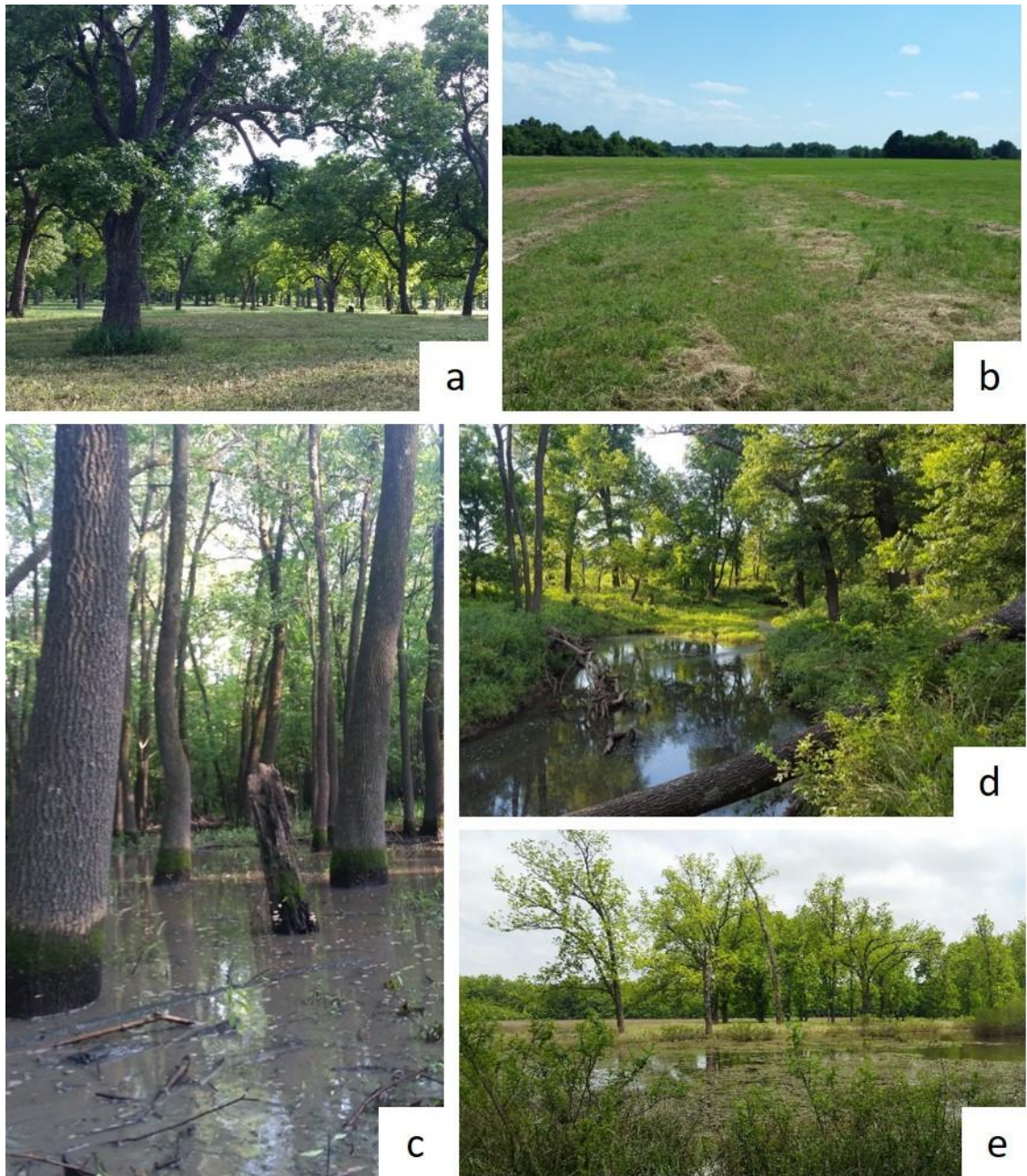


Figure 1.1: A pecan orchard (a), open farmland (b), bottomland hardwood forest wetland ecosystem (c), riverine ecosystem (Elm Creek) (d), and oxbow lake (e) present within the Neosho Bottoms

The Elm Creek watershed extends into portions of the Tar Creek Superfund Site. Elm Creek consist of two main branches (east and west) that join to form one stream. The east branch of Elm Creek originates within the Tar Creek Superfund Site and the perennial portion flows south a total distance of 10.5 kilometers before its confluence

with the West branch. The source of the west branch of Elm Creek is located outside of the Tar Creek Superfund Site and the perennial portion flows a total distance of 12 km before converging with the east branch. After the confluence of both branches, Elm Creek extends six and a half kilometers, traveling through the GRDA-owned properties, before entering the Neosho River. The Neosho River then flows southeast and discharges into Grand Lake of the Cherokees. The proximity of both water sources to the Tar Creek Superfund Site exposes them to potential trace metals contamination from the abandoned mining operations. The GRDA properties in focus consist of an approximately 7.2 square kilometer area and the locations of the Tar Creek Superfund Site, Elm Creek, Elm Creek watershed, the Neosho River, and the GRDA-owned properties of interest can be seen in Figure 1.2.

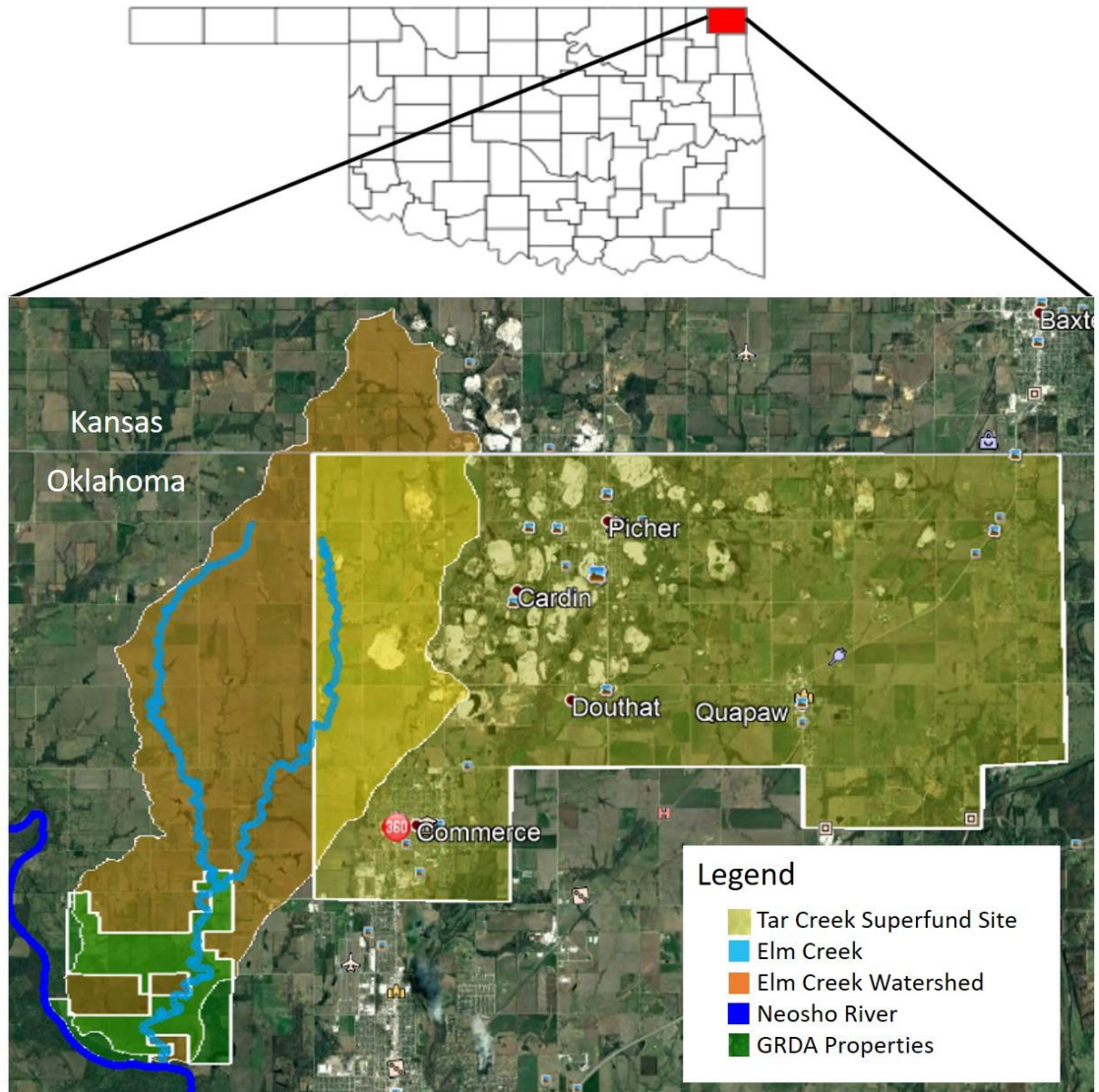


Figure 1.2: The locations of the Tar Creek Superfund Site, Elm Creek, Elm Creek watershed, the Neosho River, and the GRDA-owned properties with respect to each other

Metals contamination within Elm Creek has been previously documented and a record of trace metal deposition within the riparian area has been determined (Nairn, 2014a; USFWS, 2012). Questions regarding the impacts that the metals contamination may have on riparian soils and nearby upland soils (due to the possibility of metals deposition during seasonal fluctuations in water levels in the creek from large rain events) need to be addressed.

1.4 Hypotheses

The six hypotheses for this project are as follows:

1. The east branch of Elm Creek, nearest the mining influence, will have greater metals concentrations than the west branch of Elm Creek, further away from the mining influence, when comparing samples collected at equal distances upstream from the creek confluence.
2. Sampling locations hydrologically closer to mining influences will have soil lead, zinc, and cadmium concentrations exceeding background levels.
3. Upland lead, zinc, and cadmium soil concentrations will be lesser than concentrations present in stream terraces.
4. *In situ* XRF readings with moisture content exceeding 20% will report lesser metals concentrations than laboratory XRF readings where the soil was homogenized, dried, and sieved.
5. Homogenized, dried, and sieved soils analyzed by the XRF in the laboratory will yield concentrations not statistically different from ICP-OES metals concentrations.
6. Consumption of white-tailed deer tissue from within a mining impacted watershed, will expose humans to unacceptable risk for lead, zinc, and cadmium.

1.5 Objectives

To assess the defined hypotheses, the following objectives will be completed:

1. Evaluate soil lead, zinc, and cadmium concentrations in stream terraces and upland environments of a mining impacted agricultural watershed.
2. Generate a spatial perspective of the distribution of lead, zinc, and cadmium concentrations.
3. Compare the accuracy of metals concentrations derived from *in situ* XRFs measurements, laboratory XRFs measurements (where samples were dried and sieved), and ICP-OES analyses.
4. Estimate and quantify potential ingestion and uptake of lead, zinc, and cadmium by white-tailed deer living in a mining-impacted watershed.
5. Evaluate the human health risk associated with the consumption of white-tailed deer tissue harvested from a lead and zinc mining impacted watershed.

Chapter II: A Comparison of Methods for Analyses of Soil Trace Metals in A Mining Impacted Agricultural Watershed

2.1 Introduction

Field portable X-ray fluorescence spectroscopy (XRFS) has become an increasingly popular technology for *in situ* screening detection of trace metals (Bastos et al., 2012; Congiu et al., 2013; Coronel et al., 2014; Shand and Wendler, 2014; Galuszka et al., 2015). This technology allows for rapid screening of inorganic environmental contaminants when compared to other methods such as inductively coupled plasma-optical emission spectrometry (ICP-OES) and inductively coupled plasma-mass spectrometry (ICP-MS) which are both time consuming and costly (Kalnicky and Singhvi, 2001; Melquiades and Appoloni, 2004; Bastos et al., 2012; Shand and Wendler, 2014; Ravansari and Lemke, 2018). The ability for the field portable XRFS devices to be taken out into the field is one of the most important attributes of the technology (Potts and West, 2006; Coronel et al., 2014; Galuska et al. 2015). Many of these devices are small and light enough to be carried around in the analyst's hand which makes them especially useful in remote locations or in developing countries (Melquiades and Appoloni, 2004; Higuera et al., 2012; McComb et al., 2014). The XRFS detection limit for toxic trace elements often fall below the regulatory concentrations, making these instruments ideal for initial screening of heavily polluted areas (Galuska et al. 2015). Common applications of XRFS technologies involve environmental assessments on metals contaminated sites from mining activities, zinc smelting, industrial use, and military use (Crooks et al., 2006; Kilbride et al., 2006; Coronel et al., 2014; Rouillon and Taylor, 2016; Sahraoui and

Hachicha, 2016; Schneider et al., 2016). XRF technologies are also used to assess lead concentrations in residential areas affected by lead contamination (Reames and Lance, 2002; Binstock et al., 2008). Other applications of XRF technologies include metals analysis of lake and ocean sediments, soils amended with treated waste water, agricultural soils, and historical analyses (Ge et al., 2004; Coronel et al., 2014; McComb et al., 2014; Schneider et al., 2016; Sahraoui and Hachicha, 2017). The use of XRF technologies for the determination of trace metals in soils is utilized heavily across many research fields.

2.1.1 XRF Technology

The accuracy and precision of published data produced by an XRF only used *in situ* has been questioned (Pyle and Nocerino, 1996; Lin, 2009; Melquiades and Appoloni, 2004; McComb et al., 2014). Often, results obtained using the XRF *in situ* are reported as lower than laboratory-based methods (Alloway, 2012; Sahraoui and Hachicha, 2016). Soil samples in *in situ* environments often have surface irregularities, soil moisture, organic matter, and varying particle sizes, which can all impact XRF readings (Kalnicky and Singhvi, 2001; Ge et al., 2005; Crooks et al., 2006; Lin, 2009; Löwemark et al., 2011; Bastos et al., 2012; Sahraoui and Hachicha, 2017; Ravansari and Lemke, 2018). Researchers have found that soil samples with a moisture content greater than 20% can cause error in the readings (often underreporting values) due to the interaction with X-rays and water (Ge et al., 2005; Crooks et al., 2006; Bastos et al., 2012; Schneider et al., 2016; Sahraoui and Hachicha, 2017). Organic content of soil greater than 10% have been documented to decrease the detection of multiple elements (Lin, 2009; Coronel et al.,

2014; Shand and Wendler, 2014; Ravansari and Lemke, 2018). The particle size of soils analyzed has also been documented to affect the accuracy of XRF readings (Datin and Cates, 2002; Crooks et al., 2006; Kilbride et al., 2006). Trace metals concentrations are often associated with the fine soil fractions and therefore multiple researchers recommend sieving soil samples before analysis (Lewin and Macklin, 1987; Maxfield, 2000; Binstock and Gutknecht, 2002; Datin and Cates, 2002; Walling and Owens, 2003; Crooks et al., 2006; Binstock et al., 2008; Coronel et al., 2014; Schaidler et al. 2014). Results from these studies agree that samples should be dried and sieved past the 250 μm or #60 sieve fraction at minimum to determine the most accurate XRF concentration reading.

2.1.2 XRF and ICP-OES Method Comparison

ICP-OES and ICP-MS are EPA approved methods for the determination of trace metals in both soil and water as they are considered reliable and sensitive (Pyle and Nocerino, 1996). The microwave-assisted acid digestion that precedes ICP analysis, is considered most suitable method for trace metals extraction (Pyle and Nocerino, 1996; Bettinelli et al., 2000; Sahraoui and Hachicha, 2017; Taha, 2017). Atomic absorption spectrophotometry (AAS) and atomic fluorescence spectrometry (AFS) are also methods to determine trace metals (Sahraoui and Hachicha, 2017). All of these methods are costly and time consuming and therefore XRF, a faster and more cost-effective method, has been compared extensively to ICP-OES to determine if XRF will yield similar results to ICP-OES analysis (Wilson et al., 1995; Pyle and Nocerino, 1996; Datin and Cates, 2002; Ge et al., 2005; Kilbride et al., 2006; McComb et al., 2014; Rouillon and Taylor, 2016;

Sahraoui and Hachicha, 2016; Schneider et al., 2016; Taha, 2017). Results from these studies conclude that for XRF results to be most comparable to ICP values, samples must be homogenized, dried, and sieved before XRF analysis (Ge et al., 2005; Crooks et al., 2006; Binstock et al., 2008; McComb et al., 2014; Rouillon and Taylor, 2016; Schneider et al., 2016). Homogenized, dried, and sieved XRF concentrations often yield close to 1:1 relationships for trace elements (Pyle and Nocerino, 1996; Maxfield, 2000; Binstock and Gutknecht, 2002; Crooks et al., 2006; Binstock et al., 2008; McComb et al., 2014). Differences between ICP and XRF readings have been reported for zinc, as zinc is often overreported by the XRF (Wilson et al., 1995; Kilbride et al., 2006; Sahraoui and Hachicha, 2016). Lead concentrations reported by the ICP and XRF are repeatedly reported as statistically similar, however, lead concentrations reported by the ICP are often greater than XRF readings (Pyle and Nocerino, 1996; Binstock et al., 2008; Sahraoui and Hachicha, 2016). Regression analysis between ICP and XRF values for lead and zinc often yield $r^2 > 0.90$ for both metals and sieved samples often have $r^2 > 0.99$ (Datin and Cates, 2002; Crooks et al. 2006; Kilbride et al., 2006; McComb et al., 2014; Sahraoui and Hachicha, 2016; Schneider et al., 2016).

The primary objective associated with this portion of the study was to compare the accuracy of metals concentrations derived from *in situ* XRF measurements, laboratory XRF measurements (where samples were dried and sieved), and ICP-OES analyses. The two hypotheses were: 1) *In situ* XRF readings with moisture content exceeding 20% will report lesser metals concentrations than laboratory XRF readings where the soil was homogenized, dried, and sieved and 2) homogenized, dried, and

sieved soils analyzed by the XRFs in the laboratory will yield concentrations not statistically different from ICP-OES metals concentrations. For this study, lead and zinc were the major elements of focus. Secondary objectives of this study involved analyzing the effect of organic matter on XRFs readings and determining a mathematical relationship for the estimation of cadmium when zinc XRFs measurements are provided.

2.2 Methods

2.2.1 Site Description

The Elm Creek watershed located in Ottawa County, Oklahoma, is impacted by trace metal contamination from the Tar Creek Superfund Site, which is the Oklahoma portion of the Tri-State Lead and Zinc Mining District (USFWS, 2013; Nairn, 2014a). Extensive mining operations for zinc and lead, beginning in the 1890s and continuing until the 1970s, left extensive trace metal contamination on the surface which remains exposed to this day (USEPA, 1997; Datin and Cates, 2002; White, 2006; USEPA, 2008; Andrews, 2011; USFWS, 2013). Trace metals concentrations of the Superfund site tailings (known as “chat”) can exceed 2,200 mg/kg lead, 34,400 mg/kg zinc, and 96 mg/kg cadmium (Datin and Cates, 2002). The Elm Creek watershed extends into portions of the Tar Creek Superfund Site and the east branch of Elm Creek originates within the Superfund area (Figure 2.1). Within this watershed are a series of properties owned by the Grand River Dam Authority, known as the Neosho Bottoms, which may have trace metals contamination. The extent of the trace metals contamination in this area is of concern due to the ability for contaminated material to be transported by

fluvial processes (Miller, 1996). Access to these properties was granted by the GRDA to sample the soils in both the uplands and creek terraces.

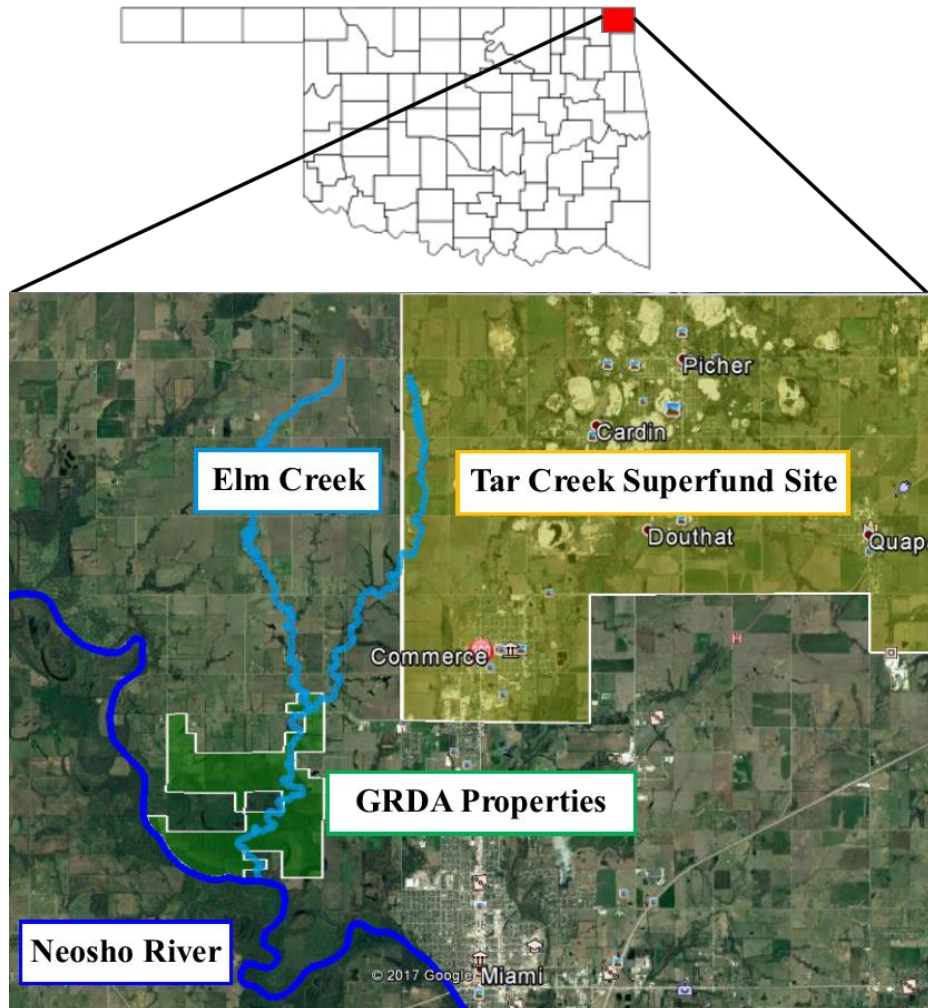


Figure 2.1: The locations of the Tar Creek Superfund Site, Elm Creek, the Neosho River, and the GRDA-owned properties with respect to each other

2.2.2 *In Situ* Soil Sample Analysis and Collection

A field portable Thermo-Fisher Scientific Niton XL3t GOLDD+ XRFs was used *in situ* within the GRDA-owned properties and at road crossings on both the east and west branches of Elm Creek for analysis of metals concentrations following USEPA Method 6200. This device was used for “rapid field screening” to obtain *in situ* metals

concentrations (USEPA, 2007c). The “All Geo mode”, which includes both the “Mining mode” (used for heavier elements) and “Soils mode” (used for lighter elements), was used to analyze samples. Sampling took place starting in January 2017 and continued through October 2017. Each soil sample location had all litter, vegetation, and roots removed before *in situ* analysis with the XRFs (Figure 2.2). Care was taken at sampling locations at Elm Creek road crossings to reduce metals influences from the road. Samples at road crossings were taken at spots furthest from the road, without trespassing onto private property. Locations with completely saturated soils did not have readings taken. Soil samples were collected using a stainless-steel shovel, excavating a 13 cm by 13 cm by 10 cm deep sample. Samples were placed in an air-tight plastic sample bags immediately upon collection. A Global Positioning System (GPS) was used to record the latitude and longitude of each sample site. A total of 278 samples were taken within areas denoted as “uplands” within the Neosho Bottoms and 106 samples were taken from stream terraces along the extent of Elm Creek. Samples were transported back to the Center for Restoration of Ecosystems and Watersheds (CREW) laboratories for further analysis.



Figure 2.2: The field portable Thermo-Fisher Scientific Niton XL3t GOLDD+ XRFs being operated *in situ* on a soil surface with all debris removed

2.2.3 Laboratory Sample Analysis

Laboratory analysis of the soil samples took place in the CREW laboratories, located in Carson Engineering Center at the University of Oklahoma. Soil samples were homogenized by hand by breaking apart larger soil clods and an aliquot was analyzed for moisture content (ASTM D2216-10). The remaining portion of the samples was air dried. After the samples air dried, they were sieved to less than the #60 soil fraction (< 250 μm). Samples were sieved using a W.S. TylerTM RO-TAPTM RX-94 electric sieve shaker for a minimum of three minutes (consisting of 278 ± 10 oscillations per minute and 150 ± 10 taps per minute with a 2.5 kg hammer) and sieves were cleaned after every sample using coarse and soft brushes with the pan wiped down with KimWipes. If dried samples were in tight clumps, the aggregates were crushed using a mortar and pestle that was cleaned after every use with KimWipes. All sieves, brushes, the mortar and pestle, and stainless-steel pans were washed and air dried after each day of sample analysis to minimize cross contamination of soil samples. The bulk sample and the soil

fraction passing the #60 sieve were both used to determine an independent organic content for both the bulk and sieved portion of the sample (Dean, 1974). The soil fraction passing the #60 sieve was used for metals concentration laboratory analyses via field portable XRFS analyzer (EPA 6200) and Varian VistaPRO CCD Simultaneous Inductively Coupled Plasma-Optical Emission Spectrometer (ICP-OES) following (EPA 3051a and EPA 6010c). Table 2.1 summarizes the methods used for each analysis and the sample size fraction analyzed.

Table 2.1: Laboratory analysis and corresponding methods

Analysis	Method	Particle Size Fraction Analyzed
Moisture Content	ASTM D2216-10	Bulk sample
Organic Content	Dean, 1974	Bulk and sieved Fraction (< 250 μm)
XRFS Analyses	EPA 6200	Bulk and sieved Fraction (< 250 μm)
ICP-OES Analyses	EPA 3051a; EPA 6010c	Sieved Fraction (< 250 μm)

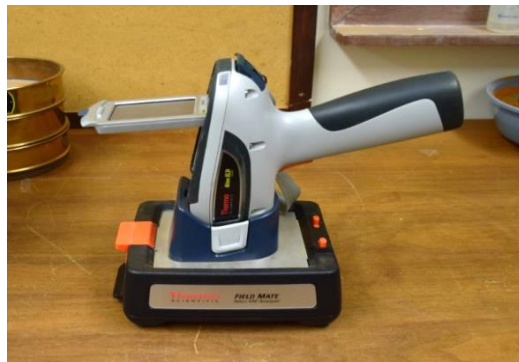
2.2.3.1 Laboratory XRFS Analysis

Air dried soil from the < #60 soil fraction was packed into circular XRFS sample cups for each sample and analyzed with the XRFS operated via personal computer in a shielded, Field Mate test stand for a total run time of 60 seconds in the All Geo mode. The XRFS sample cups were 32 mm in diameter and covered with 4.0 μm polypropylene X-ray film (Figure 2.3). Enough soil was added to the cups to ensure that the full film surface was covered, and glass wool was added into the remaining cup space to keep the sample pressed against the film window. The Field Mate test stand allows for hands free and stable analysis by locking the XRFS into place with the nose of the XRFS pointing downward at a sample cup film surface (Figure 2.4 (a)) (Thermo Scientific, 2010). The circular sample cup is securely fastened in the Field Mate test stand while the XRFS

reading takes place (Figure 2.4 (b)). The stand also shields the operator from scattered X-rays.



Figure 2.3: Packed circular XRF soil sample cups lined with polypropylene X-ray film for analysis



(a)



(b)

Figure 2.4: (a) Thermo Scientific Field Mate test stand is used to lock in the Thermo-Fisher Scientific Niton XL3t GOLDD+ XRF with the nose of the device pointing towards the sample cup; (b) The Field Mate holds the circular sample cup within the base

2.2.3.2 ICP-OES Analysis

ICP-OES analyses were conducted on the air-dried and homogenized soil fraction passing the #60 sieve ($< 250 \mu\text{m}$). A total of 79 soil samples (20%) were hot acid microwave digested with concentrated HNO_3 following USEPA Method 3051a (USEPA, 2007b) and then underwent analysis by ICP-OES following USEPA Method 6010c (USEPA,

2007a) to measure total metals concentrations for Al, As, Ca, Cd, Co, Cr, Cu, Fe, K, Mg, Mn, Na, Ni, Pb, and Zn. These 79 samples were selected based on Pb and Zn concentrations determined by the laboratory XRF reading. Samples ranging from lowest to highest laboratory XRF Pb and Zn concentrations were selected along equal concentration intervals to ensure that the full range of concentrations for both metals would be analyzed.

2.2.4 Quality Assurance / Quality Control

For each USEPA method, a minimum of one in every 10 samples was a duplicate, following USEPA guidelines for QA/QC (USEPA, 2007a; USEPA, 2007c). The same protocol (taking a duplicate for every 10 samples) was followed for both moisture content and organic content methods.

2.2.5 Statistical Analysis

Statistical analyses were performed on each of the datasets generated and analyzed with Microsoft Excel and IBM SPSS Statistics software. The Kolmogorov-Smirnov and Shapiro-Wilk tests were used to determine the normality of the dataset. The Wilcoxon signed rank test was used to determine statistical similarities or differences for non-parametric datasets containing two related samples. Regression analysis was conducted using Microsoft Excel to determine if a relationship between datasets exists. The 95% confidence interval was used for all analysis.

2.3 Results and Discussion

2.3.1 Comparison of XRFS *In Situ* and XRFS Laboratory Concentration Readings

The relationship between all collected XRFS *in situ* readings compared to the XRFS laboratory readings was analyzed for lead and zinc. Cadmium was not compared as the XRFS concentration readings for both *in situ* and laboratory tests did not generate reliable cadmium values. The data were compared two different ways. The first comparison uses the Wilcoxon signed ranks test to compare the field XRFS reading to its corresponding laboratory XRFS reading for each metal, which provides the number of readings that reported greater or lesser values for each reading type. It also provides an overall p-value for the entire paired dataset. A p-value greater than 0.05 means acceptance of the null hypothesis that the median difference between pairs is equal, while a p-value less than 0.05 causes a rejection of the null hypothesis. The second comparison uses linear regression to assess the predictability of the data. Note that although there was a total of 384 samples collected, the number of samples analyzed for both tests is lower. This is due to XRFS outputs reporting at the limit of detection for either the field or laboratory sample (around 15 mg/kg for zinc and 10 mg/kg for lead). In these cases, no numerical value was provided, and samples could not be compared. Table 2.2 and Table 2.3 outline the statistical values returned from the Wilcoxon signed ranks test and test p-value for field and laboratory XRFS readings for lead and zinc.

Table 2.2: Descriptive statistics for field and laboratory XRFS readings for lead and zinc

	Reading Type	n	Mean (mg/kg)	Median (mg/kg)	Std. Deviation (mg/kg)	Minimum (mg/kg)	Maximum (mg/kg)
Pb	Field XRFS	370	45.8	22	75.7	5.12	927
	Laboratory XRFS	370	67.0	33	100	10.0	926
Zn	Field XRFS	372	463	130	781	16.1	5100
	Laboratory XRFS	372	535	174	922	22.1	7700

Table 2.3: Wilcoxon signed ranks test distribution and p-value for the comparison of laboratory XRFS and field XRFS readings for lead and zinc

		n	p-value ¹	Null Hypothesis ²
Pb	Laboratory XRFS < Field XRFS	64	6.78E-39	Rejected (Distributions not equal)
	Laboratory XRFS > Field XRFS	305		
	Laboratory XRFS = Field XRFS	1		
	Total	370		
Zn	Laboratory XRFS < Field XRFS	109	9.34E-12	Rejected (Distributions not equal)
	Laboratory XRFS > Field XRFS	263		
	Laboratory XRFS = Field XRFS	0		
	Total	372		

¹p-value greater than 0.05 = acceptance of null hypothesis

²Null hypothesis = The median difference between pairs is equal.

Results found that there was no statistically significant relationship between field and laboratory XRFS readings for lead or zinc ($p < 0.05$) meaning that distributions were different for both metals. In most cases, laboratory XRFS reported greater readings than field XRFS readings. These results are not surprising as there is an abundance of research on how *in situ* conditions (surface irregularities, varying particle size, and presence of organic and moisture content) all impact the readings of the XRFS (Kalnicky and Singhvi, 2001; Ge et al., 2005; Crooks et al., 2006; Lin, 2009; Löwemark et al., 2011; Bastos et al., 2012; Sahraoui and Hachicha, 2017; Ravansari and Lemke, 2018). Coronel et al., (2014) mentioned that field moisture and high organic content caused lower concentration readings for *in situ* XRFS readings for zinc. The presence of moisture is widely accepted by researchers who use XRFS technologies as the major

influencing factor for underreporting of elemental concentrations (Ge et al., 2005; Crooks et al., 2006; Bastos et al., 2012; Schneider et al., 2016; Sahraoui and Hachicha, 2017). Field moisture content percentages in this study ranged from 4.5% to 66% and the organic content percentage of the field samples ranged from 0.7% to 53%. The laboratory samples in this study were dried and sieved and therefore are a different subset of the bulk sample. Many researchers stress the need to dry, crush, and sieve soil samples before the XRF reading is taken to ensure the most accurate XRF reading is provided (Lewin and Macklin, 1987; Maxfield, 2000; Binstock and Gutknecht, 2002; Walling and Owens, 2003; Crooks et al., 2006; Binstock et al., 2008; Coronel et al., 2014; Schaidler et al. 2014). The results of this comparison display that *in-situ* samples with no alterations made to the soil surface before XRF readings are conducted do not yield comparable XRF results to samples that were dried and sieved in the laboratory.

The field XRF and laboratory XRF readings were also plotted against each other and a linear regression was conducted for each metal. Figure 2.5 and Figure 2.6 present the regression of field XRF measurements against laboratory XRF measurements. The estimated relationship (dashed line) and 100% recovery (solid red line) are shown in each plot.

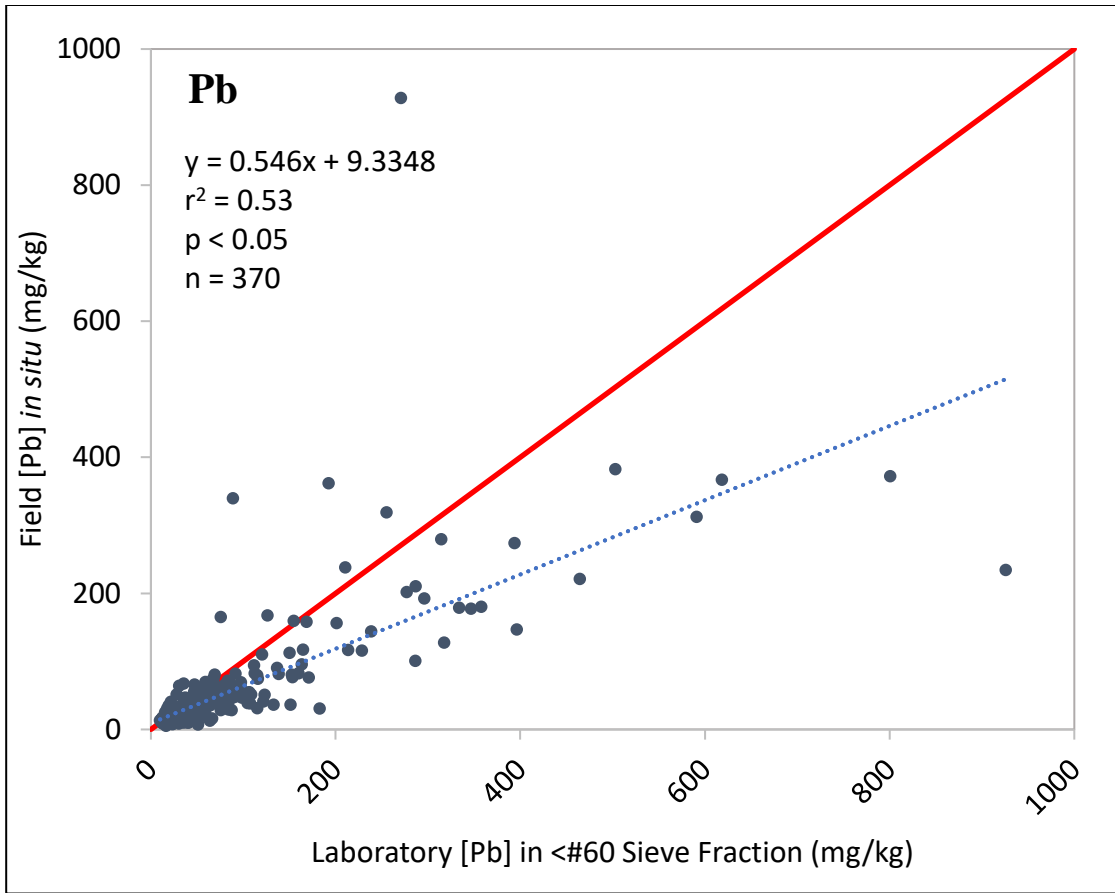


Figure 2.5: Regression of field XRFs measurements against laboratory XRFs measurements for lead. The estimated relationship (dashed line) and 100% recovery (solid red) are provided.

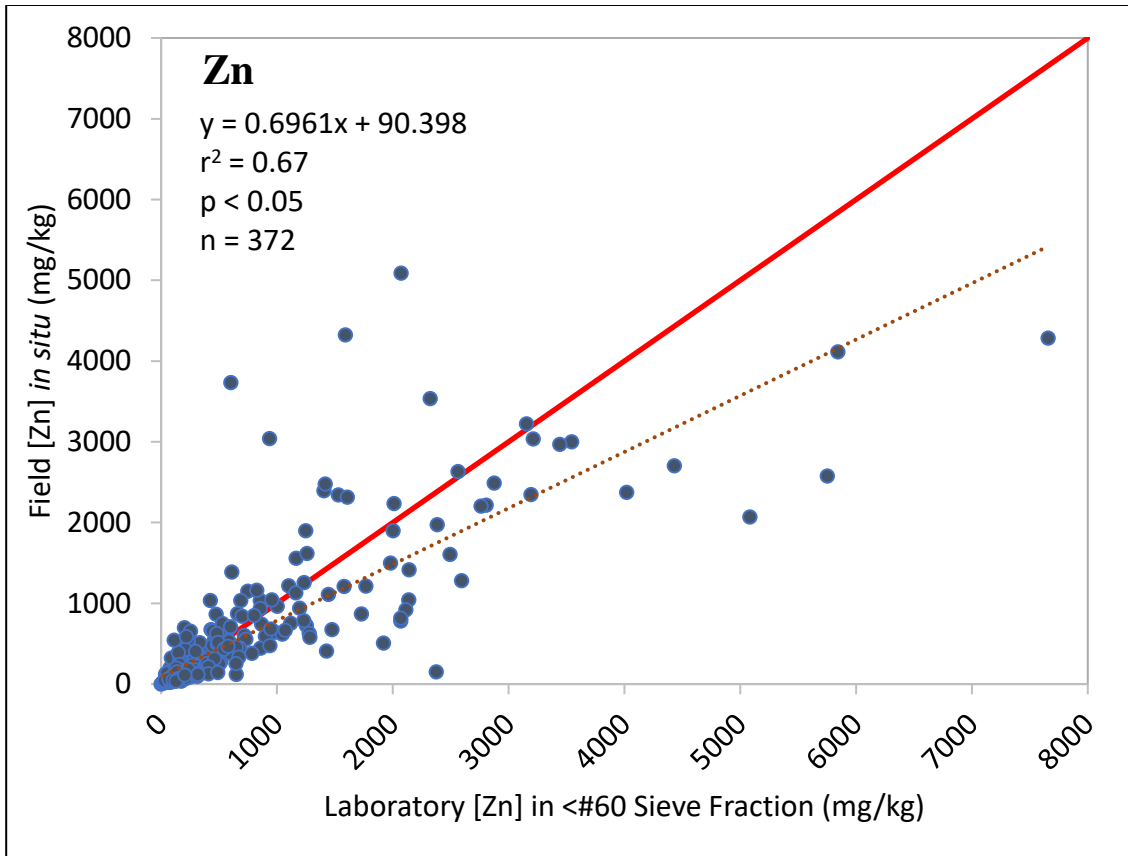


Figure 2.6: Regression of field XRF measurements against laboratory XRF measurements for zinc. The estimated relationship (dashed line) and 100% recovery (solid red) are provided.

The regression indicated that there is a statistically significant trend for both lead and zinc ($p < 0.05$). The trendline indicates that field readings are often underreported when compared to laboratory XRF readings. The laboratory XRF is taken on the finer fraction and therefore the “dilution” caused by *in situ* particle irregularities is eliminated. The regression equation can aid future researchers who are assessing *in situ* XRF readings by allowing them to predict laboratory readings.

2.3.2 Moisture Content Effect on XRF Readings

The relationship between different moisture content ranges on XRF readings was analyzed. The distributions of the field and laboratory XRF readings were analyzed using the Wilcoxon signed ranks test to determine if the distributions were equal. The field and laboratory XRF data for lead and zinc for all data collected with the corresponding field moisture contents were used. Field moisture contents ranged from 4.5%-66.4%. All laboratory XRF samples had moisture contents less than 15%. Cases where XRF readings for lead or zinc were reported at the limit of detection for a sample were not used as no numerical concentration was provided by the XRF. Field and laboratory XRF readings for lead and zinc were split into three field moisture content ranges: less than 10% moisture content, less than 20% moisture content, and greater than 20 % moisture content. The data for each group was paired and groups were analyzed independently. Table 2.4 and Table 2.5 outline the statistical values returned from the Wilcoxon signed ranks test and test p-value for field and laboratory XRF readings for lead and zinc.

Table 2.4: Descriptive statistics for field and laboratory XRF readings for lead and zinc split into less than 10% moisture content, less than 20% moisture content, and greater than 20% moisture content

	Field moisture content range (%)	Reading Type	n	Mean (mg/kg)	Median (mg/kg)	Std. Dev. (mg/kg)	Min. (mg/kg)	Max. (mg/kg)
Pb	< 10%	Field XRF	14	32.3	25.1	17.1	13.2	60.6
		Laboratory XRF	14	45.0	30.4	45.0	11.5	182
	< 20%	Field XRF	111	51.6	25.2	72.0	8.62	371
		Laboratory XRF	111	72.9	22.6	133	11.5	925
	> 20%	Field XRF	255	38.1	20.5	50.6	5.12	382
		Laboratory XRF	255	63.4	36.1	82.8	9.90	618
Zn	< 10%	Field XRF	14	252	118	228	34.3	601
		Laboratory XRF	14	525	207	734	32.2	2380
	< 20%	Field XRF	115	603	135	1002	16.2	5090
		Laboratory XRF	115	617	132	1080	23.6	5750
	> 20%	Field XRF	257	400	128	652	20.2	4280
		Laboratory XRF	257	500	185	844	22.2	7660

Table 2.5: Wilcoxon signed ranks test distribution and p-value for the comparison of laboratory XRFs and field XRFs readings for lead and zinc in different moisture content ranges

	Field moisture content range (%)	n	p-value ¹	Null Hypotheses ²	
Pb	< 10%	Laboratory XRFs < Field XRFs	6	0.30	Accepted (Distributions are equal)
		Laboratory XRFs > Field XRFs	8		
		Laboratory XRFs = Field XRFs	0		
		Total	14		
	< 20%	Laboratory XRFs < Field XRFs	34	2.60E-06	Rejected (Distributions not equal)
		Laboratory XRFs > Field XRFs	77		
		Laboratory XRFs = Field XRFs	0		
		Total	111		
	> 20%	Laboratory XRFs < Field XRFs	26	1.86E-37	Rejected (Distributions not equal)
		Laboratory XRFs > Field XRFs	228		
		Laboratory XRFs = Field XRFs	1		
		Total	255		
Zn	< 10%	Laboratory XRFs < Field XRFs	6	0.27	Accepted (Distributions are equal)
		Laboratory XRFs > Field XRFs	8		
		Laboratory XRFs = Field XRFs	0		
		Total	14		
	< 20%	Laboratory XRFs < Field XRFs	45	0.24	Accepted (Distributions are equal)
		Laboratory XRFs > Field XRFs	70		
		Laboratory XRFs = Field XRFs	0		
		Total	115		
	> 20%	Laboratory XRFs < Field XRFs	64	1.70E-13	Rejected (Distributions not equal)
		Laboratory XRFs > Field XRFs	193		
		Laboratory XRFs = Field XRFs	0		
		Total	257		

¹p-value greater than 0.05 = acceptance of null hypothesis

²Null hypothesis = The median difference between pairs is equal.

Results of these tests showed that samples with field moisture contents less than 10% did not have statistically different readings when comparing field XRFs and laboratory XRFs readings for both lead and zinc. Samples with less than 20% moisture content had statistically similar XRFs readings for zinc, but dissimilar XRFs readings for lead. Samples with greater than 20% field moisture contents had statistically different

readings for both lead and zinc when comparing field XRFs and laboratory XRFs readings. These results suggest that using the XRFs *in situ* on a dry soil surface (moisture less than 10%) could yield results statistically similar to the laboratory results. Reames and Lance (2002), also observed similar results when analyzing for lead in dry and silty soil samples in residential yards from housing units built before 1978 in the San Francisco bay area. Reames and Lance (2002) found significant correlation between soil lead concentrations measured by an XRFs *in situ* and on ground and sieved soil samples also measured by the XRFs. The *in situ* soils in the study by Reames and Lance (2002) were described as dry and silty with relatively low moisture content suggesting that dry and fine *in situ* soil samples yield comparable results to laboratory XRFs readings. Crooks et al., (2006) found that lead concentrations were not affected at moisture concentrations less than 20% which contrast from this studies results, however Crooks et al., (2006) also observed that lead concentrations greater than 20% caused reductions in XRFs readings.

The results also showed that the laboratory XRFs readings were reported as greater than the field XRFs readings which suggests that field moisture causes underreporting of *in situ* XRFs readings. This observation is supported by Sahraoui and Hachicha (2017) who stated that “water in soil acts as both an adsorption layer and a scattering layer” which fluoresces decreased characteristic X-rays back to the XRFs causing underreporting of elemental concentrations. These observations also reflect the results from multiple researchers who also observed elemental underreporting for lead and zinc when moisture contents were above 20% (Ge et al., 2005; Kido et al., 2006;

Bastos et al., 2012; Sahraoui and Hachicha, 2016; Schneider et al., 2016). Soil texture and organic content are both known to directly influence water retention in soil and therefore the combination of water content, organic matter, and differing soil textures in *in situ* soils may all be affecting XRF outputs (Gupta and Larson, 1979; Zhuang et al., 2001; Ankenbauer and Loheide, 2016).

The field and laboratory XRF readings were also plotted against each other, however this time points are separated into field moisture content ranges. This was done for the uplands samples and for the creek samples independently. Concentrations in the creek terraces were much greater than lead and zinc concentrations in the uplands which made the range of concentrations much larger and impaired the viewability of the relationships and therefore presented in a separate figure. Figure 2.7 and Figure 2.8 present the upland XRF data and the creek XRF data for lead with moisture content ranges increasing by 10% increments. Figure 2.9 and Figure 2.10 present the upland XRF data and the creek XRF data for zinc with moisture content ranges increasing by 10% increments. Each figure has the trendlines for each range (dashed line) and 100% recovery (solid red) presented.

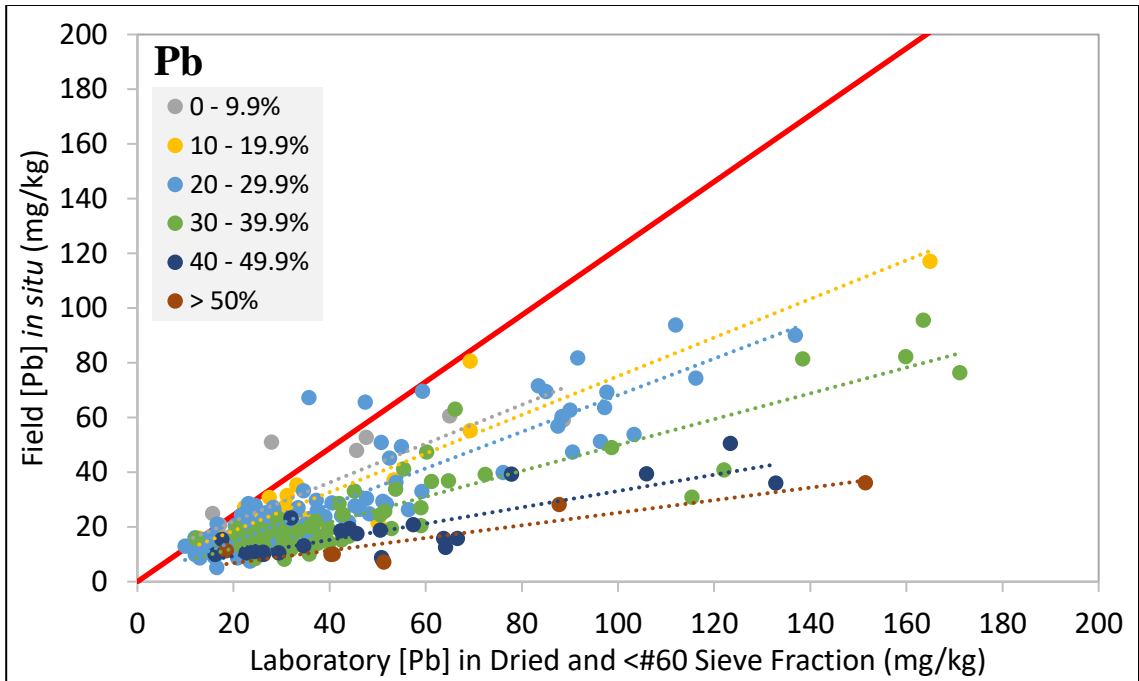


Figure 2.7: Upland XRFs data with field XRFs measurements against laboratory XRFs measurements for lead separated into moisture content ranges. The trendlines for each range (dashed line) and 100% recovery (solid red) are presented.

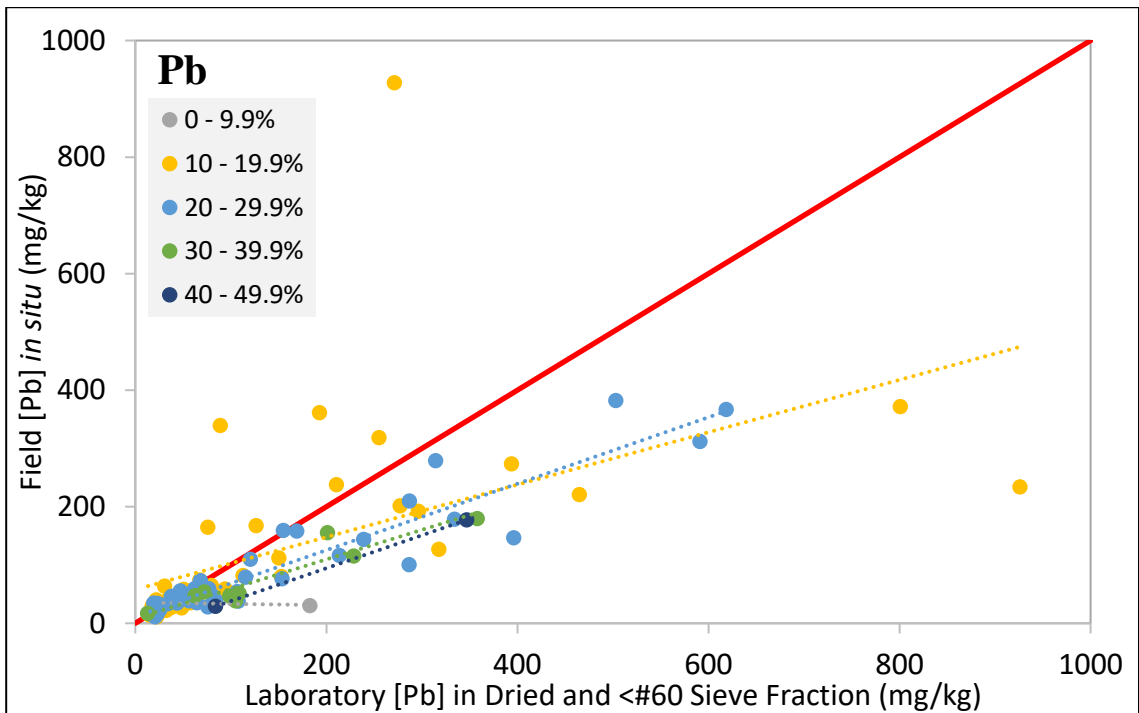


Figure 2.8: Creek XRFs data with field XRFs measurements against laboratory XRFs measurements for lead separated into moisture content ranges. The trendlines for each range (dashed line) and 100% recovery (solid red) are presented.

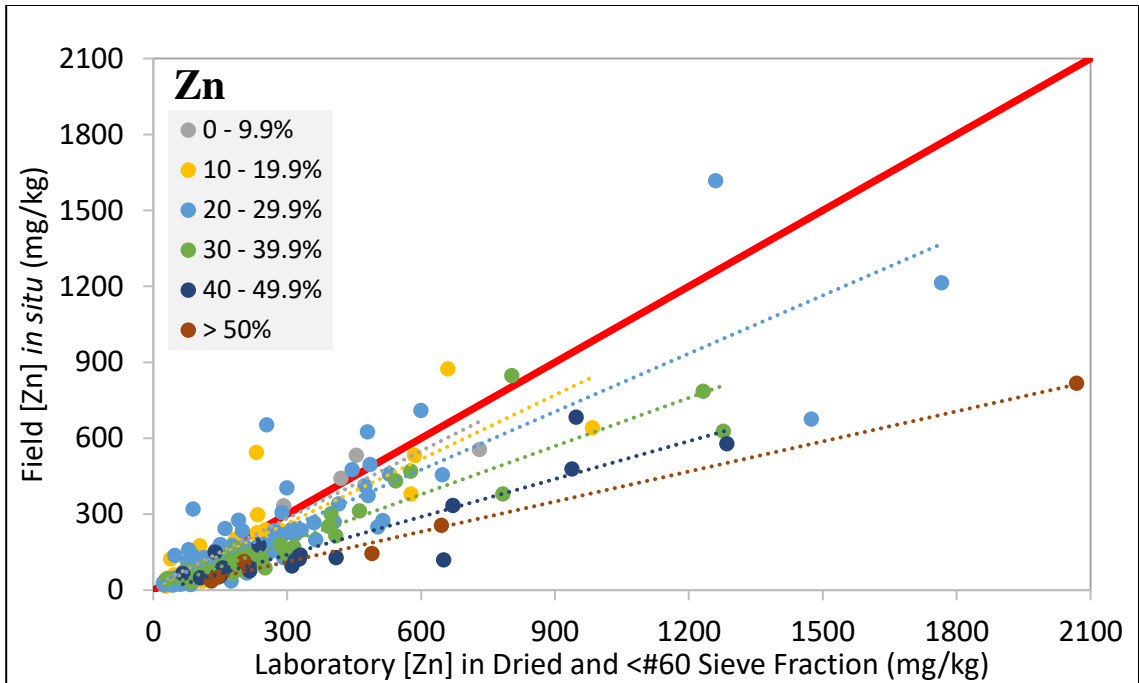


Figure 2.9: Upland XRFs data with field XRFs measurements against laboratory XRFs measurements for zinc separated into moisture content ranges. The trendlines for each range (dashed line) and 100% recovery (solid red) are presented.

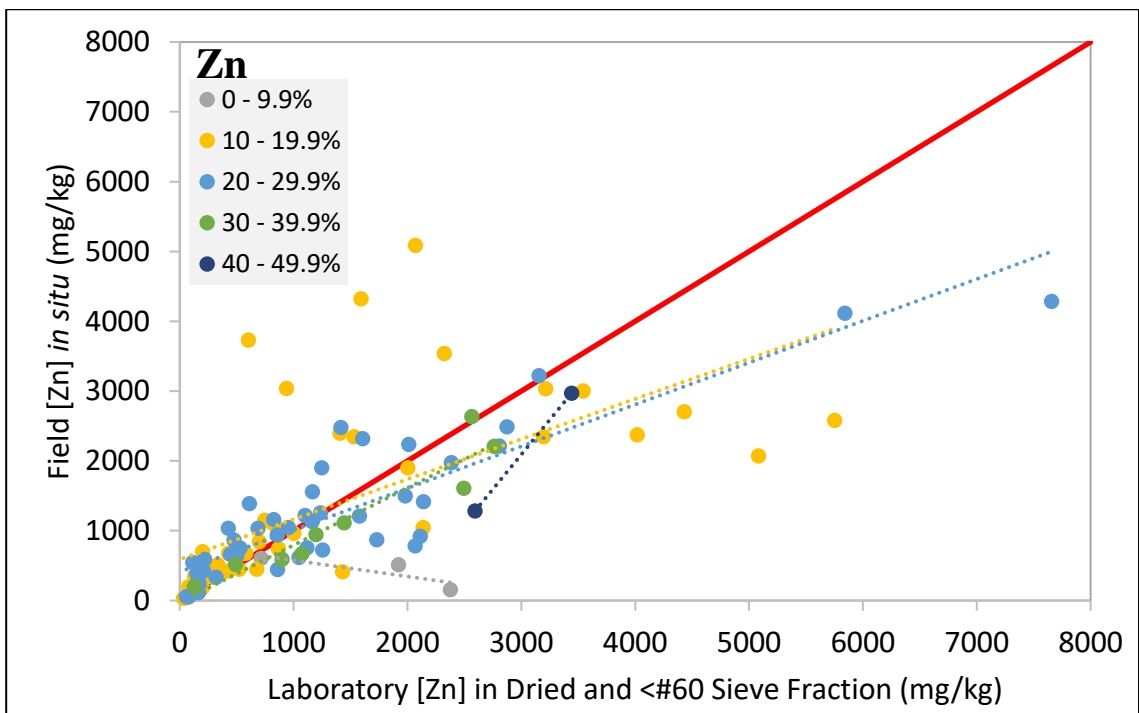


Figure 2.10: Creek XRFs data with field XRFs measurements against laboratory XRFs measurements for zinc separated into moisture content ranges. The trendlines for each range (dashed line) and 100% recovery (solid red) are presented.

The figures with just the uplands plotted graphically demonstrate a decreasing slope as moisture content increases. The 0-9.9% moisture content trendline is closest to the 100% recovery line, while the >50% moisture content range is the furthest. They indicate that as moisture content increases, *in situ* XRFs measurements decrease. Although the decreasing slope cannot be entirely related to moisture content alone since the *in situ* and laboratory samples are physically different, these figures provide a possible relationship between moisture content and the underreporting of XRFs readings. The figures with the creek data plotted do not show the same trend. The concentrations in the creek were greater than the upland samples as contamination from the Tar Creek Superfund Site was deposited within the terraces. This contamination also has greater concentrations associated with the smaller particle size fraction (Datin and Cates, 2002). Because the figures with the creek information show that samples at lower moisture content ranges falling further from the 1:1 line suggests that moisture content is not the major influence in differences in concentrations. The concentration differences in upland samples may be more affected by moisture content as they are less likely to be influenced by contamination from the Superfund site. The creek terrace samples, however, are more likely to have concentration differences due to particle size and moisture due to proximity to the stream which transports the smaller, more contaminated particles, and provides moisture which both affect XRFs readings (Wilson et al., 1995; Ge et al., 2005; Crooks et al., 2006; Kilbride et al., 2006; Bastos et al., 2012; Schneider et al., 2016; Sahraoui and Hachicha, 2016; Sahraoui and Hachicha, 2017).

The hypothesis that *in situ* XRF readings with moisture contents exceeding 20% will report lesser metals concentrations than laboratory XRF readings where the soil was homogenized, dried, and sieved was accepted. The results suggest that for the most comparable results from *in situ* and laboratory XRF readings, *in situ* XRF readings should be taken on dry surfaces (< 10% moisture content for lead and < 20% moisture content for zinc). If *in situ* soil samples are wet, results suggest that soil samples should be prepared before XRF analysis by drying and sieving the soils before a XRF reading is taken. Drying and sieving samples takes time (several hours) and often is completed in a laboratory environment. Having to prepare samples before XRF analysis takes away from the benefits of having a field portable device. In the future, the relationships between *in situ* soil moisture and field XRF values could be explored. Although laboratory preparations will take longer, outputs from the XRF are much faster than other wet chemistry analysis.

2.3.3 Organic Content Effect and XRF Readings

The presence of organic content in soils has also been known to have an impact on XRF readings (Lin, 2009; Shand and Wendler, 2014; Ravansari and Lemke, 2018). The effect of organic matter in soils on XRF readings were determined by comparing laboratory XRF readings, with known organic content percentages, to ICP values. All 384 samples collected were analyzed for organic content in the <#60 sieve (< 250 μm particle size fraction) which was the same fraction analyzed for metals by the XRF in the laboratory and by the ICP. A total of 314 samples also had the organic content determined for the bulk sample that was homogenized, but not sieved. Initial analysis

attempted to find a relationship for *in situ* organic content within the *in situ* XRF readings and laboratory XRF readings following the same approach as the analysis of water content. However, sieving the soil samples past the #60 sieve (< 250 μm particle size fraction) did not reduce the soil organic content down to a common percentage range for all samples. Analysis between the organic content percentages for the #60 soil fraction and the bulk soil revealed that sieving bulk samples caused a statistically significant ($p < 0.05$) reduction in organic content in the #60 soil fraction. Although organic content was reduced by sieving soils, analyzing possible relationships between *in situ* and laboratory XRF readings was both challenging and inconclusive. To determine if a relationship between XRF readings and organic matter did exist, laboratory XRF readings and the corresponding organic contents were compared to ICP results. ICP analyses are not impacted by the presence of organic matter as organic matter is mineralized in the acid digestion process (USEPA, 2007a, 2007b). All samples run in the ICP ($n=79$) were split into two organic concentration ranges: less than 10% and greater than 10% organic matter. It is important to note that the entire dataset (all XRF samples) had organic contents ranging from 0.20% to 53.8%, however since only a subset of samples were analyzed via ICP, the corresponding XRF/ICP samples that were compared had an organic content range of 2.44% to 49.5%. Of the ICP/XRF dataset that was greater than 10% ($n=25$), 23 of the 25 samples fell between 10%-30% organic content, and the remaining two samples had organic matter percentages of 43.2% and 49.5%. Differences between XRF laboratory and ICP concentration outputs for lead and zinc in each organic matter range were analyzed using the Wilcoxon signed ranks

test. Test statistics are presented for each dataset in Table 2.6 and the Wilcoxon signed ranks output and corresponding p-value are presented in Table 2.7.

Table 2.6: Descriptive statistics for laboratory XRFs readings and ICP values for lead and zinc split into less than 10% organic content and greater than 10% organic content for soils passing the #60 sieve fraction

	Organic content range (%)	Reading Type	n	Mean (mg/kg)	Median (mg/kg)	Std. Deviation (mg/kg)	Min. (mg/kg)	Max. (mg/kg)
Pb	< 10%	Laboratory XRF	54	118	56.1	154	11.6	800
		ICP	54	115	62.2	148	13.5	830
	> 10%	Laboratory XRF	25	63.4	46.3	41.9	16.8	160
		ICP	25	66.7	51.0	38.4	22.9	155
Zn	< 10%	Laboratory XRF	54	1080	446	1570	23.7	7700
		ICP	54	1200	368	1980	21.4	8700
	> 10%	Laboratory XRF	25	560	265	646	78.0	2600
		ICP	25	422	182	475	51.6	1630

Table 2.7: Wilcoxon signed ranks test distribution and p-value for the comparison of laboratory XRFs readings and ICP values for lead and zinc in less than 10% organic content and greater than 10% organic content for soils passing the #60 sieve fraction

	Organic content range (%)		n	p-value ¹	Null Hypothesis ²
Pb	< 10%	ICP < Laboratory XRF	24	0.81	Accepted (Distributions are equal)
		ICP > Laboratory XRF	30		
		ICP = Laboratory XRF	0		
		Total	54		
	> 10%	ICP < Laboratory XRF	6	0.007	Rejected (Distributions not equal)
		ICP > Laboratory XRF	19		
		ICP = Laboratory XRF	0		
		Total	25		
Zn	< 10%	ICP < Laboratory XRF	41	0.008	Rejected (Distributions not equal)
		ICP > Laboratory XRF	13		
		ICP = Laboratory XRF	0		
		Total	54		
	> 10%	ICP < Laboratory XRF	25	1.23E-05	Rejected (Distributions not equal)
		ICP > Laboratory XRF	0		
		ICP = Laboratory XRF	0		
		Total	25		

¹p-value greater than 0.05 = acceptance of null hypothesis

²Null hypothesis = The median difference between pairs is equal.

Lead concentration distributions between the laboratory XRF readings and ICP results were not statistically different from each other when samples had less than 10% organic content, however samples with greater than 10% organic content were found to be statistically different. Zinc distribution between the laboratory XRF reading and ICP results were statistically different for both organic content ranges.

Trace metals are known to bind to the organic fraction of soil and lead, specifically, has been documented to be held more tightly to organic material than other metals (Tidball, 1976; John and Leventhal, 1995; Turer and Maynard, 2003; Giacalone et al., 2005). This relationship could explain why the ICP returned greater lead concentrations than the XRF when organic contents exceeded 10%. The organic content in the soil could either be causing a dilution effect for the XRF readings or the lead could be bound to the organic matter and unreachable by the X-rays (Löwemark et al., 2011). This relationship is important for researchers analyzing soils that have an organic content exceeding 10% with an XRF. For most accurate lead concentrations in soils with high organic content, researchers should consider ICP analysis. The results for lead contrast with research conducted by Shand and Wendler, (2014) who found that XRF readings for a certified reference peat soils (>37.5% organic matter), where the metals concentrations were known in advance, were accurate for lead. Similar results from this study were observed for lead, but not zinc in research conducted by Lin (2009). Lin (2009) found that soils amended with 10% organic content had no significant effect on lead or zinc XRF readings when compared to samples with no organic content. Ravansari and Lemke (2018) found that XRF concentration reading decreased with

increasing organic content for lead and zinc when studying organic content amended soils with organic percentages increasing from 0-30%. The difference in zinc concentrations from XRFs readings and ICP values suggest that deviations in readings have to do with something else entirely.

2.3.4 Comparison of ICP-OES and Laboratory XRFs Concentration Readings

The relationship between ICP-OES and XRFs laboratory concentration readings were analyzed for lead and zinc. Trace metals concentrations determined by the ICP-OES are considered the most accurate values as ICP-OES analysis is a USEPA approved method. First the distributions of the laboratory XRFs and ICP readings were analyzed using the Wilcoxon signed ranks test to determine if the distributions were equal and then a linear regression was conducted to assess the predictability of the data. Table 2.8 and Table 2.9 outline the statistical values returned from the Wilcoxon signed ranks test and test p-value for field and laboratory XRFs readings for lead and zinc.

Table 2.8: Descriptive statistics for laboratory XRFs readings and ICP results for lead and zinc

	Reading Type	n	Mean (mg/kg)	Median (mg/kg)	Std. Deviation (mg/kg)	Minimum (mg/kg)	Maximum (mg/kg)
Pb	Laboratory XRFs	79	100	52.4	132	11.5	800
	ICP	79	100	58.1	125	13.5	830
Zn	Laboratory XRFs	79	915	360	1370	23.6	7660
	ICP	79	950	283	1700	21.3	8680

Table 2.9: Wilcoxon signed ranks test distribution and p-value for the comparison of laboratory XRFS readings and ICP results for lead and zinc

		n	p-value ¹	Null Hypothesis ²
Pb	ICP < Laboratory XRFS	30	0.12	Accepted (Distributions are equal)
	ICP > Laboratory XRFS	49		
	ICP = Laboratory XRFS	0		
	Total	79		
Zn	ICP < Laboratory XRFS	66	4.56E-06	Rejected (Distributions not equal)
	ICP > Laboratory XRFS	13		
	ICP = Laboratory XRFS	0		
	Total	79		

¹p-value greater than 0.05 = acceptance of null hypothesis

²Null hypothesis = The median difference between pairs is equal.

Results found that there was a statistically significant relationship between laboratory XRFS readings and ICP results for lead ($p > 0.05$), but no statistically significant relationship for zinc ($p < 0.05$). Therefore, the hypothesis that homogenized, dried, and sieved soils analyzed by the XRFS in the laboratory will yield concentrations not statistically different from ICP-OES metals concentrations was accepted for lead but rejected for zinc. The results from this test agree with a laboratory XRFS/ICP-OES study completed by Sahraoui and Hachicha (2016) where paired t-tests found no statistical differences in lead concentrations between the two methods but showed significant differences in zinc concentrations. Binstock et al., (2008) also found no statistical differences between mean XRFS and ICP soil lead concentrations. For lead, the ICP reported more samples with greater values than laboratory XRFS readings. Pyle and Nocerino (1996) also found that lead concentrations from a hazardous waste that was dried, sieved, and homogenized and analyzed using an XRFS produced readings that were lower or equal to concentrations determined by ICP-OES. This may have to do with the relationship between organic matter and lead discussed in the previous section.

These results present a strong case for the determination of lead concentrations by XRFs on sieved and dried samples. With proper sample preparation for lead, XRFs readings comparable to ICP values can be obtained in a fast and cost-efficient way.

For zinc, the XRFs reported greater values than the ICP. In a comparison of concentrations obtained from XRFs and ICP readings for zinc, Wilson et al. (1995) also observed that XRFs readings reported higher values than results obtained by the ICP. McComb et al. (2014) found that the XRFs reported greater zinc values when compared to certified values in standard soils. Overreporting of zinc XRFs concentrations may be because zinc is a lighter element than lead. Overreporting of XRFs values was also observed for other light metals determined in this study (Al, K, Ca, Cr, Fe, and Cu). Laboratory XRFs and ICP concentrations from Al, K, Ca, Cr, Fe, and Cu, which are all lighter elements than Zn, were plotted in Figure 2.11. Figure 2.11 also contains laboratory XRFs and ICP concentration plots for lead and zinc.

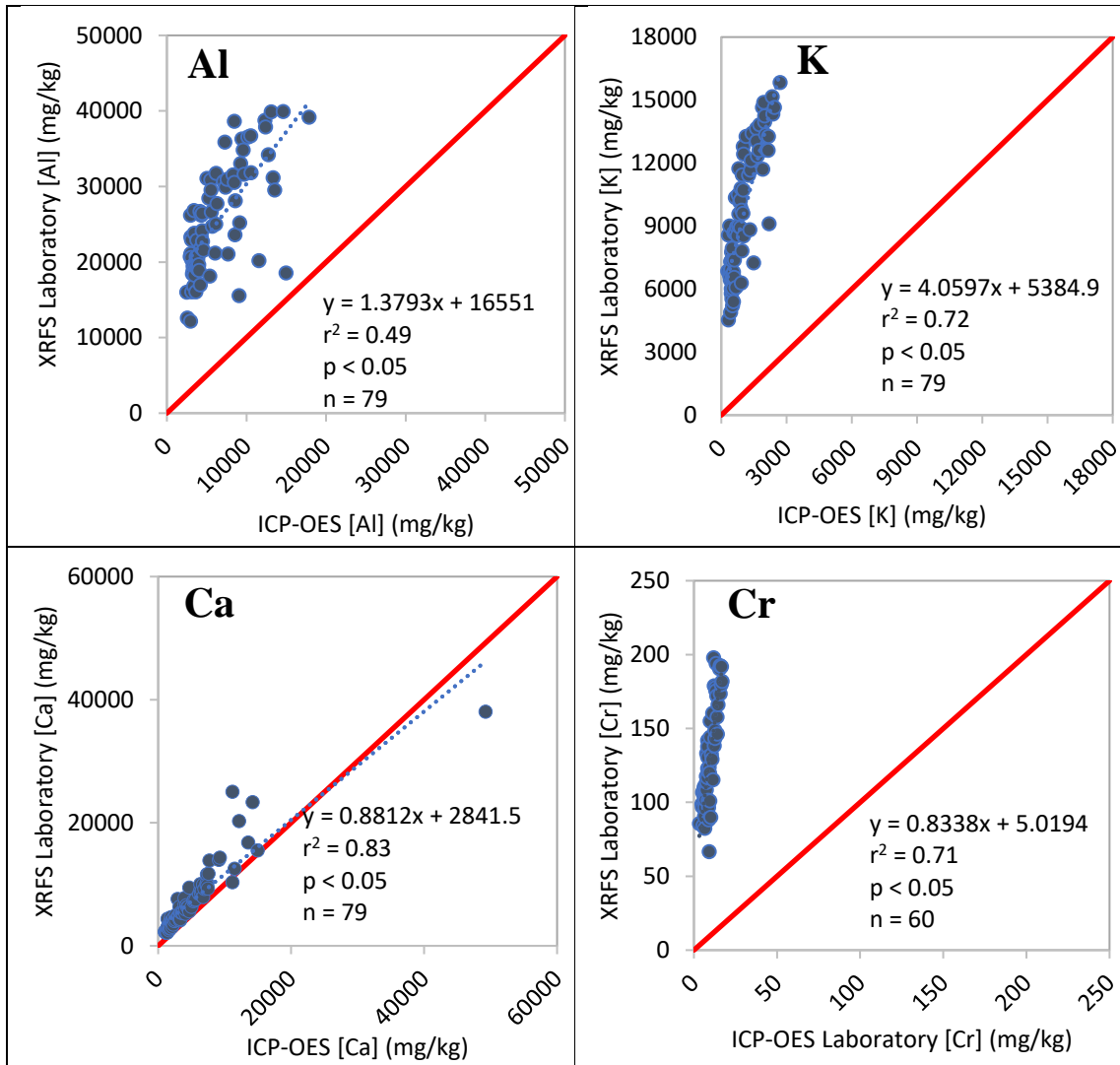


Figure 2.11: Regression for laboratory XRFs measurements against ICP for K, Ca, Cr, Fe, Cu, Zn, and Pb. The relationship (dashed line) and 100% recovery (solid red) are shown in each plot (Figure continued on next page)

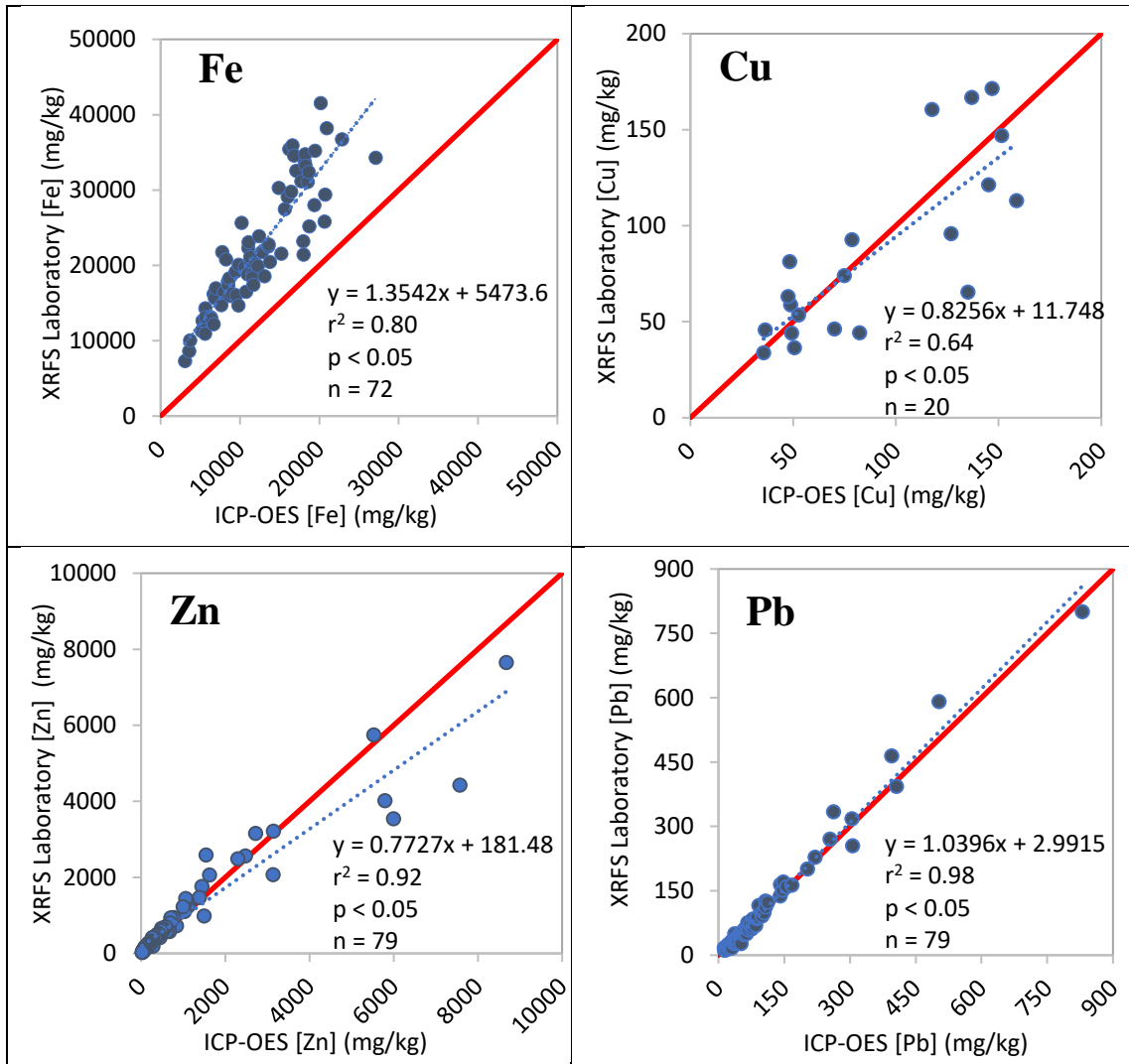


Figure 2.11: (Continued) Regression for laboratory XRF measurements against ICP for K, Ca, Cr, Fe, Cu, Zn, and Pb. The relationship (dashed line) and 100% recovery (solid red) are shown in each plot

Figure 2.11 shows that lighter elements, especially Al, K, Ca, Cr, and Fe all report greater XRF values when compared to ICP values. Lead, which is considered a heavier element, does not show overreporting. This could mean that lighter elements cause over reporting with this XRF. Regression analysis was conducted on ICP and laboratory XRF datasets for lead and zinc. Figure 2.12 and Figure 2.13 includes the same information for lead and zinc presented in Figures 2.11, however these figures include upper and lower confidence limits.

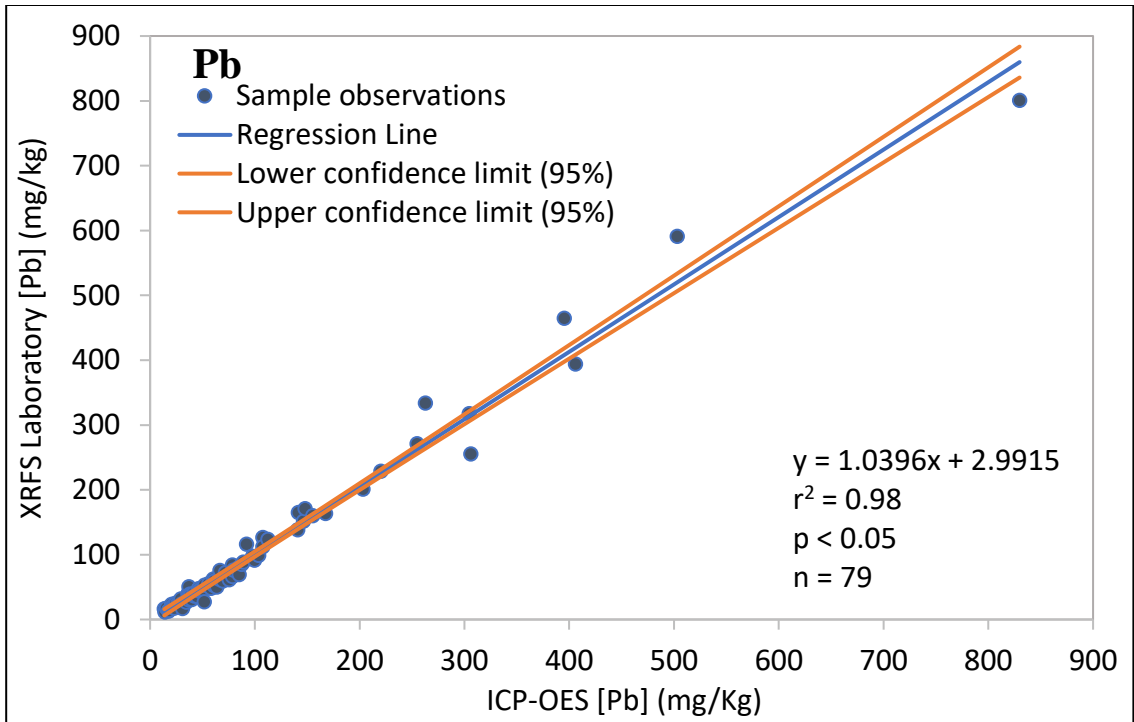


Figure 2.12: Regression of lead laboratory XRFs measurements plotted against ICP-OES. Upper and lower confidence limits are presented in the plot.

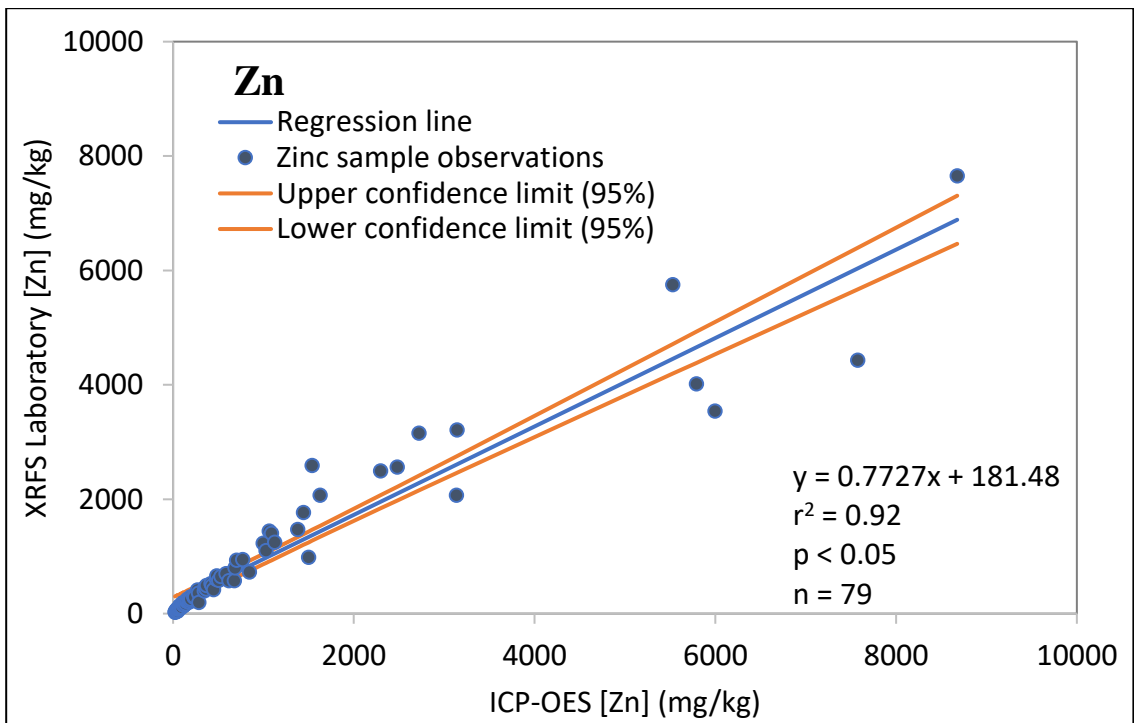


Figure 2.13: Regression of zinc laboratory XRFs measurements plotted against ICP-OES. Upper and lower confidence limits are presented in the plot.

Regression analysis for lead and zinc yielded statistically significant relationships: lead ($r^2=0.98$) and zinc ($r^2=0.92$). Similar regression coefficients for lead and zinc were determined in studies comparing ICP and XRF results by Crooks et al., (2006) (Pb $r^2=0.99$), Kilbride et al., (2006) (Pb $r^2=0.97$; Zn $r^2=0.94$), McComb et al., (2014) (Zn $r^2=0.76$), Rouillon and Taylor (2016) (Pb $r^2=0.99$; Zn $r^2=0.99$), and Schneider et al., (2016) (Pb $r^2=0.99$), when laboratory XRF samples were homogenized, dried, and sieved to past the 250 μm particle size fraction. Wilson et al. (1995) also found agreement between samples sieved past the 100 μm mesh for both methods for lead and zinc, however no r^2 values were provided. These studies had the samples analyzed by the XRF sieved to a smaller particle size than this study ($<250 \mu\text{m}$). Most of the regression coefficients for sieved soils smaller than 150 μm particle size fraction were closer to 1 suggesting that sieving particles past the 150 μm size fraction will yield a regression coefficient closer to 1.

2.3.5 Prediction of Cadmium Concentrations from Zinc Concentrations

The XRF did not provide reliable cadmium concentrations for the soil samples analyzed, however cadmium concentrations were determined by ICP-OES analysis. Zinc and cadmium are isotopic elements (elements with similar structures) and are often found together in the environment (ATSDR, 2005; Kabata-Pendias and Pendias, 2001). Because of this relationship, the ICP-OES concentrations for cadmium and zinc were plotted against each other to analyze the relationship between the two elements within this dataset. Figure 2.14 plots all 79 ICP-OES zinc and cadmium concentrations. Zinc

ICP-OES concentrations ranged from 21.3-8,680 mg/kg for and cadmium ICP concentrations ranged from 0.304-63.4 mg/kg.

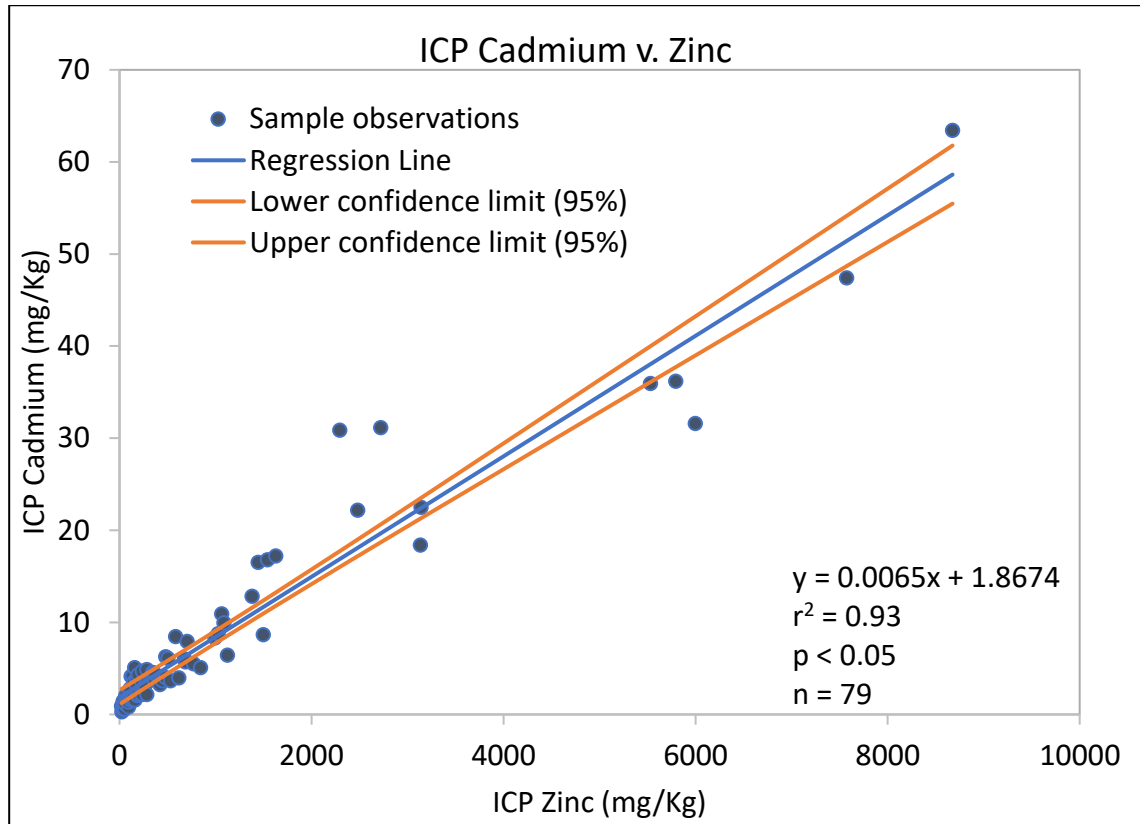


Figure 2.14: Regression of zinc and cadmium concentrations determined by ICP-OES. Upper and lower confidence limits are presented in the plot.

Combining the linear relationship between laboratory XRF zinc readings and ICP readings (Eq. 2.1) with the linear relationship between ICP cadmium and zinc (Eq. 2.2) allows for the prediction of cadmium concentrations when laboratory XRF zinc concentrations are given (Eq. 2.3). An example calculation is also included.

$$z = 0.7727x + 181.48 \quad (\text{Eq.2.1}) \text{ From Figure 2.11}$$

$$[Cd] = 0.0065x + 1.8674 \quad (\text{Eq.2.2}) \text{ From Figure 2.12}$$

$$[Cd] = 0.00841z + 0.34078 \quad (\text{Eq.2.3})$$

Where:

z = Laboratory XRFs zinc concentrations (mg/kg)

x = ICP zinc concentrations (mg/kg)

$[Cd]$ = Predicted cadmium concentrations (mg/kg)

Example calculation:

Eq.2.1
$$z = 0.7727x + 181.48$$

Solve for x :
$$x = \frac{z - 181.48}{0.7727}$$

Substitute into Eq. 2.2:
$$[Cd] = 0.0065 \left(\frac{z - 181.48}{0.7727} \right) + 1.8674$$

Simplify:
$$[Cd] = 0.00841z + 0.34078$$

This relationship provides a useful tool for researchers using the XRFs in this mining site. Because ICP-OES and laboratory XRFs readings for zinc provide a statistically significant trend, the XRFs laboratory zinc concentrations can be used to predict a cadmium concentration for the same sample. Having this tool can shorten analysis times and costs for cadmium as cadmium concentrations in the soil can be predicted before analyzing samples in the ICP-OES. Equation 2.3 was applied to the zinc laboratory XRFs readings also read by the ICP to determine estimated cadmium concentrations.

Figure 2.15 plots the estimated cadmium concentrations to the actual cadmium concentrations determined by ICP analysis.

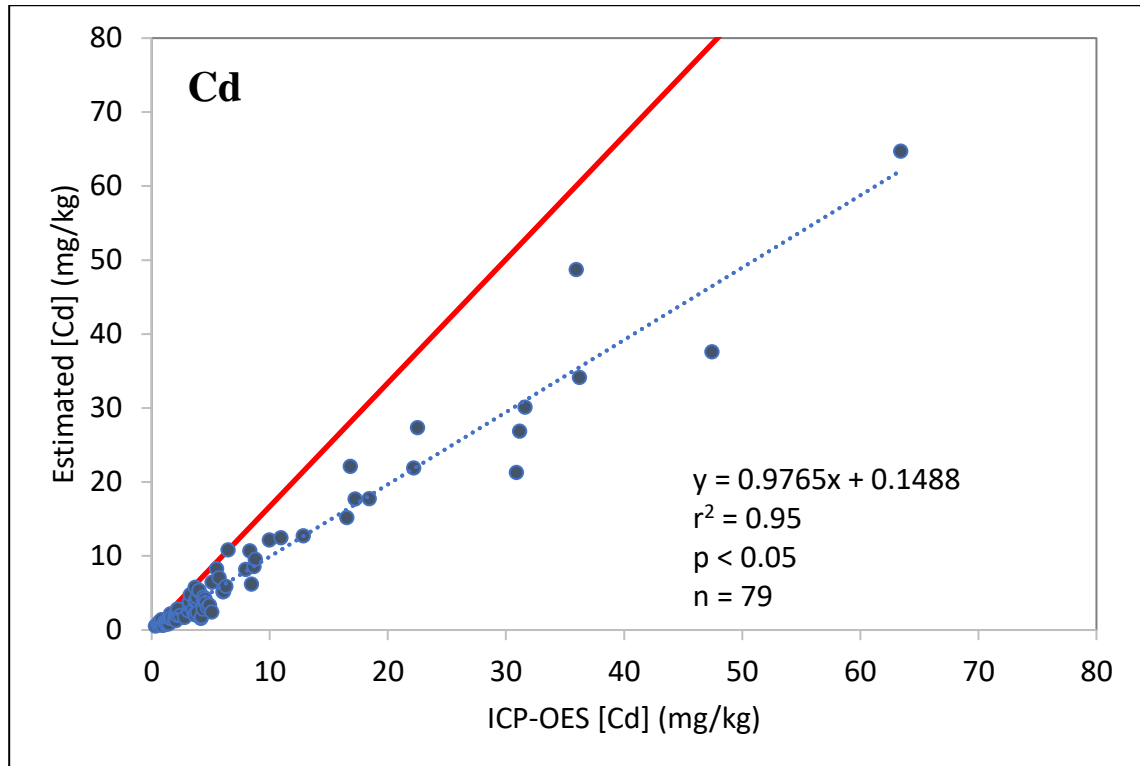


Figure 2.15: Estimated cadmium and ICP cadmium values

2.4 Conclusions

In situ analysis of 384 soil samples showed that XRFs readings in *in situ* environments showed statistically different results for lead or zinc when compared to XRFs readings on samples that were dried and sieved. *In situ* analysis on samples with less than 10% moisture content yielded statistical similarities to laboratory XRFs concentrations for lead and zinc where the samples were homogenized, dried and sieved. The hypothesis that *in situ* XRFs readings with moisture contents exceeding 20% will report lesser metals concentrations than laboratory XRFs readings where the soil was homogenized, dried, and sieved was accepted as there was no statistical

relationship between lead or zinc values within this moisture content range. Organic content less than 10% was found to have no effect on laboratory XRFs and ICP lead concentrations, however organic contents greater than 10% caused underreporting of lead XRFs values when compared to ICP concentrations. When comparing ICP and laboratory XRFs concentrations, results found that concentrations were statistically similar for lead, but statistically different for zinc. The hypothesis that homogenized, dried, and sieved soils analyzed by the XRFs in the laboratory will yield concentrations not statistically different from ICP-OES metals concentrations was therefore accepted for lead but rejected for zinc. Regression analysis for lead and zinc yielded statistically significant relationships lead ($r^2=0.98$) and zinc ($r^2=0.92$). The regression equations for zinc and cadmium allowed the estimation of cadmium from zinc XRFs values. The estimated XRFs cadmium and ICP cadmium concentrations yielded a statistically significant relationship ($r^2=0.95$).

The results of this study suggest that for the most accurate results for *in situ* measurements compared to laboratory XRFs readings, *in situ* XRFs readings should be taken on dry surfaces clear of debris. If *in situ* soil samples are wet, samples should be prepared before XRFs analysis by drying and sieving the soils. Soil samples with greater than 10% organic content report inaccurate XRFs lead concentrations and therefore, should be analyzed by the ICP. Future researchers should also be aware of the overreporting of laboratory XRFs zinc concentrations when compared to ICP values. This research shows that XRFs may not be suited for *in situ* soil analysis due to variability in field conditions and on the determination of lead in soils with elevated organic

contents. Additional sample preparation (drying and sieving), which slows down the data generation process and negates one of the benefits from this device, is necessary to generate reliable values. Although XRFs sample times are much faster and cheaper than ICP analysis, the XRFs may only operate as a screening tool for zinc due to overreporting. Additionally, understanding how different sample conditions affect the accuracy of XRFs readings will aid future analysts in yielding the most comparable results to the ICP (Pyle and Nocerino, 1996; Melquiades and Appoloni, 2004; Kalnicky and Singhvi, 2001; Ge et al., 2005; Crooks et al., 2006; Lin, 2009; Löwemark et al., 2011; Bastos et al., 2012; McComb et al., 2014; Schneider et al., 2016; Sahraoui and Hachicha, 2017; Ravansari and Lemke, 2018).

Chapter III: Geospatial Distribution of Trace Metals in Soils of a Mining Impacted Agricultural Watershed

3.1 Introduction

Mining is a major source of trace metals pollution to soils and their impacts have gained global attention due to the extensive adverse effects to both the environmental and human health (ATSDR, 2005; ATSDR, 2007; ATSDR, 2012; Qin et al., 2012; Lee et al., 2016; Kim and Choi, 2017; Wang and Nie, 2017). Although natural levels of trace metals in soils are found in the environment, elevated concentrations of trace metals from mining can cause significant damage to surrounding ecosystems (Kabata-Pendias and Mukherjee, 2007; Tchounwou et al., 2012; Alloway, 2012; Kim and Choi, 2017; Wang and Nie, 2017). Metals toxicity in animals and plants has been documented in areas close to mines and risks to human health have been studied (USACHPPM, 1995; Sileo et al., 2003; French and Mateo, 2005; White, 2006; Zota et al., 2011; Soto-Ríos et al., 2017). Phelps and Mcbee (2009) found that rodents residing in a trace metal contaminated habitat had reduced species diversity, richness, and evenness when compared to reference sites. Decreased motor function and low body weight were observed in wild birds and waterfowl near the Tar Creek Superfund Site (Sileo et al., 2003; French and Mateo, 2005). Children living near mining sites contaminated with lead were found to have elevated blood lead levels which can lead to poor academic performance and cognitive disorders (Zota et al., 2011; Soto-Ríos et al., 2017). Because of the human health and ecological risks associated with exposure to trace metal pollution in soils, researchers stress the need for investigation and quantification of soil trace metals

within potentially impacted areas (Imperato et al., 2003; Juracek and Drake, 2016; Wang and Nie, 2017; Yang et al., 2018).

3.1.1 Determination of Soil Metals Concentrations

Inductively coupled plasma-optical emission spectrometry (ICP-OES), inductively coupled plasma-mass spectrometry (ICP-MS), atomic absorption spectrophotometry (AAS), and atomic fluorescence spectrometry (AFS) are effective methods for the determination of trace metals in both soil and water (Pyle and Nocerino, 1996; Bettinelli et al., 2000; Sahraoui and Hachicha, 2017). These methods however, require acid digestion of the sample which is both time consuming and costly, and destroys the sample (Pyle and Nocerino, 1996; Bettinelli et al., 2000; Sahraoui and Hachicha, 2017; Taha, 2017). Because of the time consuming, costly and destructive nature of these methods, researchers have used X-ray fluorescence spectroscopy (XRFS) technologies as an alternative (Wilson et al., 1995; Pyle and Nocerino, 1996; Datin and Cates, 2002; Reames and Lance, 2002; Ge et al., 2005; Kilbride et al., 2006; Binstock et al., 2008; Coronel et al., 2014; McComb et al., 2014; Rouillon and Taylor, 2016; Sahraoui and Hachicha, 2016; Schneider et al., 2016; Taha, 2017). These technologies allow for quick analysis (often less than 90 seconds), are cost-effective when compared to wet chemistry methods, and are nondestructive (Kalnicky and Singhvi, 2001; Melquiades and Appoloni, 2004; Bastos et al., 2012; Shand and Wendler, 2014; Lee et al., 2016; Kim and Choi, 2017; Ravansari and Lemke, 2018). Inaccuracies in XRFS data have been reported and researchers recommend that XRFS data be validated by inductively coupled plasma-optical emission spectrometry (ICP-OES) or other EPA approved wet

chemistry analyses, especially if trace metals concentrations are to be used for decision making (Wilson et al., 1995; Ge et al., 2005; Crooks et al., 2006; Kilbride et al., 2006; Bastos et al., 2012; Schneider et al., 2016; Sahraoui and Hachicha, 2016; Sahraoui and Hachicha, 2017).

A study completed by Ge et al., (2005) found that elevated soil moisture (<20%) content caused under-reporting of elemental concentrations by XRFs. Ravansari and Lemke (2018) found that XRFs concentration readings decreased with increasing organic content for all elements analyzed (As, Cr, Cu, Fe, Mn, Pb, Rb, Sr, Th, Ti, V, Zn, and Zr). In a laboratory XRFs/ICP-OES comparison study completed by Sahraoui and Hachicha (2016) on soils surrounding a mine in Tunisia, t-tests showed no statistical differences in lead concentrations between the two methods but showed significant differences in zinc and cadmium concentrations. Wilson et al. (1995) observed that XRFs zinc readings reported higher values than results obtained by the ICP, however did not provide an explanation as to why.

3.1.2 Trace Metals in Soils and Sediments

Trace metals contamination from mining operations may be relatively easily dispersed and can cause widespread problems (Macklin et al., 2006; Lee et al., 2016; Kim and Choi, 2017). Movement of the contaminated material by fluvial processes, wind, or even by humans can cause contamination of otherwise unimpacted areas (Lewin and Macklin, 1987; Swennen et al., 1994; Jung and Thornton, 1996; Miller, 1997). Storm water runoff can carry the smallest particles, which often contain the greatest

concentrations, downstream and deposit them in stream terraces or beds (Miller, 1997; Datin and Cates, 2002). Flooding can cause remobilization of metals and can deposit trace metals in floodplain and upland areas outside of the stream banks (Horowitz, 1991; Swennen et al., 1994; Miller, 1997). Lewin and Macklin, (1987) concluded that flood waters transporting trace metals will leave a fine, thin layer of suspended metals contamination over the horizontal reach of the flood plain. Swennen et al., (1994) and Dennis et al., (2009) found that floodplains within 200 m of a river were highly contaminated from upstream mining wastes. Brewer and Taylor (1997) observed that the distribution of trace metals within the floodplain and stream terraces is “spatially complex”, with vertical and lateral channel instability, flood frequency and magnitude, and terrace height, all affecting deposition.

Although metals concentrations have been found to decrease as distance from the source increases, concentrations that exceed remedial limits or pose risk to human health have been found beyond the defined borders of contaminated sites (Jung and Thornton, 1996; Maxfield and McBratney, 2001; Quin et al., 2012; Avila et al., 2012; USFWS, 2013; Lee et al., 2016). A study within the Tar Creek Superfund Site in northeastern Oklahoma found that Pb, Zn, and Cd exceeded EPA action level concentrations 600 feet outside of the site boundaries (USFWS, 2013). Jung and Thornton (1996) found that vegetation grown outside of mine boundaries posed significant risk to human health.

3.1.3 Spatial Distribution of Trace Metals

Understanding the spatial distribution of metals in these contaminated areas is important to reduce associated health risks and to apply proper remediation or management to these areas (Zhang et al., 2008; Juracek and Drake, 2016; Kim and Choi, 2017). Because many areas near mining operations contain widespread contamination, understanding the spatial variation of metals concentrations can be difficult (Dennis et al., 2009; Bird et al., 2010; Lee et al., 2016; Juracek and Drake, 2016; Kim and Choi, 2017). To study the spatial variability, many researchers generate spatial perspectives of trace metals distributions using geographical information systems (GIS) software combined with geostatistical methods (Imperato et al., 2003; Cheng et al., 2007; Zhang et al., 2008; Quin et al., 2012; Avila et al., 2012; Lee et al., 2016; Kim and Choi, 2017). Geostatistical methods are used extensively in environmental fields for spatial estimation as they help to understand and predict the spatial distribution of trace metals where no data have been collected (Blöschl, 2002; Zhang et al., 2008; Kim and Choi, 2017; Krivoruchko, 2017). GIS tools apply these methods and allow for analysis, interpretation, and presentation of spatial data (Burrough, 2001). Extensive sampling of an area can be costly, time consuming, and unrealistic, therefore interpolation techniques such as kriging and natural neighbor, which provide an estimation of a variable in an unsampled location, have been applied extensively in trace metals contaminated soils research (Steiger et al., 1997; Cattle et al., 2002; Imperato et al., 2003; Cheng et al., 2007; Zhang et al., 2008; Quin et al., 2012; Avila et al., 2012; Lee et al., 2016). Interpolation techniques provide a continuous map outlining the estimated concentration

distributions of metals and can help identify patterns or sources of contamination (Imperato et al., 2003; Cheng et al., 2007; Zhang et al., 2008; Quin et al., 2012; Avila et al., 2012; Lee et al., 2016; Wang and Nie, 2017). Geostatistics can also identify statistically significant hotspots, spatial clusters, and spatial outliers (Zhang et al., 2008; McClintock, 2012; Kim and Choi, 2017).

Two parameters for the measurement of spatial autocorrelation are the local Moran's I index and Getis-Ord G_i^* (Zhang et al., 2008; Kim and Choi, 2017). Both autocorrelation methods use a comparison of nearest neighbors to identify areas of interest (Zhang et al., 2008; Kim and Choi, 2017). Kim and Choi (2017) tested the use of the Getis-Ord G_i^* statistic on soil samples at an abandoned mine in Korea and determined that the statistical method was accurate in predicting hot spots in soils. McClintock (2012) used the Getis-Ord G_i^* statistic to determine lead hot spots in soils in residential areas in Oakland, California and observed more lead hotspots in the oldest and poorest communities than newer and wealthier areas. The local Moran's I statistic was applied by Zhang et al., (2008) to determine lead hotspots in urban soils and found that although the statistic was effective of identifying hotspots, extreme values affected results by indicating larger areas of high value spatial clusters.

The overlay of site specific data such as topography or geographical maps can be applied to help identify relationships between spatial datasets. Imperato et al. (2003), found that copper accumulated around railways in Naples, Italy and that concentration increases of Cu, Pb, and Zn since 1974 were greatest near major roadways suggesting that vehicle emissions were the source. In studies analyzing trace metals contamination

in soils near mining operations, Quin et al., (2012) and Avila et al., (2012), determined that wind direction and topography were major influences on metals dispersion downwind and downgradient.

3.1.4 Contaminants of Primary Concern

Elevated concentrations of lead, zinc, and cadmium from mining wastes have been found to be toxic to organisms and humans and have been identified as Contaminants of Primary Concern (COPC) by the United States Environmental Protection Agency (USEPA) (Żukowska and Biziuk, 2008; Kabata-Pendias and Mukherjee, 2007; USEPA, 2008; Zota et al., 2011). The COPC are designated hazardous substances by the USEPA and are listed as such in the Code of Federal Regulations 40 C.F.R §116.4 and are also listed as toxic pollutants in 40 C.F.R §401.15 (USFWS, 2013). Exposure to COPC pose potential ecological risk and have been shown to cause adverse biological effects (USEPA, 2010; USFWS, 2013; ATSDR, 2005). The USEPA defines COPC within the Tar Creek Superfund Site as “chemical substances found at the site that the EPA has determined pose an unacceptable risk to human health or the environment” (USEPA, 2017a). At this site, lead, zinc, and cadmium are the COPC at Tar Creek (USEPA, 2010; USFWS, 2013; Dames and Moore, 1993).

The two objectives of this study were to evaluate soil lead, zinc, and cadmium concentrations in stream terraces and upland environments of a mining impacted agricultural watershed and to generate a spatial perspective of the distribution of lead, zinc, and cadmium concentrations. The three related hypotheses were: 1) the stream

branch nearest the mining influence will have greater metals concentrations than the stream branch further away from the mining influence when comparing samples collected at equal distances upstream from the creek confluence, 2) sampling locations hydrologically closer to mining influences will have soil lead, zinc, and cadmium concentrations exceeding background levels, and 3) upland lead, zinc, and cadmium soil concentrations will be lesser than concentrations present in stream terraces.

3.2 Methods

3.2.1 Site Description

The study area is situated within the Elm Creek watershed located in Ottawa County, Oklahoma. The area is between 36 58'20.40" N and 36 53'28.50" N longitudes and 94 57'16.70" W and 94 53'25.40" W latitudes. The Elm Creek watershed is impacted by trace metal contamination from the Tar Creek Superfund Site, which is the Oklahoma portion of the Tri-State Lead-Zinc Mining District (TSMD) (USFWS, 2013; Nairn, 2014a). Extensive mining operations for zinc and lead, beginning in the 1890s and continuing until the 1970s, left extensive trace metal contamination on the surface which remains exposed to this day (USEPA, 1997; Datin and Cates, 2002; White, 2006; USEPA, 2008; Andrews, 2011; USFWS, 2013). Trace metals concentrations of the Tar Creek Superfund Site tailings, known as "chat", can exceed 2,200 mg/kg lead, 34,400 mg/kg zinc, and 96 mg/kg cadmium (Datin and Cates, 2002). Soils over 600 feet away from delineated Superfund boundaries have been found to exceed the Remedial Goals (RGs) for lead, zinc, and cadmium (USFWS, 2013). The USEPA determined enforceable RGs for transition soil metals concentrations within the areas of Ottawa County impacted by

mining wastes under Operable Unit 4 (USEPA, 2008). These goals were selected with the intent to decrease human exposure to COPCs from soil (USEPA, 2008). The USEPA-selected remedial goals for transition zone soils for lead, zinc, and cadmium are 500 mg/kg, 1,100 mg/kg, and 10 mg/kg, respectively (USEPA, 2008). If the soil trace metal concentrations exceed the values listed above, the USEPA Record of Decision calls for the excavation of the contaminated soil down to native soils (USEPA, 2008).

Along with the TSMD RGs, non-enforceable TSMD-specific Sediment Quality Guidelines (SQGs) address threshold concentrations for stream and lake sediments. Ingersoll et al., (2009) determined SQGs from probable effect concentrations (PECs) in sediments within Grand Lake of the Cherokees into which TSMD waters flow. These concentrations are 150 mg/kg for lead, 2,100 mg/kg for zinc, and 11.1 mg/kg for cadmium. At these concentrations, adverse health effects (survival or growth) are likely to occur in organisms (MacDonald et al., 2000; Ingersoll et al., 2009). Remedial Goals (RGs) and Sediment Quality Guideline (SQG) concentrations were used as threshold concentrations to identify areas in need of focus, for lead, zinc, and cadmium within this watershed.

The Elm Creek watershed extends into portions of the Tar Creek Superfund Site. Elm Creek consist of two main branches (east and west) that join to form the main stem stream. The east branch of Elm Creek originates within the Tar Creek Superfund Site and flows south a total distance of 10.5 kilometers before its confluence with the West branch. The source of the west branch of Elm Creek is located outside of the Tar Creek Superfund Site and flows a total distance of 12 km before converging with the east

branch. After the confluence of both branches, Elm Creek extends six and a half kilometers before entering the Neosho River (Figure 3.1). Within this watershed are a series of properties owned by the Grand River Dam Authority, known as the Neosho Bottoms. The confluence of Elm Creek is at the most northern point within these properties and the main stem flows directly through them. The extent of the trace metals contamination in this area is of concern due to the probability of trace metals contaminated material to be transported by fluvial processes (Miller, 1997). Access to these properties was granted by the GRDA to sample the soils in both the uplands and creek terraces. The GRDA properties consist of an approximately 7.2 square kilometer area.

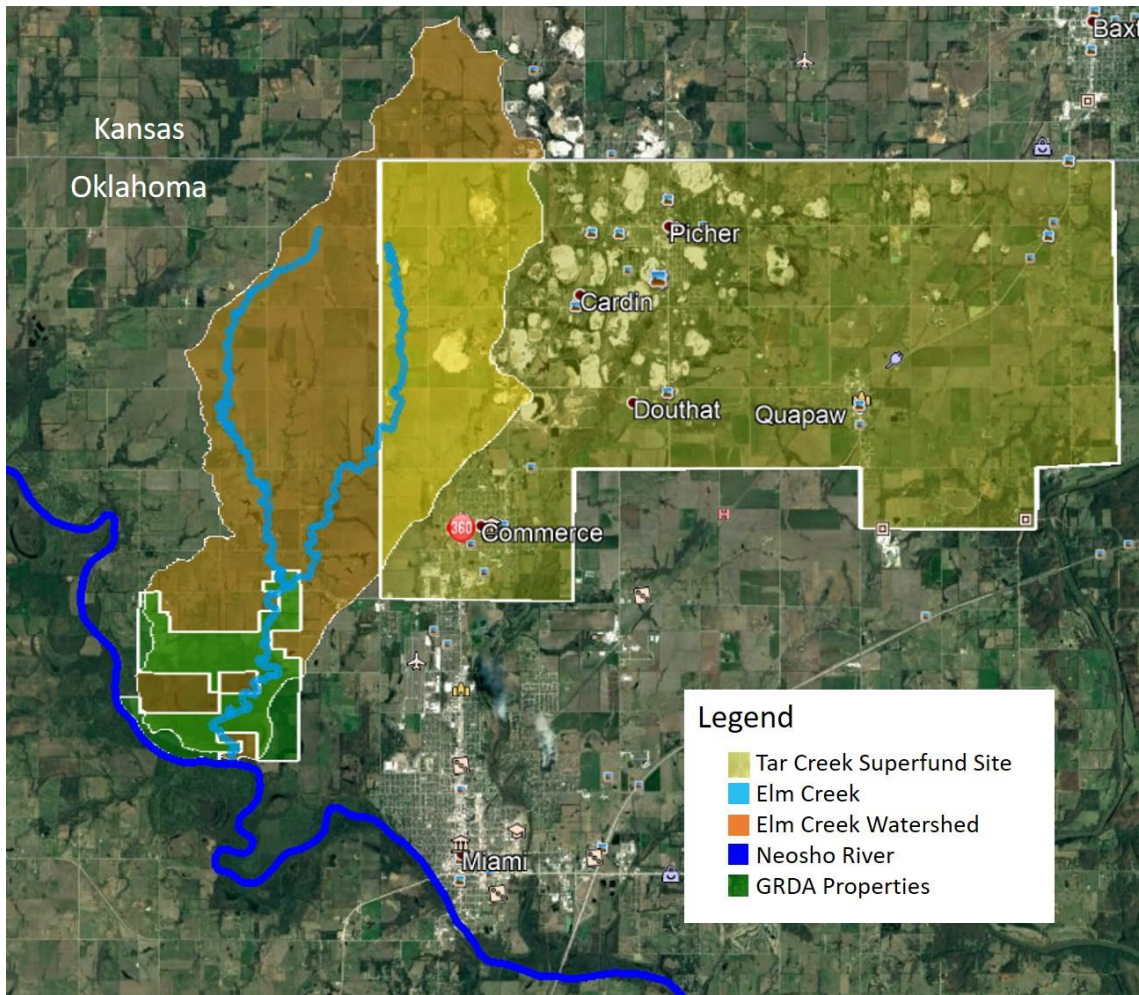


Figure 3.1: The GRDA-owned properties (highlighted in green) proximity to the Neosho River, Elm Creek and The Tar Creek Superfund Site

3.2.2 Determination of Minimum Sample Size

The minimum number of soil samples necessary to meet a confidence level of 80%, power of 90% and minimum relative detectable difference of 20% was calculated using Equation 3.1 (USEPA, 1991; Datin and Cates, 2002). These statistical parameters were selected to match the statistical values used by Datin and Cates (2002) in determining a sample size for the analysis of chat within the Tar Creek Superfund Site. The same statistical parameters from Datin and Cates (2002) were applied to this work as both take place in the same area of contamination.

$$n > 112.8(CV)^2 + 0.354 \quad (\text{Eq. 3.1})$$

Where:

- n = required number of samples
- CV = coefficient of variation = (s/x)
- s = standard deviation
- x = mean

Using an XRF dataset completed over a subset of these locations in 2014, the minimum number of samples necessary to meet the above statistical performance objectives for the Elm Creek riparian zone and upland transects are 31 and 276 samples, respectively (Nairn, 2014b). The summary statistics from this dataset for the Elm Creek riparian sampling locations are presented in Table 3.1 and the summary statistics for the upland sampling locations are presented in Table 3.2.

Table 3.1: Summary statistics for Elm Creek riparian area soil lead, zinc, and cadmium concentrations (mg/kg) from Nairn (2014b)

	Lead	Zinc	Cadmium
# analyses	20	20	8
Mean	125	1010	21.0
Median	47.7	652	19.2
Maximum	774	4500	40.0
Minimum	9.07	45.5	9.47
Standard Deviation	196	1280	10.7

Table 3.2: Summary statistics for Elm Creek upland soil lead, zinc, and cadmium concentrations (mg/kg) from Nairn (2014b)

	Lead	Zinc	Cadmium
# analyses	23	23	1
Mean	17.6	102	16.8
Median	16.8	87.7	16.8
Maximum	45.0	280	16.8
Minimum	4.60	48.2	16.8
Standard Deviation	7.63	53.4	

3.2.3 Sampling Locations

Soil samples were obtained from the Elm Creek riparian zone throughout the watershed and the upland environments of GRDA-owned properties. Within Elm Creek riparia, samples were taken from the streambank terraces on both the left and right banks defined when facing upstream. The top of bank, primary terrace, and lower terrace were each sampled if present at each location (Figure 3.2).



Figure 3.2: Image of Elm Creek, located in Ottawa County, Oklahoma, in October 2016 with the stream terraces clearly identified

Fifteen locations were selected as sampling sites along Elm Creek to satisfy the minimum sample size for Elm Creek riparian zones. Seven sites were located at road crossings in the northern stretch of the creek (at locations not owned by GRDA but accessible to the public via county road crossings) and the remaining eight sampling sites were located within the GRDA-owned properties. Figure 3.3 highlights the Elm Creek

sampling locations for the Elm Creek riparian zone inside and outside of the GRDA-owned properties.

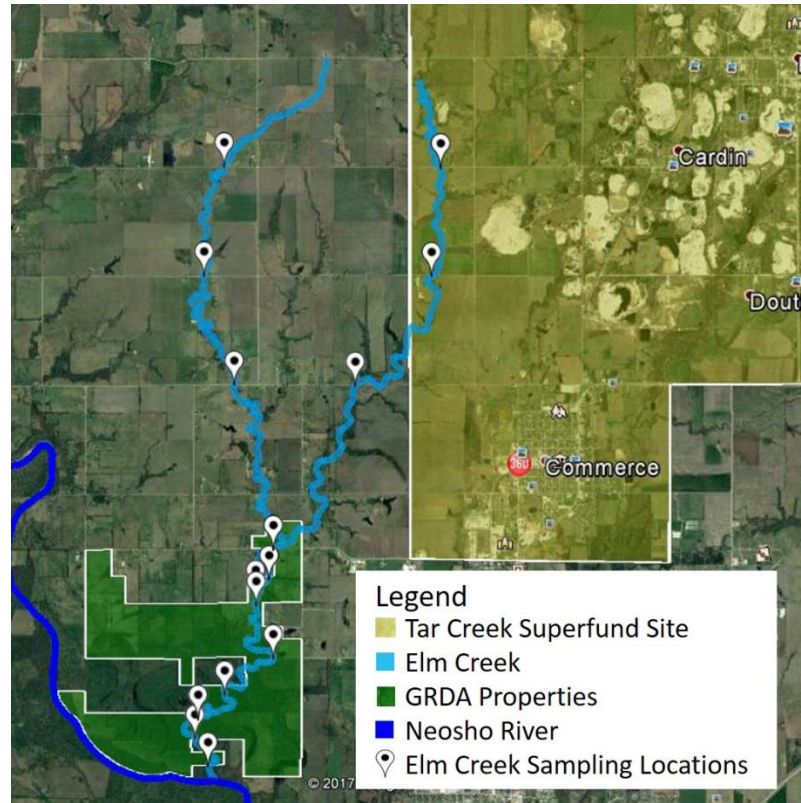


Figure 3.3: Elm Creek riparian zone sampling sites

Two hundred and seventy-eight samples were obtained from the upland environments within the area of interest to meet the minimum sample size requirements. A series of transects that intersect or run parallel to Elm Creek were developed to generate an effective representation of soil concentrations at different distances from the stream (Figure 3.4). The total length of all the transects combined extends just over 20 kilometers (13 miles). Soil samples were taken approximately every 110 m (360 feet) along the transects to ensure the minimum number of samples were collected within the uplands. Sampling locations were determined in advance of field

sampling and a global positioning system (GPS) was used in the field to locate sampling spots.

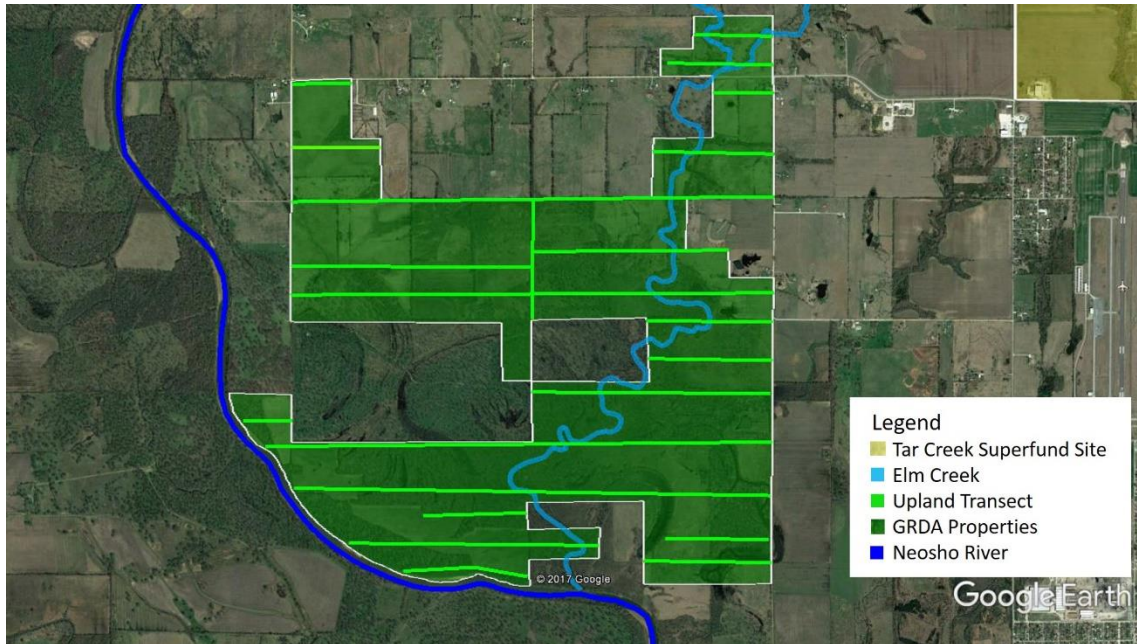


Figure 3.4: Developed upland transect locations within the GRDA-owned properties

3.2.4 Soil Sample Collection

Soil sampling and collection took place starting in January 2017 and continued through October 2017. A field portable Thermo-Fisher Scientific Niton XL3t GOLDD+ XRFS was used *in situ* within the GRDA-owned properties and at road crossings on both the east and west branches of Elm Creek for analysis of metals concentrations following USEPA Method 6200. This device was used for “rapid field screening” to obtain *in situ* metals concentrations (USEPA, 2007c). The “All Geo” mode, which includes both the “Mining mode” (used for heavier elements) and “Soils mode” (used for lighter elements), was used to analyze samples. Soil samples were collected using a stainless-steel shovel, excavating a 13 cm by 13 cm by 10 cm deep sample. Samples were placed

in air-tight plastic sample bags immediately upon collection. A GPS was used to record the latitude and longitude of each sample location. Samples at road crossing were taken at spots furthest from the road, without trespassing onto private property. Samples were transported back to the laboratory for XRF analysis. Although *in situ* XRF data were collected, they were not used in this chapter.

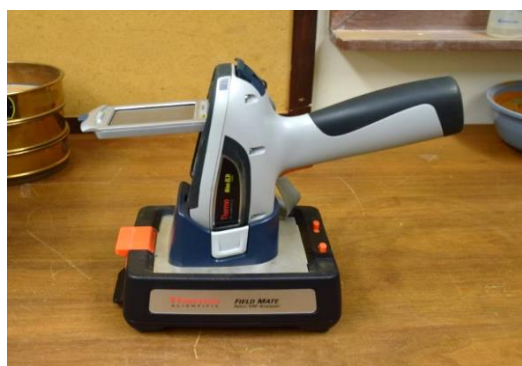
3.2.5 Laboratory Sample Analysis

Laboratory XRF analysis of the soil samples took place in the Center for Restoration of Ecosystems and Watersheds (CREW) laboratories, located in Carson Engineering Center at the University of Oklahoma. Soil samples were homogenized by hand by breaking apart larger soil clods and then air dried. After the samples air dried, they were sieved to less than the #60 soil fraction ($< 250 \mu\text{m}$). Samples were sieved using a W.S. Tyler™ RO-TAP™ RX-94 electric sieve shaker for a minimum of three minutes (consisting of 278 ± 10 oscillations per minute and 150 ± 10 taps per minute with a 2.5 kg hammer) and sieves were cleaned after every sample using course and soft brushes with the pan wiped down with KimWipes. If dried samples were in tight clumps, the aggregates were crushed using a mortar and pestle that was cleaned after every use with KimWipes. All sieves, brushes, the mortar and pestle, and stainless-steel pans were washed and air dried after each day of sample analysis to minimize cross contamination of soil samples. The soil fraction passing the #60 sieve was used for metals concentration analyses using a field portable XRF analyzer.

Air dried soil from the < #60 soil fraction were packed into circular XRF sample cups for each sample and analyzed with the XRF operated via personal computer in a shielded, Field Mate test stand for a total run time of 60 seconds in the All Geo mode following USEPA Method 6200. The XRF sample cups were 32 mm in diameter and covered with 4.0 μm polypropylene X-ray film (Figure 3.5). Enough soil was added to the cups to ensure that the full film surface was covered, and glass wool was added into the remaining cup space to keep the sample pressed against the film window. The Field Mate test stand allows for hands free and stable analysis by locking the XRF into place with the nose of the XRF pointing downward at a sample cup film surface (Figure 3.6 (a)) (Thermo Scientific, 2010). The circular sample cup is securely fastened in the Field Mate test stand while the XRF reading takes place (Figure 3.6 (b)). The stand also shields the operator from scattered X-rays. A minimum of one in every 10 samples was a duplicate, following USEPA guidelines for QA/QC.



Figure 3.5: Packed circular XRF soil sample cups lined with polypropylene X-ray film for analysis



(a)



(b)

Figure 3.6: (a) Thermo Scientific Field Mate test stand is used to lock in the Thermo-Fisher Scientific Niton XL3t GOLDD+ XRF with the nose of the device pointing towards the sample cup; (b) The Field Mate holds the circular sample cup within the base

3.2.5.1 ICP-OES Analysis

ICP-OES analyses were conducted on the air-dried and homogenized soil fraction passing the #60 sieve ($< 250 \mu\text{m}$). A total of 79 soil samples (20%) were hot acid microwave digested with concentrated HNO_3 following USEPA Method 3051a (USEPA, 2007b) and then underwent analysis by ICP-OES following USEPA Method 6010c (USEPA, 2007a). Concentrations obtained by the XRF that exceeded the RGs and SQGs for samples within the GRDA properties were validated by ICP-OES analysis and part of the total dataset.

3.2.6 Estimation of Cadmium

Cadmium concentrations were not generated by the XRFs and were therefore predicted from zinc XRFs values. The combination of the linear relationship between laboratory XRFs zinc readings and ICP readings with the linear relationship between ICP cadmium and zinc determined in Chapter 2 of this work allowed for the accurate estimation of cadmium concentrations when laboratory XRFs zinc concentrations were given. Equation 3.2 was applied to XRFs zinc concentrations to estimate cadmium.

$$[Cd] = 0.00841z + 0.34078 \quad (\text{Eq.3.2})$$

Where:

$$\begin{aligned} z &= \text{Laboratory XRFs zinc concentrations (mg/kg)} \\ [Cd] &= \text{Predicted cadmium concentrations (mg/kg)} \end{aligned}$$

Note that because cadmium concentrations were determined using this relationship, all XRFs cadmium concentrations used in this work are considered “estimated”, unless stated as ICP cadmium concentrations.

3.2.7 Statistical Analysis

Statistical analyses were performed on each of the datasets generated and analyzed with Microsoft Excel and IBM SPSS Statistics software. The Kolmogorov-Smirnov and Shapiro-Wilk tests were used to determine the normality of the dataset. All datasets were non-parametric, therefore non-parametric tests were used for all statistical analysis. The Wilcoxon signed rank test was used to determine statistical similarities or differences for datasets containing two related samples. The Friedman test was used to determine if differences existed between several related samples. The

Mann-Whitney U test and the Kruskal-Wallis Test were used for comparisons of two-independent samples and several independent samples, respectively. The null hypothesis for each non-parametric test was that the distributions between variables are not different. A p-value greater than 0.05 means acceptance of the null hypothesis. The 95% confidence interval was used for all analysis.

3.2.8 Geospatial Analysis

ArcGIS Pro software was used for the creation of interpolating maps and geostatistical analysis for the upland soil concentrations. Spatial maps outlining the concentration distributions of metals from the XRFS datasets were created using inverse distance weighted (IDW) and ordinary kriging interpolation methods in ArcGIS Pro. The IDW function interprets the values of unsampled locations by averaging the values of nearest neighbors to create a continuous surface model (Cheng et al., 2006; Avila, 2013; ESRI, 2016). Points closer to the spot of interest have a more influence on the averaging process. Although the exact algorithm equation used by the software is not given, the formula follows that of a weighted moving average. The output from this function provides a visual “heatmap”. The strength of the relationship between weighting and distance is determined by the input “power”. A power of 0 means influence of points will not decrease with distance, and as the power increases, further points have less influence. The default power of two was used in this analysis. Spatial maps outlining the concentration distributions of metals were also created using ordinary kriging in ArcGIS Pro which also provide a heatmap of concentrations. Kriging and IDW interpolation are similar, however IDW interpolation is based on local deterministic

methods while kriging uses weights from a semi-variogram which is dependent on the spatial structure of the data rather than on actual values (Arun, 2013; Bhunia et al., 2016; Shit et al., 2016; Kim and Choi, 2017). IDW maps are guaranteed to reflect the values from the input data while ordinary kriging maps reduce bias from input values (Arun, 2013; Bhunia et al., 2016; Shit et al., 2016). Both methods have been used extensively to map soils in trace metals contaminated areas and are considered effective for soil concentration mapping (Steiger et al., 1997; Cattle et al., 2002; Cheng et al., 2006; Quin et al., 2012; Shit et al., 2016). Maps using both methods were generated to allow for the best understanding of the concentration distributions in the uplands.

In this study, statistically significant spatial clusters and outliers were determined using the local Moran's I and Getis-Ord Gi* statistic, using a built-in function in ArcGIS pro. The local Moran's I compares one point or concentration to its nearest neighbors within a radius. All the points that fall within the radius are used in the comparison analysis. The local Moran's I index is defined by:

$$I_i = \frac{x_i - \bar{X}}{\sigma^2} \sum_{j=1, j \neq i}^n [w_{ij}(x_j - \bar{X})] \quad \text{Eq. (3.3)}$$

Where x_i is the value of the attribute at location i , \bar{X} is the mean of the attributes with sample size n , σ^2 is the variance of the attributes, x_j is the value of the other variables at other locations, and w_{ij} is the spatial weight between feature i and j (Zhang et al., 2008; ESRI, 2017a). A positive I value identifies high-high clusters (areas with similarly high values near each other) which can be regarded as regional hot spots and low-low

clusters (areas with similarly low values near each other) which are designated as cold spots (Zhang et al., 2008). A negative I value identifies spatial outliers which consist of high-low outliers (points in which a high value is surrounded by low values) and a low-high outlier (points in which a low value is surrounded by high values). In soil pollution, Zhang et al., (2008) states that high-low outliers can be considered individual hotspots.

Hot spot analysis was also conducted using a z-score based on the Getis-Ord G_i^* statistic. The Getis-Ord G_i^* statistic also uses nearest neighbors to identify areas of interest and is defined by:

$$G_i^* = \frac{\sum_{j=i}^n w_{i,j} x_j - \bar{X} \sum_{j=1}^n w_{i,j}}{S \sqrt{\frac{[n \sum_{j=1}^n w_{i,j}^2 - (\sum_{j=1}^n w_{i,j})^2]}{n-1}}} \quad \text{Eq. (3.4)}$$

Where:

$$\bar{X} = \frac{\sum_{j=1}^n x_j}{n} \quad \text{Eq. (3.5)}$$

$$S = \sqrt{\frac{\sum_{j=1}^n x_j^2}{n} - (\bar{X})^2} \quad \text{Eq. (3.6)}$$

Where x_j is the attribute value for feature j , w_{ij} is the spatial weight between feature being analyzed and j , and n is the total number of features analyzed (ESRI, 2017b; Kim and Choi, 2017). The G_i^* statistic is a z-score and a larger and more positive z-score indicates hot spots, while lower and more negative z-scores indicate cold spots (Kim and Choi, 2017).

A distance band or “sphere of influence” of 300 m was selected for these analyses. This distance allowed for the analysis of multiple neighbors as it was longer than the sampling interval of 110 m which is recommended for these analyses (Zhang et al., 2008; ESRI, 2018). It is also the distance in which minimum point clustering occurred. The applied spatial relationship used the inverse distance method, which analyzes points within the specified distance with points further away from the point of interest having less of an impact while points closer have more influence (ESRI, 2017a). The local Moran’s I and Getis-Ord G_i^* both answer similar questions, however the major difference between methods is the Local Moran’s I does not include the value for the feature being analyzed in the calculations. The Getis-Ord G_i^* includes the feature being analyzed with all the nearest neighbors.

3.3 Results and Discussion

3.3.1 Elm Creek Riparian Concentration Distribution

The east branch and main stem of Elm Creek were analyzed for trace metals to observe how metals distribution changes with distance. The east branch was assumed to be the major contributor of trace metals due to its proximity to the Tar Creek Superfund Site. Figure 3.7 presents the sampling locations marked with each points distance (in kilometers) from the headwaters.

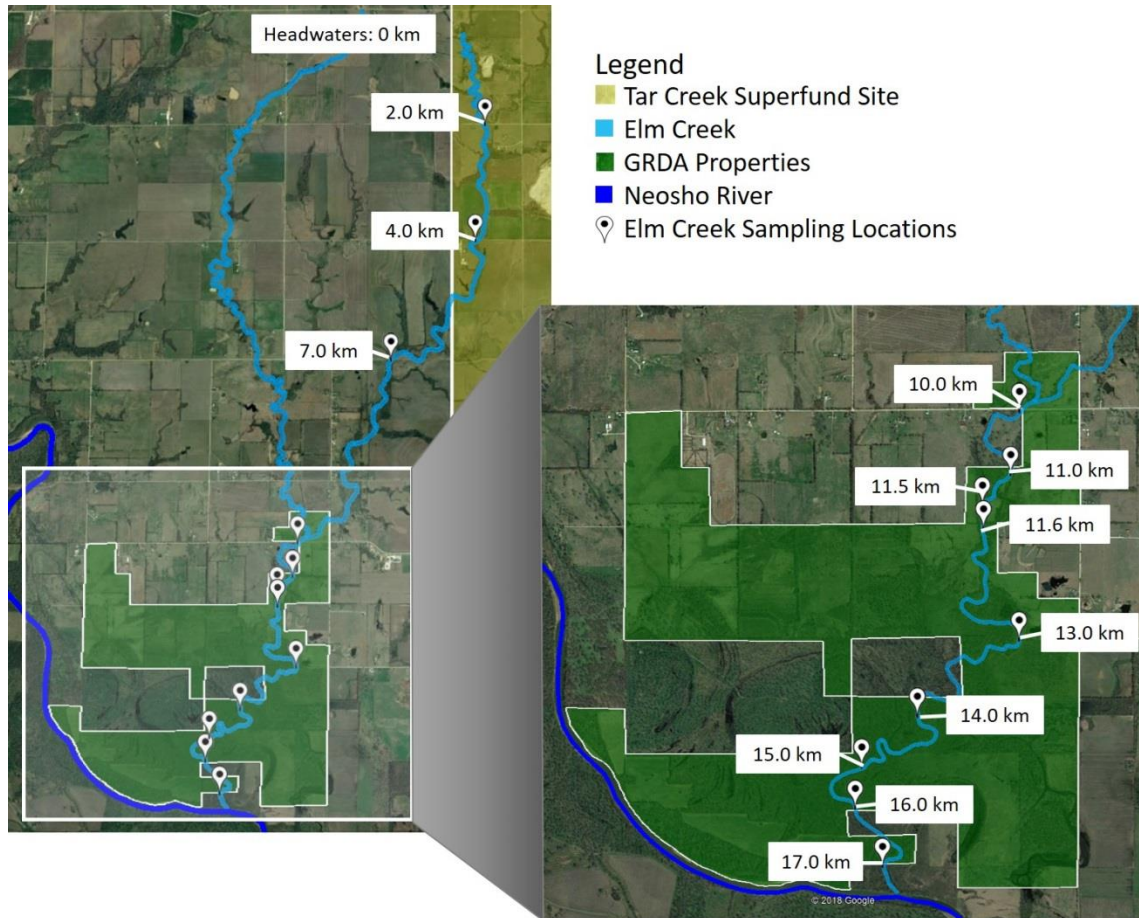


Figure 3.7: Elm Creek sampling locations marked with distances (in kilometers) from creek headwaters

Figures 3.8 through 3.13 present the concentration distributions of lead, zinc, and cadmium for each sampling location in the stream terraces (top of bank, primary terrace, and lower terrace) for the left and right banks. The x-axis distances correspond to the locations marked in Figure 3.7 with the first location (2.0 km) closest to the headwaters and moving downstream to the final sampling location (17.0 km). The SQG for each trace metal are also indicated in each figure. Left and right banks are denoted facing upstream or north in this case.

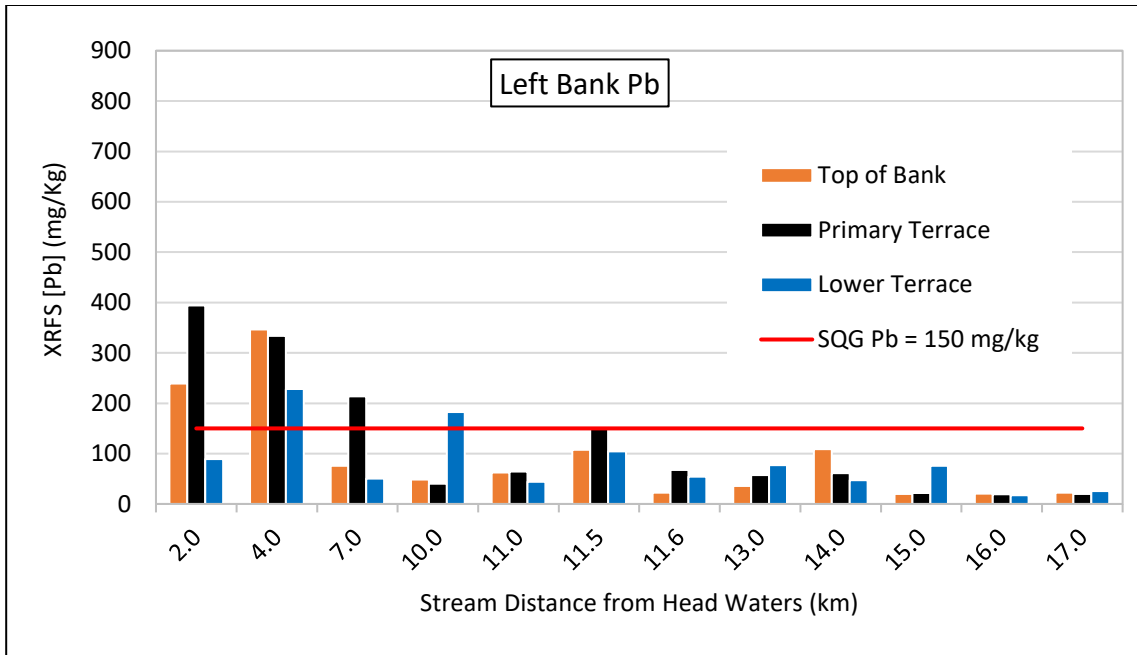


Figure 3.8: Elm Creek lead concentrations on the left bank for each sampling location starting closest to the headwaters and continuing downstream. Concentrations for the top of bank, primary terrace, and lower terrace are presented with the SQG for lead indicated in red.

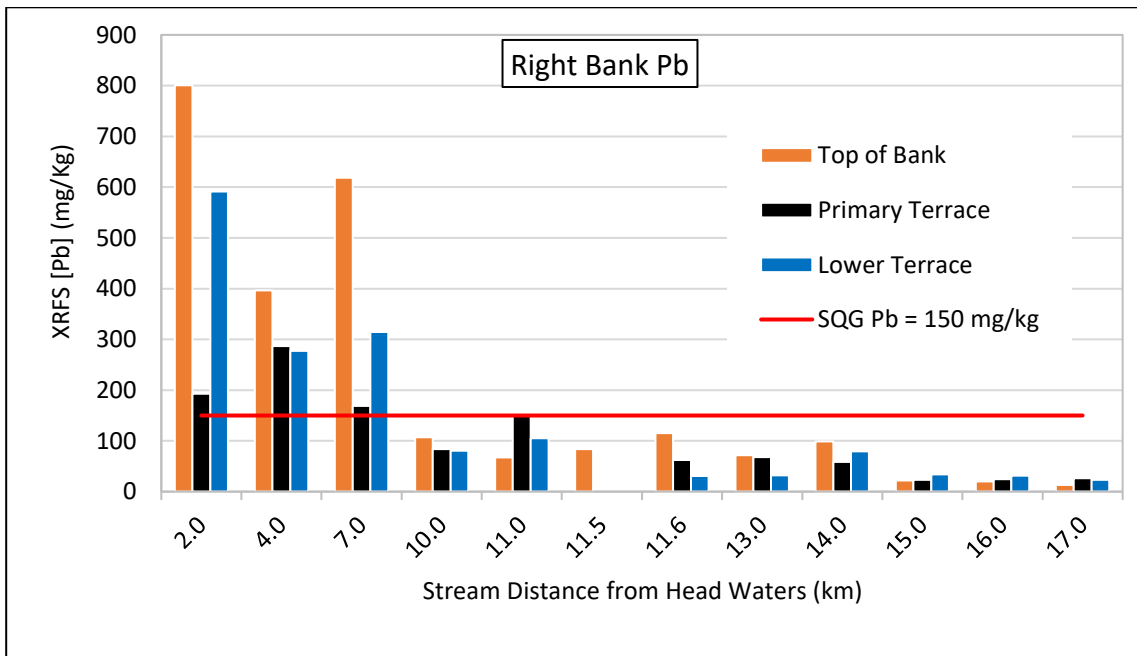


Figure 3.9: Elm Creek lead concentrations on the right bank for each sampling location starting closest to the headwaters and continuing downstream. Concentrations for the top of bank, primary terrace, and lower terrace are presented with the SQG for lead indicated in red.

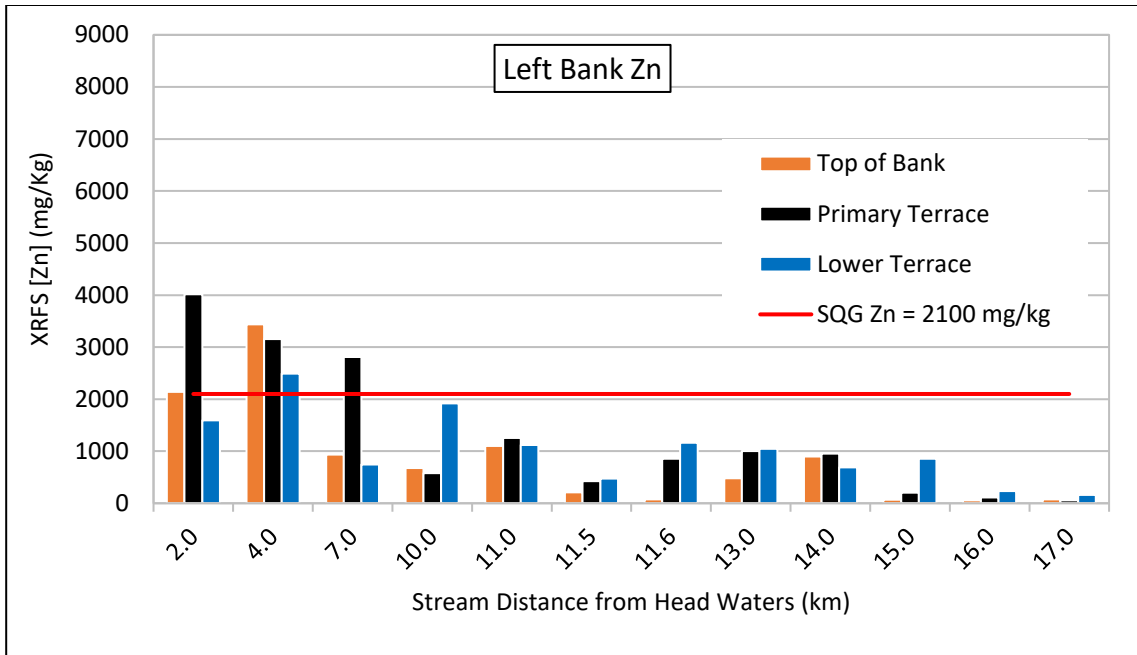


Figure 3.10: Elm Creek zinc concentrations on the left bank for each sampling location starting closest to the headwaters and continuing downstream. Concentrations for the top of bank, primary terrace, and lower terrace are presented with the SQG for zinc indicated in red.

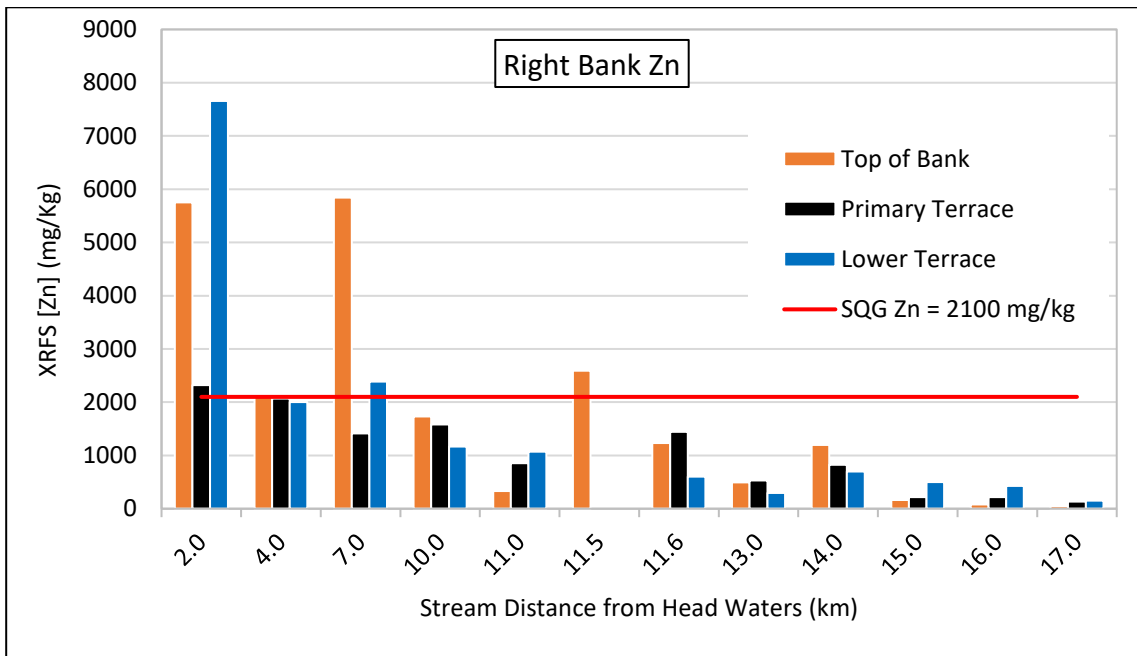


Figure 3.11: Elm Creek zinc concentrations on the right bank for each sampling location starting closest to the headwaters and continuing downstream. Concentrations for the top of bank, primary terrace, and lower terrace are presented with the SQG for zinc indicated in red.

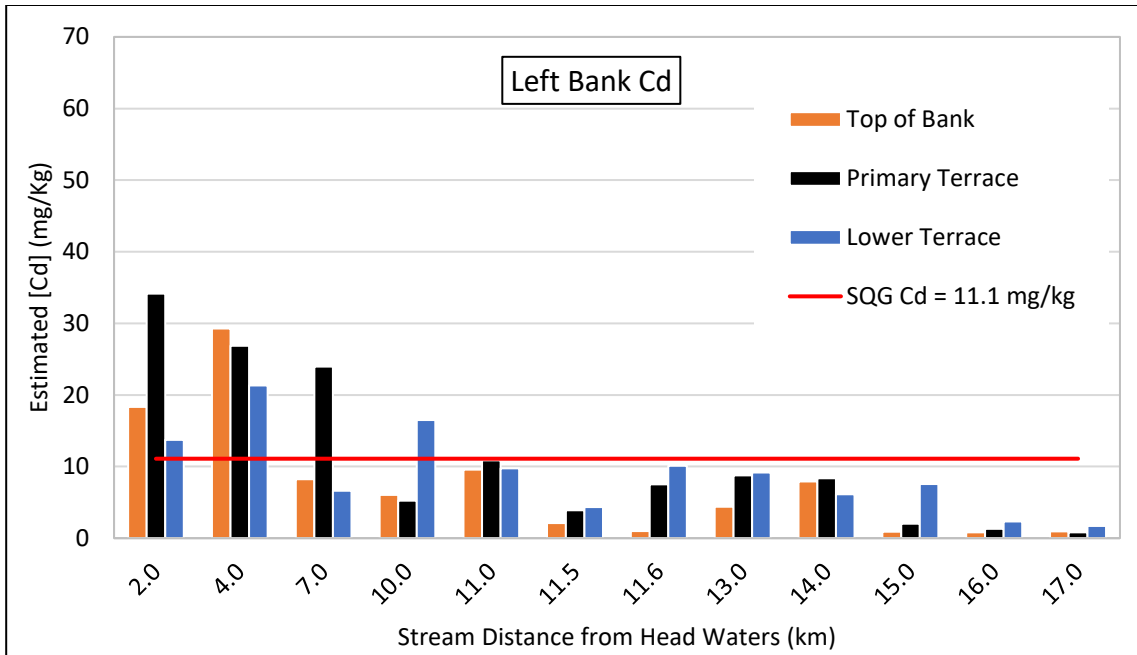


Figure 3.12: Elm Creek estimated cadmium concentrations on the left bank for each sampling location starting closest to the headwaters and continuing downstream. Concentrations for the top of bank, primary terrace, and lower terrace are presented with the SQG for cadmium indicated in red.

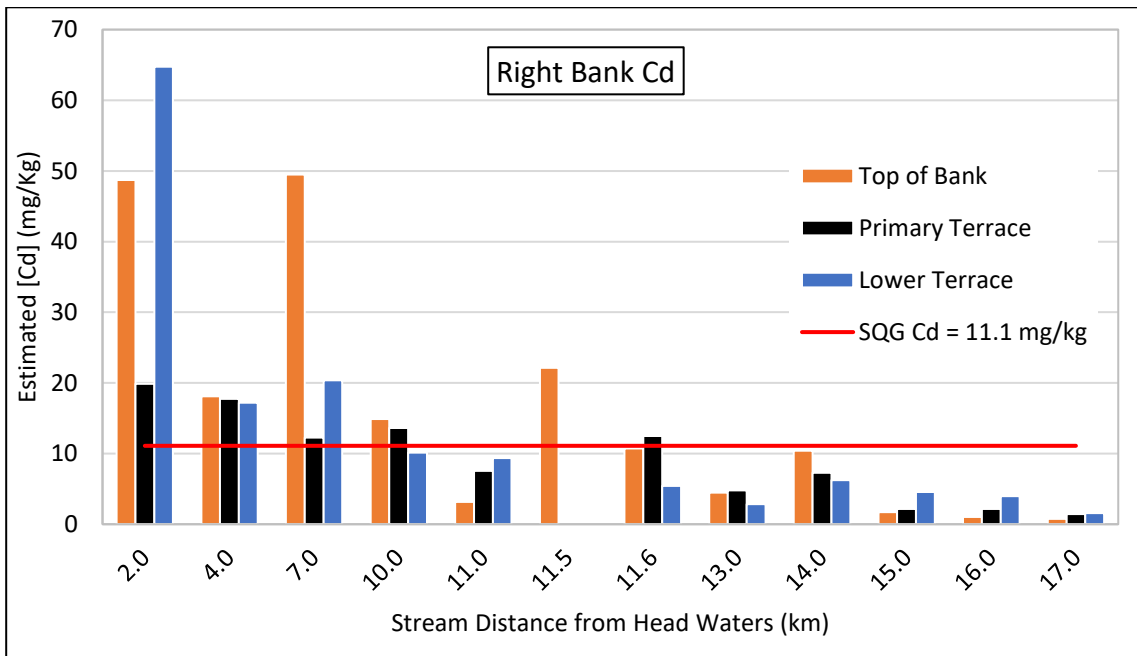


Figure 3.13: Elm Creek estimated cadmium concentrations on the right bank for each sampling location starting closest to the headwaters and continuing downstream. Concentrations for the top of bank, primary terrace, and lower terrace are presented with the SQG for cadmium indicated in red.

These figures show a decreasing trend in trace metals concentrations as distance downstream increases. The three locations closest to the Tar Creek Superfund Site have the greatest concentrations of trace metals suggesting that the bulk of the contamination is from this area. Also, the right bank in the first three sites had higher concentrations than the left bank which provides more evidence that the contamination is coming from the Tar Creek Superfund Site as more runoff from the superfund site will likely enter the creek on the right bank than the left. Contamination from this site is likely influencing soil metal concentrations downstream, especially since smaller particles from the waste material have been found to have the greatest trace metals concentrations and are more easily transported downstream (Horowitz, 1991; Miller, 1997; Datin and Cates, 2002). The natural meandering of Elm Creek may act as a removal mechanism of the trace metals as meandering streams have point bars which accumulate sediment over time (Lewin and Macklin, 1987, Miller, 1997, USGS, 2009). This could account for the decreasing metals concentrations as distance increases. Juracek and Drake (2016) stated that sediment concentrations from mining-related trace metals typically decrease as downstream distance increases. The trend in the figures presented reflect the statement made by Juracek and Drake (2016) as concentrations in the stream terraces appear to decrease as distance from the source increases. Although this study looks at soil terrace concentrations, studies analyzing the distribution of trace metals contaminated sediments reflect similar findings (Swennen et al., 1994; Carter et al., 2006; Dennis et al., 2009; Bird et al., 2010; Wang and Nie, 2017). Researchers studying trace metal contaminated alluvial sediments have found

that concentrations close to the source of contamination reflected similar concentration to that of the source, however distributions downstream were often unevenly distributed (Swennen et al., 1994; Wang and Nie, 2017). Carter et al., (2006) observed a clear decrease in Pb, Cu, and Cr sediment concentrations as distance from industrial effluents increased in the Rivers Aire and Carter.

The first three locations (2.0 km, 4.0 km, and 7.0 km) have the greatest number of samples that exceed the SQGs for each metal. The cadmium SQG is exceeded in the fourth location (10.0 km) in three of the six terraces. The first four sampling locations are not within the GRDA properties (the fourth location (10.0 km) may appear to be within the property, however this sampling spot falls just outside of the property line).

Within the GRDA owned properties, the SQG for lead is exceeded at two points along the creek. The left primary terrace at location 11.5 km reported lead concentrations of 153 mg/kg and the right primary terrace at location 11.0 km downstream reported lead concentrations of 152 mg/kg. Zinc and cadmium exceeded the SQGs at location 11.5 km on the top of the right bank with concentrations of 2,590 mg/kg and 22.1 mg/kg respectively. Cadmium also exceeded the SQG at location 11.6 km on the right bank with a primary terrace concentration of 12.5 mg/kg. Although the SQG's are non-enforceable, the concentrations at points that exceeded SQGs within the GRDA properties for lead, zinc, and cadmium were confirmed with ICP-OES analysis. Table 3.3 outlines the lead and zinc concentrations reported by XRFs and estimated cadmium concentrations with the ICP values for each Elm Creek terrace location within the GRDA properties that exceeded SQGs.

Table 3.3: Lead and zinc concentrations reported by XRFs and estimated cadmium concentrations with the corresponding ICP values for each Elm Creek terrace location within the GRDA properties that exceeded SQGs.

Location	Terrace	SQG	Pb (mg/kg)		Zn (mg/kg)		Cd (mg/kg)	
			XRFs	ICP	XRFs	ICP	Estimated	ICP
			150		2100		11.1	
11.0 km	Right Primary		152	140				
11.5 km	Left Primary		153	133				
11.5 km	Right Top				2590	1540	22.1	16.8
11.6 km	Right Primary						12.5	11.0

All ICP concentrations reported lower values than the XRFs and supports the statement made in Chapter 2 regarding the XRFs being used only as a screening tool. Lead and zinc ICP concentrations report values lower than the SQGs, while only one cadmium ICP value remained greater than SQG. If XRFs values were not confirmed with ICP analyses, a greater riparian area would be in focus for remediation.

The stretch of Elm Creek that extends between locations 11.0-11.5 km may be considered an area for possible remediation as concentrations fall both near SQGs for lead and over the SQG for cadmium. Also, because location 10.0 km reported concentrations exceeding the SQGs for lead and cadmium, the stretch of the stream north of this point that fall within the GRDA properties could also be an area in need of remediation. Negating property lines and boundaries, the stretch of Elm Creek that extends from the headwaters of the creek to 11.5 km downstream should be considered for remediation with the stretch closest to the Tar Creek Superfund Site receiving greatest attention. This contamination is being transported downstream and if measures are not taken to prevent the contamination from entering the stream, any remediation downstream will likely be ineffective as the source has not been addressed.

3.3.1.1 Terrace analysis:

The east branch and main stem of Elm Creek terraces were analyzed to visualize the distribution of metals within the different terraces (e.g., Does the lower terrace generally have greater metals concentrations than the top or primary terrace?). The Friedman test was used to assess if any differences occurred between the top, primary, and lower terraces for each metal using the XRF datasets. Table 3.4 outlines the descriptive statistics and p-value for each metal. Note that sample taken at location 11.5 km on the right side of the creek was not used as only the top terrace was sampled.

Table 3.4: The descriptive statistics and p-value (Friedman test) for lead, zinc, and estimated cadmium concentrations in the top, primary or lower terraces of the east branch and main stem of Elm Creek.

		n	Mean (mg/kg)	Median (mg/kg)	Std. Dev. (mg/kg)	Min. (mg/kg)	Max. (mg/kg)	p- value ¹	Null Hypothesis ²
Pb	Top	23	150	72.1	205	13.2	800	0.437	Accepted
	Primary	23	112	64.3	107	19.2	393		
	Lower	23	112	76.0	132	17.4	591		
Zn	Top	23	1270	676	1670	50.7	5840	0.437	Accepted
	Primary	23	1180	857	1070	55.2	4020		
	Lower	23	1280	858	1550	140	7660		
Cd	Top	23	11.0	6.00	14.0	0.77	49.5	0.437	Accepted
	Primary	23	10.2	7.60	8.98	0.81	34.1		
	Lower	23	11.1	7.60	13.0	1.60	64.7		

¹p-value greater than 0.05 = acceptance of null hypothesis

²Null hypothesis = There are no differences between the variables.

These results show no statistically significant differences between trace metal concentrations in the terraces. The lower terrace was thought to have the greatest concentrations because the lower terrace is most likely to be influenced by trace metals deposited from the stream however, the deposition of trace metals in Elm Creek appears to be much more spatially complex. Brewer and Taylor (1997) found that the

distribution of trace metals within stream terraces was spatially complex, and deposition of metals was influenced by vertical and lateral channel instability, flood frequency and magnitude, and terrace height. Because the stream morphology and terrace slopes for this study were not mapped, understanding how varying terrace heights and locations affect the concentration distribution would prove exceptionally challenging but may require further inquiry.

3.3.1.2 Analysis of the East and West Branch of Elm Creek

The east and west branches of Elm Creek were sampled in August 2017 and concentrations from each branch were compared to determine if there was a difference between creek branches. This was the second time the east branch of Elm Creek was sampled as data collected within the same day would allow for the most accurate comparison. Note that the east branch data collected in January 2017 and August 2017 were not statistically different from each other. Figure 3.14 shows the sampling locations on Elm Creek at the east and west branches with the E30, E40, and E50 County Road crossings marked. The E30, E40, and E50 County Road crossings on the east branch correspond to the 2.0 km, 4.0 km, and 7.0 km locations, respectively, used in the analysis prior to this section. Figures 3.15 through 3.17 present the metals concentrations for lead, zinc, and cadmium for the east and west branches split into left and right banks. The SQG for each metal is presented in red.

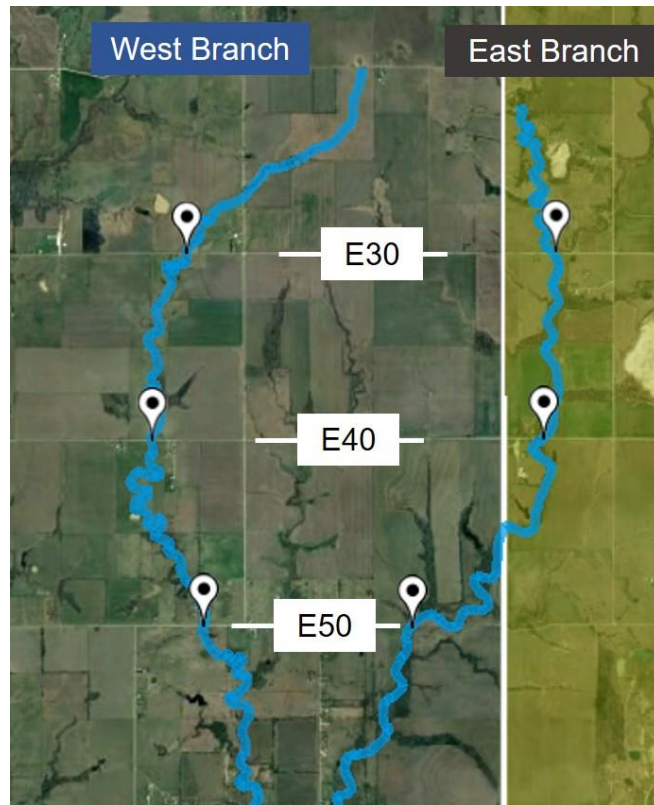


Figure 3.14: Elm Creek sampling locations on the east and west branches at the E30, E40, and E50 County Road crossings.

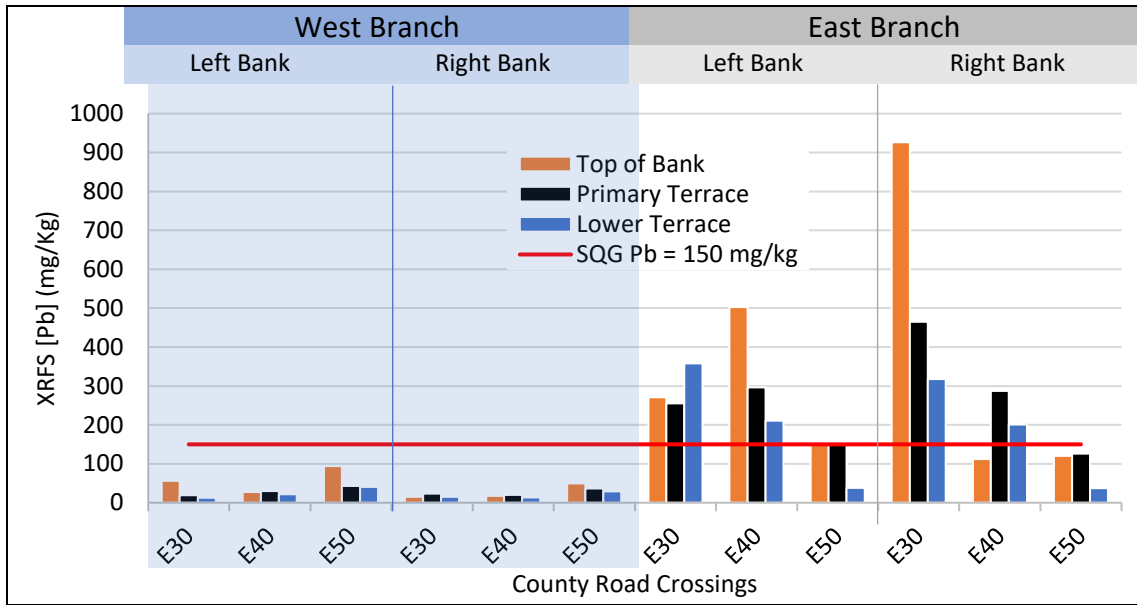


Figure 3.15: Elm Creek east and west branch lead concentrations. Each branch presents concentrations for the top of bank, primary terrace, and lower terrace for the left and right banks at each road crossing. The SQG is marked in red.

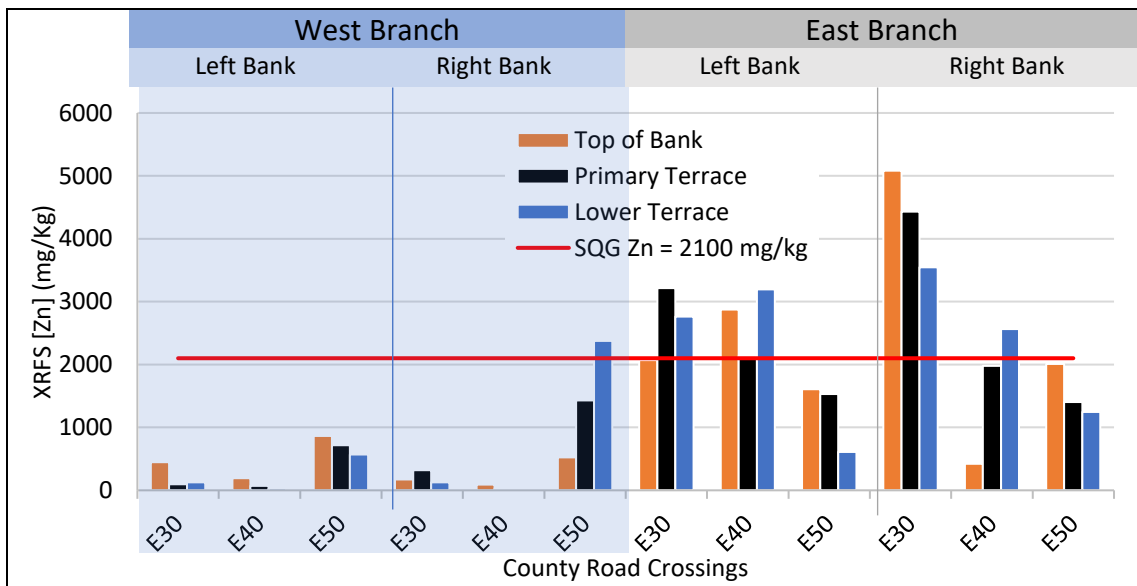


Figure 3.16: Elm Creek east and west branch zinc concentrations. Each branch presents concentrations for the top of bank, primary terrace, and lower terrace for the left and right banks at each road crossing. The SQG is marked in red.

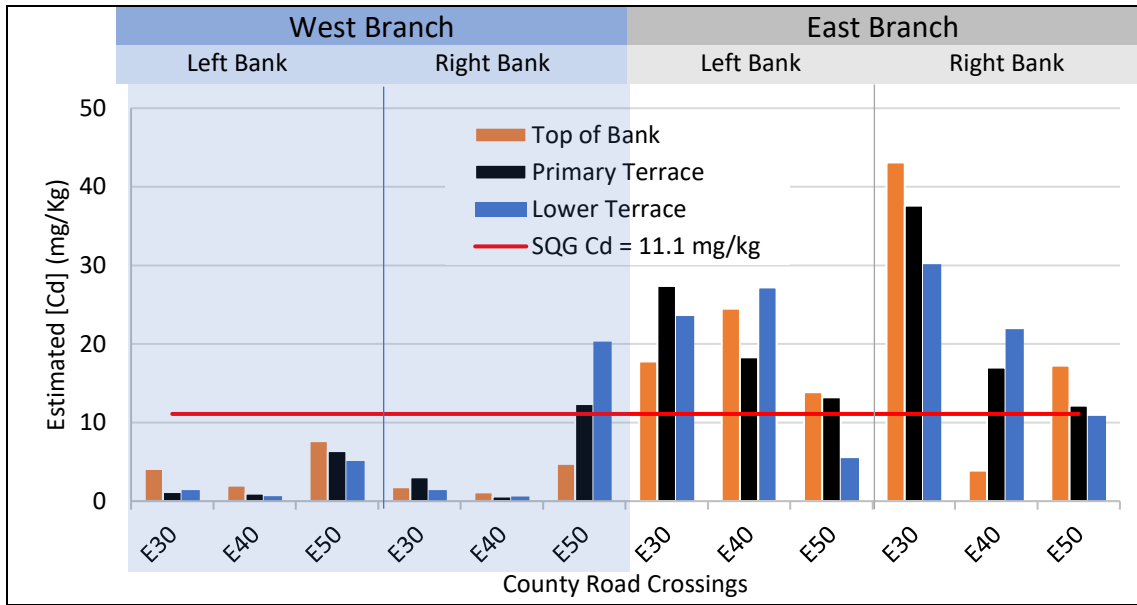


Figure 3.17: Elm Creek east and west branch estimated cadmium concentrations. Each branch presents concentrations for the top of bank, primary terrace, and lower terrace for the left and right banks at each road crossing. The SQG is marked in red.

The Mann-Whitney U-test was used to determine if there were differences between creek branches. Table 3.5 outlines the descriptive statistics and p-values for each metal in the east and west branches.

Table 3.5: The descriptive statistics and p-value (for Mann-Whitney U-test) for lead, zinc, and predicted cadmium in the east and west branches of Elm Creek

	Branch	n	Mean (mg/kg)	Median (mg/kg)	Std. Dev. (mg/kg)	Min. (mg/kg)	Max. (mg/kg)	p-value ¹	Null Hypothesis ²
Pb	East	18	268	232	209	37.5	925	1.52E-06	Rejected
	West	18	31.5	25.3	20.2	12.7	94.0		
Zn	East	18	2370	2100	1230	421	5080	8.16E-06	Rejected
	West	18	456	182	604	31.4	2370		
Cd	East	18	20.2	18.0	10.3	3.89	43.1	8.16E-06	Rejected
	West	18	4.18	1.88	5.09	0.610	20.3		

¹p-value greater than 0.05 = acceptance of null hypothesis

²Null hypothesis = The distributions between variables are identical

The results from this analysis show that the east and west branches were statistically different and that the west branch had statistically lower trace metals

concentrations than the east branch for lead, zinc, and cadmium. The #50 road crossing on the west branch did show greater metals concentrations than the #30 and #40 locations on the same branch. Until the early 2000s, chat, the mining waste material was used as gravel on county roads without any encapsulation or stabilization. After publication of the “chat rule” in the Federal Register in 2007 , its use is now restricted as aggregate in paving material. It is likely that chat entered the streambed during storm events and through airborne deposition after disturbance by vehicles (40 CFR Parts 260 and 278) (FRC, 2007).

The hypothesis that the stream branch nearest the mining influence (east branch) will have greater metals concentrations than the stream branch further away from the mining influence (west branch) when comparing samples collected at equal distances upstream from the creek confluence was therefore accepted. The assumption made earlier that the east branch was the main source of trace metals to the main stem is also confirmed by this analysis.

3.3.2 Uplands Concentration Distribution

The 278 upland sampling locations in the GRDA properties are shown in Figure 3.18. Due to the scale of the sampling location markers, some sample points appear to be within Elm Creek. Each of these samples was taken with proximity to the creek and terrace sampling locations which are not marked.

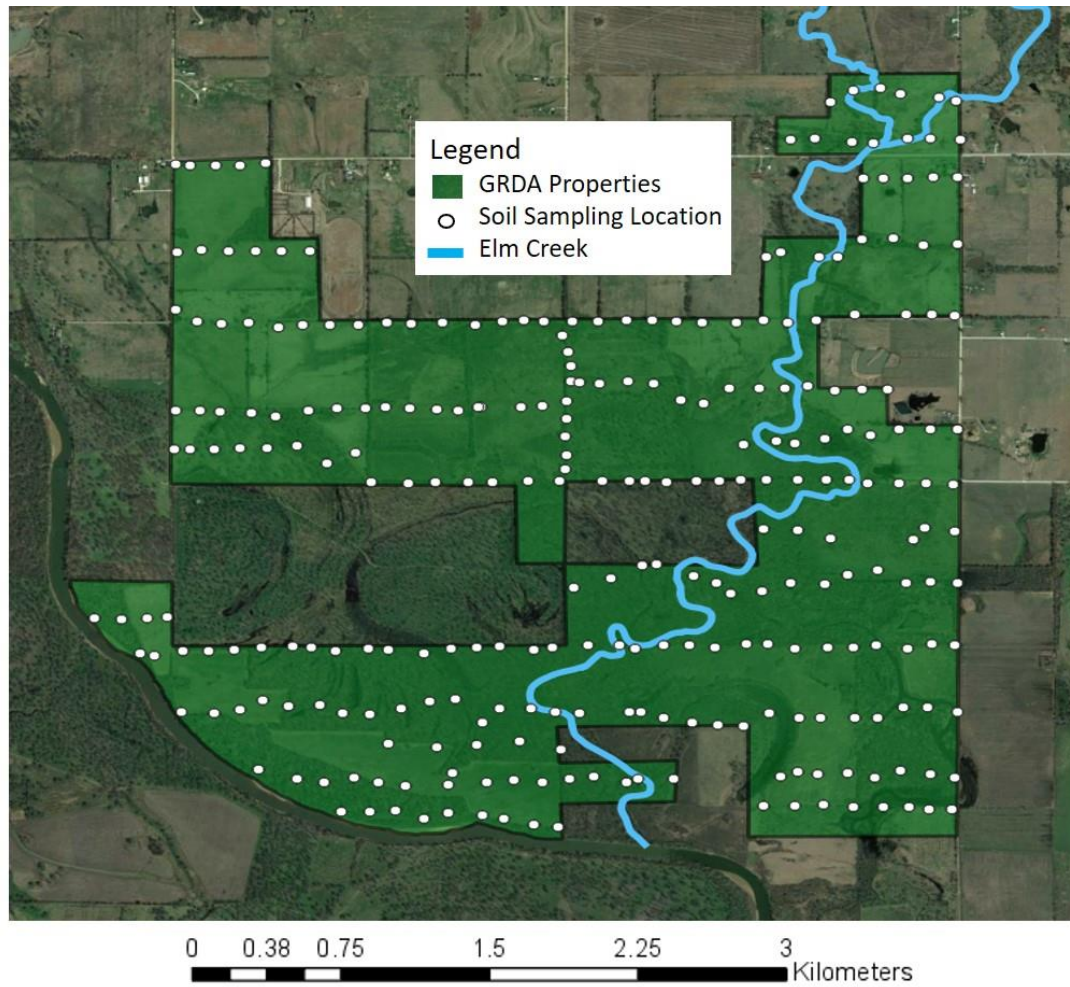


Figure 3.18: The 278 sampling locations for all soil samples in the GRDA Properties.

The upland soil concentrations were split into frequency distribution for lead, zinc, and cadmium in Figure 3.19. These figures show the number of samples that fell within a given concentration range for each metal.

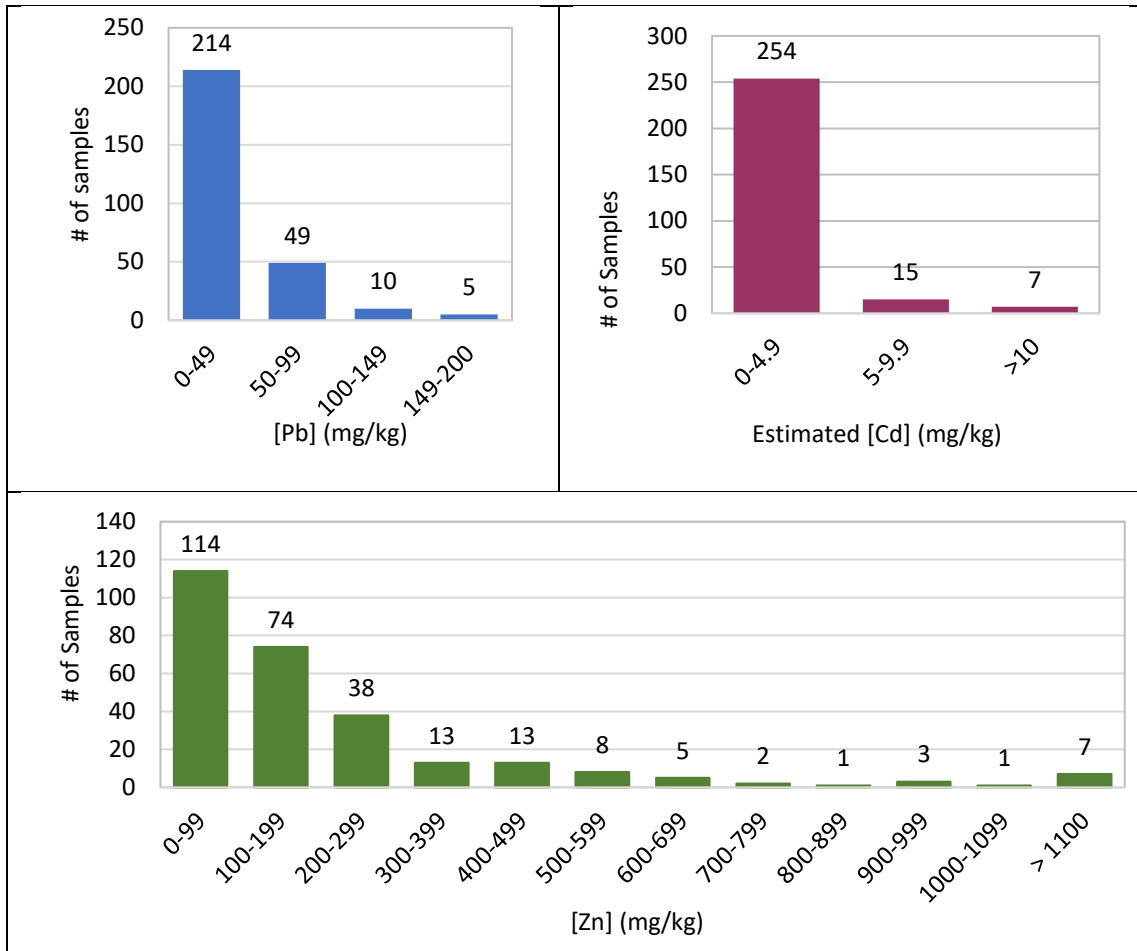


Figure 3.19: The frequency distributions for lead, zinc, and cadmium concentrations in upland soils.

The number of samples in each concentration bracket decreases as concentration increases for each metal. None of the samples exceed the RG for lead (500 mg/kg), however, the RG's are exceeded for the same seven samples for both zinc (RG = 1,100 mg/kg), and cadmium (RG = 10 mg/kg). All seven soil samples had trace metals concentrations determined by ICP analysis. Figure 3.20 shows the locations of the seven samples that exceeded the RG for zinc and cadmium. Table 3.6 outlines the XRFs and ICP concentrations for each site.

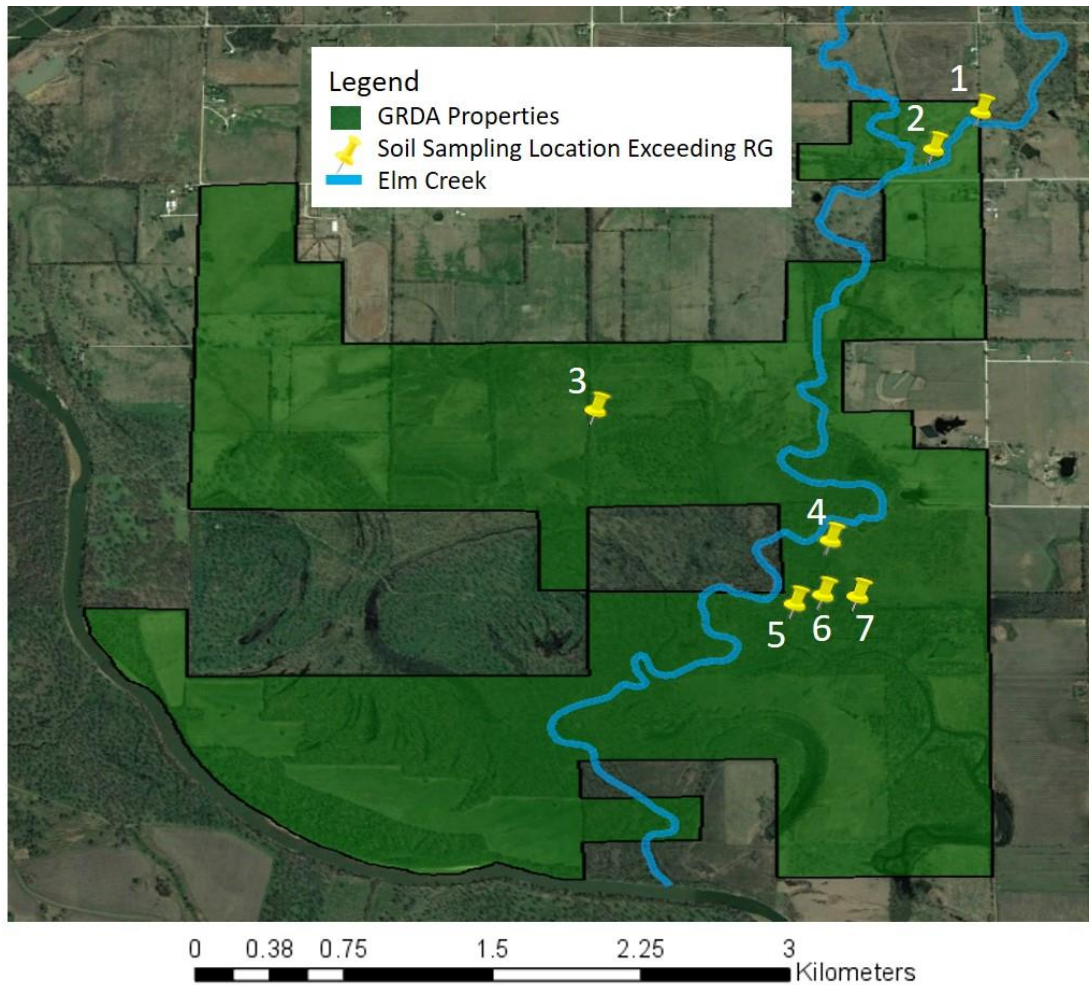


Figure 3.20: Locations where samples exceed the RG's for zinc and cadmium

Table 3.6: Zinc and cadmium concentrations determined by XRFs and ICP analysis for soil samples in the uplands with XRFs values exceeding the RG

Location	Zn (mg/kg)		Cd (mg/kg)	
	XRFS	ICP	Estimated	ICP
RG	1100		10.0	
1	1260	1070	10.9	9.80
2*	1766	1440	15.2	16.5
3*	1474	1380	12.7	12.8
4*	2068	1630	17.7	17.2
5*	1277	1200	11.1	10.0
6	1232	995	10.7	8.31
7**	1285	1230	11.1	9.50

*RG exceedance confirmed by ICP analysis for zinc and cadmium

**RG exceedance confirmed by ICP analysis for zinc only

The ICP analysis confirmed that five of the seven samples exceeded the RG for zinc (locations 2, 3, 4, 5, and 7), while only four of the seven samples were confirmed for cadmium (locations 2, 3, 4, and 5). Two samples (locations 1 and 6) had ICP concentrations less than the RGs for zinc and cadmium. The results from the XRFS and ICP confirm the need for ICP validation especially in regulatory situations such as this. If validation via ICP was not conducted, a much larger area would need attention which would increase remediation costs. Further analysis of the geospatial distribution of trace metals was completed using GIS and geostatistical methods.

3.3.2.1 IDW and Ordinary Kriging Interpolation

Spatial maps outlining the concentration distributions of lead, zinc, and cadmium were created using the inverse distance weighted (IDW) interpolation and ordinary kriging methods with the XRFS and estimated cadmium dataset. Each metal therefore has two maps and were presented next to each other in Figure 3.21, Figure 3.2.2, and Figure 3.23. The map developed using IDW interpolation is on the top (a), while the map generated using ordinary kriging is on the bottom (b). The RG for each trace metal is marked in the legend next to the corresponding concentration. Note that because lead did not exceed the RG at any points, the RG falls at a different color (red) than it does for zinc and cadmium (yellow).

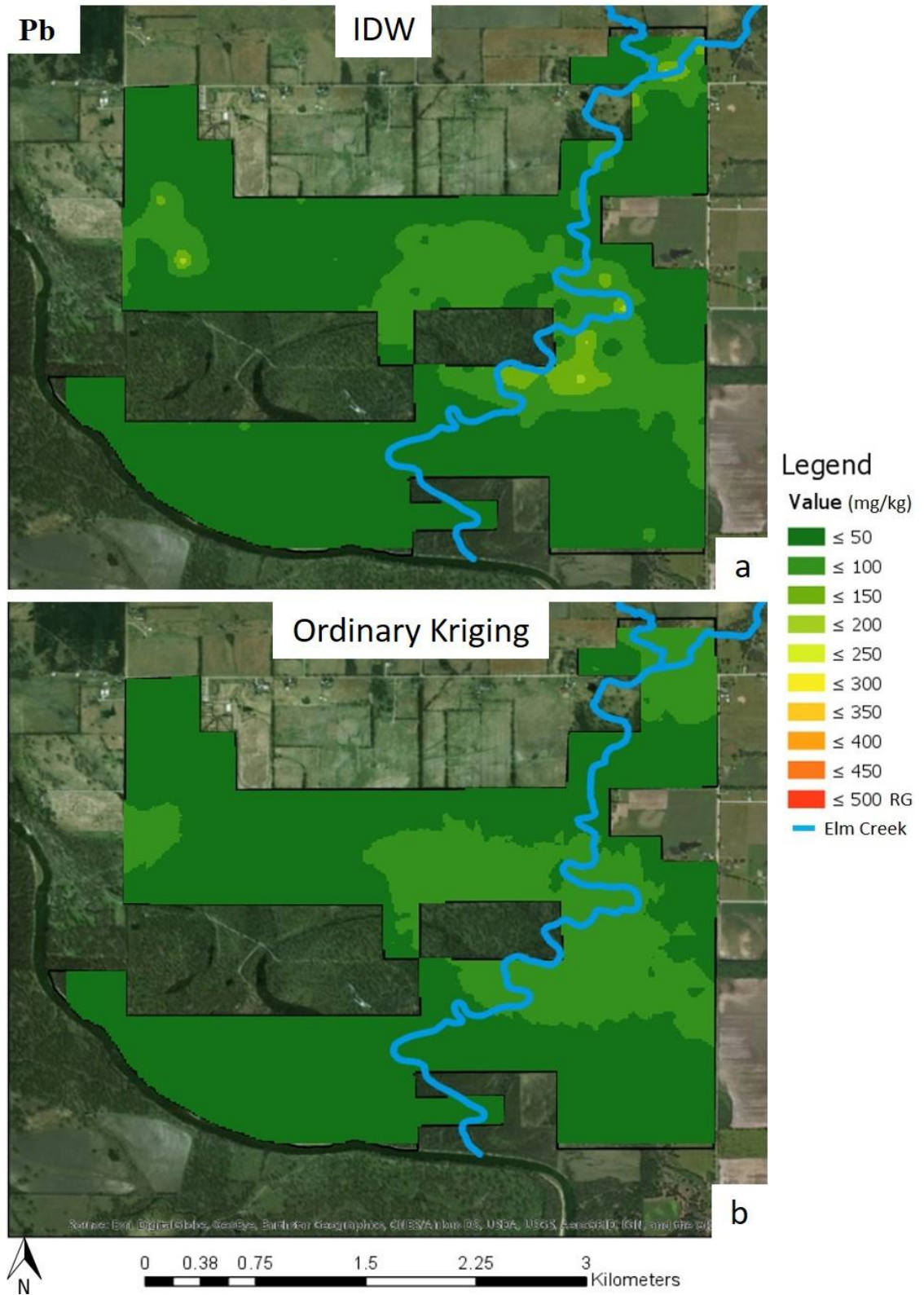


Figure 3.21: The (a) IDW geospatial interpretation and (b) ordinary kriging maps for lead in the uplands

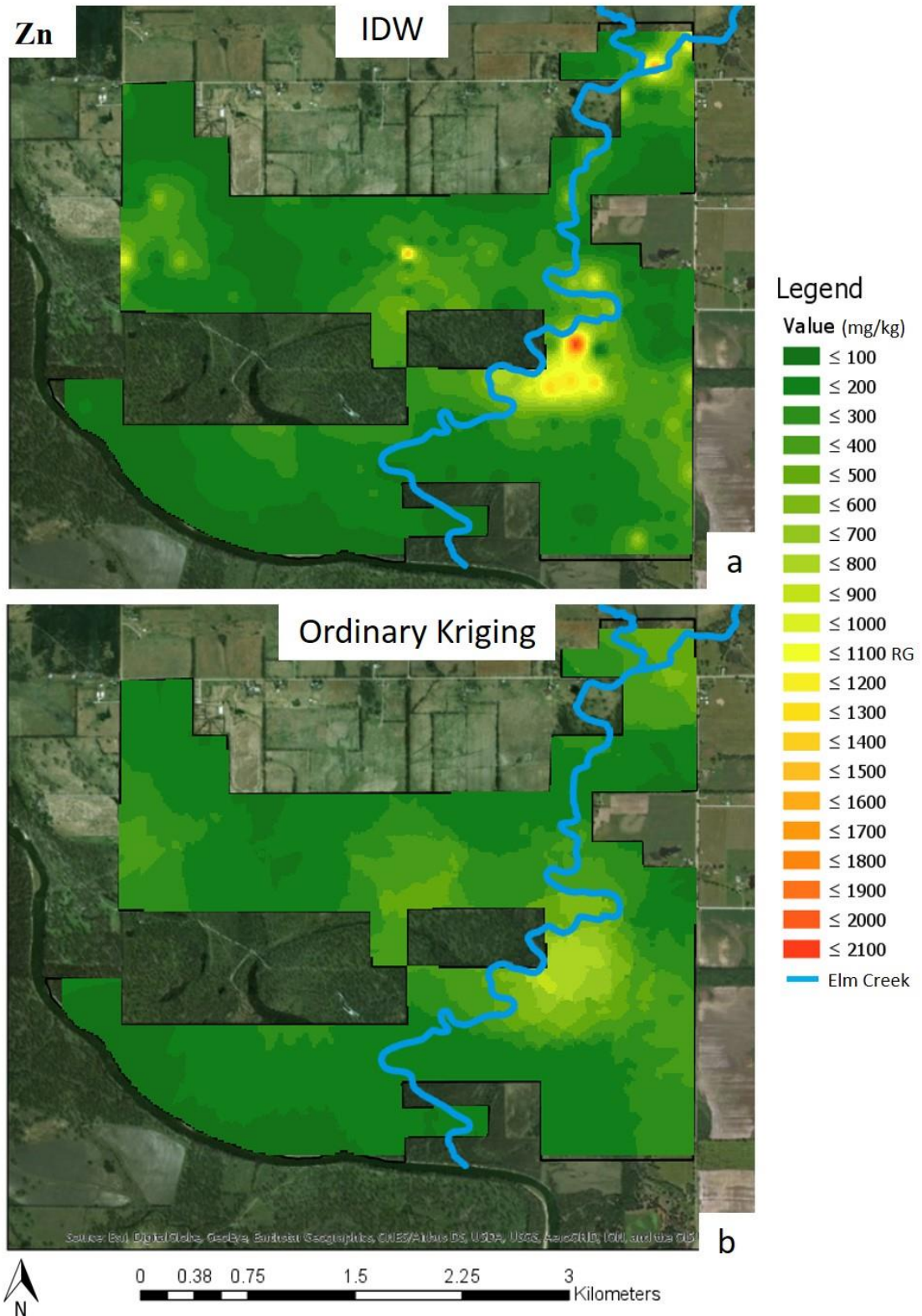


Figure 3.22: The (a) IDW geospatial interpretation and (b) ordinary kriging maps for zinc in the uplands

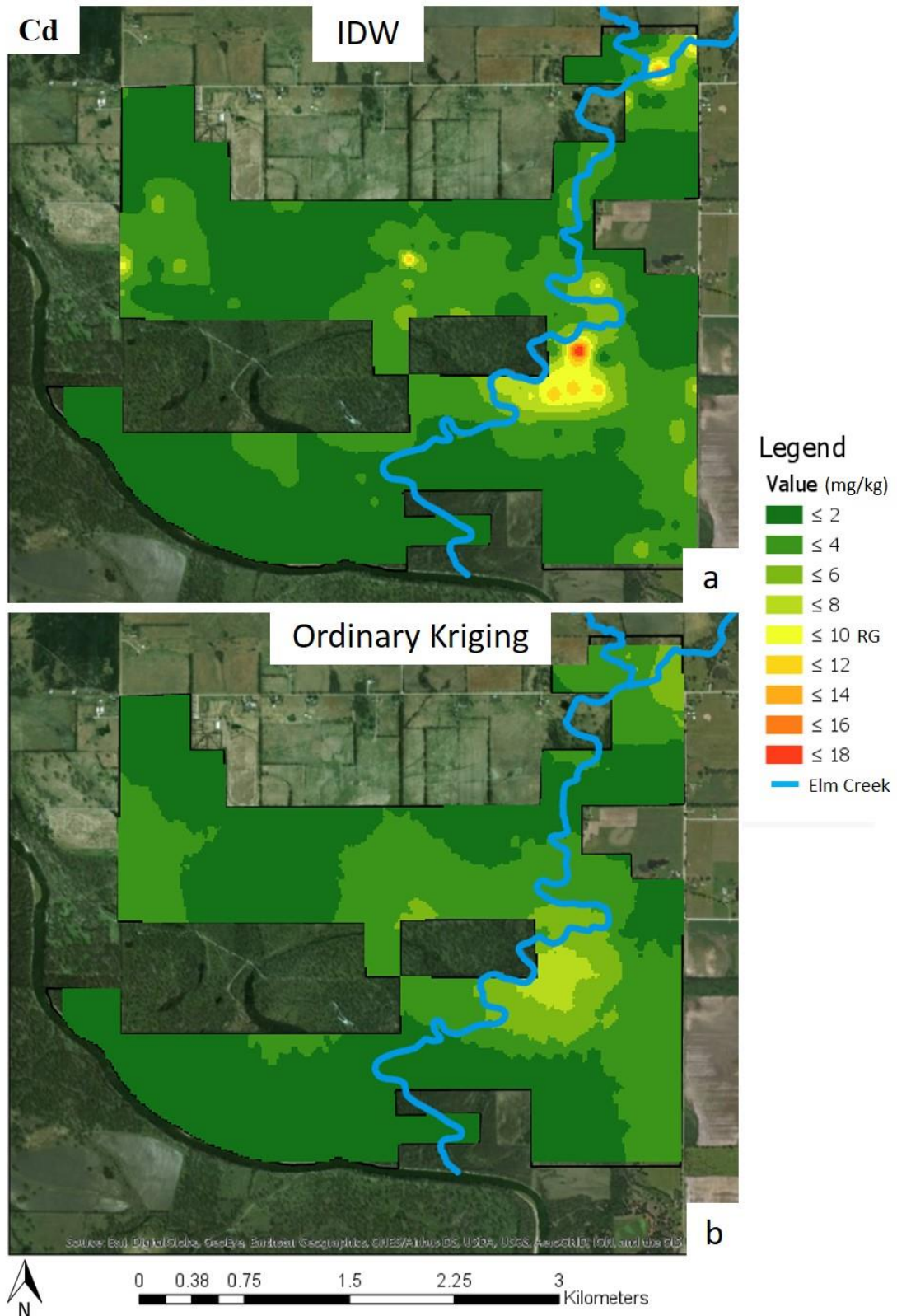


Figure 3.23: The (a) IDW geospatial interpretation and (b) ordinary kriging maps for estimated cadmium in the uplands

Both interpolation maps for each metal highlight areas of greater concentration at the top right corner of the properties near the creek confluence and surrounding the creek midway into the east portion of the property. The IDW map presents the actual concentrations determined by the XRFs while the ordinary kriging leveled out areas of greater concentration identified in the IDW maps. The IDW map also outlined areas that could possibly exceed the RGs for zinc and cadmium (in yellow), while the ordinary kriging maps predict the concentration distributions will remain below RG values. Studies comparing both methods are contradictory on which method is best and the most accurate method is debated among researchers (Arun, 2013; Bhunia et al., 2016; Shit et al., 2016; Wang and Nie, 2017), therefore both maps were generated and appear to highlight the same areas of interest. To further analyze the distribution of metals, statistically significant points were determined using hotspot analysis techniques.

3.3.2.2 Hotspot Identification

Hotspots were identified using the local Moran's I and the Getis-Ord G_i^* statistic. Figures 3.24-3.26 present the high-high clusters, low-low clusters, high-low outliers, and low-high outliers for each metal determined by the local Moran's I in the first map (a). The hot spot and cold spot identification using the Getis-Ord G_i^* spatial statistics are shown in the second (b). An inverse distance band of 300 m was used for both analysis. Points were overlain on the IDW maps for each metal to aid in data interpretation and visualization. Note that this is not a comparison of methods as both techniques have different approaches to identifying statistically significant points.

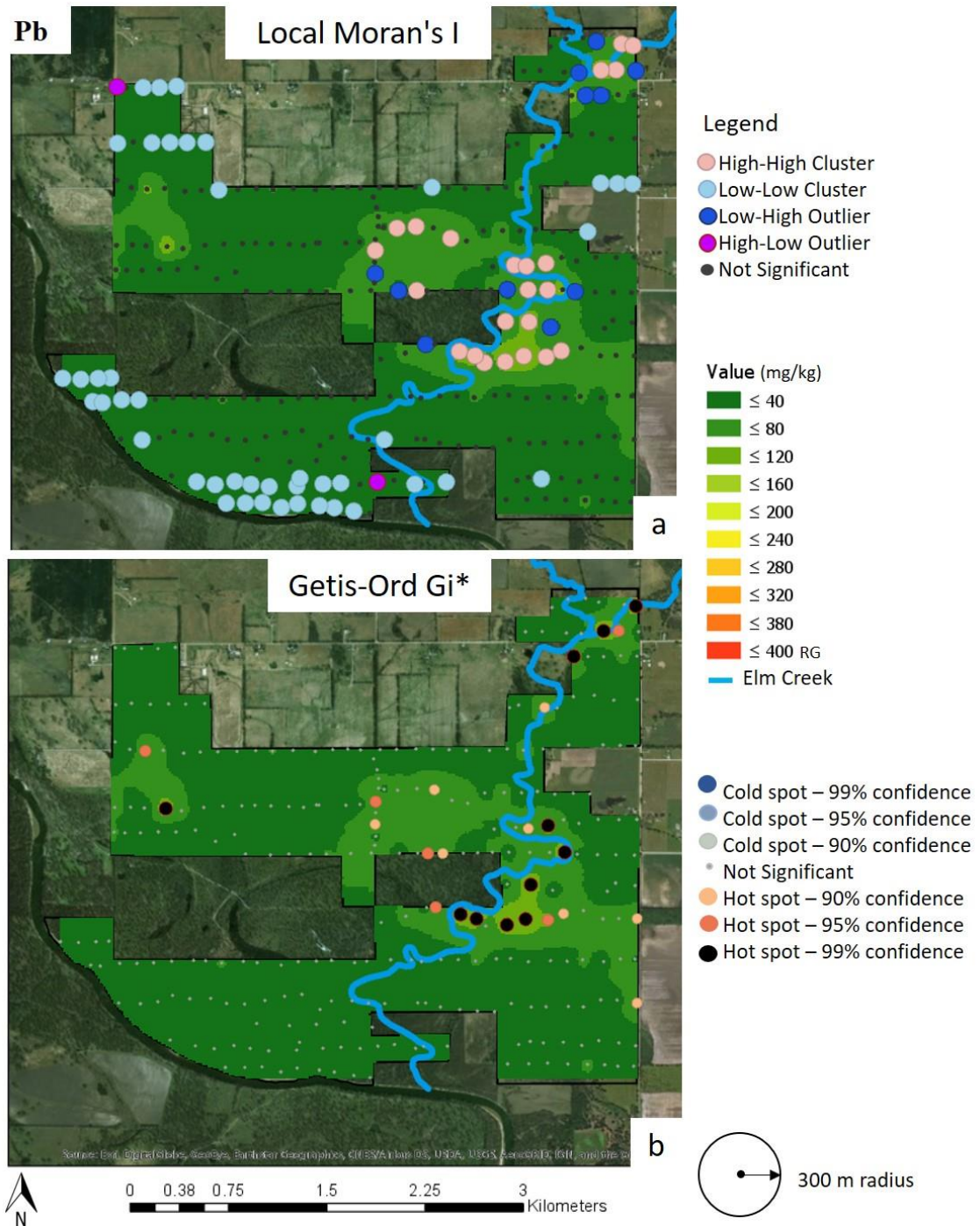


Figure 3.24: The spatial distribution map of significant hotspot clusters and cold spot clusters using the (a) local Moran's I spatial statistic for identification of clusters and (b) the Getis-Ord G_i^* spatial statistic for identification of hot and cold spots for lead concentrations in the uplands. An inverse distance band of 300 m was used for both methods. Points are overlain on IDW interpolation map

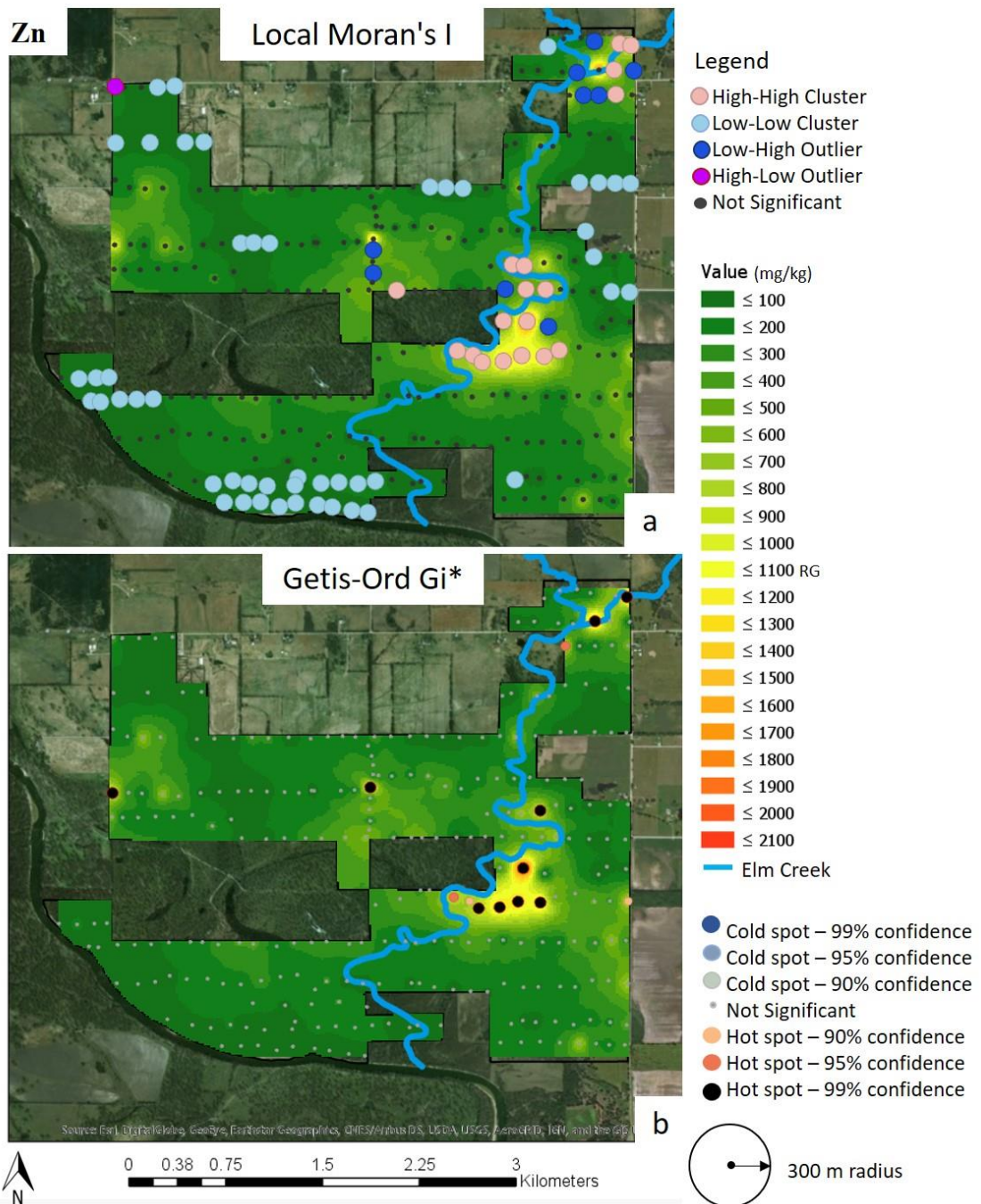


Figure 3.25: The spatial distribution map of significant hotspot clusters and cold spot clusters using the (a) local Moran's I spatial statistic for identification of clusters and (b) the Getis-Ord Gi* spatial statistic for identification of hot and cold spots for zinc concentrations in the uplands. An inverse distance band of 300 m was used for both methods. Points are overlain on IDW interpolation map

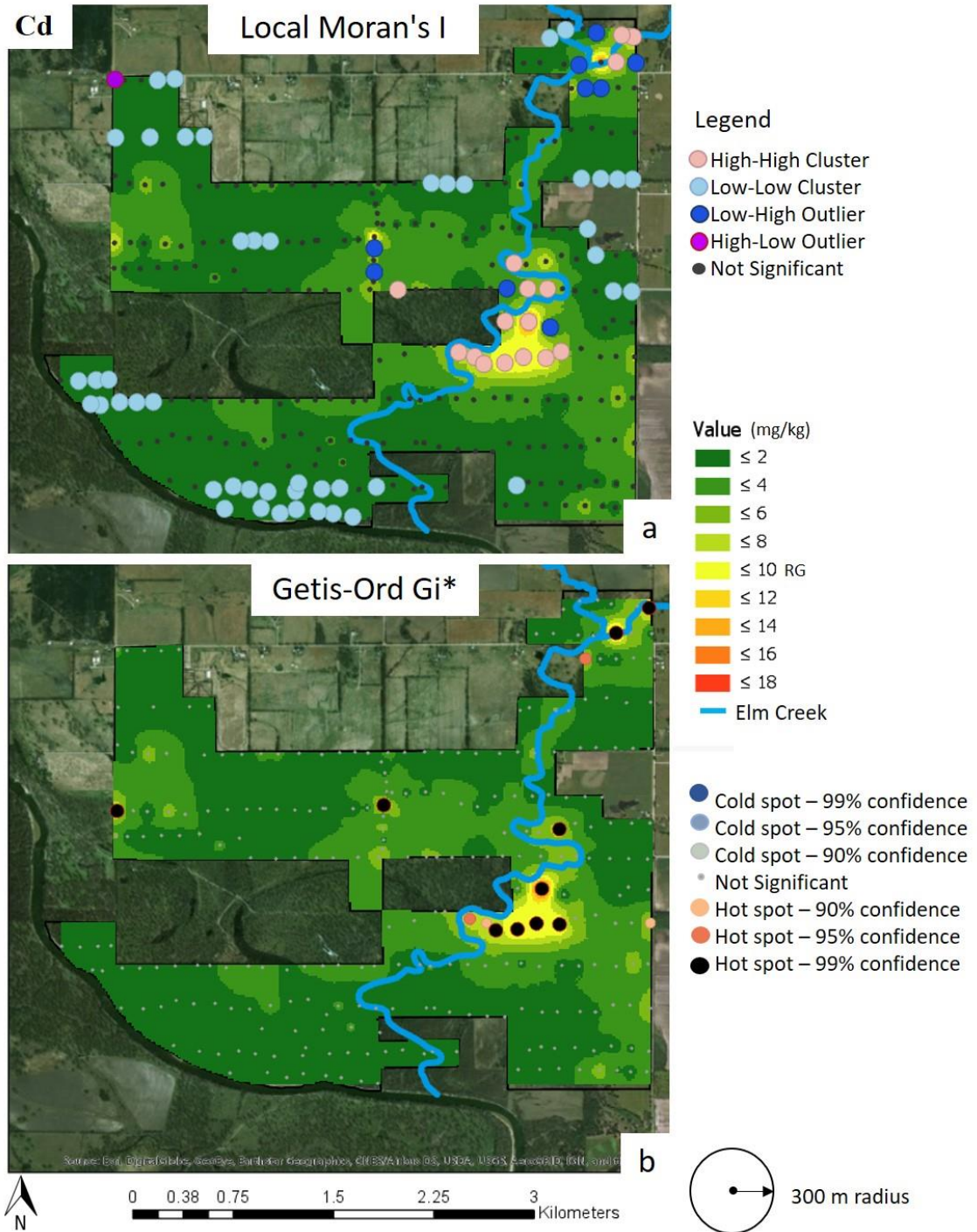


Figure 3.26: The spatial distribution map of significant hotspot clusters and cold spot clusters using the (a) local Moran's I spatial statistic for identification of clusters and (b) the Getis-Ord G_i^* spatial statistic for identification of hot and cold spots for estimated cadmium concentrations in the uplands. An inverse distance band of 300 m was used for both methods. Points are overlain on IDW interpolation map

The high-high clusters for each trace metal determined by the local Moran's I are located near the creek confluence in the northeastern corner of the maps and midway down the creek. The map for lead also has high-high clustering in the center of the map to the west of the creek. The Getis-Ord G_i^* spatial statistic also identified the same areas as high-high clustering to have statistically significant hot spots. Low-low clustering occurred in the same areas for all metals. No statistically significant cold spots were identified. Low-high outliers appear in transition areas where low concentrations were near high-high clustering. One high-low outlier is present in each map in the northwestern corner (this point has statistically higher concentrations than its neighbors) which are marked as low-low clusters. The statistically greater concentrations at this point are most likely due to metals influence from the roadway as this sampling location was closest to a gravel road rural intersection. That could have been used in the making of the gravel road and vehicles driving by kick up dust from the road which could settle in sampling locations close to roadways. This can also be said for the hot spots identified near the east and west boundaries by the Getis-Ord G_i^* spatial statistic. All samples (aside from the most north eastern location next to the creek) were near unpaved roads or gates that allowed for vehicle access to the property. Soil concentrations could be influenced by the movement of road material being airborne in high winds or from vehicles or by road material being tracked into the properties on the tires of vehicles. One other high-low outlier is present near low-low clustering in the map for lead in the south portion of the property. All high-low outlier

points were identified because they are surrounded by areas of low concentrations and are of no concern as they do not exceed any RGs.

The interpolation methods and geostatistical methods highlighted two areas of interest for lead, zinc, and cadmium: the most northeastern part of the map just before the creek confluence and midway down the creek on the eastern side on the property. A third location is identified for zinc and cadmium near the center of the map. For simplicity, Figure 3.27 outlines these locations as A, B, and C on the zinc IDW contour map.

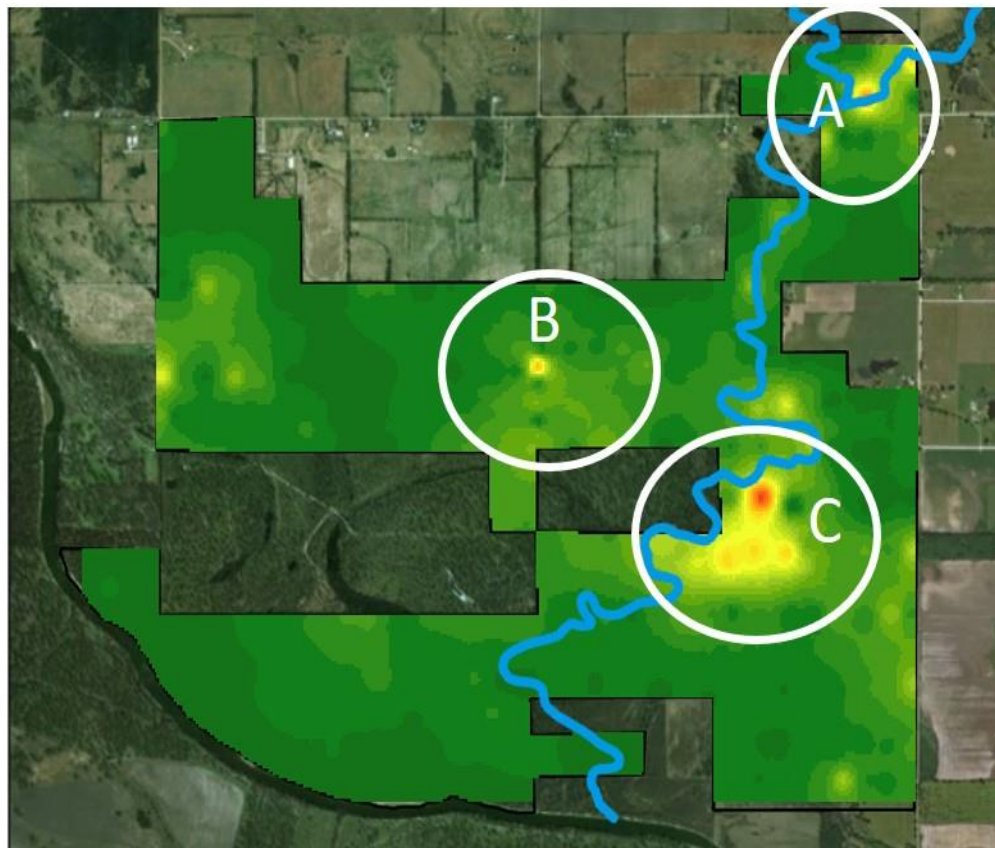


Figure 3.27: Reference map for the identification of areas A, B, and C

Locations A and C are located adjacent to Elm Creek. Location A had upland maximum concentrations of 140 mg/kg for lead, 1,440 mg/kg for zinc, and 16.5 mg/kg

for cadmium, and the creek sampling location closest to this area had similar or greater maximum concentrations of 182 mg/kg for lead, 1,920 mg/kg for zinc, and 16.5 mg/kg for cadmium. The maximum concentrations in the creek terraces at the 13.0 km location, which was closest to the C area, were 76.0 mg/kg for lead, 1,050 mg/kg for zinc, and 9.5 mg/kg for cadmium. The upland concentration highlighted in red on the IDW maps for zinc and cadmium had concentrations of 160 mg/kg for lead, 1,630 mg/kg for zinc, and 17.2 mg/kg for cadmium which were greater than the max concentrations present in the creek. The yellow/orange cluster which occurred in the zinc and cadmium IDW maps below the red point, reflected the maximum creek concentrations for zinc and cadmium in this area. The similarities between the creek concentrations near the areas identified as hotspots or high-high clusters and the upland concentrations within these clusters suggest that contamination from the creek is impacting upland concentrations in these locations. These areas also fall within lower elevation areas which are susceptible to pooling during flood events (Lewin and Macklin, 1987; Miller, 1997). Figure 3.28 presents an elevation contours within the GRDA properties and the Elm Creek watershed boundary is highlighted in grey.

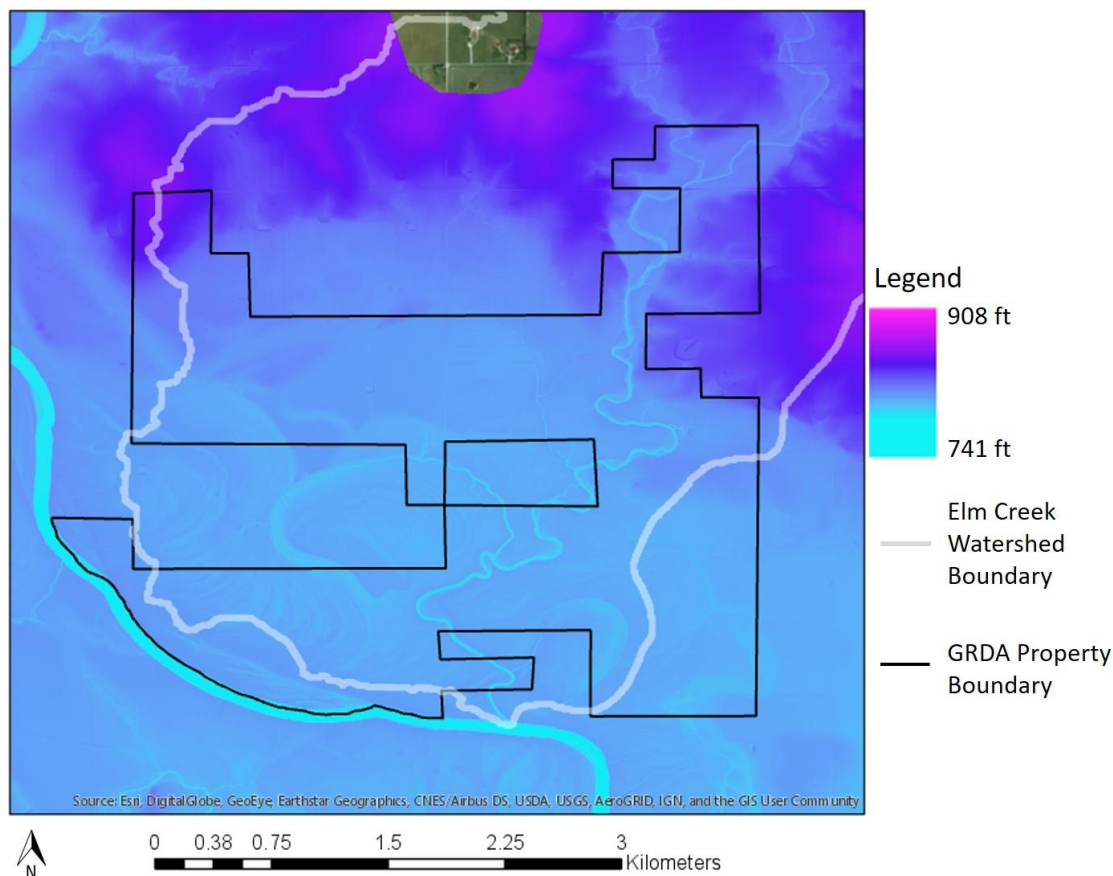


Figure 3.28: Elevation contours within the GRDA properties with the Elm Creek Watershed outlined in grey

Point A has a creek elevation of 760 ft while the uplands have an elevation of 766 ft. The creek near location C has an elevation of 752 feet while the area of hotspot clustering has elevations of 760 feet. A USGS has a stream discharge gauging station at the #65 road crossing, the same location as the creek sampling site at 10.0 km downstream, just past the confluence of the east and west branches (USGS, 2018). Data from this station shows that Elm Creek has relatively low flows throughout most of the year (around 1 cfs), however storm events in the spring can cause significant increases in flows. Figure 3.29 presents the USGS discharge rates (in cfs) for Elm Creek over

January-October 2017 and Figure 3.30 presents the water surface elevation (ft) at the same location (#65 road crossing) over the same time frame.

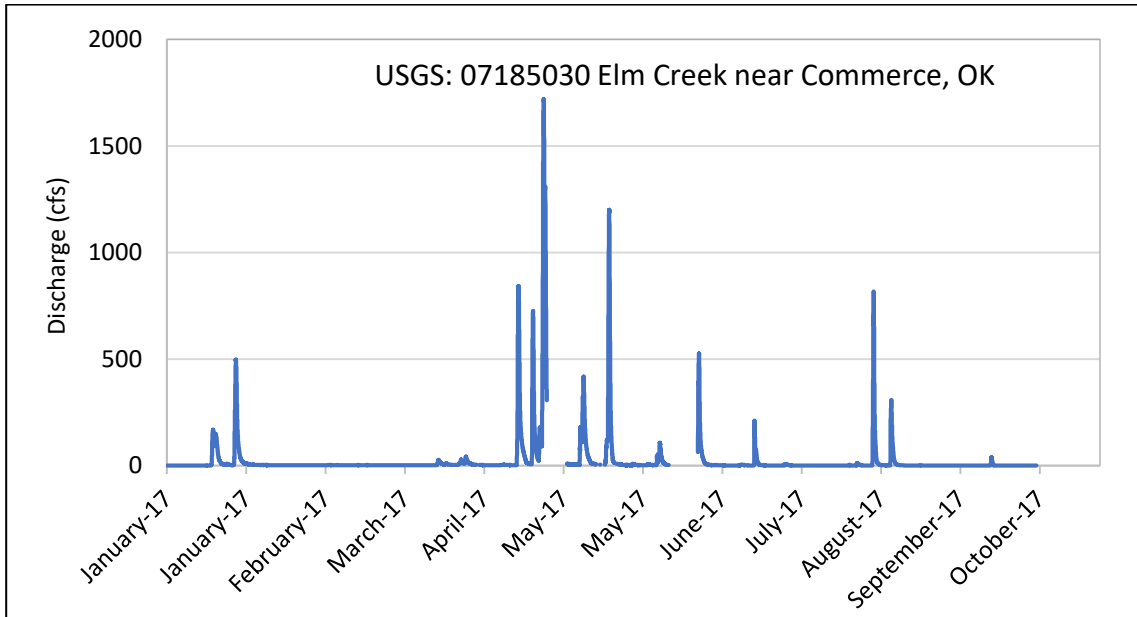


Figure 3.29: USGS discharge rates for Elm Creek gauge station at the #65 road crossing from January to October 2017. Data from USGS, 2018.

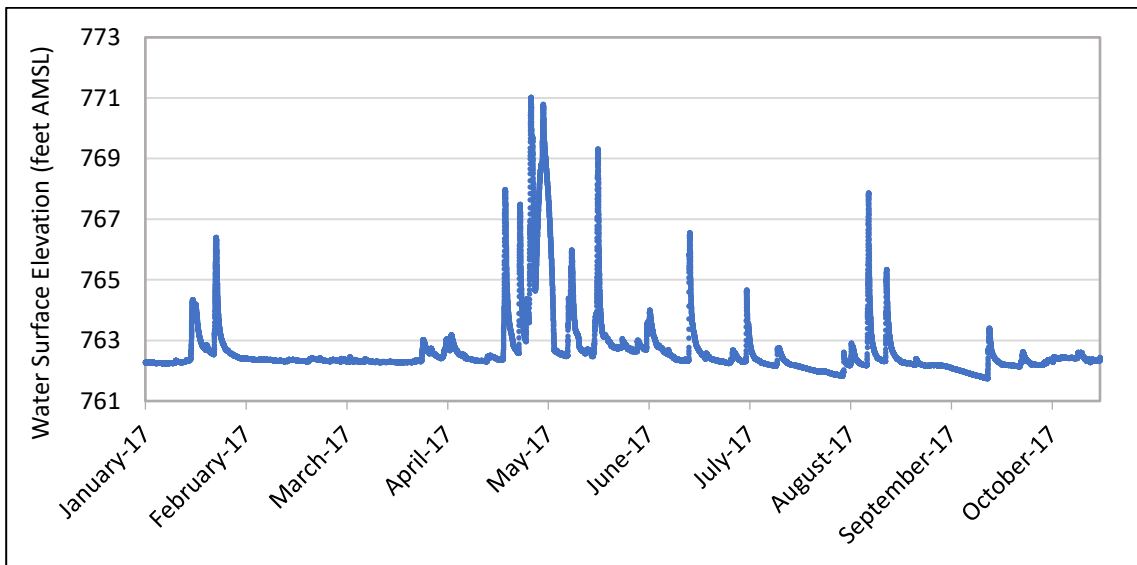


Figure 3.30: USGS water surface elevation at the #65 road crossing at the Elm Creek gauge station from January to October 2017. Data from USGS, 2018.

Reported flows of over 1,500 cfs would most likely cause significant flooding of the upland areas with low elevations around the creek and these flows will likely have

mobilized contamination from runoff. During the high flow in May 2017, the gauge height reported an increase of eight feet which would cause flooding in areas A and C. Swennen et al., (1994) and Dennis et al., (2009) observed greatest concentrations of metal accumulation within lower floodplain areas impacted upstream mining and that uplands 200 m away from the river could also present elevated concentrations. During seasons of high flows and rain, the Neosho river also experiences elevated water levels. This could cause Elm Creek to “backup”, holding water in the uplands for longer durations.

Location B was near a gravel road that ran in the north-south direction within the property. The road was identified before sampling and care was taken to sample off the road. The elevated concentrations at this point could be attributed to possible uses of chat in the dirt road that could be moved by rain, wind or vehicles, however multiple samples were taken along the north/south transect and no other spot reported high concentrations. The lack of other high concentrations makes the origin or cause of this hotspot challenging to identify.

3.3.3 Analysis of the Creek and Uplands

To answer the second hypothesis which stated that sampling locations hydrologically closer to mining influences will have soil lead, zinc, and cadmium concentrations exceeding background levels, soil metals concentrations at increasing distances downstream were compared to background soil concentrations found within

the TSMD. Table 3.7 outlines average background concentrations for lead, zinc, and cadmium found in the Oklahoma, Kansas, and Missouri portions of the TSMD.

Table 3.7: Average background soil concentrations for lead, zinc, and cadmium found in the Oklahoma, Kansas, and Missouri portions of the TSMD

	Oklahoma ¹	Kansas	Missouri
Pb (mg/kg)	31.2	17.0	91.0
Zn (mg/kg)	83.3	44.0	433
Cd (mg/kg)	0.730	0.400	4.10

¹Oklahoma RGs: Pb=500 mg/kg, Zn=1,100 mg/kg, Cd=10.0 mg/kg

*from USFWS (2013), Tri-State Transition Zone Assessment Study

Elm Creek was split into six different groups based on increasing hydraulic distances from the Tar Creek Superfund Site with Group 1 being closest to the Superfund Site and Group 6 being the furthest. Table 3.8 outlines the distance from the headwaters, ending distance, and total distance for each group. Elm Creek terrace soil samples and uplands soil samples that fell within 100 m of the creek for each group were compared to TSMD average background soil concentrations. Upland samples within 100 m of the creek were used as they likely fell within the floodplain and therefore are most likely to have soil trace metals concentrations influenced by the creek. Figure 3.31 presents the locations of each group and the locations of the creek and upland soil sampling locations. The Kruskal-Wallis test was used to compare the lead, zinc, and cadmium background soil concentrations to the soil concentrations in each group. Table 3.9 outlines the descriptive statistics for lead, zinc, and cadmium concentrations in each group and the p-value from the statistical test.

Table 3.8: The distance from the headwaters, ending distance, and total distance for Groups 1-6

	Distance from Headwaters (km)	Ending Distance (km)	Total Length (km)
Group 1	2	7	5
Group 2	9.5	10.5	1
Group 3	10.5	11.5	1
Group 4	11.5	13.5	2
Group 5	13.5	15	2
Group 6	15	17	1.5

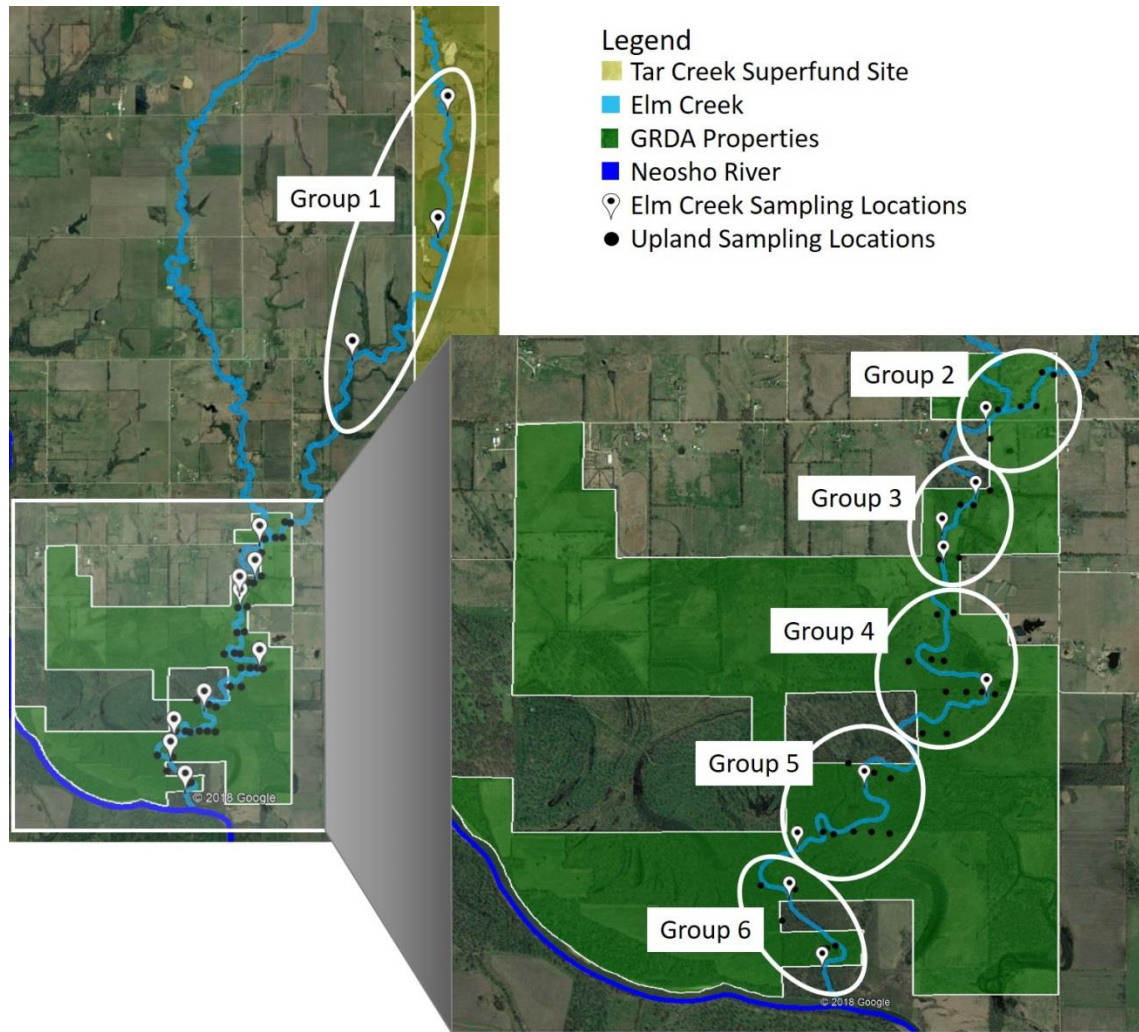


Figure 3.31: The locations of each tested group with Elm Creek terrace sampling locations and upland sampling locations marked within each boundary. All upland samples fell within a 100 m radius of Elm Creek

Table 3.9: The descriptive statistics for lead, zinc, and cadmium concentrations within Groups 1-6 and the corresponding p-value when concentrations are compared to TSMD background concentrations

		n	Mean (mg/kg)	Median (mg/kg)	Std. Dev. (mg/kg)	Min. (mg/kg)	Max. (mg/kg)	p- value ¹	Null Hypothesis ²
Group 1	Pb	18	347	281	190	88.8	800	0.016	Rejected
	Zn	18	3230	2350	1810	1590	7660	0.007	Rejected
	Cd	18	27.5	20.1	15.2	13.7	64.7	0.007	Rejected
Group 2	Pb	12	101	96.0	48.8	35.0	182	0.083	Accepted
	Zn	12	1060	984	587	167	1920	0.014	Rejected
	Cd	12	9.27	8.62	4.94	1.75	16.5	0.014	Rejected
Group 3	Pb	21	86.2	66.0	40.1	22.2	153	0.239	Accepted
	Zn	21	864	856	672	76.8	2590	0.040	Rejected
	Cd	21	8.37	7.54	5.29	2.10	22.1	0.032	Rejected
Group 4	Pb	17	52.1	55.0	20.4	27.5	87.7	0.368	Accepted
	Zn	17	450	474	325	77.7	1050	0.081	Accepted
	Cd	17	4.13	4.32	2.74	1.00	9.15	0.064	Accepted
Group 5	Pb	21	54.2	55.5	31.3	19.7	108	0.570	Accepted
	Zn	21	606	586	368	69.6	1200	0.106	Accepted
	Cd	21	5.44	5.27	3.10	0.93	10.4	0.061	Accepted
Group 6	Pb	17	22.0	20.6	4.76	13.2	31.6	0.266	Accepted
	Zn	17	146	112	108	50.7	429	0.874	Accepted
	Cd	17	1.57	1.30	0.91	0.77	3.95	0.368	Accepted

¹p-value greater than 0.05 = acceptance of null hypothesis

²Null hypothesis = The distributions between variables are identical.

The closest group to the Tar Creek Superfund Site (Group 1) was statistically different from background concentrations for all the metals of interest. The three closest groups to the Tar Creek Superfund Site (Group 1-3) were not like background concentrations for zinc and cadmium. Lead concentrations 9.5 km downstream of the creek origin (within Groups 2-6) reflected background soil concentrations and both zinc and cadmium reflected background soil concentrations two kilometers further at 11.5 km downstream from the creek origin. Because samples hydrologically closer to the Tar Creek Superfund Site exceed background concentrations for lead, zinc, and cadmium, while locations further from the Tar Creek Superfund Site reflected background

concentrations, the hypothesis that sampling locations hydrologically closer to mining influences will have soil lead, zinc, and cadmium concentrations exceeding background levels was accepted.

Finally, the concentrations of trace metals present in the uplands and creek terraces were compared to answer the third hypothesis which stated that upland lead, zinc, and cadmium soil concentrations will be lesser than concentrations present in the stream terraces. All upland samples were compared to the Elm Creek samples taken from terraces in the main stem (10.0 km-17.0 km). The Mann-Whitney U-test was used to determine if there were differences between the uplands and creek concentrations. Table 3.10 outlines the descriptive statistics for lead, zinc, and cadmium in the uplands and creek terrace locations and the corresponding test p-value for each metal.

Table 3.10: Descriptive statistics for lead, zinc, and cadmium in the uplands and creek terrace locations and the test p-value for each metal

	Location	n	Mean (mg/kg)	Median (mg/kg)	Std. Dev. (mg/kg)	Min. (mg/kg)	Max. (mg/kg)	p-value ¹	Null Hypothesis ²
Pb	Uplands	276	39.4	28.3	30.1	9.90	171	1.01E-4	Rejected
	Creek	52	60.0	55.9	39.4	13.2	182		
Zn	Uplands	273	220	172	273	21.1	2070	9.49E-11	Rejected
	Creek	52	680	555	556	50.7	2590		
Cd	Uplands	273	2.22	1.80	1.79	0.67	12.7	9.49E-11	Rejected
	Creek	52	6.05	5.00	4.68	0.77	22.10		

¹p-value greater than 0.05 = acceptance of null hypothesis

²Null hypothesis = The distributions between variables are identical.

The statistical analysis revealed differences between the metals concentrations present the uplands and within the samples taken from the riparian zone of Elm Creek that fall within the GRDA property. The uplands concentrations were lower than the creek concentrations and therefore the hypothesis that the upland lead, zinc, and cadmium

soil concentrations will be lesser than concentrations present in the stream terraces was accepted. This conclusion is logical because trace metals concentrations within the Elm Creek terraces are more likely to meet elevated concentrations from contamination originating in the Tar Creek Superfund Site. The uplands are less likely to be influenced by the Tar Creek Superfund site contamination as they are at greater elevations than the stream terraces and are further away from Elm Creek.

3.4 Conclusions

Analyses of the east branch and main stem of Elm Creek revealed that trace metals concentrations in the terraces decreased with distance from the Tar Creek Superfund Site. No relationship between trace metals concentration and stream terraces could be established. The east and west branches of Elm Creek were found to have statistically different trace metals concentrations and the west branch had statistically lower trace metals concentrations than the east branch for lead, zinc, and cadmium. The hypothesis that the stream branch nearest the mining influence (east branch) will have greater metals concentrations than the stream branch further away from the mining influence (west branch) when comparing samples collected at equal distances upstream from the creek confluence was therefore accepted. The east branch of Elm Creek was found to be the major source of contamination downstream.

Geospatial analysis of the upland environments provided effective visuals and analysis that allowed for determination of areas of interest and reasons for possible contamination. Generated maps revealed two main areas of interest, both falling within

the creek floodplain. Analysis of elevations and creek flow rates during rainfall events revealed that the uplands could easily flood, and high flows could carry trace metals from upstream runoff and deposited them within these areas. Higher concentrations observed near the east and west property boundaries were most likely due to influence from mining waste material, which contains elevated trace metals concentrations, used in the road material (FRC, 2007). Because samples hydrologically closer to the Tar Creek Superfund Site exceed background soil concentrations for lead, zinc, and cadmium, while locations further from the Tar Creek Superfund Site reflected background soil concentrations, the hypothesis that sampling locations hydrologically closer to mining influences will have soil lead, zinc, and cadmium concentrations exceeding background levels is accepted. Statistical analysis found differences between the metals concentrations present the uplands and within the samples taken from the riparian zone of Elm Creek that fell within the GRDA property. The upland concentrations were lower than the creek concentrations and the hypothesis that the upland lead, zinc, and cadmium soil concentrations will be lesser than concentrations present in the stream terraces was accepted.

Areas identified within the creek terraces and upland environments that exceed SQGs and RSs should be resampled and if necessary remediated while areas with no metals impact could be used as areas for mitigation purposes. However, since these elevated concentrations are likely due to upstream source materials being transported downstream, the most effective approach would be to address the problem at the source. Once the source is addressed, downstream concentrations in the riparian and

upland areas close to the stream are likely experience lesser trace metals concentrations as new, cleaner sediment will dilute areas with high trace metals concentrations or “dirtier” riparian soils will be eroded and transported downstream (Miller, 1997). If the source is not addressed, trace metals within the riparian area may compound over time and be much harder to remediate in the future (Juracek and Drake, 2016). The information presented in this study will allow for the GRDA to make educated decisions on land use practices.

Chapter IV: Analysis of Potential Ingestion and Uptake of Lead, Zinc, and Cadmium by White-tailed Deer (*Odocoileus virginianus*) and Associated Human Health Risk in the Elm Creek Watershed

4.1 Introduction

The white-tailed deer (*Odocoileus virginianus*) is one of the most popular big game animals in North America (Bidwell et al., 2017; ODWC, 2017). They are hunted for food as well as for sport. White-tailed deer live in every state in the United States (US) except in more arid regions west of the Rocky Mountains including parts of California, Nevada, Utah, Arizona, New Mexico and Colorado (Deckman, 2003; Bidwell et al., 2017). White-tailed deer live 4.5 years on average with males and females typically living 2.9 and 6.5 years, respectively (Lopez et al., 2003). White-tailed deer are non-migratory and have a relatively small home range of 0.6-5.2 km² and therefore are considered biological indicators of trace metals contamination as residuals in their tissues can be directly associated with a small geographic area (Progulske and Baskett, 1958; Larson et al., 1978; Sawicka-Kapusta, 1979; Sample and Sutter, 1994; Conder and Lanno, 1999; Campbell et al., 2004; Gallina and Lopez, 2016). Vegetation, soil, and water can all be ingestible sources of trace metals to white-tailed deer in contaminated areas (Sample and Sutter, 1994; Beyer et al., 1994; Conder and Lanno, 1999; White, 2006; Garvin et al., 2017).

Many researchers have studied trace metals concentrations in tissues and bones of white-tailed deer in North America (Kocan et al., 1980; Woolf et al., 1982; Sileo and Beyer, 1985; Storm et al., 1994; USACHPPM, 1995; Conder and Lanno, 1999; CH2M, 2017). Studies have found that trace metals, specifically lead, zinc, and cadmium, taken

up into the tissues of white-tailed deer tend to concentrate in the bone, livers, and kidneys (Kocan et al., 1980; Sileo and Beyer, 1985; Storm et al., 1994; Conder and Lanno, 1999; Andrews, 2010; CH2M, 2017). Trace metals concentrations in white-tailed deer liver, kidneys, and heart can be present in equal or greater concentrations than those in the meat (USACHPPM, 1995; Andrews, 2010; CH2M, 2017). The greatest concentrations of lead, zinc, and cadmium were found in the bones (mandibles) in white-tailed deer in the Palmerton Zinc Pile in Pennsylvania and in the Tar Creek Superfund Site in Oklahoma (Storm et al., 1994; Conder and Lanno, 1999). These two sites are listed on the US Environmental Protection Agency's (EPA) National Priorities List and have extensive surface trace metals contamination (Sileo and Beyer, 1985; Storm et al., 1994; USEPA, 1997; Conder and Lanno, 1999; Andrews, 2010; CH2M, 2017). The Palmerton Zinc Pile's trace metals contamination originates from zinc smelting processes which began in the early 1900s and released arsenic, cadmium, chromium, copper, lead, manganese, and zinc via air emissions into the surrounding environment (PDEP, 2010). The Tar Creek Superfund Site in Oklahoma's surface trace metals contamination originates from waste material from underground lead and zinc mining from the late 1800s = to mid-1900s which was left on the surface after operations ceased (USEPA, 2008). White-tailed deer from both locations have been studied for tissue and bone trace metals concentrations, specifically lead, zinc, and cadmium, and were compared to white-tailed deer from background locations (Sileo and Beyer, 1985; Storm et al., 1994; Conder and Lanno, 1999; Andrews, 2010; CH2M, 2017). This study focuses on white-tailed deer residing within the Elm Creek watershed with proximity to the Tar Creek Superfund Site.

4.1.1 Estimating Exposure of Trace Metals Intake into White-tailed Deer

The exposure of any contaminant to wildlife can occur through oral ingestion, dermal contact, or inhalation (Sileo and Beyer, 1985; Sample and Sutter, 1994; Conder and Lanno, 1999; Carpenter et al., 2004; French and Mateo, 2005). The primary exposure pathway of trace metals into white-tailed deer is through oral ingestion of contaminated food, water, and soil (Sample and Sutter, 1994). Exposure from inhalation and dermal contact are considered negligible as ground cover and hair provide effective barriers which reduce possible contact (Camner et al., 1979; Sample and Sutter, 1994). Understanding the life history of a white-tailed deer is necessary to estimate exposure. These site-specific data include body weight, food, water, and soil consumption rates, diet composition, home range, and available habitat (Sample and Sutter, 1994; USACHPPM, 1995; Opresko et al., 1996). These parameters are rarely available for a given area and therefore must be estimated based on existing literature or on estimations from site-specific conditions.

Estimating oral ingestion is often completed by summing the exposure dose of contaminant from food, soil, and water (Sample and Sutter, 1994; USACHPPM, 1995; Opresko et al., 1996). These oral exposure estimates may then be compared to toxicological doses for white-tailed deer estimated by Opresko et al. (1996). Opresko et al., (1996) estimated no observable adverse effects levels (NOAELs) and lowest observable adverse effects levels (LOAELs) for 85 hazardous substances, including lead, zinc, and cadmium, on nine mammalian wildlife species from studies conducted primarily on laboratory rodents. NOAELs are the highest doses that will produce no-

effect or nonhazardous reactions in a population, while LOAELs represent threshold levels where adverse health effects are likely to become apparent (Opresko et al., 1996; Watts, 1998). No visible adverse health effects from lead, zinc, or cadmium poisoning in white-tailed deer were mentioned in any of the studies involving trace metals in tissues of white-tailed deer, therefore, comparing the calculated doses to developed NOAEL and LOAEL data may be the only way to determine poisoning (Sileo and Beyer, 1985; Storm et al., 1994; USACHPPM, 1995; USFWS, 2006).

4.1.2 Human Health Effects Associated with Consumption of Lead, Zinc, and Cadmium

White-tailed deer hunted in areas with trace metals contamination may be a source of trace metals to humans who consume the deer tissue (USACHPPM, 1995; Lopez et al., 2003; Bidwell et al., 2017; ODWC, 2017). Human consumption of materials containing trace metals can lead to a variety of health problems (Smith and Huyck, 1999; ATSDR, 2005; Kabata-Pendias and Mukherjee, 2007; ATSDR, 2007; Żukowska and Biziuk, 2008; ATSDR, 2012). Lead and cadmium are considered probable human carcinogens and lead also is known to directly impact the nervous system of adults. In children, lead is a potent neurotoxin and can cause brain damage, kidney damage, and developmental disorders (ATSDR, 2007; Zota et al., 2011; ATSDR, 2012). Ingestion of cadmium can also cause kidney damage and bone diseases (ATSDR, 2012; Monitha et al., 2012; Qi et al., 2016). Zinc is an essential micronutrient in the human body, however ingestion over the daily recommended 12-15 mg of zinc can decrease the amount of iron in the body, inhibit healing processes and decrease the ability to defend against foreign disease

(NRC, 1989; Gunderson, 1995; Smith and Huyck, 1999; ATSDR, 2005; Kabata-Pendias and Mukherjee, 2007; Roohani et al., 2013).

The determination of safe levels of ingestion of trace metals can be determined by comparing the daily ingested concentration to Minimum Risk Levels (MLRs). MLRs for the oral consumption of contaminants are daily exposure concentrations that exude no substantial risk of adverse health effects (ATSDR, 2005; 2007; 2012; 2017). MLRs for the oral consumption of both zinc and cadmium have been established and are equal to the USEPA's Reference Dose (RfD) values. RfDs are doses based on the NOAEL for a substance and often contain multiple safety factors (Watts, 1998). No oral MRLs or RfDs currently exist for lead, as any exposure is considered to provide unacceptable risk (ATSDR, 2007). Based on the MLRs and RfD values for zinc and cadmium, concentrations exceeding 21 mg/kg of zinc and 0.035 mg/kg of cadmium per day for a 70 kg individual would expose the individual to the possibility of adverse health effects (Watts, 1998; ATSDR, 2005; 2007; 2012). There is no published oral RfD for lead as neurological effects on children can occur at blood lead levels so low that a threshold value could not be established (IRSI, 2004). The World Health Organization (WHO) developed a provisional tolerable weekly intake (PTWI) for lead. The PTWI is the provisional tolerable intake level used for trace metals with cumulative properties (ENHIS, 2009; WHO, 2011). WHO (1993) estimated that a weekly intake of 25.0 μg of lead per kilogram of body weight (0.0036 mg/kg/day) for a 10-kg child multiplied by a conversion factor of 0.160 μg of lead/dL of blood per μg of lead intake per day would result in a blood concentration of 5.70 $\mu\text{g}/\text{dL}$. An example of this calculation is provided below in Equation 4.1.

$$\left(25.0 \frac{\mu g \text{ Pb intake}}{kg \cdot week}\right) \left(\frac{1 \text{ week}}{7 \text{ days}}\right) (10 \text{ kg}) \left(0.160 \frac{\mu g \text{ Pb in blood} \cdot \text{day}}{dL \text{ blood} \cdot \mu g \text{ Pb intake}}\right) \quad (\text{Eq. 4.1})$$

$$= 5.70 \frac{\mu g \text{ Pb}}{dL}$$

This lead concentration of 5.70 µg/dL is below the 7.00 µg/kg lead exposure value that has been shown to cause evidence of causing cognitive defects in children. The U.S. Centers for Disease Control and Prevention uses a reference blood level of 5.00 µg/dL to identify children who have been exposed to lead and will require care from medical professionals (WHO, 1993; CDC, 2017c). This PTWI was extended to both adults and children (WHO, 2011). In 2011, WHO concluded that it was not possible to establish a new PTWI as recent dose-response analysis did not provide any indication of a threshold effect of lead, however, this value is subject to review as new information becomes available (WHO, 2011).

Due to the toxic effects of elevated trace metals in the human body, the uptake of metals from white-tailed deer in contaminated areas poses questions and concerns about the human health risk associated with consuming tissue from these animals (Kocan et al., 1980; Sileo and Beyer, 1985; USACHPPM, 1995; Conder and Lanno, 1999). The human health risk is the likelihood or probability that a harmful consequence or adverse impact will occur as the result of an action or condition (Cardenas, 1999; Tejaswi and Samuel, 2017). Assessing human health risks involves evaluation of both hazards and exposure to an individual or population. Results from these assessments help predict the likelihood of adverse impacts and aid in the implementation of preventative measures or legislation (Cardenas, 1999; Tejaswi and Samuel, 2017).

At this time, only one study was identified that explicitly assessed the human health risks associated with consuming white-tailed deer from a trace metals contaminated area. This study was conducted by the US Army Center for Health Promotion and Preventative Medicine (USACHPPM) at the Aberdeen Proving Ground (APG) located in the upper Chesapeake Bay, Maryland. The APG is a US Army installation for chemical manufacturing. Testing of munitions and military vehicles began in 1917 and is still currently in operation (USACHPPM, 1995; ATSDR, 2008a). Because of chemical manufacturing and munitions testing, the APG is contaminated with organochlorine pesticides, polychlorinated biphenyls, and trace metals (USACHPPM, 1995; ATSDR, 2008a). Concentrations of lead, cadmium, chromium, mercury, and arsenic were measured in the meat, livers, and kidneys of white-tailed deer hunted within the APG and deer from a background area not affected by contamination (USACHPPM, 1995). The USACHPPM (1995) assessed noncancer risk by calculating the daily oral intake of trace metals to humans from consuming deer tissue. The cancer risk from oral ingestion could not be calculated because the slope factors (SF) that are used to determine the probability of carcinogenic effects do not currently exist for the oral ingestion of trace metals (USACHPPM, 1995; Watts, 1998). Parameters for intake were determined by having hunters fill out a questionnaire which helped researchers determine how many years they have been hunting near the APG, how many deer they harvest per year, and what parts of the deer the families consumed (USACHPPM, 1995). The hazard quotient (HQ) for each trace metal was determined by dividing the intake over the RfDs. The hazard index (HI), the calculated parameter for the determination of

noncarcinogenic risk, was determined by summing all the HQ's for arsenic, cadmium, chromium, and mercury. A HI less than 1 indicates that no adverse human health effects from exposure to given concentrations are expected to occur, while a HI exceeding 1 indicates that exposure to the given concentrations of contaminants may cause harm to human health (USACHPPM, 1995; Watts, 1998). Arsenic (HQ=1.2) contributed most to the potential risk from the consumption of meat, however, researchers determined that this was an overestimation as the toxicity values were derived from inorganic arsenic instead of the less toxic organic form. The researchers did not know if the arsenic in the deer was organic or inorganic but assumed that it was mostly organic arsenic. The study found that the HI exceeded 1.0 for consumption of the meat (HI=1.5), but not the liver (HI=0.30) from a white-tailed deer within the APG. The HI for the consumption of the kidney was not calculated as only one of the 103 individuals surveyed ate the kidney. Although the HI exceeded 1.0 for the APG deer meat, researchers concluded that the consumption of APG deer should not present an elevated human health hazard due to possible overestimation of the risk from arsenic.

Human health risks within the Tar Creek Superfund Site have been linked to trace metals exposure from the mining waste (Wright et al., 2006; Neuberger et al., 2009; Zota et al., 2011). Wright et al., (2006) found that the IQ scores of students in the local school system were inversely related to verbal IQ scores and hair manganese and arsenic concentrations (Wright et al., 2006). Neuberger et al., (2009) studied the mortality of community members and found that from 1980 to 1985 there were a statistically significant number of deaths from heart disease, stroke, and kidney disease which are

all linked to exposure to lead and cadmium (ATSDR, 2007; 2012). Neuberger et al., (2009) concluded that although deaths in the community related to such issues are declining, (possibly due to members moving away), there is rising concern about the safety of eating locally grown food, fish, and other sources of food from this area has risen due to possible metals exposure (USEPA, 1997). The Oklahoma Department of Environmental Quality recommended that individuals restrict consumption of catfish and non-game fish from the surrounding rivers (Neosho and Spring Rivers) and from Grand Lake as these fish had high enough lead concentrations to cause human harm (ODEQ, 2008). Garvin et al., (2017) found that plants within the floodplain of the Tar Creek Superfund Site contained greatest metals concentrations in the roots and “low-lying leafy greens” and posed a significant health risk to natives who gather local plants.

There were two objectives associated with this portion of the study: 1) estimate and quantify potential ingestion and uptake of lead, zinc, and cadmium by white-tailed deer living in a mining-impacted watershed and 2) evaluate the human health risk associated with the consumption of white-tailed deer tissue harvested from a lead and zinc mining impacted watershed. It was hypothesized that consuming white-tailed deer tissue from within a mining impacted watershed, specifically the Elm Creek Watershed in Ottawa County, Oklahoma, will expose humans to unacceptable risk for lead, zinc, and cadmium.

4.2 Methods

4.2.1 Site Description

The Elm Creek watershed located in Ottawa County, Oklahoma, is impacted by trace metal contamination from the Tar Creek Superfund Site, which is the Oklahoma portion of the Tri-State Lead and Zinc Mining District (USFWS, 2013; Nairn, 2014a). Extensive mining operations for zinc and lead, beginning in the 1890s and continuing until the 1970s, left extensive trace metal contamination on the surface which remains exposed to this day (USEPA, 1997; Datin and Cates, 2002; White, 2006; USEPA, 2008; Andrews, 2011; USFWS, 2013). These residuals, which are readily transportable by water and wind, pose potential human health and ecological risks (Miller, 1997; USEPA, 2008; ATSDR 2008). Lead, zinc, and cadmium concentrations surrounding the Tar Creek Superfund Site are of primary concern due to their ability to have toxic effects on the human body (USEPA, 2008).

A portion of the east branch of the Elm Creek watershed is in the Tar Creek Superfund Site (Figure 4.1). This branch of Elm Creek can transport and deposit trace metals to portions of the watershed outside of the Superfund boundaries as water can easily carry the small particulates (Miller, 1997).

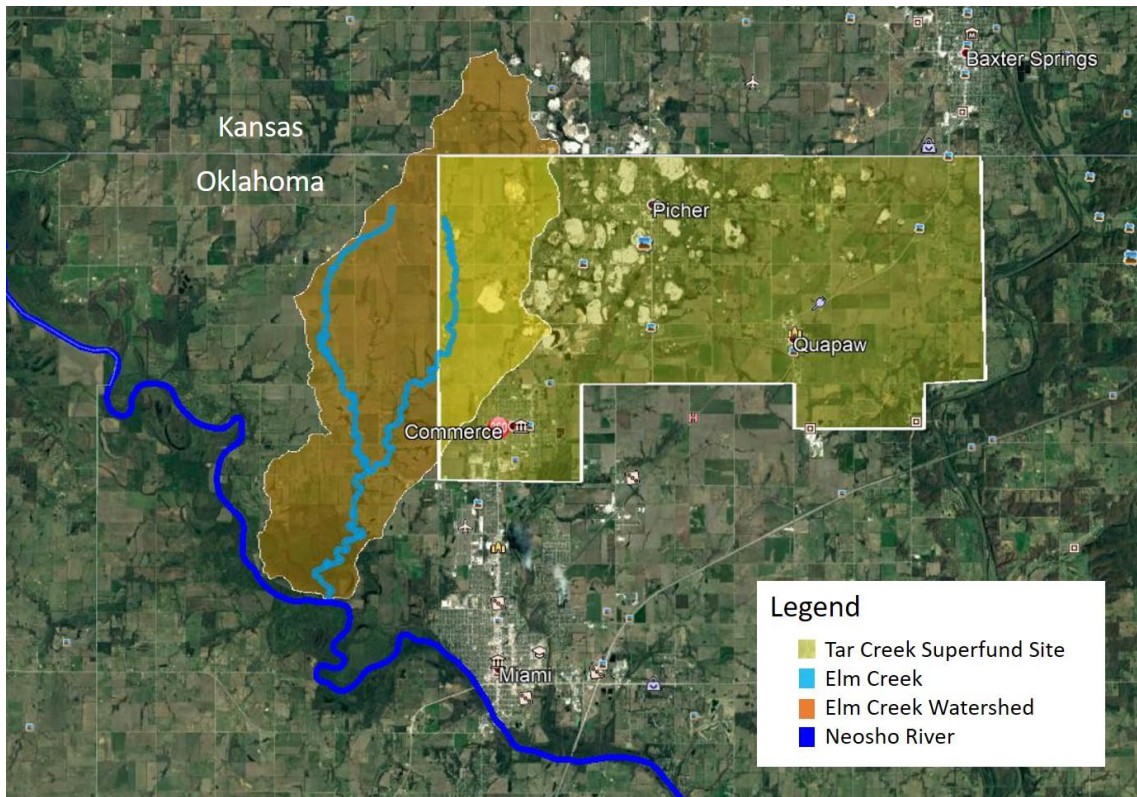


Figure 4.1: The Elm Creek watershed, Elm Creek, and Tar Creek Superfund Site locations and areas, Ottawa County, Oklahoma (Google Earth, 2018)

White-tailed deer that live within this watershed are exposed to trace metals through ingestion of local water, soils, and forage (Figure 4.2) (Sample and Sutter, 1994; Beyer et al., 1994; White, 2006; Conder and Lanno, 1999; Garvin et al., 2017). These deer are potential sources of contaminated flesh, organs, and by-products to humans who eat deer hunted in this area (Conder and Lanno, 1999; Andrews, 2010; CH2M, 2017; ODWC, 2017). The Oklahoma Department of Wildlife Conservation (ODWC) reported that 1,351 deer were harvested by hunters in Ottawa County in 2016 (ODWC, 2017). Although the Tar Creek Superfund Site and portions of the Elm Creek watershed have trace metals contamination, hunting in these areas is not restricted (Conder and Lanno, 1999; CH2M, 2017). The Grand River Dam Authority (GRDA) partners with the Mid-

America Chapter of the Paralyzed Veterans of America (PVA), which allows paralyzed veterans to hunt white-tailed deer on properties owned by the GRDA in the Elm Creek Watershed (GRDA, 2016).



Figure 4.2: Two white-tailed deer grazing in the GRDA-owned properties in the Elm Creek Watershed on August 5, 2017. Photo provided by Aaron Roper of GRDA

4.2.2 Estimation of Lead, Zinc, and Cadmium Ingestion and Uptake by White-Tailed Deer

A model was developed to estimate ingestion and uptake of lead, zinc, and cadmium to white-tailed deer living within the Elm Creek Watershed. The ingestion model assumes that ingestion through dermal and inhalation are negligible and therefore the total exposure is equal to the oral exposure. Oral exposure is broken down

into ingestion of lead, zinc, and cadmium through consumption of vegetation, soil, and water.

4.2.2.1 Estimated Ingestion from Plant Matter

Adult white-tailed deer weigh between 45-68 kg and eat a wide variety of browse (leaves, twigs, nuts, and woody plants), forbs (weeds, broad-leafed vegetation, flowering plants), and grasses (including sedges and rush families) (Sample and Sutter, 1994; Gee et al., 2011; Bidwell et al., 2017). Bidwell et al. (2017) estimated that a healthy 65 kg white-tailed deer eats on average 8.1 kg or 12.5% of its body weight of forage per day and prefers forbs and grasses when available. A detailed breakdown of white-tailed deer diets in the Cross Timbers ecoregion of Oklahoma, a region close Ottawa County, was presented in Gee et al. (2011). The report by Gee et al. (2011) estimated that deer consume approximately 41% browse, 44% forbs, and 15% grasses annually. The percentages of annual forage described by Gee et al. (2011) were multiplied by median trace metals concentrations in grasses, forbs, and browse for lead, zinc and cadmium to determine the weighted average concentration for each trace metal.

Median trace metals concentrations in grasses were determined by White (2006) from trace metals concentrations present in species listed in Table 4.1 grown on mine tailings from the Tar Creek Superfund Site. Mine tailings are mining wastes that contain elevated concentrations of trace metals (White, 2006). Grasses grown on metals-rich mine tailings may not lead to higher aboveground biomass trace metals concentrations when compared to grasses grown in a sand or washed quartz gravel (Levy et al., 1999;

White, 2006). Levy et al. (1999) found no significant differences in trace metals concentrations of copper, cadmium, iron, lead, and zinc in big bluestem and switchgrass grown in mine tailings and a control media of washed quartz. White (2006) found that big bluestem and switchgrass roots accumulate the bulk of the trace metals and therefore making the availability of trace metals to wildlife less likely. The median metals concentrations in forbs was determined from trace metals concentrations in forb-like plants listed in Table 4.1 in a study by Garvin et al. (2017) near Elm Creek. Median metals concentrations in browse were determined from a study by Andrews (2011), where upland trees in the Tri-State Mining District were sampled for trace metal concentrations in the bark, twigs, leaves and nuts of a variety of tree species listed in Table 4.1. Table 4.2 summarizes the median lead, zinc, and cadmium concentrations for grasses, forbs, and browse.

Table 4.1: The common and scientific names for each plant used to determine forage trace metals concentrations from White (2006), Garvin et al., (2017), and Andrews (2011)

Forage Type	Common Name	Scientific Name	Source
Grasses	Big bluestem	<i>Andropogon gerardi</i>	White (2006)
	Indian grass	<i>Sorghastrum nutans</i>	
	Little bluestem	<i>Schizachyrium scoparium</i>	
	Switchgrass	<i>Panicum virgatum</i>	
Forbs	Black brush	<i>Coleogyne ramosissima</i>	Garvin et al. (2017)
	Broadleaf plantain	<i>Plantago major</i>	
	Buttercup	<i>Ranunculus repens</i>	
	Common milkweed	<i>Asclepias syriaca</i>	
	Curlydock	<i>Rumex crispus</i>	
	Dandelion	<i>taraxacum</i>	
	Elderberry	<i>Sambucus</i>	
	Green dragon	<i>Arisaema dracontium</i>	
	Greenbrier	<i>Smilax rotundifolia</i>	
	Pawpaw	<i>Asimina trilobal</i>	
Wild blackberry	<i>Rubus occidentalis</i>		
Browse	American elm	<i>Ulmus americana</i>	Andrews (2011)
	American sycamore	<i>Platanus occidentalis</i>	
	Black hickory	<i>Carya texana</i>	
	Black oak	<i>Quercus velutina</i>	
	Pin oak	<i>Quercus palustrus</i>	
	Plains cottonwood	<i>Populus deltoides monilifera</i>	
River birch	<i>Betula nigra</i>		

Table 4.2: Median concentrations of lead, zinc, and cadmium in potential forage for white-tailed deer in the Elm Creek Watershed

Forage Type	Estimated percentage of annual diet	Lead (mg/kg)	Zinc (mg/kg)	Cadmium (mg/kg)	Source
Grasses	15%	43.1	622	7.57	White (2006)
Forbs	44%	10.9	220	2.04	Garvin et al. (2017)
Browse	41%	4.00	500	4.00	Andrews (2011)
Weighted means of median plant concentrations	100%	12.9	395	3.67	

4.2.2.2 Estimated Ingestion from Soil

In addition to ingesting metals from plant materials, a relatively small amount of soil is ingested by deer from consumption of roots from forbs and grasses, grooming, and direct ingestion of soil for minerals (Sample and Sutter, 1994; Beyer et al., 1994). Beyer et al., (1994) found that up to 2% of the white-tailed deer daily diet can consist of direct ingestion of soil for sodium needs. For this study, an assumption that 4% of the overall daily food consumption for deer was soil was used. This value will account for direct consumption of soil for minerals and salt (2% from Beyer et al., (1994)), ingestion of soil from roots (1%), and ingestion of soil from grooming (1%) (Sample and Sutter, 1994; Beyer et al., 1994).

Median concentrations of lead (28.5 mg/kg) and zinc (126 mg/kg) from soils in the Elm Creek watershed were determined from 277 and 275 soil samples, respectively, using a handheld field portable X-ray fluorescence (XRF) spectrometer following USEPA Method 6020. The median cadmium concentration (1.40 mg/kg) was determined via

regression from XRFs zinc concentrations from the same dataset (n=275). Table 4.3 summarizes the soil metals concentrations for lead, zinc, and cadmium.

Table 4.3: Summary statistics of lead, zinc, and cadmium concentrations in soil samples collected in the Elm Creek watershed upland environment.

Metal	n	Mean (mg/kg)	Median (mg/kg)	Max. (mg/kg)	Min. (mg/kg)	Std. Dev. (mg/kg)	Std. Error (mg/kg)
Pb	277	39.2	28.5	171	9.90	30.0	1.81
Zn	275	220	126	2070	21.2	272	16.4
Cd	275	2.20	1.40	17.7	0.520	2.30	0.138

4.2.2.3 Estimated Ingestion from Water

Estimated ingestion of trace metals in water by white-tailed deer was based on a daily water intake of 0.063 L/kg-day (4.28 L/day for a 68 kg deer) (Bidwell et al., 2017). Average trace metals concentrations in unfiltered water samples from Elm Creek were determined by the Center for Restoration of Ecosystems and Watersheds (CREW) laboratory at the University of Oklahoma from 2005-2008 for lead (0.04 mg/L), zinc (4.88 mg/L), and cadmium (0.031 mg/L). Samples were obtained from the County Road E30 road crossing over Elm Creek’s east branch (Figure 4.3). Table 4.4 summarizes the water trace metals concentrations for lead, zinc, and cadmium.

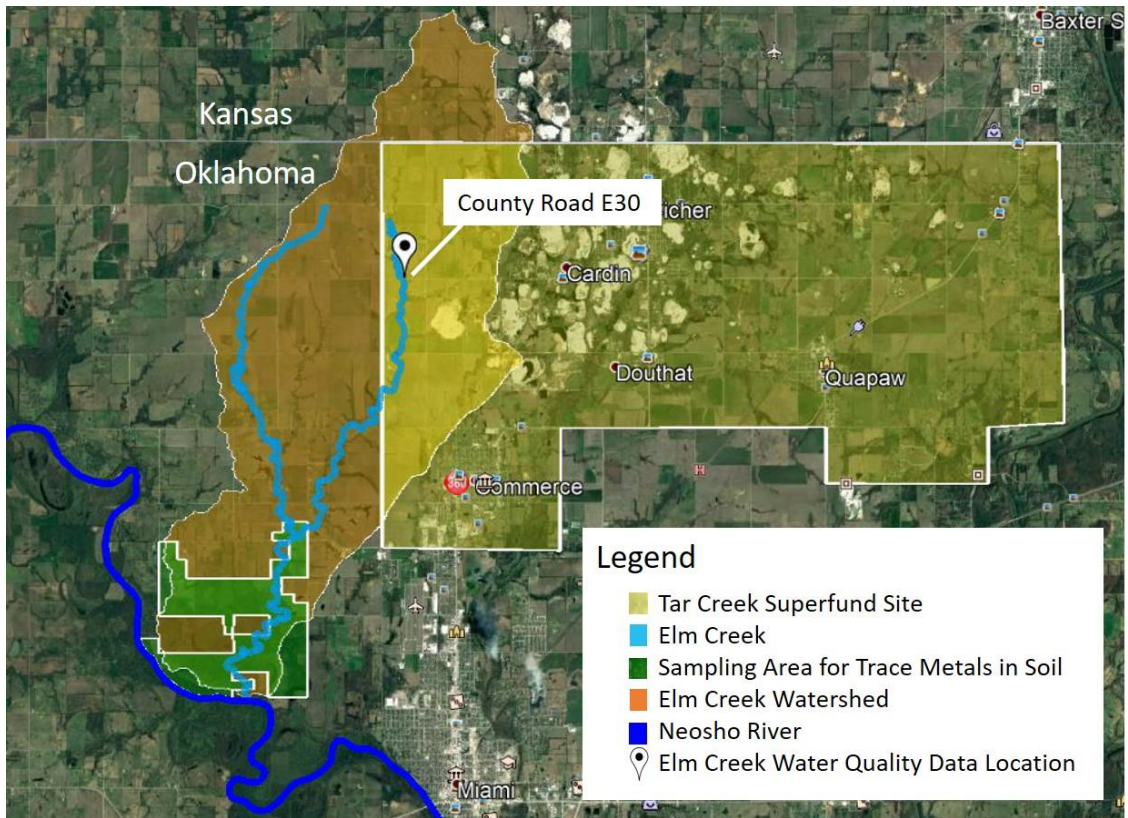


Figure 4.3: The locations of the Tar Creek Superfund Site, Elm Creek, Elm Creek watershed, the water quality data location, and the soil trace metal concentration area, located in Ottawa County, OK (Google Earth, 2018)

Table 4.4: Summary statistics of unfiltered lead, zinc, and cadmium concentrations in water samples collected by CREW at the east Elm Creek County Road E30 road crossing, Ottawa County, OK, 2005-2008

Metal	n	Range (mg/L)	Mean (mg/L)	Median (mg/L)	Standard Error (mg/L)
Pb	21	0.013-0.081	0.040	0.033	0.004
Zn	24	0.910-12.9	4.88	3.89	0.670
Cd	24	0.007-0.077	0.031	0.025	0.004

4.2.2.4 Estimated Total Ingestion

For this model, total ingestion was calculated for a 68 kg white-tailed deer. Assumptions on the percent intake from food (split into plant matter and soil) and water per day based on literature from Sample and Sutter (1994), Beyer et al. (1994), and Bidwell et al. (2017) are summarized in Table 4.5. The daily mass and volume

consumption of plant matter, soil, and water for a 68 kg deer are also presented in Table 4.5.

Table 4.5: Daily food and water consumption values for a 68 kg white-tailed deer

	Total % of Body Weight Consumed per Day		Daily Consumption for 68 kg Deer		Source
Food	12.5%	Plant Matter	8.16	kg/day	Bidwell et al. (2017)
		Soil (4% of daily food)	0.340	kg/day	Sample and Sutter (1994); Beyer et al. (1994)
Water	6.3%		4.28	L/day	Bidwell et al. (2017)

The daily consumption rates for a 68 kg deer were multiplied by the median trace metals concentrations for lead, zinc, and cadmium in the plant matter (Equation 4.2), soil (Equation 4.3), and water (Equation 4.4). These values were then summed to determine total ingestion (Equation 4.5). The total ingestion was multiplied by a transfer coefficient for each metal determined by the International Atomic Energy Agency (IAEA, 2010) to determine an estimated tissue concentration (Equation 4.6). The transfer coefficients provided by IAEA are for the prediction of radioisotope transfer into the meat of ruminants. Although different isotopes for an element have variances in nuclear stability, they still share similar chemical properties and in many cases the radioisotope of an element will be present in identical proportions to their stable counterpart in an organism (National Academy of Sciences, 1971; Philips and Rainbow, 1993). Therefore, the transfer coefficients determined by IAEA for sheep will be used for white-tailed deer as both animals are ruminants and share similar gastrointestinal

tracts (Huston et al., 1986). Sheep have a greater ability to digest organic matter than deer, so the minimum transfer coefficient values for sheep will be used for white-tailed deer in this study (Huston et al., 1986). Currently there are no data for trace metal transfer coefficients into the meat of white-tailed deer.

$$I_{Plant\ Matter} = (C_{Plant\ Matter} \times D_{Plant\ Matter}) \quad (\text{Eq.4.2})$$

$$I_{Soil} = (C_{Soil} \times D_{Soil}) \quad (\text{Eq.4.3})$$

$$I_{Water} = (C_{Water} \times D_{Water}) \quad (\text{Eq.4.4})$$

Where:

$I_{Plant\ Matter}$ = Estimated daily intake for plant items ($\text{mg}_{\text{metal}}/\text{day}$)
 $C_{Plant\ Matter}$ = Plant matter trace metal concentration ($\text{mg}_{\text{metal}}/\text{kg}$)
 $D_{Plant\ Matter}$ = Daily plant matter consumption (kg/day)

I_{Soil} = Estimated daily intake for soil ($\text{mg}_{\text{metal}}/\text{day}$)
 C_{Soil} = Soil trace metal concentration ($\text{mg}_{\text{metal}}/\text{kg}$)
 D_{Soil} = Daily soil consumption (kg/day)

I_{Water} = Estimated daily intake for water ($\text{mg}_{\text{metal}}/\text{day}$)
 C_{Water} = Water metal concentration ($\text{mg}_{\text{metal}}/\text{L}$)
 D_{Water} = Daily water consumption (L/day)

$$TI = \sum I_{Plant\ Matter} + I_{Soil} + I_{Water} \quad (\text{Eq.4.5})$$

Where:

TI = Total Ingestion ($\text{mg}_{\text{metal}}/\text{day}$)
 $I_{Plant\ Matter}$ = Estimated daily intake for plant items ($\text{mg}_{\text{metal}}/\text{day}$)
 I_{Soil} = Estimated daily intake for soil ($\text{mg}_{\text{metal}}/\text{day}$)
 I_{Water} = Estimated daily intake for water ($\text{mg}_{\text{metal}}/\text{day}$)

$$ETC = TC \times TI \quad (\text{Eq.4.6})$$

Where:

- ETC = Estimated Tissue Concentration (mg_{metal}/day)
- TC = Transfer Coefficient (day/kg)
- TI = Total Ingestion (mg_{metal}/day)

4.2.3 Evaluation of Risk to Humans from Consumption of White-Tailed Deer

To investigate the potential health risks to people in Ottawa County, Oklahoma, the average daily dose (ADD) of trace metals through oral ingestion of white-tailed deer meat was calculated. The ADD is the amount of trace metal ingested per kilogram of body weight per day. The calculated ADD (Equation 4.7) was used to estimate the hazard quotient (HQ) for consumption of lead, zinc, and cadmium individually. These HQ's were then summed to determine the hazard index (HI) for lead, zinc, and cadmium.

$$ADD = \frac{CW \times IR \times EF \times ED}{BW \times AT} \quad (\text{Eq.4.7})$$

Where:

- ADD = average daily dose (mg/kg/day)
- CW = contaminant concentration (mg/kg)
- IR = ingestion rate (kg/day) or (kg/meal)
- EF = exposure frequency (days/year) or (meals/year)
- ED = exposure duration (years)
- BW = body weight (kg)
- AT = averaging time (days) (ED · 365 days/year)

The contaminant concentration (CW) is the average trace metal tissue concentration present in the white-tailed deer (mg/kg). The ingestion rate (IR) is the mass of deer tissue ingested per day. For this study, an 8 oz (0.23 kg) steak size per day will be used. The exposure frequency (EF) is the total time of exposure to the contaminant. This study assumes that the individual will consume deer meat once a

week. Exposure duration (ED) is the time that the individual is exposed to the source of contamination. The ED for this report is the number of years a human eats animal tissue in their lifetime. Assuming the average person consumes animal tissue starting at eight years old, and the average lifespan of an average American is 78 years, an ED of 70 years will be used (CDC, 2017a). Body weight (BW) is the average weight of the individual studied during the exposure period. Although the standard value for body weight is 70 kg, today the average American adult weights 83 kg with the obesity rate in Oklahoma at 35.2% (2% higher than the national average) (CDC, 2016; CDC, 2017b). For this calculation, a BW of 83 kg will be used as it is representative for a population in the State of Oklahoma. The averaging time (AT) is average time for exposure and for non-carcinogens the AT is the ED multiplied by 365 days/year (Watts, 1998; Garrido et al., 2017). This method follows a conservative approach which tries to simulate a “worst-case” scenario as this amount of deer consumption is unlikely for the length of time designated. The input parameters for the ADD are summarized in Table 4.6.

Table 4.6: Input parameters to determine the average daily dose for lead, zinc, and cadmium for humans consuming white-tailed deer within the Elm Creek Watershed

Parameter		Value		Explanation
Contaminant Concentration	CW		mg/kg	Dependent on each trace metal (Pb, Zn, and Cd) tissue concentration in white-tailed deer
Ingestion Rate	IR	0.23	kg/meal	Assuming one 8 oz “steak” is consumed per meal (converted to kg)
Exposure Frequency	EF	52	meals/year	Consumption of deer tissue once a week
Exposure Duration	ED	70	years	Number of years an individual eats deer tissue in their lifetime
Body Weight	BW	83	kg	Average American body weight in 2017
Averaging Time	AT	25550	days	ED × 365 days/year

The potential for adverse health effects to occur was evaluated by comparing the oral ingestion of metals to the oral RfD. The HQs were calculated for lead, zinc, and cadmium (Equation 4.8). The HQ is the ratio of the daily intake or ADD to the RfD for each trace metal and represents the probability of absence or presence of harm resulting from exposure to a single noncarcinogen (Watts, 1998). A HQ less than 1 indicates that no adverse human health effects from exposure to a given concentration of a single noncarcinogens are expected to occur (USACHPPM, 1995). A HQ exceeding 1 indicates that exposure to the given contaminant concentration can cause harm to human health (USACHPPM, 1995; Watts, 1998).

$$HQ = \frac{ADD}{RfD} \quad (\text{Eq.4.8})$$

Where:

- HQ = the hazard quotient (dimensionless)
- ADD = average daily intake (mg/kg/day)
- RfD = reference dose (mg/kg/day)

Non-carcinogenic risk was calculated by summing the hazard quotients for lead, zinc, and cadmium to determine a hazard index value (HI) (Equation 4.9).

$$HI = \sum HQ \quad (\text{Eq.4.9})$$

Where:

- HI = the hazard index (dimensionless)
- HQ = the hazard quotients (dimensionless)

A HI less than 1 indicates that no adverse human health effects are expected to occur from exposure to given concentrations (USACHPPM, 1995; Watts, 1998). A HI exceeding 1 indicates that exposure to the given concentrations of contaminants may cause harm to human health (USACHPPM, 1995; Watts, 1998). There is no published oral RfD for lead as neurological effects on children can occur at blood lead levels so low that a threshold value could not be established (IRSI, 2004). The World Health Organization (WHO) developed a provisional tolerable weekly intake (PTWI) for lead (2011). For this study, the PTWI of 0.0036 mg/kg/day was used as an oral RfD for lead. Established oral RfD for zinc (0.3 mg/kg/day) and cadmium (0.0005 mg/kg/day) were also used to calculate the HI (Watts, 1998; ATSDR, 2017).

4.3 Results and Discussion

4.3.1 Determination of Possible Adverse Effects to White-tailed Deer

The estimated total ingestion in mg/kg/day for ingestion of plant matter, soil, and water are presented in Table 4.7. To determine if adverse health effects would be apparent from the trace metals ingestion by white-tailed deer within the Elm Creek watershed, the estimated total ingestion was compared to NOAEL and LOAEL values estimated for white-tailed deer by Opresko et al., (1996). Because no visible adverse health effects from lead, zinc, or cadmium poisoning in white-tailed deer were mentioned in any of the studies involving trace metals in tissues of white-tailed deer, comparing the calculated doses to developed NOAEL and LOAEL data may be the only way to determine poisoning (Sileo and Beyer, 1985; Storm et al., 1994; USACHPPM, 1995; USFWS, 2006). The daily ingestion for white-tailed deer within the Elm Creek Watershed for plant matter, soil, water, and the total sum, are presented in Table 4.7. The NOAEL and LOAEL for white-tailed deer estimated by Opresko et al. (1996) are also included in Table 4.7 for reference.

Table 4.7: The daily ingestion of lead, zinc, and cadmium for plant matter, soil, and water and corresponding NOAELs and LOAELs for the consumption of lead, zinc, and cadmium for white-tailed deer determined by Opresko et al. (1996)
[all units in mg/kg/day]

	Plant Matter Ingestion	Soil Ingestion	Water Ingestion	Total Ingestion	NOAEL	LOAEL
					Opresko et al. (1996)	
Pb	1.54	0.142	0.0025	1.69	2.24	22.4
Zn	47.4	0.632	0.307	48.3	50.0	90.0
Cd	0.440	0.007	0.002	0.449	0.271	2.71

The total daily ingestion for lead and zinc falls below the NOAEL and LOAEL for white-tailed deer and therefore lead and zinc consumption by white-tailed deer are unlikely to observe adverse health effects based on the concentrations ingested. The total daily ingestion for cadmium exceeds the NOAEL but not the LOAEL. This daily ingestion concentration of cadmium could possibly cause adverse health effects to white-tailed deer within this watershed, although the concentration does fall closer to the NOAEL. This information was presented to evaluate possible adverse health effects to white-tailed deer from estimated consumption of trace metals.

4.3.2 Estimation of Tissue Concentration in White-tailed Deer

Estimated ingestion rates and the tissue concentration for a 68 kg white-tailed deer are presented in Table 4.8. These values were calculated by multiplying the values from Table 4.7 by a 68 kg deer body mass.

Table 4.8: Estimated ingestion rates for a 68 kg white-tailed deer in the Elm Creek watershed

	Plant Matter Ingestion (mg/d)	Soil Ingestion (mg/day)	Water Ingestion (mg/day)	Total Ingestion (mg/day)	Transfer Coefficient* (d/kg)	Estimated Tissue Concentration (mg/kg)
Pb	105	9.69	0.171	115	0.004	0.460
Zn	3220	42.9	20.9	3290	0.020	65.7
Cd	29.9	0.476	0.133	30.5	0.007	0.217

*from International Atomic Energy Agency (2011) for minimum radionucleotide transfer to sheep meat

The soil trace metals concentrations determined within the Elm Creek watershed in Chapters 3 had little impact on the overall trace metals tissue concentration in the white-tailed deer. Trace metals from ingested plant matter had the greatest influence

on the total ingestion for white-tailed deer while ingestion from water had the least influence. Plant matter made up of most of the white-tailed deer diet while soils only made up 4%. Although the white-tailed deer was estimated to drink 4.58 L of water per day, the median concentrations of trace metals were the lowest when compared to concentrations in soil and plant matter.

In November 2017, as part of U.S. EPA Tar Creek Operable Unit 5 efforts, white-tailed deer tissues were “opportunistically” sampled during the deer hunting season and the tissues collected were analyzed for trace metals concentrations in Ottawa County, OK (CH2M, 2017). Four male white-tailed deer (three killed in the Elm Creek Watershed and one killed in the Tar Creek Superfund Site just outside of the Elm Creek watershed) weighing 60 kg on average, had trace metal tissue concentrations averaged for heart, liver, and meat. The one deer killed in the Tar Creek Superfund Site deer had concentrations for trace metals in the kidneys, however since kidney data were not provided for the other three deer, kidney metals concentrations were not used in this analysis. It is important to note that the Tar Creek Superfund Site white-tailed deer was the youngest and smallest (by weight) of all four-white-tailed deer and had comparable tissue concentrations to the older and larger Elm Creek white-tailed deer. The breakdown of ages and weights for all four deer are provided in Table 4.9. The approximate locations where these white-tailed deer were harvested and the locations where water, soil, and food trace metals concentration data used in the model are all within a 40 km² area (Figure 4.4).

Table 4.9: The breakdown of all four white-tailed deer genders, ages, and approximate weights from CH2M (2017)

	Watershed	Gender	Deer Age (years)	Approximate Weight (kg)
Elm Creek Deer 1	Elm Creek	Male	3-4	68
Elm Creek Deer 2	Elm Creek	Male	1-2	55
Elm Creek Deer 3	Elm Creek	Male	5-6	80
Tar Creek Deer 1	Tar Creek	Male	1	36

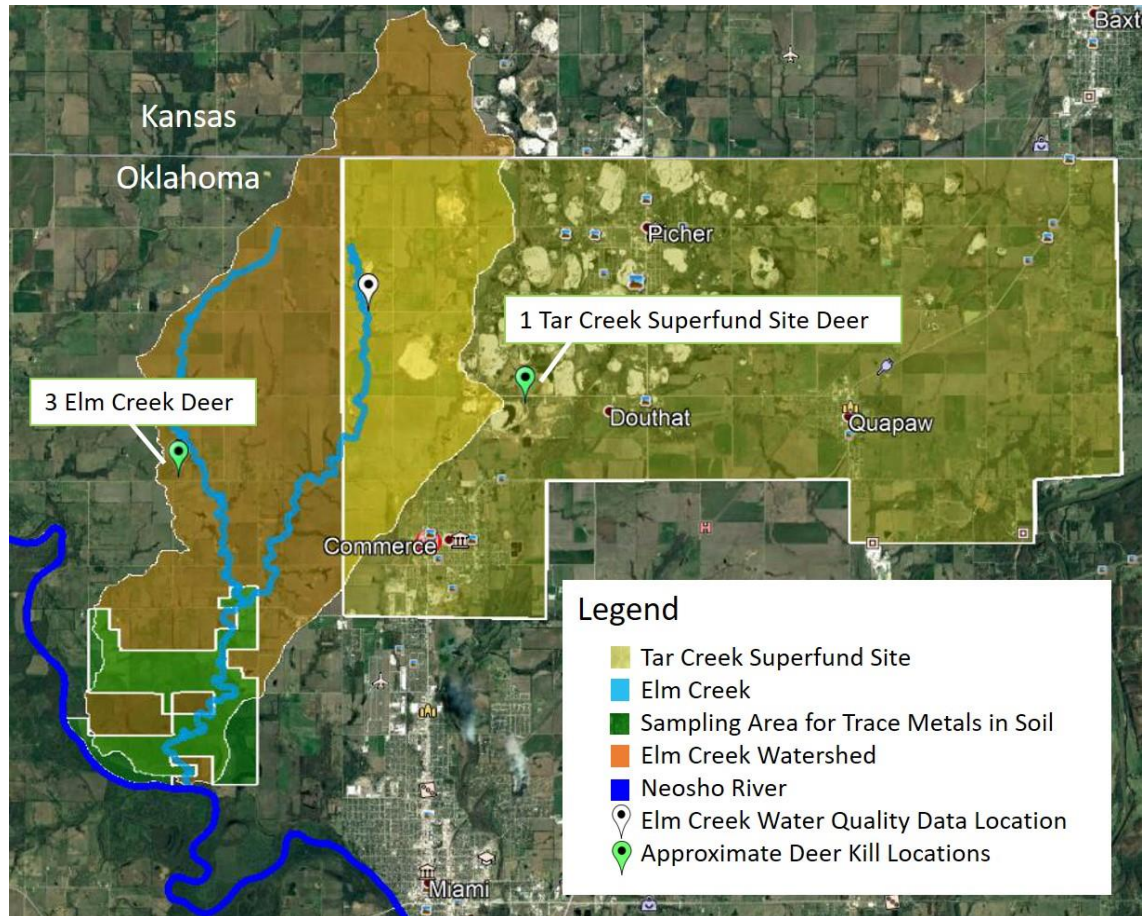


Figure 4.4: The locations of the Tar Creek Superfund Site, Elm Creek and corresponding watershed, the water quality data location, and the soil trace metal concentration area with respect to where the white-tailed deer were hunted, Ottawa County, OK

Due to the proximity of hunted white tailed deer and the location of model parameters, the trace metal tissue concentrations estimated in this study’s model and the actual trace metals concentrations in white-tailed deer determined by the CH2M (2017) study were compared. Table 4.10 outlines the average weighted tissue

concentrations for the heart, liver, meat, and total average for the harvested white-tailed deer, along with the estimated tissue concentrations from this study's model. Average weighted tissue concentrations for a 68 kg deer were determined by assuming a mass of 0.500 kg for the heart (0.74% of body weight), a mass of 1.40 kg for the liver (0.02% of body weight), and a mass of 35.4 kg for muscle (52% of body weight) (McCullough and Ullrey, 1983; Parra, 2012).

Table 4.10: The tissue concentrations for the heart, liver, meat, and total weighted average for white-tailed deer determined by CH2M (2017) along with the estimated tissue concentrations from this study

	Average Heart Tissue (mg/kg)	Average Liver Tissue (mg/kg)	Average Meat Tissue (mg/kg)	Average Total Tissue (mg/kg)	Estimated Tissue Concentration (mg/kg)
	(Deer tissue samples from CH2M (2017))				(this study model)
Pb	0.450	0.420	0.460	0.450	0.460
Zn	18.0	35.9	29.3	29.4	65.7
Cd	0.310	0.340	0.160	0.170	0.221

The estimated concentration of lead and cadmium in white-tailed deer tissue was similar to the actual average concentration in the samples harvested from the area. Lead concentrations in all tissue types was consistent, however, more cadmium was present in the heart and liver tissue than the meat tissue for the CH2M (2017) white-tailed deer. The literature states that cadmium accumulates in the livers and kidneys of deer and therefore different transfer coefficient into different organs are likely to apply (Sileo and Beyer, 1985; Conder and Lanno, 1999). Each transfer coefficient used for lead, zinc, and cadmium in the model was specific to transfer into only the meat of sheep and therefore more accurate organ-specific transfer coefficients are necessary to predict

cadmium in the heart and liver of the white-tailed deer. The estimated concentration of zinc is 2.2 times the actual average tissue concentration in the white-tailed deer sample. The overestimation of zinc may be due to differences in behavior of zinc as a trace element than as a radionuclide, however it is most likely due to zinc's properties as a required nutrient (National Academy of Sciences, 1971; Philips and Rainbow, 1993). Zinc is an essential micronutrient and is poorly stored in the tissues of white-tailed deer and therefore acts differently than lead and cadmium which concentrate in tissues (USFWS, 2006). Zinc concentrations in deer tissues may not be a good estimate of concentrations in the body as zinc is metabolized and must be constantly present in the diet of white-tailed deer (USFWS, 2006).

This model provides the ability to predict trace metals transfer coefficients into the heart, liver, and meat tissues of white-tailed deer. Dividing the actual tissue concentrations (mg/kg) of white-tailed deer in this area by the estimated total ingestion value (mg/day) will yield a transfer coefficient (d/kg) for trace metals into each tissue type (Equation 4.10). The estimated transfer coefficients for trace metals into the heart, liver, and meat for lead, zinc, and cadmium are provided in Table 4.11.

$$TC = \frac{ATC}{TI} \quad (\text{Eq.4.10})$$

Where:

TC	=	Transfer Coefficient (day/kg)
ATC	=	Actual Tissue Concentration (mg _{metal} /day)
TI	=	Total Ingestion (mg _{metal} /day)

Table 4.11: Estimated transfer coefficients for lead, zinc, and cadmium into the heart, liver, and meat of a white-tailed deer living in the around the Elm Creek Watershed

	Heart (d/kg)	Liver (d/kg)	Meat (d/kg)	Total Average (d/kg)
Pb	0.004	0.004	0.004	0.004
Zn	0.005	0.011	0.009	0.008
Cd	0.010	0.011	0.005	0.009

These transfer coefficients can be applied to the ingestion model for white-tailed deer to further improve the estimation of trace metals uptake into the meat, heart, and liver. Lesser concentrations of cadmium predicted by the model relative to concentrations present in the heart and liver tissue of the actual white-tailed deer may be due to underestimations of the ingestion of cadmium. This model uses median trace metals concentrations from water, soil, and forage within a 40 km² area while the home range of a white-tailed deer vary from 0.6-5.2 km² (Sample and Sutter, 1994; Gallina and Lopez, 2016). The trace metals contamination in this area is not spatially homogeneous like the model assumes, therefore the home range area may have a greater influence and be a more accurate predictor of trace metal exposure to white-tailed deer. The area where the soil metals concentrations were determined is also further from the Tar Creek Superfund Site (the major source of trace metals) than the collection locations of both forage and water which may cause an underprediction in tissue concentrations even though soil is a very small part of the white-tailed deer diet.

For this study, inhalation as an exposure route was not considered. In northeastern Oklahoma specifically, wind speeds can reach over to 65 kilometers per hour and areas with concentrated trace metals contamination are exposed and not covered by vegetation (White, 2006; OCS, 2017). High wind speeds allow for the

mobilization of the smallest size fractions, which also are also known to have elevated trace metal concentrations (Datin and Cates, 2002). Deer living closest to the Tar Creek Superfund Site may have additional ingestion through inhalation of trace metals picked up by the wind. This local factor may increase the chances of metals uptake and therefore oral ingestion may not be the only route of trace metals exposure.

Although the white-tailed deer living within the Elm Creek Watershed and Tar Creek Superfund Site have concentrations of trace metals in their tissues, these concentrations cannot be considered “elevated” in reference to other white-tailed deer from non-trace metal contaminated areas across the State of Oklahoma. An interesting observation between multiple studies where white-tailed deer tissue and bone metals concentrations revealed that white-tailed deer living in trace metals contaminated areas do not always have greater trace metal tissue concentrations when compared to white-tailed deer from background locations in Oklahoma (Table 4.12) (Kocan et al., 1980; Conder and Lanno, 1999; Andrews, 2010; CH2M, 2017).

Table 4.12: Mean metals concentrations of meat, liver, kidneys, and other tissues in white-tailed deer from studies conducted in the State of Oklahoma

Metal	Meat	Liver	Kidney	Heart	Bone	n	Location	Source
Pb ¹	0.456	0.422	0.270*	0.452	--	4	Elm Creek and Tar Creek Superfund Site, Ottawa County, OK	CH2M (2017)
Zn ¹	29.2	35.9	31.9*	17.9	--	4		
Cd ¹	0.16	0.34	1.50*	0.310	--	4		
Pb ¹	0.4	0.48	0.41	0.740	--	1		
Zn ¹	31.5	42.6	22.6	15.3	--	1		
Cd ¹	0.14	0.13	0.74	0.37	--	1		
Pb	0.009	0.099	--	--	--	1	Picher, OK	Andrews (2010)
Zn	72.4	62.6	--	--	--	1		
Cd	0.011	0.040	--	--	--	1		
Pb	0.217	--	--	--	--	1	Love County, OK	
Zn	27.9	--	--	--	--	1		
Cd	0.004	--	--	--	--	1		
Pb	--	--	--	--	1.43	19	Near Picher, OK	Conder and Lanno (1999)
Zn	--	--	--	--	77.1	20		
Cd	--	--	--	--	--	--		
Pb	--	--	--	--	0.170	8	Background area in North Central OK	
Zn	--	--	--	--	66.5	8		
Cd	--	--	--	--	--	--		
Pb	--	--	0.574	--	--	64	Multiple counties in OK (not including Ottawa County)	Kocan et al. (1980)
Zn	--	--	--	--	--	--		
Cd	--	--	6.96	--	--	64		

[-- no data collected, all units in mg/kg, tissue concentrations are means of wet weights, bone tissue concentrations are means of dry weights unless otherwise noted

¹ Analysis on wet or dry weight not mentioned in study

* Kidney data only applies to the "Tar Creek Deer" n=1

The study by CH2M (2017) found little difference between the mean metals concentrations in the four-white-tailed deer closest to the Superfund site and one

background white tailed-deer harvested in an area with no mining influence, approximately 13 km south of the Tar Creek Superfund Site. In the study by Andrews (2010), tissue from a white-tailed deer killed in Picher, OK, a town within the boundaries of the Tar Creek Superfund Site, had far lower concentrations of lead and cadmium in the meat and liver, but over double the zinc concentrations found in meat and liver from the averaged four-white-tailed deer closest to the Superfund site determined by CH2M (2017). Kocan et al. (1980) found substantial differences in lead and cadmium concentrations in kidneys of white-tailed deer across the State of Oklahoma. Counties across the state with no known trace metals contamination had lead and cadmium kidney concentrations exceeding the kidney concentrations determined by CH2M (2017) (Kocan et al., 1980). However, the study by Kocan et al., was conducted in 1980 and research technologies and detection limits have changed. Lead and zinc concentrations in the mandibles (jaw bone) of white-tailed deer were higher in white tailed deer killed closest to the Tar Creek Superfund Site in a study conducted by Conder and Lanno (1999).

The observation that white-tail deer tissue concentrations are not elevated substantially in areas of trace metal contamination within Oklahoma could mean that trace metals have lesser tissue affinity and are more likely to concentrate in the bones or that trace metal contaminated areas have minimal influence on the body burden in white-tailed deer. There are relatively few studies conducted on the trace metal concentrations in the tissues of white-tailed deer in Oklahoma and therefore expansion on this area of research would help develop a better understanding on the relationship

between trace metals uptake by white-tailed deer in both contaminated and uncontaminated areas.

4.3.3 Evaluation of Human Health Risk

The ADD was calculated for each tissue type using the average tissue trace metal concentrations from the four-white-tailed deer hunted in the Elm Creek watershed and Tar Creek Superfund Site (CH2M, 2017). The ADD and oral RfD for each metal are presented in Table 4.13. The HQ for lead, zinc, and cadmium for each tissue type and corresponding HI were calculated and are presented in Table 4.14.

Table 4.13: The oral RfD for each trace metal and ADD for each tissue from white-tailed deer hunted in the Elm Creek watershed

Parameter	Tissue Type	Pb	Zn	Cd
Oral RfD (mg/kg/day)	---	3.60×10^{-3}	0.300	5.00×10^{-4}
ADD (mg/kg/day)	Heart	1.76×10^{-4}	7.00×10^{-3}	1.20×10^{-4}
	Liver	1.64×10^{-4}	0.014	1.32×10^{-4}
	Meat	1.77×10^{-4}	0.011	6.22×10^{-5}
	Average	1.72×10^{-4}	0.010	1.05×10^{-4}

Table 4.14: The HQ for lead, zinc, and cadmium and corresponding HI for each tissue type in white-tailed deer hunted in the Elm Creek Watershed

Tissue Type	HQ			HI
	Pb	Zn	Cd	
Heart	0.048	0.023	0.241	0.313
Liver	0.045	0.046	0.264	0.357
Meat	0.049	0.037	0.124	0.211
Average	0.047	0.035	0.210	0.294

The HQ for each trace metal does not exceed 1.0 in all tissue types for each metal for the consumption of one 0.23 kg serving of tissue once a week for 70 years for an 83 kg individual. The HI also does not exceed 1.0 and therefore, there is no likelihood of

associated health risk from the consumption of white-tailed deer tissue following the stated ADD parameters. The number of days an individual consumed white-tailed deer tissues per year was adjusted to determine how many days one can eat deer products per week before the HI exceeded 1.0. The HI exceeded 1.0 for liver after 146 days, heart after 166 days, and meat after 246 days, suggesting individuals should not consume liver more than two times per week, heart more than three days per week, and meat more than four days per week for 70 years to minimize risk associated with the trace metals concentrations in these tissues.

The likelihood of someone consuming a liver more than twice a week out of the year is small since a white-tailed deer only has one liver with the estimated liver weight being 1.4 kg for a 68 kg animal (Parra, 2012). The hunter will only be able to get six servings of the liver from one white-tailed deer and to eat liver for 146 days out of the year (HI=1), one would have to obtain 24 livers. If one 68 kg deer yields 30 kg of meat, it would provide the hunter with 130 meals which is well under the 246 days per year necessary to assume possible risk. In a survey conducted by the USACHPPM (1995), researchers found that hunters usually harvest two deer on average and share the meat with friends and family, and feed some of the meat to pets and therefore it is unlikely that one hunter will consume an entire deer within a year by themselves. Even then, no risk is assumed if a hunter ate all the meat by themselves. Risk could be assumed if the hunter ate two deer all by themselves.

This model considered the extreme scenario and it is unlikely that an individual would only eat deer tissues for this duration especially due to the diversity in diets,

accessibility to supermarket foods, and foods from restaurants in the area. A larger sample size of white-tailed deer tissue concentrations from white-tailed deer killed within the Elm Creek Watershed would assist in producing a more accurate model for future work. Also, interviewing hunters within this watershed on how much white-tailed deer they eat, how often they eat it, and what tissue types they eat, would aid in selecting the most accurate parameters for the determination of the ADD.

4.4 Conclusions

The estimation of lead, zinc, and cadmium intake into white-tailed deer and the associated human health risks are both based on a variety of site-specific information and assumptions. All assumptions used in the calculations were based on previous literature. These calculations suggest that the model developed to quantify lead, zinc, and cadmium uptake into the tissue of white-tailed deer living in the Elm Creek watershed was accurate for the prediction of lead and cadmium. The model initially incorrectly predicted the tissue concentrations of zinc. The zinc transfer coefficient was adjusted to predict the concentrations in collected tissue samples from a separate study, thus improving the accuracy of the model. The same dataset used for the calibration of zinc concentrations in tissue in white-tailed deer was used to develop separate transfer coefficients for the metals of interest into the meat, heart, and liver tissues to further improve the accuracy of the model or to aid in the prediction of tissue concentrations in the future. The soil trace metals concentrations generated in this study as a whole, had little impact on the overall trace metals tissue concentration in the white-tailed deer. Trace metals from ingested plant matter had the greatest influence on the total

ingestion for white-tailed deer. A larger sample size of white-tailed deer tissue concentrations from white-tailed deer killed within the Elm Creek Watershed would assist in producing a more accurate model for future work.

The risk characterization approach in this study assessed risk to an 83 kg individual who consumed 0.23 kg of white-tailed deer tissues once a week for 70 years of their life, a conservative approach from a risk perspective. Tissue trace metals concentrations came from mean tissue concentrations from actual white-tailed deer analyzed by CH2M (2017). Using these parameters, this study concluded that the consumption of white-tailed deer from the Elm Creek Watershed would not likely present a human health hazard. The hypothesis that consuming white-tailed deer tissue harvested within the Elm Creek watershed would expose the consumers to unacceptable risk for lead, zinc, and cadmium was rejected. Neither the HQs for each metal and tissue type nor the overall HI for each tissue type exceeded 1.0 based on the ADD parameters selected. The largest HI value was for the liver (HI=0.357) and the lowest was for meat (HI=0.211) with cadmium (HQ=0.124-0.264) being the major contributor for each tissue type. The model suggests limiting consumption of the liver to no more than two times per week, heart no more than three days per week, and meat no more than four days to prevent unacceptable risk. Interviewing hunters within this watershed regarding deer consumption would aid in selecting the most reflective parameters for the determination of the ADD for individuals in this area. The most important conclusion to take away from this portion of the study is consuming white-

tailed deer poses no adverse health effects based on the model developed for the Elm Creek watershed.

Chapter V: Conclusions and Future Work

5.1 Conclusions

The Elm Creek watershed located in Ottawa County, Oklahoma, is an area in need of conservation (Brabander et al., 1985; Ducks Unlimited, 2012). This watershed contains portions of the Tar Creek Superfund site and is impacted by trace metal contamination from the abandoned mining operations within the Superfund area (USFWS, 2013; Nairn, 2014a). Substantial portions of this watershed were acquired by the GRDA to be used as offsite mitigation for impacts under the Pensacola Dam hydropower license under FERC.

The proximity of these properties to the Tar Creek Superfund Site raised questions and concern about the extent of metals contamination and viability of this area to be used for offsite habitat mitigation. Soil samples were taken from this site and from upstream riparian terrace locations to help understand and evaluate the trace metals distribution within this portion of the watershed. This study consisted of three major sections: (1) a comparison of analytical methods for the detection of trace metals in soils, (2) analysis of the distribution of trace metals in the creek terraces and uplands soils and, (3) analysis of trace metals uptake into white-tailed deer and the human health risk associated with consumption of these deer.

5.1.1 Comparison of Methods

The comparison of trace metals concentrations determined by *in situ* XRFs and laboratory XRFs (where samples were homogenized, dried and sieved) yielded

statistically different results for lead and zinc. When samples with less than 10% field moisture content were compared, *in situ* and laboratory XRF concentrations for lead and zinc were statistically similar. Organic content greater than 10% caused underreporting of lead XRF values when compared to ICP concentrations. Laboratory XRF concentrations were statistically similar to ICP values for lead, but statistically different for zinc. The XRF overreported zinc concentrations when compared to ICP values. Regression analysis for laboratory XRF and ICP values for lead and zinc yielded statistically significant relationships lead ($r^2=0.98$) and zinc ($r^2=0.92$). Regression equations for ICP-derived zinc and cadmium concentrations allowed the estimation of cadmium from zinc XRF values. The estimated XRF cadmium and ICP cadmium concentrations yielded a statistically significant relationship ($r^2=0.95$). Results from this study recommend that to yield the most comparable XRF readings, *in situ* XRF readings should be taken on dry soils. Wet *in situ* soils should be homogenized, dried, and sieved before XRF analysis and soils with greater than 10% organic content should be analyzed via ICP to yield the most accurate concentrations.

This research shows that XRF may not be suited for *in situ* soil analysis due to variability in field conditions and on the determination of lead in soils with elevated organic contents. Additional sample preparation (drying and sieving), which slows down the data generation process and negates one of the benefits from this device, is necessary to generate reliable values. Although XRF sample times are much faster and cheaper than ICP analysis, the XRF may only operate as a screening tool for zinc due to overreporting.

5.1.2 Distribution of Trace Metals in Elm Creek

The east branch of Elm Creek was found to be the major transporter of contamination from the Tar Creek Superfund Site to downstream locations. The west branch of Elm Creek displayed significantly lower concentrations of lead, zinc, and cadmium than the east branch. Although no relationship between trace metals concentration and stream terraces could be established, analyses of the east branch and main stem of Elm Creek revealed that trace metals concentrations in the terraces decreased with distance from the Tar Creek Superfund Site. Upstream deposition of trace metals may be the cause of reduced concentrations at lower reaches of the creek. Lower trace metals concentrations may also be due to lower reaches experiencing greater soil erosion from the compounding flows upstream during storm events.

5.1.3 Distribution of Trace Metals in Uplands

Geospatial interpolation methods and geostatistical analyses revealed concentrations that reflected background values with exception of two areas falling within the Elm Creek floodplain and one spot at the center of the properties. Hotspots and clusters near the creek were likely due to deposition from contaminated runoff from upstream as they both fell at lower elevations. Hotspots on the property boundaries and at the center of the property were likely due to tailings material used on rural roads or tracked in on vehicle tires. Although ICP validation of trace metals concentrations in samples exceeding the RG reported lower trace metals concentrations in almost every sample, the RG remained exceeded at five points for zinc, and at three of the five points for cadmium. More sampling in and around these areas is necessary to determine the

extent of concentrations exceeding RGs. Areas of the properties furthest to the west and south display the lowest metals concentrations because they are furthest (upland or downstream) from trace metals influence.

5.1.4 Estimation of Trace Metals Uptake in White-Tailed Deer

The estimation of trace metals uptake into white-tailed deer from watershed-specific trace metals concentrations in water, forage, and soil, reflected actual tissue concentrations for lead and cadmium in deer harvested from the Elm Creek watershed. Concentrations of zinc were overestimated as zinc is an essential micronutrient and is poorly stored in the tissues of white-tailed deer and therefore acts differently than lead and cadmium which concentrate in tissues (USFWS, 2006). White-tailed deer-specific transfer coefficients of lead, zinc, and cadmium into the heart, liver, and meat were predicted based on actual tissue concentrations.

5.1.5 Human Health Risk Evaluation

The human health risk evaluation followed conservative approach and assessed risk to an 83 kg individual who consumed 0.23 kg of white-tailed deer tissues once a week for 70 years of their life. The HQ from consuming this amount of the heart, liver, and meat was evaluated for lead, zinc, and cadmium. HQ's for each metal were summed to determine an overall HI for each of the tissues. The largest HI value was for the consumption of the white-tailed deer liver (HI=0.357) and the lowest was for the deer meat (HI=0.211). Cadmium (HQ=0.124-0.264) was the major contributor to the HI for each tissue type. Neither the HQs for each metal nor the overall HI for each tissue type

exceeded 1.0 based on the dose parameters selected. This study concluded that the consumption of white-tailed deer from the Elm Creek Watershed would not likely present a human health hazard as the conservative approach overestimated deer consumption.

5.1.6 Final Comments

The information presented in this study will allow for future researchers to utilize XRFS in the most effective manner. Understanding soil conditions and how these conditions impact XRFS output values before sampling will aid in effective sampling and analysis plans. The geospatial distribution of trace metals in the creek and uplands areas will hopefully aid GRDA to make educated decisions on land use practices. Areas identified within the creek terraces and upland environments that exceed SQGs and RSs should be resampled and if necessary remediated while areas with no metals impact could be used as areas for mitigation purposes. However, since these elevated concentrations are likely due to upstream source materials being transported downstream, the most effective approach would be to address the problem at the source. Based on conservative assumptions, a risk estimation found that white-tailed deer from this area are safe for human consumption.

References

- Alloway, B. J., (2012). *Heavy Metals in Soils* 3rd ed., Springer, New York, ISBN 978-94-007-4469-1, 615 pages.
- Andrews, W. J., (2010). "Plant uptake, time trends, and natural attenuation of lead, zinc, and other selected metals in the abandoned tri-state mining district of northeastern Oklahoma, southeastern Kansas, and southwest Missouri", The University of Oklahoma, Unpublished Dissertation. 328 pages.
- Andrews W. J., (2011). "Plant uptake, time trends, and natural attenuation of selected metals in an abandoned mining district", The University of Oklahoma, Dissertation. 131 pages.
- Ankenbauer, K. J. and Loheide, S. P., (2016). "The effects of soil organic matter on soil water retention and plant water use in a meadow of the Sierra Nevada, CA", *Hydrological Processes*. Vol. 31, pp. 891-901
- Arun, P. V., (2013). "A comparative analysis of different DEM interpolation methods", *The Egyptian Journal of Remote Sensing and Space Sciences*. Vol. 16, pp. 133-139
- ASTM, (November 2016). "Standard test methods for laboratory determination of water (moisture) content of soil and rock by mass", Method D2216-10, American Society for Testing and Materials.
- ASTM, (November 2013). "Standard test methods for loss on ignition (LOI) of soil combustion residues", Method D7348-13, American Society for Testing and Materials.
- ATSDR, (2005). "Toxicological profile for zinc", United States Department of Health and Human Services, Agency for Toxic Substances and Disease Registry. 352 pages.
- ATSDR, (2007). "Toxicological profile for lead", United States Department of Health and Human Services, Agency for Toxic Substances and Disease Registry. 582 pages.
- ATSDR, (2008a). "Public health assessment for U.S. Army Aberdeen Proving Ground, Edgewood area, Aberdeen, Hartford County, Maryland", United States Department of Health and Human Services. Agency for Toxic Substances and Disease Registry. 83 pages.
- ATSDR, (2008b). "Public health assessment for occurrence of selected health conditions in Ottawa County, Oklahoma," Agency for Toxic Substances and Disease Registry. 38 pages.

ATSDR, (2012). "Toxicological profile for cadmium", United States Department of Health and Human Services, Agency for Toxic Substances and Disease Registry. 487 pages.

ATSDR, (2017). "Minimal Risk Levels (MRLs)", Agency for Toxic substances and Disease Registry. https://www.atsdr.cdc.gov/mrls/pdfs/atsdr_mrls.pdf

Avila, M., Perez, G., Esshaimi, M., Mandi, L., Ouazzani, N., Brianso, J. L., and Valiente, M., (2012). "Heavy metal contamination and mobility at the mine area of Draa Lasfar (Morocco)", *The Open Environmental Pollution & Toxicology Journal*. Vol. 3, pp.2-12

Bettinelli, M., Beone, G. M., Spezia, S., and Baffi, C., (2000). "Determination of heavy metals in soils and sediments by microwave-assisted digestion and inductively coupled plasma optical emission spectrometry analysis", *Analytica Chimica Acta*. Vol. 424, pp. 289-296

Bastos, R. O., Melquiades, F. L., and Biasi, G. E. V., (2012). "Correction for the effect of soil moisture on *in situ* XRF analysis using low-energy background", *X-Ray Spectrometry*. Vol. 41, pp. 304-307

Beyer, W.N., (1988). "Damage to the forest ecosystem on Blue Mountain from zinc smelting", *Trace Substances in Environmental Health*. Vol. 22, pp. 249-262

Beyer, N., Connor, E. E., and Gerould, S., (1994). "Estimates of soil ingestion by wildlife", *Journal of Wildlife Management*. Vol. 58(2), pp. 375-382

Bhunja, G. S., Shit, P. K., and Maiti, R., (2016). "Comparison of GIS-based interpolation methods for spatial distribution of soil organic carbon (SOC)", *Journal of the Saudi Society of Agricultural Sciences*.

Bidwell, T. G., Elmore, D. R., and Bartholomew, E. M., (2017). "White-tailed deer habitat evaluation and management guide", *Oklahoma State University Division of Agricultural Sciences and Natural Resources*, Oklahoma Cooperative Extension Service. 32 pages.

Binstock, D. A. and Gutknecht, W. F., (2002). "Final report for research to develop a cost-effective approach to residential soil-lead risk assessment", HUD Cooperative Agreement NCLH R0055-99.

Bird, G., Brewer, P. A., Macklin, M. D., Nikolova, M., Kotsev, T., Mollov, M., and Swain, C., (2010). "Dispersal of contaminant metals in the mining-affected Danube and Maritsa Drainage Basins, Bulgaria, Eastern Europe", *Water, Air, and Soil Pollution*. Vol. 206, pp. 105-127

- Blöschl, G., (2002). "Geostatistics for environmental scientists", *Vadose Zone*. Vol. 1, page 321
- Brabander, J. J., Masters, R. E., and Short, R. M., (1985). "Bottomland hardwoods of eastern Oklahoma", United States Fish and Wildlife Service. 164 pages.
- Brewer, P. A. and Taylor, M.P., (1997). "The spatial distribution of heavy metal contaminated sediment across terraced floodplains", *Catena*. Vol. 30, pp. 229-249
- Burrough, P. A., (2001). "GIS and geostatistics: Essential partners for spatial analysis", *Environmental and Ecological Statistics*. Vol. 8, pp. 361-377
- Camner, P., Clarkson, T. W. and Nordberg, G. F., (1979). "Routes of exposure, dose and metabolism of metals", in *Handbook on the toxicology of metals*, Friberg, L., Nordberg, G.F., and Vouk, V.B., eds. Amsterdam, The Netherlands: Elsevier/North-Holland Biomedical Press
- Campbell, T. A., Laseter, B. R., Ford, W. M., and Miller, K. V., (2004). "Movements of female white-tailed deer (*Odocoileus virginianus*) in relation to timber harvests in the central Appalachians", *Forest Ecology and Management*. Vol. 199, pp. 371-387
- Cardenas, M. L., (1999). "Environmental risk assessment (EnRA)", United Nations Environmental Programme, Technical workbook on environmental management tools for decision analysis. Accessed on February 19, 2018 at URL: <http://www.unep.or.jp/ietc/publications/techpublications/techpub-14/1-EnRA1.asp>
- Carpenter, J.W., Andrews, G.A., and Beyer, W.N., (2004). "Zinc toxicosis in a free-flying trumpeter swan (*Cygnus buccinator*)", *Journal of Wildlife Diseases*. Vol. 40(4), pp. 769-774
- Carroll, S.A., O'Day, P.A., and Piechowski, M., (1998). "Rock-water interactions controlling zinc, cadmium, and lead concentrations in surface waters and sediments, US Tri-State Mining District. 1. Geochemical interpretation", *Environmental Science and Technology*. Vol. 32, pp. 956-965
- Carter, J., Walling, D. E., Owens, P. N., and Leeks, G. J. L., (2006). "Spatial and temporal variability in the concentration and speciation of metals in suspended sediment transported by the River Aire, Yorkshire, UK", *Hydrological Processes*. Vol. 20, pp. 3007-3027
- Cattle, J. A., McBratney, A. B., and Minasny, B., (2002). "Kriging method evaluation for assessing the spatial distribution of urban soil lead contamination", *Journal of Environmental Quality*. Vol. 31(5), pp. 1576-1589

CDC, (2017a). "Life expectancy", Centers for Disease Control and Prevention. Accessed on February 11, 2018 at URL: <https://www.cdc.gov/nchs/fastats/life-expectancy.htm>

CDC, (2017b). "Body measurements", Centers for Disease Control and Prevention. Accessed on February 11, 2018 at URL: <https://www.cdc.gov/nchs/fastats/body-measurements.htm>

CDC, (2017c). "Blood lead levels in children", Centers for Disease Control and Prevention. Accessed on February 10, 2018 at URL: https://www.cdc.gov/nceh/lead/acclpp/lead_levels_in_children_fact_sheet.pdf

CFR. (2007). "Criteria for the safe and environmentally protective use of granular mine tailings known as "chat" 40 CFR Parts 260 and 278", Environmental Protection Agency, Federal Register, Vol. 72 (137), pp. 39331-39353

CH2M, (2017). "Tar Creek Superfund Site, Ottawa County, Oklahoma, Opportunistic deer tissue sample laboratory analysis", Technical Memorandum prepared for USEPA Region 6. CH2M Project No. 664457.RR.01

Chaney, R.L., (2010). "Cadmium and zinc", In P. S. Hooda (Ed.), Trace elements in soils, (pp. 410-439). London, England: Wiley-Blackwell.

Cheng, J., Shi, Z., and Zhu, Y., (2006). "Assessment and mapping of environmental quality in agricultural soils of Zhejiang Province, China", *Journal of Environmental Sciences*. Vol. 19, pp. 50-54

Conder, J. M. and Lanno, R. P., (1999). "Heavy metal concentrations in mandibles of white-tailed deer living in the Picher mining district", *Bulletin of Environmental Contamination and Toxicology*. Vol. 63, pp. 80-86

Coronel, E. G., Bair, D. A., Brown, C. T., and Terry, R. E., (2014). "Utility and limitations of portable X-ray fluorescence and field laboratory conditions on the geochemical analysis of soils and floors at areas of known human activities", *Soil Science*. Vol. 179(5), pp. 258-271

Crooks V., Simpson, P., Rawson, b., and Wake, D., (2006). "Investigation of PXRf procedures for measuring contaminated land", Health and Safety Laboratory, Vol. 102, 49 pages.

Dames and Moore, (1993). "Final remedial investigation for Cherokee County, Kansas, CERCLA Site, Baxter Springs/Treece Sub-sites." Denver, CO. 285 pages.

Datin, D.L. and Cates, D.A., (2002). "Sampling and metal analysis of chat piles in the Tar Creek Superfund Site", Prepared for the Oklahoma Department of Environmental Quality, Oklahoma City, Oklahoma.

Deckman, D., (2003). "North American white-tailed deer: Distribution and subspecies", Whitetails Unlimited, Inc. Accessed on February 19, 2018 at URL: https://www.whitetailsunlimited.com/i/p/bk_distribution.pdf

Dennis, I. A., Couthard, T. J., Brewer, P., and Macklin, M. G., (2009). "The role of floodplains in attenuating contaminated sediment fluxes in formerly mined drainage basins", Earth Surface Processes and Landforms. Vol. 34, pp. 453-466

Ducks Unlimited, (2012). Neosho bottoms restoration plan, Volume 1. Submitted to Oklahoma Department of Wildlife Conservation, 48 pages.

Ducks Unlimited. 2012a. Neosho Bottoms Restoration Plan, Volume 2, Study Unit Report. Submitted to Oklahoma Department of Wildlife Conservation, 130 pages.

Ecology and Environment, Inc., (1996). "Supplement to the site assessment report, residential soil, Tar Creek Superfund Site, Statistical correlations between the ICP and XRF Data and AA and XRF Data", Prepared for the U.S. Environmental Protection Agency Region 6.

ENHIS, (2009). "Exposure of children to chemical hazards in food", European Environment and Health Information System. Fact Sheet 4.4, Code RPG4_Food_Ex1. http://www.euro.who.int/data/assets/pdf_file/0004/97042/4.4.-Exposure-of-children-to-chemical-hazards-in-food-EDITED_layouted.pdf

ESRI. (2016). "Comparing interpolation methods", ESRI Spatial Statistics. Accessed on March 23, 2018 at URL: <http://desktop.arcgis.com/en/arcmap/10.3/tools/3d-analyst-toolbox/comparing-interpolation-methods.htm>

ESRI. (2017a). "How cluster and outlier analysis (Anselin Local Moran's I) works", ESRI Spatial Statistics. Accessed on March 23, 2018 at URL: <http://pro.arcgis.com/en/pro-app/tool-reference/spatial-statistics/h-how-cluster-and-outlier-analysis-anselin-local-m.htm>

ESRI. (2017b). "How hot spot analysis (Getis-Ord Gi*) works", ESRI Spatial Statistics. Accessed on March 24, 2018 at URL: <http://pro.arcgis.com/en/pro-app/tool-reference/spatial-statistics/h-how-hot-spot-analysis-getis-ord-gi-spatial-stati.htm>

ESRI. (2018). "Conceptualization of spatial relationships", ESRI Spatial Statistics. Accessed on March 23, 2018 at URL

http://resources.esri.com/help/9.3/arcgisdesktop/com/gp_toolref/spatial_statistics_toolbox/modeling_spatial_relationships.htm

French, J. B. and Mateo, R., (2005). "Zinc and lead poisoning in wild birds in the Tri-State Mining District (Oklahoma, Kansas, and Missouri)", *Archives of Environmental Contamination and Toxicology*. Vol. 48, pp. 108-117

Gallina, S. and Lopez, A. H., (2016). "Odocoileus virginianus. The IUCN Red List of Threatened Species 2016: e.T42394A22162580", International Union for Conservation of Nature and Natural Resources. Accessed on February 2, 2018 at URL: <http://dx.doi.org/10.2305/IUCN.UK.2016-2.RLTS.T42394A22162580>

Galuszka, A., Migaszewski, Z. M., and Namienik, J., (2015). "Moving your laboratories to the field – Advantages and limitations of the use of field portable instruments in environmental sample analysis", *Environmental Research*. Vol. 140, pp. 593-60

Garrido, A. E., Strosnider, W. H. J., Wilson, R. T., Condori, J., and Nairn, R. W., (2017). "Metal-contaminated potato crops and potential human health risk in Bolivian mining highlands", *Environmental Geochemistry and Health*. Vol. 39, pp. 681-700

Garvin, E. M., Bridge, C. F., and Garvin, M. S., (2017). "Edible wild plants growing in contaminated floodplains: implications for the issuance of tribal consumption advisories within the Grand Lake watershed of northeastern Oklahoma, USA", *Environmental Geochemistry and Health*. pp. 1-27

Ge, L., Lai, W., and Lin, Y., (2005). "Influence of and correction for moisture in rocks, soils and sediments on *in situ* XRF analysis", *X-Ray Spectrometry*. Vol. 34, pp. 28-34

Gee, K. L., Porter, M. D., Demarais, S., and Bryant, F. C., (2011). "White-tailed deer: Their foods and management in the cross timbers", (3rd edition) NF-WF-11-02. Noble Foundation, Ardmore, Oklahoma

Giacalone, A., Gianguzza, A., Orecchio, S., Piazzese, D., Dongarrà, G., Sciarrino, S., and Varrica, D., (2015). "Metals distribution in the organic and inorganic fractions of soil: a case study on soils from Sicily", *Chemical Speciation and Bioavailability*. Vol. 17(3), pp. 83-93

GRDA, (2016). "GRDA to make more land available for PVA hunts along Neosho River", Grand River Dam Authority. Press release October 24, 2016. Accessed on February 14, 2018 at URL: <http://www.grda.com/grda-to-make-more-land-available-for-pva-hunts-along-neosho-river/>

Gunderson, E. L., (1995). "FDA Total Diet Study, July 1986-April 1991, dietary intakes of pesticides, selected elements, and other chemicals", *Journal of the Association of Official Analytical Chemists International*. Vol.78, pp. 1353-1362

Gupta, S. C. and Larson, W. E., (1979). "Estimating soil water retention characteristics from particle size distribution, organic matter percentage, and bulk density", *Water Resources Research*. Vol. 15(6), pp. 1633-1635

Higuera, P., Oyarzun, R., Iraizoz, J. M., Lorenzo, S., Esbri, J. M., and Martinez-Coronado, A., (2012). "Low-cost geochemical surveys for environmental studies in developing countries: Testing a field portable XRF instrument under quasi-realistic conditions", *Journal of Geochemical Exploration*. Vol. 113, pp. 3-12

Horowitz, A. J., (1985). "A primer on trace metal-sediment chemistry," Submitted to the US Geological Survey. 72 pages.

Horowitz, A. J., (1991). "A primer in sediment-trace element chemistry," Submitted to the US Geological Survey. 142 pages.

Huston, J. E., Rector, B.S., Ellis, W. C., and Allen, M. L., (1986). "Dynamics of digestion in cattle, sheep, goats and deer", *Journal of Animal Science*. Vol. 62, pp. 208-215

Imperato, M., Adamo, P., Naimo, D., Arienzo, M., Stanzione, D., and Violante, P. (2003). "Spatial distribution of heavy metals in urban soils of Naples city (Italy)", *Environmental Pollution*. Vol. 124, pp. 247-256

Ingersoll, C. G., Ivey, C. D., Brumbaugh, W. G., Besser, J. M., and Kemble, N. E., (2009). "Toxicity assessment of sediments from the Grand Lake O' the Cherokees with the amphipod *Hyalella Azteca*", Submitted to the US Fish and Wildlife Service. Administrative Report CERC-8335-FY09-20-01

IRIS, (2004). "Lead and compounds (inorganic); CASRN 7439-92-1", Integrated Risk Information System, Chemical Assessment Summary. U.S. Environmental Protection Agency. Accessed on February 6, 2018 at URL: https://cfpub.epa.gov/ncea/iris/iris_documents/documents/subst/0277_summary.pdf

John, D. A. and Leventhal, J. S. (1995). "Bioavailability of metals", U.S. Geology Survey Open File Report 95-831, pp. 10-18

Jung, M. C., and Thornton, I., (1996). "Heavy metal contamination of soils and plants in the vicinity of a lead-zinc mine, Korea", *Applied Geochemistry*. Vol. 11, pp. 53-59

Juracek, K. E. and Drake, K. D., (2016). "Mining-related sediment and soil contamination in a large superfund site: characterization, habitat implications, and remediation", *Environmental Management*. Vol. 58, pp. 721-740

Kabata-Pendias A. and Pendias, H. (2001). Trace elements in soils and plants, 3rd ed., Boca Raton, Florida: CRC Press LLC.

Kabata-Pendias, A. and Mukherjee, A. B., (2007). Trace elements from soil to human, Heidelberg, Germany: Springer Verlag, 550 pages.

Kalnicky, D.J. and Singhvi, R.S., (2001). Field Portable XRF Analysis of Environmental Samples. *Journal of Hazardous Materials*. 83 pp. 93-122

Kido, Y., Koshikawa, T., and Tada, R., (2006). "Rapid and quantitative major element analysis method for wet fine-grained sediments using an XRF microscanner", *Marine Geology*. Vol. 229, pp. 209-225

Kilbride, C., Poole, J., and Hutchings, T. R., (2006). "A comparison of Cu, Pb, As, Cd, Zn, Fe, Ni and Mn determined by acid extraction/ICP-OES and ex situ field portable X-ray fluorescence analyses", *Environmental Pollution*. Vol. 143(1), pp. 16-23

Kim, S. and Choi, Y., (2017). "Assessing statistically significant heavy-metal concentrations in abandoned mine areas via hot spot analysis of portable XRF data", *International Journal of Environmental Research and Public Health*. Vol. 14, pp. 654-670

Kocan, A. A., Shaw, M. G., Edwards, W. C., Eve, J. H., (1980). "Heavy metals concentrations in the kidneys of white tailed deer in Oklahoma", *Journal of Wildlife Diseases*. Vol. 16(4), pp. 593-596

Krivoruchko, K., (2017). "Introduction to modeling spatial processes using geostatistical analyst", Esri Press, 27 pages. Accessed on March 22, 2018 at URL: <http://www.esri.com/library/whitepapers/pdfs/intro-modeling.pdf>

Larson, T. J., Rongstad, O. J., and Terbilcox, F. W., (1978). "Movement and habitat use of white-tailed deer in south central Wisconsin", *Journal of Wildlife Management*. Vol. 42, pp. 113-117

Levy, D., Redente, E., and Uphoff, G., (1999). "Evaluating the phytotoxicity of Pb-Zn tailings to big bluestem (*Andropogon gerardii* Vitman) and switchgrass (*Panicum virgatum* L.)", *Soil Science*. Vol. 146(6), pp. 363-375

Lewin, J. and Macklin, M.G., (1987). "Metal mining and floodplain sedimentation in Britain", *International Geomorphology*. Wiley, London, pp. 1009-1027

Lin, J. (2009). "Performance of the Thermo Scientific Niton XRF Analyzer: The effects of particle size, length of analysis, water, organic matter, and soil chemistry", Master's Thesis, University of California, Berkeley, California.

Lopez, R. R., Vieira, M. E., Silvy, N. J., Frank, P. A., Whisenant, S. W., Jones. D. A., (2003). "Survival, mortality, and life expectancy of Florida key deer", *Journal of Wildlife Management*. Vol. 67 (1), pp. 34-45

Löwemark, L., Chen, H. F., Yang, T. N., Kylander, M., Yu E. F., Hsu, Y. W., Lee, T. Q., Song, S. R., and Jarvis, S., (2011). "Normalizing XRF-scanner data: A cautionary note on the interpretation of high-resolution records from organic-rich lakes", *Journal of Asian Earth Sciences*. Vol. 40, pp. 1250-1256

MacDonald, D. D., Ingersoll, C. G., and Berger, T. A., (2000). "Development and evaluation of consensus-based sediment quality guidelines for freshwater ecosystems", *Archives of Environmental Contamination and Toxicology*. Vol. 39, pp. 20-31

Macklin, M. G., Brewer, P. A., Hudson-Edwards, K. A., Bird, G., Coulthard, T. J., Dennis, I. A., Lechler, P.J., Miller, J. R., Turner, J. N., (2006). "A geomorphological approach to the management of rivers contaminated by metal mining", *Geomorphology*. Vol. 79, pp. 423-447

Markus, J. and McBratney, A. B., (2001). "A review of the contamination of soil with lead II. Spatial distribution and risk assessment of soil lead", *Environmental International*. Vol. 27, pp. 399-411

Maxfield, R. (2000). "A community based environmental lead assessment and remediation program", Presented at the 2000 National Lead Grantee Conference. Atlanta, GA.

McClintock, N., (2012). "Assessing soil lead contamination at multiple scales in Oakland, California: Implications for urban agriculture and environmental justice", *Applied Geography*. Vol. 35, pp. 460-473

McComb, J. Q., Rogers, C., Han, F. X., and Tchounwou, P. B., (2014). "Rapid screening of heavy metals and trace elements in environmental samples using portable X-ray fluorescence spectrometer, a comparative study", *Water, Air, and Soil Pollution*. Vol. 225, pp. 2168-2178

McCullough, D. R. and Ullrey, D. E., (1983). "Proximate mineral and gross energy composition of white-tailed deer", *The Journal of Wildlife Management*. Vol. 47(2), pp. 430-441

Melquiades, F. L. and Appoloni C. R., (2004). Application of XRF and field portable XRF for environmental analysis", *Journal of Radioanalytical and Nuclear Chemistry*. Vol. 262(2), pp. 533-541

Miller, R. J., (1997). "The role of fluvial geomorphic processes in the dispersal of heavy metals from mine sites", *Journal of Geochemical Exploration*. Vol. 58, pp. 101-118

Monitha, M., Jayakumar, C., and Nagendra Gandhi, N., (2012). "Environmental toxicology-assessment and remediation of toxic metals in soil", *International Journal of Environmental Biology*. Vol. 2(2), pp. 59-66

Nairn, R. W., (2014a). "Elm Creek, Elm Creek prairie and Miami bottoms wetland development areas, Ottawa County, OK," Submitted to the Grand River Dam Authority. Unpublished work.

Nairn, R. W., (2014b). Elm Creek XRF data. Center for Restoration of Ecosystems and Watersheds, The University of Oklahoma. Unpublished work.

National Academy of Sciences, (1971). Radioactivity in the Marine Environment, Prepared by the Panel on Radioactivity in the Marine Environment of the Committee on Oceanography National Research Council, Washington, D.C. 272 Pages.

NRC, (1989). Recommended Dietary Allowances. 10th Ed. National Research Council (US), Washington, DC: National Academies Press (US). doi: 10.17226/1349

Neuberger, J. S., Hu, S. C., Drake, K. D., and Jim, R., (2009). "Potential health impacts of heavy-metal exposure at the Tar Creek Superfund site, Ottawa County, Oklahoma", *Environmental Geochemistry and Health*. Vol. 31, pp. 47-59

OCS, (2017). "Oklahoma Mesonet: Severe Winds", Oklahoma Climatological Survey. Accessed on February 12, 2018 at URL: <http://www.mesonet.org/index.php/weather/category/wind>

O'Day, P.A., Carroll, S.A., and Waychunas, G.A., (1998). "Rock-water interactions controlling zinc, cadmium, and lead concentrations in surface waters and sediments, US Tri-State Mining District. 1. Molecular identification using X-ray absorption spectroscopy", *Environmental Science and Technology*. Vol. 32, pp. 943-955

ODEQ, (2008). "Fish tissues metal analysis in the Tri-state mining area follow up study", State of Oklahoma Department of Environmental Quality, Section 106 Water Quality Management Program. 45 pages.

ODWC, (2017). "2016-2017 Big game report: 2016 Deer harvests by county, season, and sex", Oklahoma Department of Wildlife Conservation. Accessed on February 2, 2018 at URL: <https://www.wildlifedepartment.com/hunting/species/2016-2017-big-game-report>

Opresko, D. M., Sample, B. E., Sutter, G. W., (1996). "Toxicological benchmarks for wildlife: 1996 revision", Prepared for the U.S. Department of Energy, ES/ER/TM-86/R3, 217 pages.

PDEP, (2010). "Palmerton Zinc Pile Superfund Site natural resource damage assessment: Draft restoration plan and environmental assessment", Pennsylvania Department of Environmental Protection. 58 pages. Accessed on February 20, 2018 at URL: http://files.dep.state.pa.us/EnvironmentalCleanupBrownfields/SiteRemediation/SiteRemediationPortalFiles/Draft_Palmerton_RP_051910.pdf

Parra, C. A., (2012). "Body weight and age influences on liver weight in white-tailed deer (*Odocoileus virginianus*): Implications for reproductive effort", Master's Thesis, Texas State University, San Marcos, Texas. 34 pages.

Philips, D. J. H. and Rainbow, P. S., (1993). "The biomonitoring of trace metals and radionucleotides", *Biomonitoring of Trace Aquatic Contaminants*. Vol. 37, pp. 79-132

Phelps, K. L. and Mcbee, K., (2009). "Ecological characteristics of small mammal communities at a superfund site", *The American Midland Naturalist*. Vol. 161(1), pp. 57-68

Potts P. J. and West, M., (2008). "Portable X-ray fluorescence spectrometry: Capabilities for *in situ* analysis", RSC Pub, Cambridge, UK, 291 pages. ISBN 9780854045525

Pyle, S. M. and Nocerino, J. M., (1996). "Comparison of AAS, ICP-AES, PSA, and XRF in determining lead and cadmium in soil", *Environmental Science and Technology*. Vol. 30, pp. 204-213

Qi, J., Zhang, H., Li, X., and Lu, J., (2016). "Concentrations, spatial distribution, and risk assessment of soil heavy metals in a Zn-Pb mine district in southern China", *Environmental Monitoring and Assessment*. Vol. 188(143), 11 pages.

Qin, C., Luo, C., and Chen, Y., (2012). "Spatial-based assessment of metal contamination in agricultural soils near an abandoned copper mine of eastern China", *Bulletin of Environmental Contamination and Toxicology*. Vol. 89, pp. 113-118

Ravansari, R. and Lemke, L. D., (2018). "Portable X-ray fluorescence trace metal measurement in organic rich soils: pXRF response as a function of organic matter fraction", *Geoderma*. Vol. 319, pp. 175-184

Reames, G. and Lance, L. L., (2002). "Childhood lead poisoning investigators: Evaluating a portable instrument for testing soil lead", *Journal of Environmental Health*, Vol. 64(8), pp. 9-13

Roohani, N., Hurrell, R., Kelishadi, R., and Schulin, R., (2013). "Zinc and its importance for human health: An integrative review", *Journal of Research in Medical Sciences*. Vol. 18(2), pp. 144-157

Rouillon, M. and Taylor, M. P., (2016). "Can field portable X-ray fluorescence (pXRF) produce high quality data for application in environmental contamination research?" *Environmental Pollution*. Vol. 214, pp. 255-264

Sahraoui, H. and Hachicha, M., (2016). "Determination of trace elements in mine soil samples using portable X-ray fluorescence spectrometer: A comparative study with ICO-OES", *KKU Engineering Journal*. Vol. 43(3), 5 pages.

Sahraoui, H. and Hachicha, M., (2017). "Effects of soil moisture on trace elements concentrations using portable X-ray fluorescence spectrometer", *Journal of Fundamental and Applied Sciences*. Vol. 9(1), pp. 468-484

Sample, B. E. and Suter, G. W., (1994). "Estimating exposure of terrestrial wildlife to contaminants", Prepared for the U.S. Department of Energy by Oak Ridge National Laboratory, Oak Ridge, Tennessee

Sawicka-Kapusta, K., (1979). "Roe deer antlers as bioindicators of environmental pollution in southern Poland", *Environmental Pollution*. Vol. 19(4), pp.283-293

Schaider, L. A., Senn, D. B., Estes, E. R., Brabander, D. J., and Shine, J. P., (2014). "Sources and fates of heavy metals in a mining-impacted stream: Temporal variability and the role of iron oxides", *Science of The Total Environment*. Vol. 490, pp. 456-466

Schneider, A. R., Cancès, B., Breton, C., Ponthieu, M, Morvan, X., Conreux, A., and Marin, B., (2016). "Comparison of field portable XRF and aqua regia/ICPAES soil analysis and evaluation of soil moisture influence on FPXRF results", *Journal of Soils Sediments*. Vol. 16, pp. 438-448

Shand, C. A. and Wendler, R., (2014). "Portable X-ray fluorescence analysis of mineral and organic soils and the influence of organic matter", *Journal of Geochemical Exploration*. Vol. 143, pp. 31-42

Shit, P. K., Bhunia, G. S., and Maiti, R., (2016). "Spatial analysis of soil properties using GIS based geostatistics models", *Modeling Earth Systems and Environment*. Vol. 2(107), 6 pages.

Sileo, L., Beyer, W. N., and Mateo, R., (2003). "Pancreatitis in wild zinc-poisoned waterfowl", *Avian Pathology*. Vol. 32(6), pp. 655-660

Sileo, L. and Beyer, W. N., (1985). "Heavy metals in white-tailed deer living near a zinc smelter in Pennsylvania", *Journal of Wildlife Diseases*, Vol. 21(3), pp. 289-296

Smith, K. S. and Huyck, H. L. O., (1999). "An overview of the abundance, relative mobility, bioavailability, and human toxicity of metals", *Reviews in Economic Geology*. Vol. 6, pp. 29-70

Soto-Ríos, M. L., Juárez-Pérez, C. A., Rendón-Gandarilla, F. J., Talavera-Mendoza, O., and Aguilar-Madrid, G., (2017). "Elevated blood lead levels in children associated with living near mining waste sites in Guerrero, Mexico", *Environments*. Vol. 4(2), 9 pages.

Steiger, B., Webster, R., Schulin, R., and Lehmann, R., (1996). "Mapping heavy metals in polluted soil by disjunctive kriging", *Environmental Pollution*. Vol. 94(2), pp. 205-215

Storm, G. L., Fosmire, G. J., and Bellis, E. D., (1994). "Persistence of metals in soil and selected vertebrates in the vicinity of the Palmerton zinc smelters", *Journal of Environmental Quality*. Vol.23, pp. 508-514

Swennen, R., Van Keer, I., and De Vos, W., (1994). "Heavy metal contamination in overbank sediments of the Geul river (East Belgium): Its relation to former Pb-Zn mining activities", *Environmental Geology*. Vol. 24, pp. 12-21

Taha, K., (2017). "Heavy elements analyses in the soil using X-ray fluorescence and inductively coupled plasma-atomic emission spectroscopy", *International Journal of Advances in Science, Engineering, and Technology*. Vol 5(1), pp. 118-120

Tchounwou, P. B., Yedjou, C. G., Patlolla, A. K., and Sutton, D. J., (2012). "Heavy metals toxicity and the environment", *Molecular, Clinical and Environmental Toxicology*. Vol. 101, pp. 133-164

Tejaswi, D. and Samuel, C., (2017). "Techniques for environmental risk assessment: A review", *Rasauan Journal of Chemistry*. Vol. 10(2), pp. 499-506

Thermo Scientific, (2010). "Thermo Scientific Niton XRF Analyzers", Environmental hazards testing pamphlet. Thermo Fisher Scientific Inc.

Tidball, R. R., (1976). "Lead in the environment: Lead in soils", US Geological Survey Professional Paper. pp. 43-53

USACHPPM, (1995). "Health risk assessment of consuming deer from Aberdeen proving ground, Maryland", U.S. Department of the Army: U.S. Army Center for Health Promotion and Preventative Medicine. Field Study no. 75-23-YS50-94. 197 pages.

US Census Bureau, (2017). "Ottawa County, Oklahoma: Population estimates July 1, 2016", United States Census Bureau. Accessed on February 5, 2018 at URL: <https://www.census.gov/quickfacts/fact/table/ottawacountyoklahoma,OK/PST045217>

USEPA, (1989). "Risk assessment guidance for superfund, Volume 1, Human health evaluation manual (Part A)", United States Environmental Protection Agency, 291 pages.

USEPA, (1991). "Guidance for data usability in risk assessment (Part A)", Superfund. United States Environmental Protection Agency

USEPA, (1997). "Record of Decision, Operable Unit 2, Residential areas, Tar Creek Superfund Site, Ottawa County, Oklahoma," United States Environmental Protection Agency, 166 pages.

USEPA, (2007a). "Inductively coupled plasma-atomic emission spectrometry: Method 6010c", United States Environmental Protection Agency

USEPA, (2007b). "Microwave assisted acid digestion of sediments, sludges, soils, and oils: Method 3015a", United States Environmental Protection Agency

USEPA, (2007c). "Field portable X-ray fluorescence spectrometry for the determination of elemental concentrations in soil and sediment: Method 6200", United States Environmental Protection Agency

USEPA, (2007d). "Framework for metals risk assessment", Office of the Science Advisor: Risk Assessment Form, Washington, DC 20460

USEPA, (2007e). "Framework for metals risk assessment", United States Environmental Protection Agency. 172 pages.

USEPA, (2008). "Record of Decision, Operable Unit 4, Chat piles, other mine and mill waste and smelter waste, Tar Creek Superfund Site, Ottawa County, Oklahoma, OKD980629844," United States Environmental Protection Agency, 161 pages.

USEPA, (2010). "Fourth five-year review, Tar Creek Superfund Site, Ottawa County, Oklahoma," Prepared by Region 6 United States Environmental Protection Agency, Dallas Texas, 246 pages.

USEPA, (2017a). "Superfund site: Tar Creek, Ottawa County, OK: Site facts", United States Environmental Protection Agency. Retrieved from <https://cumulis.epa.gov/supercpad/SiteProfiles/index.cfm?fuseaction=second.contams&id=0601269>

USEPA, (2017b). "Risk assessment", United States Environmental Protection Agency. Retrieved from <https://www.epa.gov/risk>

USFWS, (2013). "Tri-State transition zone assessment study, Kansas, Missouri and Oklahoma," Prepared by U.S. Fish and Wildlife Service Oklahoma Ecological Services Field Office, Tulsa, Oklahoma, 53 pages

USGS, (2004). "Stream terraces and older surfaces", US Geological Survey. Western Region Geology and Geophysics Science Center. Retrieved from <http://pubs.usgs.gov/of/2004/1007/terraces.html>

USGS. (2018). "USGS 07185030 Elm Creek near Commerce, OK: Discharge for January-October 2017", United States Geological Survey, Water Resources. Accessed on March 27, 2018 at URL: https://nwis.waterdata.usgs.gov/ok/nwis/uv?cb_00060=on&cb_00065=on&format=gif_default&site_no=07185030&period=&begin_date=2017-01-01&end_date=2017-04-01

Walling, D. E. and Owens, P.N., (2003). "The role of overbank floodplain sedimentation in catchment contamination budgets", *Hydrobiologia*. Vol. 494, pp. 83-91

Wang, Z. and Nie, K., (2017). "Measuring spatial distribution characteristics of heavy metal contaminations in a network-constrained environment: A case study in river network of Daye, China", *Sustainability*. Vol. 9(986), 11 pages.

Watts, R. J., (1998). Hazardous Wastes: Sources, pathways, receptors, New York, NY: Wiley. 764 pages. ISBN: 0471002380

WHO, (1993). "Evaluation of certain food additives and contaminants, Forty-First Report of the Joint FAO/WHO Expert Committee on Food Additives", World Health

Organization, Geneva. Technical Report Series No 837.

http://apps.who.int/iris/bitstream/10665/36981/1/WHO_TRS_837.pdf

WHO, (2011). "Evaluation of certain food additives and contaminants, Seventy-Third Report of the Joint FAO/WHO Expert Committee on Food Additives", World Health Organization, India. Technical Report Series No 960.

http://apps.who.int/iris/bitstream/10665/44515/1/WHO_TRS_960_eng.pdf

Wilson, P., Cooke, M., Cawley, J., Giles, L., and West, M., (1995). "Comparison of the determination of copper, nickel and zinc in contaminated soils by X-Ray fluorescence spectrometry and inductively coupled plasma spectrometry", *X Ray Spectrometry*. Vol. 24, pp. 103-108

Wright, R. O., Amarasiriwardena, C., Woolf, A. D., Jim, R., and Bellinger, D. C., (2006). "Neuropsychological correlates of hair arsenic, manganese, and cadmium levels in school-age children residing near a hazardous waste site", *NeuroToxicology*, Vol. 27, pp. 210-216

Zhang, C., Luo, L., Xu, W., and Ledwith, V., (2008). "Use of local Moran's I and GIS to identify pollution hotspots of Pb in urban soils of Galway Ireland", *Science of the Total Environment*. Vol. 398, pp. 212-221

Zota, A. R., Schaider, L.A., Ettinger, A. S., Wright, R.O., Shine, J. P., and Spengler, J. D., (2011). "Metals sources and exposures in the homes of young children living near a mining-impacted superfund site", *Journal of Exposure Science and Environmental Epidemiology*, Vol. 21(5), pp. 495-505

Żukowska, J. and Biziuk, M., (2008). "Methodological evaluation of method for dietary heavy metal intake", *Journal of Food Science*, Vol.73(2), pp. 21-29

Appendix A

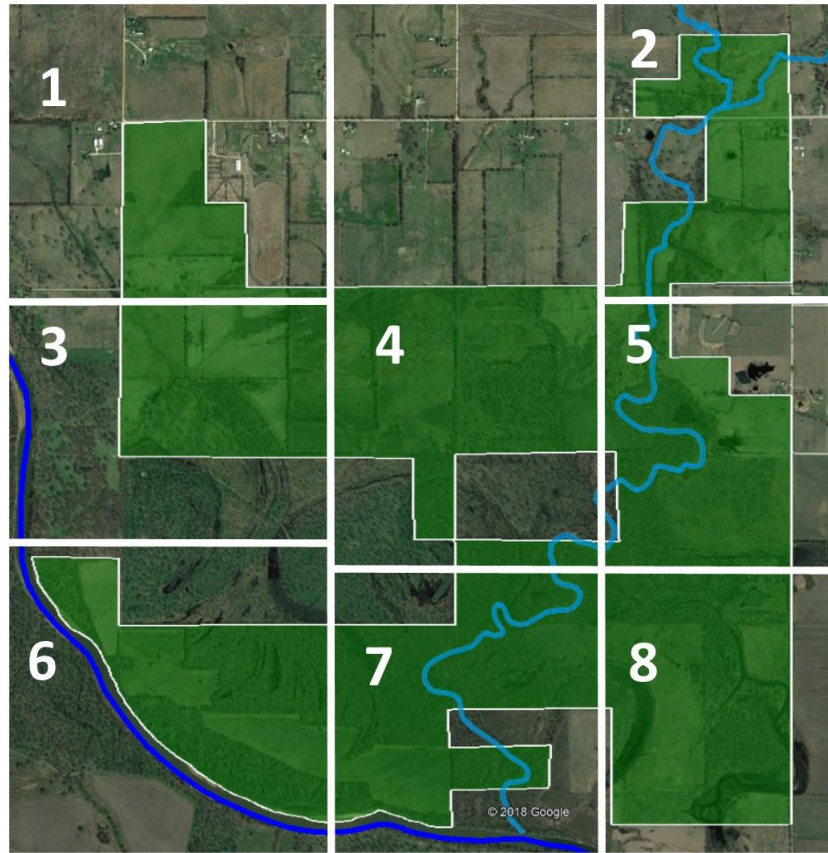


Figure A.1: GRDA properties split into eight sections

Table A.1: Upland and creek sampling site names listed in their corresponding section

Section	1	2	3	4
Upland Sites	MTA 17-25 SKA 1-5 UBA 1-6	GRA 1-13 HFA 1-5 IBA 1-8 MTA 1-4; 26-30	EOA 20-29 PTA 22-31	CRA 1-9 EOA 7-19 MTA 5-16 PTA 11-21 XPA 9-15
	Creek Sites	ECA 65, 67, 70, 72		ECA 80
Section	5	6	7	8
Upland Sites	EOA 1-7 HRA 1-8 PTA 11 PTA 1-9 STA 1-3; 6-8 XPA 1-8	BMA 22-32 JOA 1-4 LBA 1-6 OXA 22-30 TTA 5 YDA 7-9	BMA 10-21 LBA 7-16 OXA 10-21 TTA 1-4 YDA 1-6	BMA 1-9 HWA 1-8 NSA 1-8 OXA 1-9
	Creek Sites	ECA 85, 87, 90		

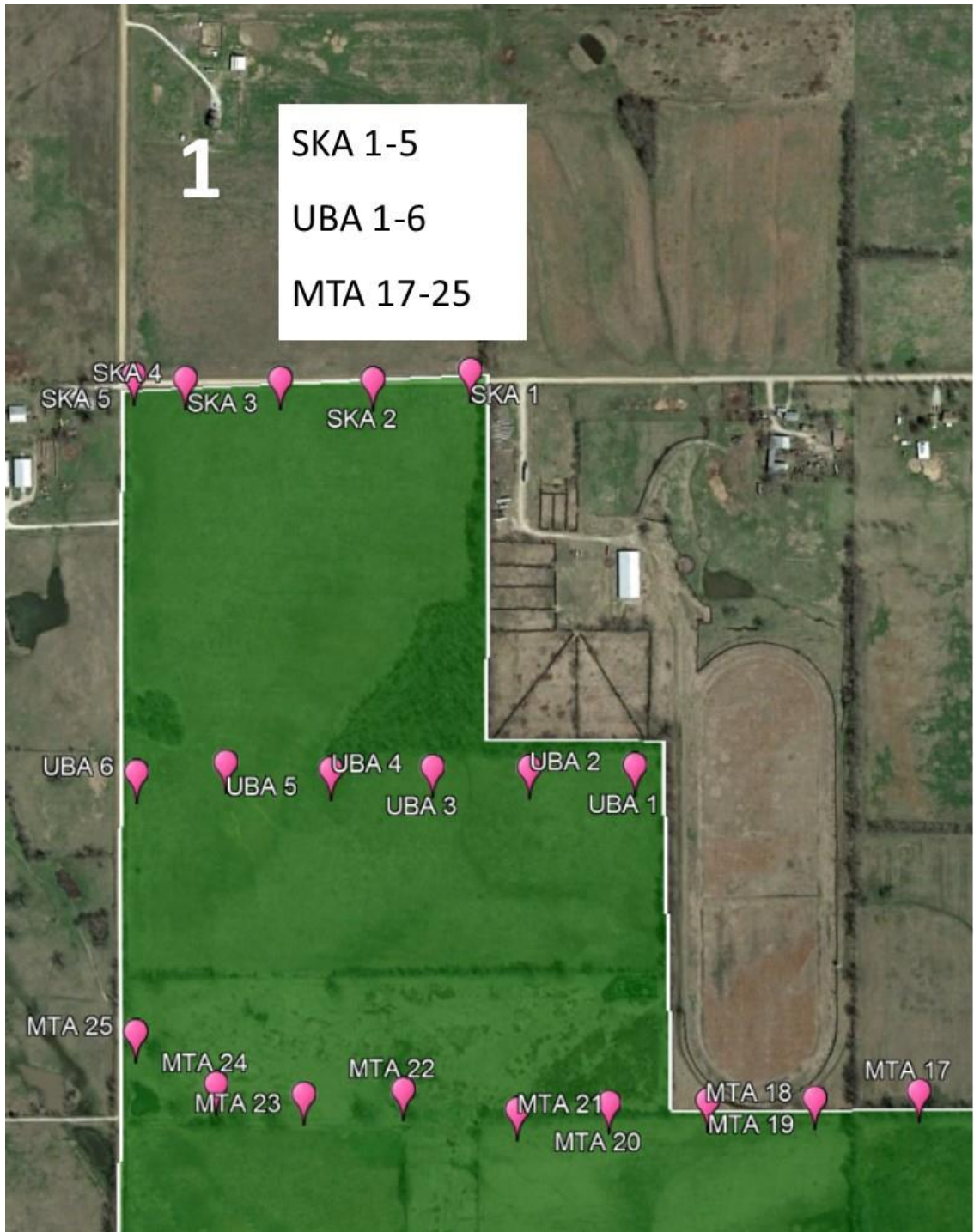


Figure A.2: Section 1 in the GRDA properties with labeled upland soil sampling locations

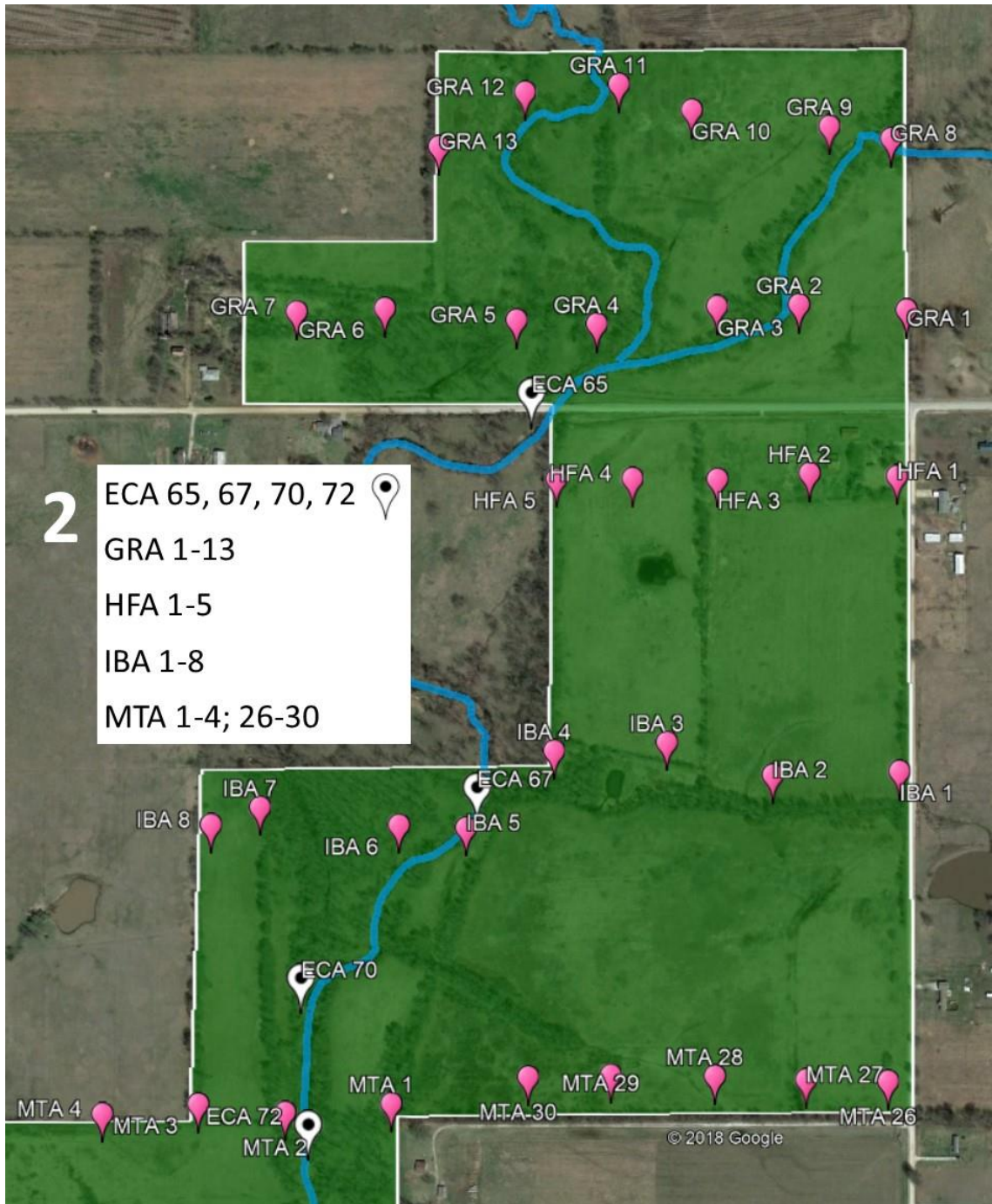


Figure A.3: Section 2 in the GRDA properties with labeled upland and creek soil sampling locations

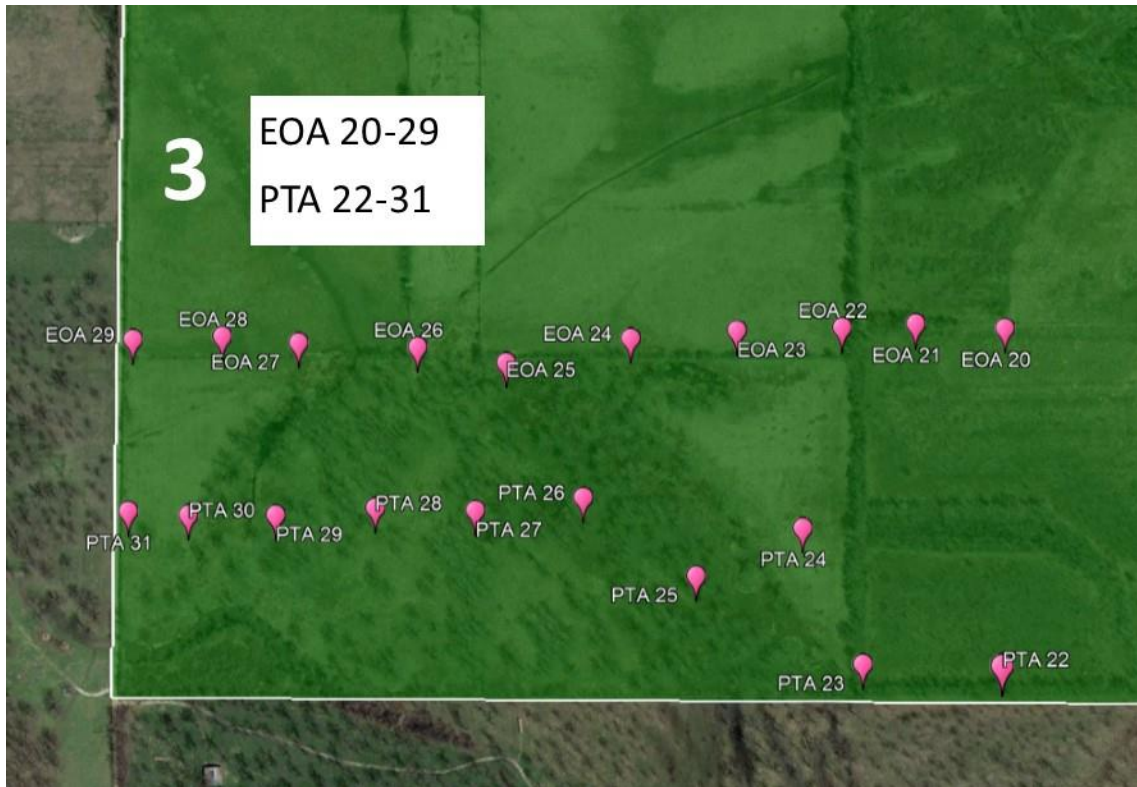


Figure A.4: Section 3 in the GRDA properties with labeled upland soil sampling locations

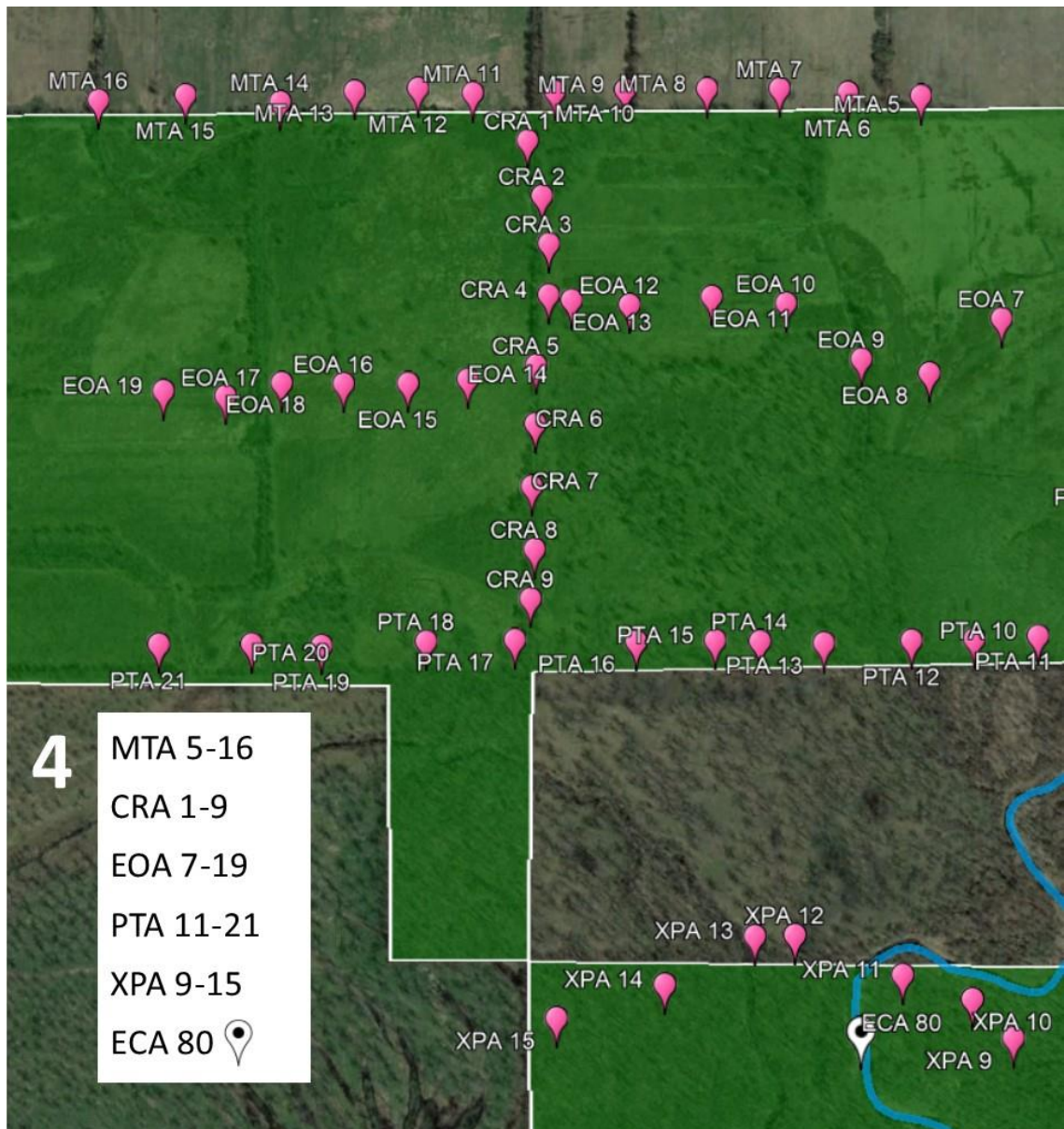


Figure A.5: Section 4 in the GRDA properties with labeled upland and creek soil sampling locations

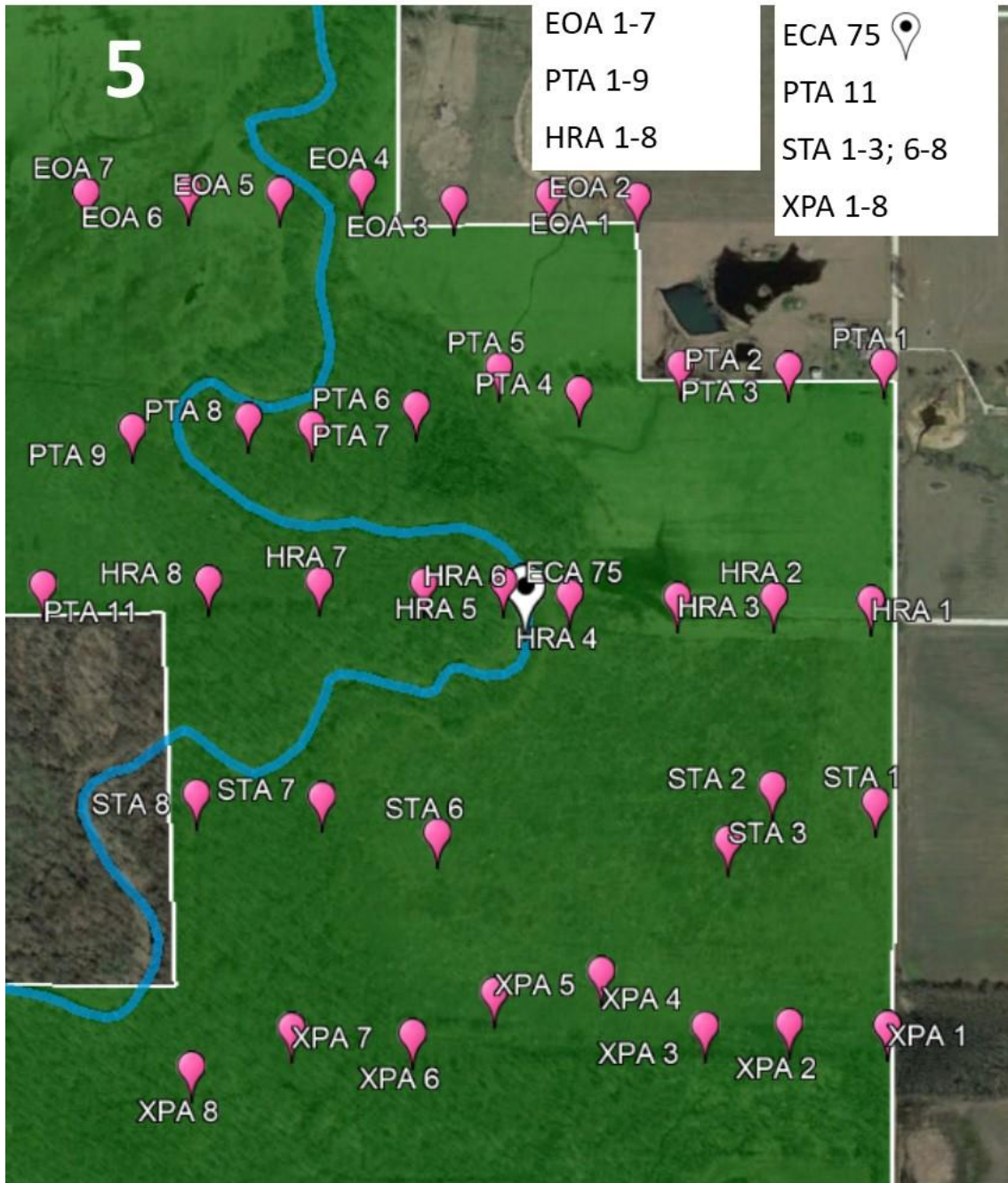


Figure A.6: Section 5 in the GRDA properties with labeled upland and creek soil sampling locations



Figure A.7: Section 6 in the GRDA properties with labeled upland soil sampling locations

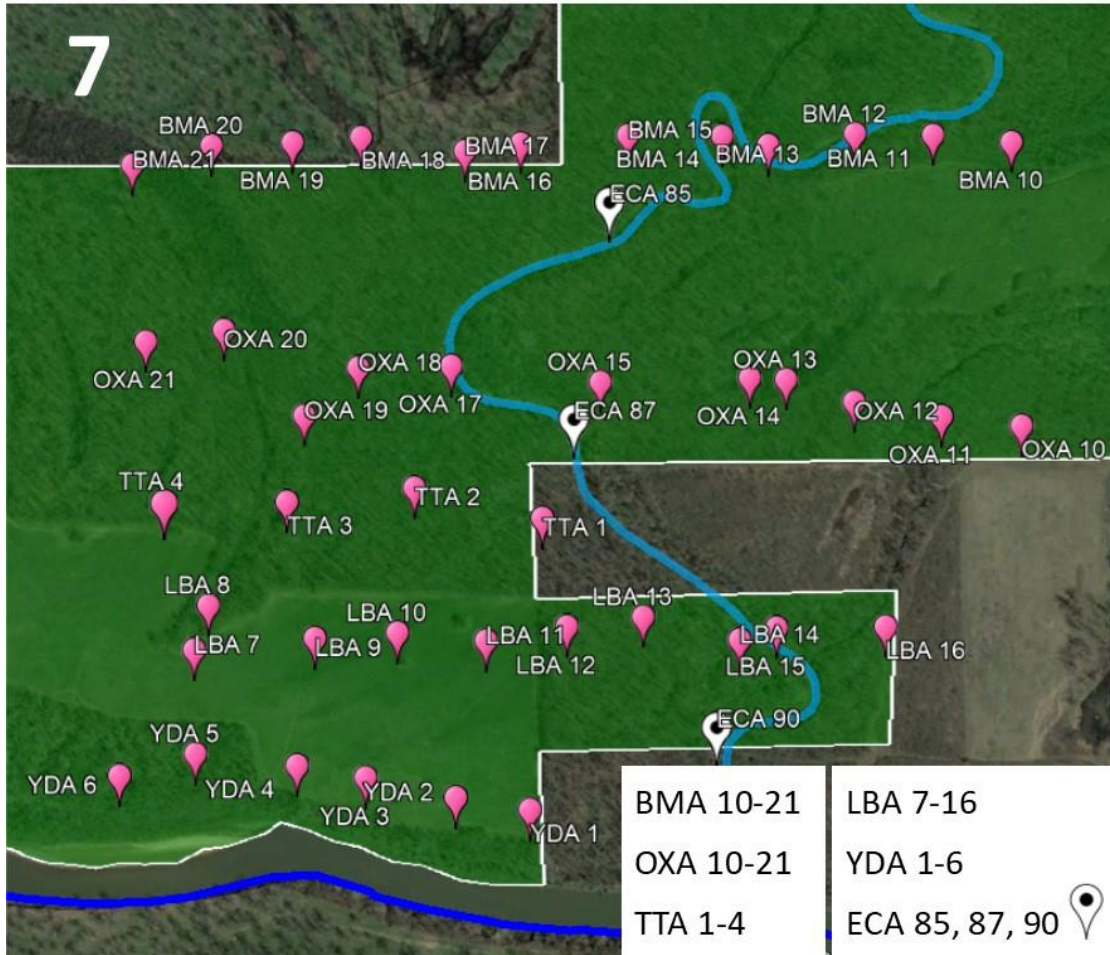


Figure A.8: Section 7 in the GRDA properties with labeled upland and creek soil sampling locations

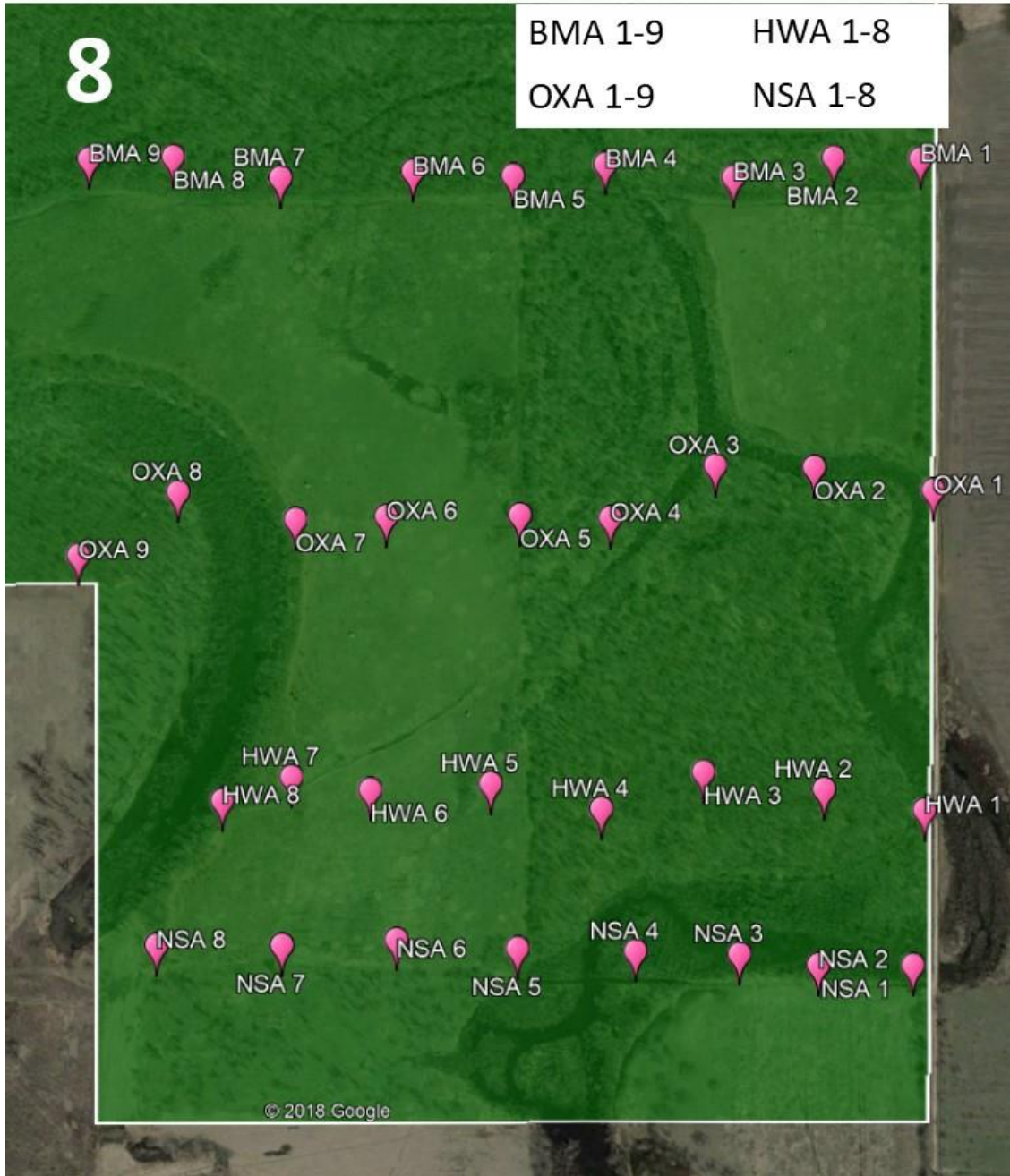


Figure A.9: Section 8 in the GRDA properties with labeled upland soil sampling locations

Table A.2: Upland soil samples-coordinates, metals concentrations, moisture content, and organic content

Sample	Latitude	Longitude	<i>In Situ</i> XRFs		Lab XRFs		Eq. 2.3	ICP-OES			Moisture Content		Organic Content
			mg/kg		mg/kg		mg/kg	mg/kg			<i>In Situ</i> (Bulk sample)	<#60 Sieved Sample	<#60 Sieved Sample
			Pb	Zn	Pb	Zn	Est. Cd	Cd	Pb	Zn			
BMA 1	36.899865	-94.913935	24.8	236	48.2	283	2.72	3.49	58.1	234	18.6%	5.9%	8.4%
BMA 2	36.899877	-94.914928	60.4	533	88.3	586	5.27				18.2%	6.6%	15.0%
BMA 3	36.899698	-94.916073	35.4	297	33.2	234	2.31				14.8%	5.4%	7.6%
BMA 4	36.899818	-94.917537	26.3	269	56.4	405	3.75				23.1%	9.1%	12.2%
BMA 5	36.899713	-94.918592	22.4	68.6	28.8	104	1.22				13.0%	4.4%	5.9%
BMA 6	36.899754	-94.919736	17.7	83.8	31.4	123	1.38				8.8%	3.9%	4.8%
BMA 7	36.899694	-94.921250	23.4	154	30.7	265	2.57	3.11	39.8	182	26.7%	7.3%	14.2%
BMA 8	36.899905	-94.922487	25.2	73.0	25.6	148	1.59	1.59	24.4	121	14.3%	3.2%	7.4%
BMA 9	36.899885	-94.923454	19.2	129	39.8	292	2.79				28.9%	7.5%	10.8%
BMA 10	36.899736	-94.924888	45.2	266	52.4	360	3.37	4.89	60.7	283	23.3%	5.8%	8.3%
BMA 11	36.899824	-94.926082	14.1	67.9	29.8	210	2.10				25.9%	6.3%	13.2%
BMA 12	36.899842	-94.927270	15.7	41.3	25.9	78.6	1.00				20.5%	3.4%	5.0%
BMA 13	36.899701	-94.928592	16.8	124	23.6	219	2.18				30.0%	13.1%	17.1%
BMA 14	36.899815	-94.929296	12.5	76.7	17.5	80.5	1.02				30.5%	5.8%	3.7%
BMA 15	36.899821	-94.930728	18.0	83.4	26.9	174	1.81	1.69	34.6	138	33.6%	7.5%	12.4%
BMA 16	36.899720	-94.932361	20.0	144	36.0	297	2.84	4.34	44.6	195	36.0%	11.1%	17.6%
BMA 17	36.899626	-94.933209	27.8	172	45.3	234	2.31				25.5%	13.2%	16.2%
BMA 18	36.899797	-94.934792	24.4	140	50.5	242	2.38	3.88	56.9	181	29.1%	8.4%	17.2%
BMA 19	36.899732	-94.935834	19.4	113	44.1	222	2.21				39.5%	7.0%	17.6%
BMA 20	36.899696	-94.937067	16.5	132	38.1	205	2.07				30.6%	9.1%	17.4%
BMA 21	36.899457	-94.938265	28.6	157	23.1	139	1.51				22.2%	3.6%	6.6%
BMA 22	36.899622	-94.939896	17.6	123	45.7	327	3.09	4.70	50.6	238	40.4%	7.4%	15.3%

Table A.2 Continued page 2: Upland soil samples-coordinates, metals concentrations, moisture content, and organic content

Sample	Latitude	Longitude	In Situ XRFs		Lab XRFs		Eq. 2.3	ICP-OES			Moisture Content		Organic Content
			mg/kg		mg/kg		mg/kg	mg/kg			In Situ (Bulk sample)	<#60 Sieved Sample	<#60 Sieved Sample
			Pb	Zn	Pb	Zn	Est. Cd	Cd	Pb	Zn			
BMA 23	36.899707	-94.940859	22.2	170	37.1	315	2.99				30.2%	7.3%	13.9%
BMA 24	36.899588	-94.942343	36.3	184	53.8	237	2.33				27.5%	6.6%	12.0%
BMA 25	36.899750	-94.943439	11.7	101	31.9	170	1.77				30.1%	9.5%	13.8%
BMA 26	36.899771	-94.944278	20.0	85.2	29.0	124	1.39				21.6%	8.2%	8.6%
BMA 27	36.899730	-94.945777	21.6	81.8	50.1	113	1.29	2.04	63.7	65.1	17.5%	3.8%	6.7%
BMA 28	36.899608	-94.947016	16.0	73.9	18.2	70.8	0.937				8.4%	3.0%	4.2%
BMA 29	36.899575	-94.948159	15.4	46.4	22.7	58.3	0.831				8.1%	2.5%	3.8%
BMA 30	36.899577	-94.949347	16.7	42.5	19.6	92.4	1.12				10.2%	2.8%	4.7%
BMA 31	36.899383	-94.950682	15.4	29.2	17.5	68.6	0.917				14.6%	2.6%	4.9%
BMA 32	36.899455	-94.951340	11.7	47.1	16.4	46.1	0.729				20.7%	2.3%	3.0%
CRA 1	36.913649	-94.931894	25.2	62.4	26.7	97.2	1.16				18.4%	7.9%	23.3%
CRA 2	36.912922	-94.931657	24.1	176	42.5	177	1.83				24.7%	5.3%	8.1%
CRA 3	36.912295	-94.931543	15.9	126	63.7	229	2.27				39.5%	6.3%	13.9%
CRA 4	36.911625	-94.931544	28.4	138	51.8	171	1.78				25.0%	7.2%	16.5%
CRA 5	36.910710	-94.931741	63.6	676	97.2	1474	12.7	12.8	97.8	1380	27.2%	4.7%	13.1%
CRA 6	36.909950	-94.931748	7.99	76.4	51.0	216	2.16				41.6%	4.6%	11.6%
CRA 7	36.909142	-94.931798	47.4	275	90.6	514	4.66				25.2%	3.0%	9.8%
CRA 8	36.908333	-94.931752	16.3	113	38.9	137	1.49				26.3%	14.9%	26.5%
CRA 9	36.907700	-94.931814	36.9	250	64.7	503	4.57				29.2%	8.1%	14.8%
EOA 1	36.911253	-94.917017	13.7	123	22.4	39.2	0.670				15.1%	2.1%	5.7%
EOA 2	36.911285	-94.918180	11.8	37.6	12.9	26.7	0.566				20.3%	1.9%	4.4%
EOA 3	36.911225	-94.919423	9.34	36.5	16.0	28.4	0.580				19.8%	3.3%	6.9%

Table A.2 Continued page 3: Upland soil samples-coordinates, metals concentrations, moisture content, and organic content

SAMPLE	Latitude	Longitude	<i>In Situ</i> XRFS		Lab XRFS		Eq. 2.3	ICP-OES			Moisture Content		Organic Content
			mg/kg		mg/kg		mg/kg	mg/kg			<i>In Situ</i> (Bulk sample)	<#60 Sieved Sample	<#60 Sieved Sample
			Pb	Zn	Pb	Zn	Est. Cd	Cd	Pb	Zn			
EOA 4	36.911416	-94.920635	14.8	114	27.6	77.8	1.00				23.1%	2.1%	5.5%
EOA 5	36.911322	-94.921715	15.1	129	29.9	113	1.29				27.4%	3.9%	6.6%
EOA 6	36.911333	-94.922916	69.7	653	59.3	254	2.48	2.19	69.4	196	22.1%	3.3%	5.9%
EOA 7	36.911316	-94.924258	26.4	244	46.3	161	1.69	1.94	51.0	106	27.0%	6.6%	19.8%
EOA 8	36.910606	-94.925426	27.1	130	59.0	150	1.60				34.9%	8.2%	12.4%
EOA 9	36.910791	-94.926515	39.9	340	76.1	415	3.84	3.18	79.5	269	26.8%	3.4%	11.6%
EOA 10	36.911518	-94.927722	51.3	220	96.3	317	3.01				28.7%	7.9%	13.7%
EOA 11	36.911605	-94.928919	33.0	136	59.2	172	1.78	1.55	61.0	121	25.6%	7.4%	16.9%
EOA 12	36.911498	-94.930242	20.5	88.5	59.0	160	1.69				35.7%	10.0%	17.6%
EOA 13	36.911558	-94.931173	16.6	134	44.0	194	1.97	2.39	46.6	108	34.1%	6.0%	11.5%
EOA 14	36.910526	-94.932836	10.1	51.4	40.8	144	1.55				50.5%	4.9%	7.3%
EOA 15	36.910475	-94.933795	17.8	64.0	30.7	102	1.20				31.3%	3.7%	8.1%
EOA 16	36.910469	-94.935658	15.7	22.5	27.0	84.2	1.05				26.9%	6.4%	15.7%
EOA 17	36.910479	-94.935822	23.8	73.9	39.0	89.6	1.09	1.08	38.0	51.6	24.9%	6.4%	20.7%
EOA 18	36.910310	-94.936721	18.8	71.3	50.5	155	1.64	1.51	36.9	81.5	41.2%	3.3%	8.4%
EOA 19	36.910376	-94.937719	9.92	36.8	40.3	130	1.44				50.7%	5.3%	12.8%
EOA 20	36.910418	-94.938947	15.8	33.7	25.3	85.5	1.06	0.616	26.6	52.5	33.3%	2.6%	3.9%
EOA 21	36.910461	-94.940047	10.1	36.3	24.5	80.6	1.02				38.2%	2.4%	4.1%
EOA 22	36.910426	-94.940955	24.9	52.5	15.6	42.1	0.695				9.9%	3.9%	5.9%
EOA 23	36.910396	-94.942251	9.87	35.3	16.1	36.8	0.650				18.1%	3.5%	17.0%
EOA 24	36.910317	-94.943561	13.8	42.0	17.7	78.0	1.00	1.21	22.9	53.2	20.9%	2.8%	10.6%
EOA 25	36.910077	-94.945094	20.9	139	57.4	330	3.11				40.3%	4.7%	7.0%

Table A.2 Continued page 4: Upland soil samples-coordinates, metals concentrations, moisture content, and organic content

Sample	Latitude	Longitude	<i>In Situ</i> XRFS		Lab XRFS		Eq. 2.3	ICP-OES			Moisture Content		Organic Content
			mg/kg		mg/kg		mg/kg	mg/kg			<i>In Situ</i> (Bulk sample)	<#60 Sieved Sample	<#60 Sieved Sample
			Pb	Zn	Pb	Zn	Est. Cd	Cd	Pb	Zn			
EOA 26	36.910231	-94.946187	95.6	469	163	576	1.00	6.04	167	677	37.0%	5.2%	8.6%
EOA 27	36.910272	-94.947655	25.9	78.8	22.8	74.4	1.29				24.6%	5.3%	7.1%
EOA 28	36.910337	-94.948596	33.3	235	34.5	199	2.48				21.5%	5.2%	7.2%
EOA 29	36.910306	-94.949698	55.2	641	69.2	984	1.69	8.67	85.0	1498	14.0%	2.6%	7.9%
GRA 1	36.922424	-94.913675	14.0	135	23.8	89.0	1.60				23.8%	3.1%	7.8%
GRA 2	36.922479	-94.915043	93.8	710	112	600	3.84	4.01	108	480	24.4%	2.9%	6.9%
GRA 3	36.922462	-94.916087	76.4	1214	171	1766	3.01	16.5	148	1443	29.7%	6.0%	8.4%
GRA 4	36.922284	-94.917619	21.0	148	35.1	167	1.78				26.5%	7.2%	8.3%
GRA 5	36.922324	-94.918641	15.4	114	32.4	134	1.69				26.1%	2.9%	6.0%
GRA 6	36.922443	-94.920319	14.9	55.5	26.9	71.3	1.97				26.6%	4.3%	10.8%
GRA 7	36.922409	-94.921443	16.5	58.9	26.4	76.6	1.55				24.1%	7.5%	8.9%
GRA 8	36.924167	-94.913872	90.1	1617	137	1260	1.20				24.5%	2.8%	7.3%
GRA 9	36.924292	-94.914658	69.5	496	85.0	485	1.05	3.83	87.3	431	28.9%	1.9%	5.8%
GRA 10	36.924458	-94.916409	15.1	111	28.6	122	1.09				19.9%	3.8%	7.1%
GRA 11	36.924721	-94.917337	13.6	31.9	19.8	49.6	1.64				17.7%	2.1%	6.4%
GRA 12	36.924640	-94.918532	16.0	111	24.6	75.3	1.44				18.6%	2.1%	6.2%
GRA 13	36.924087	-94.919629	9.64	40.3	12.8	66.5	1.06	0.784	17.8	38.0	18.5%	2.8%	6.5%
HFA 1	36.920734	-94.913797	48.0	442	45.6	420	1.02	3.67	48.4	446	4.6%	2.5%	7.0%
HFA 2	36.920765	-94.914909	37.3	227	53.4	232	0.695				10.7%	3.6%	9.5%
HFA 3	36.920705	-94.916083	15.4	91.8	13.3	75.8	0.650				16.8%	4.1%	8.4%
HFA 4	36.920712	-94.917164	15.0	36.5	13.4	41.8	1.00				24.0%	4.1%	6.5%
HFA 5	36.920707	-94.918134	81.4	848	138	803	3.11	5.71	141	686	30.0%	12.1%	18.3%

Table A.2 Continued page 5: Upland soil samples-coordinates, metals concentrations, moisture content, and organic content

Sample	Latitude	Longitude	<i>In Situ</i> XRFS		Lab XRFS		Eq. 2.3	ICP-OES			Moisture Content		Organic Content
			mg/kg		mg/kg		mg/kg	mg/kg			<i>In Situ</i> (Bulk sample)	<#60 Sieved Sample	<#60 Sieved Sample
			Pb	Zn	Pb	Zn	Est. Cd	Cd	Pb	Zn			
HRA 1	36.907021	-94.913976	27.1	180	33.4	150	1.60				22.8%	3.0%	8.2%
HRA 2	36.907058	-94.915237	18.7	56.1	27.4	91.2	1.11				30.2%	3.3%	7.6%
HRA 3	36.907056	-94.916493	24.3	160	21.7	79.3	1.01				24.5%	2.3%	6.8%
HRA 4	36.907088	-94.917892	19.7	321	36.4	88.9	1.09				20.0%	2.0%	6.1%
HRA 5	36.907216	-94.918757	117	874	165	660	5.89	6.27	141	482	15.6%	1.5%	3.3%
HRA 6	36.907204	-94.919790	71.6	413	83.4	474	4.33				22.7%	3.3%	8.7%
HRA 7	36.907220	-94.921149	49.4	221	54.9	292	2.80				21.6%	2.0%	6.3%
HRA 8	36.907231	-94.922591	67.2	276	35.7	191	1.95				21.7%	2.8%	5.2%
HWA 1	36.893904	-94.913888	29.7	237	37.2	331	3.13				28.3%	6.9%	13.5%
HWA 2	36.894094	-94.915035	11.4	67.2	35.5	178	1.84				35.2%	7.8%	21.4%
HWA 3	36.894253	-94.916415	22.0	85.1	29.3	149	1.60				32.0%	6.8%	13.5%
HWA 4	36.893917	-94.917582	19.6	83.1	20.6	151	1.61				33.0%	6.1%	12.5%
HWA 5	36.894147	-94.918848	21.0	65.7	25.5	119	1.34				11.2%	4.5%	7.6%
HWA 6	36.894090	-94.920225	19.2	68.7	20.9	64.4	0.883				11.8%	3.4%	5.0%
HWA 7	36.894208	-94.921126	11.3	42.3	22.4	83.6	1.04				17.8%	6.5%	13.0%
HWA 8	36.893980	-94.921922	19.7	112	29.0	173	1.79				26.2%	2.3%	5.0%
IBA 1	36.917732	-94.913764	15.3	95.5	14.6	125	1.39				26.6%	3.3%	9.8%
IBA 2	36.917695	-94.915377	14.7	30.8	17.5	45.8	0.726	0.532	15.6	37.4	24.3%	2.6%	7.1%
IBA 3	36.918027	-94.916727	20.6	113	20.4	96.6	1.15	1.16	22.0	57.5	26.5%	3.5%	9.9%
IBA 4	36.917940	-94.918164	12.9	97.3	26.2	104	1.21				26.0%	2.0%	7.8%
IBA 5	36.917155	-94.919286	33.1	174	45.1	205	2.06				29.5%	2.1%	7.3%
IBA 6	36.917183	-94.920143	62.7	625	90.0	480	4.38				24.6%	3.7%	9.5%

Table A.2 Continued page 6: Upland soil samples-coordinates, metals concentrations, moisture content, and organic content

Sample	Latitude	Longitude	<i>In Situ</i> XRFs		Lab XRFs		Eq. 2.3	ICP-OES			Moisture Content		Organic Content
			mg/kg		mg/kg		mg/kg	mg/kg			<i>In Situ</i> (Bulk sample)	<#60 Sieved Sample	<#60 Sieved Sample
			Pb	Zn	Pb	Zn	Est. Cd	Cd	Pb	Zn			
IBA 7	36.917365	-94.921915	13.3	28.1	24.2	22.2	0.527				23.9%	1.8%	4.7%
IBA 8	36.917186	-94.922541	7.45	20.2	23.4	42.9	0.702	0.596	20.6	39.8	27.1%	1.8%	5.6%
JOA 1	36.901065	-94.953427	11.3	32.0	18.6	46.5	0.732				21.0%	3.8%	3.3%
JOA 2	36.901005	-94.952173	13.0	61.2	21.7	115	1.31				33.8%	5.6%	12.4%
JOA 3	36.901063	-94.950969	13.1	58.6	22.6	81.4	1.03				18.7%	3.0%	5.8%
JOA 4	36.901099	-94.950100	15.6	65.6	22.6	89.9	1.10				24.6%	3.6%	7.0%
LBA 1	36.894300	-94.945883	13.2	34.2	24.2	65.5	0.892				26.5%	2.8%	5.4%
LBA 2	36.893893	-94.944142	17.4	61.0	22.0	97.9	1.16				26.6%	4.5%	7.1%
LBA 3	36.893689	-94.942857	15.6	68.4	21.5	99.2	1.18				31.7%	6.0%	10.7%
LBA 4	36.893914	-94.941492	9.92	49.3	16.2	105	1.23				48.9%	7.9%	32.1%
LBA 5	36.893713	-94.940378	14.8	67.7	19.9	79.1	1.01				21.8%	3.0%	7.2%
LBA 6	36.893550	-94.939111	15.1	49.7	19.3	72.1	0.947				18.4%	2.9%	5.9%
LBA 7	36.893597	-94.937185	22.0	89.7	27.2	93.5	1.13				17.8%	4.0%	7.5%
LBA 8	36.894129	-94.936982	26.3	107	28.5	79.7	1.01				20.4%	4.2%	8.0%
LBA 9	36.893736	-94.935377	16.3	69.1	31.7	115	1.31				25.4%	4.2%	7.9%
LBA 10	36.893802	-94.934141	21.8	90.2	32.2	101	1.19				19.3%	4.5%	7.1%
LBA 11	36.893707	-94.932814	22.8	110	26.4	108	1.25				21.5%	4.4%	7.9%
LBA 12	36.893876	-94.931603	15.2	108	42.5	172	1.79				36.7%	6.8%	15.9%
LBA 13	36.893992	-94.930459	< LOD	67.0	19.0	76.9	0.987				33.2%	4.9%	9.9%
LBA 14	36.893718	-94.929011	14.7	50.2	18.1	87.6	1.08				23.3%	3.7%	5.0%
LBA 15	36.893860	-94.928459	15.5	28.1	14.1	78.1	1.00				24.6%	2.7%	2.6%
LBA 16	36.893875	-94.926824	13.7	46.2	15.0	74.8	0.970				25.8%	3.5%	7.4%

Table A.2 Continued page 7: Upland soil samples-coordinates, metals concentrations, moisture content, and organic content

Sample	Latitude	Longitude	<i>In Situ</i> XRFS		Lab XRFS		Eq. 2.3	ICP-OES			Moisture Content		Organic Content
			mg/kg		mg/kg		mg/kg	mg/kg			<i>In Situ</i> (Bulk sample)	<#60 Sieved Sample	<#60 Sieved Sample
			Pb	Zn	Pb	Zn	Est. Cd	Cd	Pb	Zn			
MTA 1	36.914345	-94.920242	14.3	163	39.9	185	1.90	1.97	41.6	111	31.2%	3.4%	9.4%
MTA 2	36.914254	-94.921596	39.2	432	72.4	543	4.91				34.3%	4.8%	12.4%
MTA 3	36.914338	-94.922706	19.3	73.3	25.4	107	1.24				30.3%	2.8%	6.5%
MTA 4	36.914239	-94.923929	< LOD	< LOD	18.2	39.6	0.674				23.7%	1.6%	5.2%
MTA 5	36.914237	-94.925527	14.5	49.1	28.2	58.9	0.836				23.5%	2.8%	8.4%
MTA 6	36.914280	-94.926712	9.70	24.4	16.2	27.3	0.570				20.6%	2.4%	5.7%
MTA 7	36.914331	-94.927816	13.6	44.6	36.1	60.1	0.846				22.9%	3.2%	7.1%
MTA 8	36.914328	-94.928991	10.6	64.9	22.7	66.2	0.897				44.5%	3.0%	6.7%
MTA 9	36.914316	-94.930316	15.4	150	17.6	139	1.51				41.2%	4.0%	12.2%
MTA 10	36.914294	-94.931455	21.5	196	31.2	273	2.63				22.2%	2.5%	7.3%
MTA 11	36.914274	-94.932785	26.0	173	37.4	152	1.62				25.4%	3.7%	5.8%
MTA 12	36.914336	-94.933671	11.8	106	30.9	134	1.47				19.9%	2.9%	7.7%
MTA 13	36.914297	-94.934700	21.5	134	39.1	127	1.41	0.828	36.2	93.9	14.9%	1.8%	8.0%
MTA 14	36.914156	-94.935902	19.7	62.3	30.1	98.6	1.17				24.3%	3.7%	8.4%
MTA 15	36.914248	-94.937436	11.6	39.0	17.3	61.1	0.855				29.1%	2.7%	9.7%
MTA 16	36.914180	-94.938844	19.5	148	52.8	221	2.20	1.59	52.1	159	32.0%	4.0%	9.3%
MTA 17	36.914235	-94.939995	23.1	121	29.3	243	2.39				36.5%	5.7%	13.4%
MTA 18	36.914166	-94.941282	11.3	38.3	21.7	43.1	0.704				25.1%	1.9%	3.9%
MTA 19	36.914146	-94.942604	11.9	< LOD	16.9	27.5	0.572				28.8%	2.4%	4.5%
MTA 20	36.914122	-94.943823	10.4	29.4	16.4	24.2	0.545				19.8%	1.7%	5.3%
MTA 21	36.914055	-94.944952	< LOD	< LOD	17.4	< LOD					23.6%	1.2%	4.3%
MTA 22	36.914253	-94.946359	29.4	245	51.1	316	3.00				17.9%	1.9%	5.8%

Table A.2 Continued page 8: Upland soil samples-coordinates, metals concentrations, moisture content, and organic content

Sample	Latitude	Longitude	<i>In Situ</i> XRFs		Lab XRFs		Eq. 2.3	ICP-OES			Moisture Content		Organic Content
			mg/kg		mg/kg		mg/kg	mg/kg			<i>In Situ</i> (Bulk sample)	<#60 Sieved Sample	<#60 Sieved Sample
			Pb	Zn	Pb	Zn	Est. Cd	Cd	Pb	Zn			
MTA 23	36.914208	-94.947585	74.4	380	116	577	5.20	3.99	91.9	617	19.3%	2.1%	6.1%
MTA 24	36.914310	-94.948668	22.1	63.8	26.1	80.4	1.02				22.6%	2.5%	7.7%
MTA 25	36.914823	-94.949660	10.1	< LOD	22.7	92.8	1.12				27.3%	1.9%	5.5%
MTA 26	36.914577	-94.913907	8.71	66.2	20.8	65.2	0.890				20.8%	1.6%	4.3%
MTA 27	36.914591	-94.914953	9.89	27.8	12.0	32.4	0.613				21.0%	2.3%	5.8%
MTA 28	36.914628	-94.916115	< LOD	28.2	12.5	53.8	0.793				19.8%	1.5%	5.6%
MTA 29	36.914637	-94.917442	9.67	< LOD	< LOD	32.0	0.610				20.4%	1.1%	4.8%
MTA 30	36.914617	-94.918496	13.0	< LOD	9.90	21.2	0.519				23.6%	3.7%	4.4%
NSA 1	36.892482	-94.914019	30.5	235	47.6	271	2.62				24.7%	6.7%	16.4%
NSA 2	36.892486	-94.915101	30.8	109	27.4	155	1.64				15.6%	5.3%	11.3%
NSA 3	36.892585	-94.916004	23.1	135	34.8	188	1.92				13.5%	5.2%	7.5%
NSA 4	36.892610	-94.917191	12.6	119	64.1	650	5.81				40.6%	5.8%	12.8%
NSA 5	36.892636	-94.918540	14.6	90.8	30.4	203	2.05	3.70	37.0	179	29.6%	6.2%	11.6%
NSA 6	36.892717	-94.919925	22.1	59.3	23.2	98.8	1.17				19.2%	4.1%	6.6%
NSA 7	36.892666	-94.921234	19.4	68.0	27.5	97.0	1.16				21.2%	4.1%	7.7%
NSA 8	36.892648	-94.922679	14.5	36.4	25.1	109	1.26				18.0%	3.7%	5.3%
OXA 1	36.896832	-94.913789	81.8	456	91.6	648	5.79	3.67	99.8	530	24.5%	8.0%	17.1%
OXA 2	36.897042	-94.915149	28.6	199	42.0	364	3.40				28.9%	13.3%	12.9%
OXA 3	36.897059	-94.916279	21.8	165	44.0	283	2.72				27.5%	9.6%	16.3%
OXA 4	36.896579	-94.917479	< LOD	36.3	16.8	174	1.81	4.21	31.0	133	26.6%	12.5%	49.5%
OXA 5	36.896606	-94.918512	24.6	101	42.8	172	1.79				32.4%	6.8%	11.5%
OXA 6	36.896593	-94.920041	16.7	62.9	15.6	93.6	1.13				20.8%	4.8%	6.1%

Table A.2 Continued page 9: Upland soil samples-coordinates, metals concentrations, moisture content, and organic content

Sample	Latitude	Longitude	In Situ XRFS mg/kg		Lab XRFS mg/kg		Eq. 2.3 mg/kg Est. Cd	ICP-OES mg/kg			Moisture Content		Organic Content <#60 Sieved Sample
			Pb	Zn	Pb	Zn		Cd	Pb	Zn	In Situ (Bulk sample)	<#60 Sieved Sample	
OXA 7	36.896566	-94.921078	27.2	123	28.3	161	1.69				25.2%	7.0%	12.2%
OXA 8	36.896819	-94.922431	19.1	140	25.3	167	1.75				31.7%	6.1%	13.1%
OXA 9	36.896237	-94.923576	20.0	66.2	28.6	87.1	1.07				14.2%	3.8%	5.6%
OXA 10	36.896284	-94.924762	12.6	85.6	20.0	110	1.26				28.8%	5.4%	9.3%
OXA 11	36.896396	-94.925970	14.0	51.5	22.7	64.1	0.880				30.0%	2.9%	5.1%
OXA 12	36.896572	-94.927289	9.92	63.7	26.2	145	1.56				43.8%	7.2%	15.1%
OXA 13	36.896842	-94.928318	10.0	48.9	35.7	126	1.40				37.9%	6.3%	11.1%
OXA 14	36.896862	-94.928867	16.8	70.9	20.8	86.0	1.06				35.9%	7.2%	16.9%
OXA 15	36.896812	-94.931124	13.4	55.6	26.3	126	1.40				30.7%	8.3%	13.3%
OXA 16	36.896831	-94.932250	14.5	< LOD	15.9	48.1	0.745				24.4%	3.5%	2.3%
OXA 17	36.897009	-94.933385	11.5	39.4	12.8	53.2	0.788				21.2%	7.7%	5.1%
OXA 18	36.896986	-94.934788	20.5	93.1	36.1	214	2.14	3.58	42.2	150	33.6%	14.4%	14.5%
OXA 19	36.896405	-94.935591	10.5	87.8	29.4	156	1.65				41.0%	13.6%	19.0%
OXA 20	36.897440	-94.936828	16.8	62.4	35.5	107	1.24				27.2%	6.6%	10.5%
OXA 21	36.897301	-94.938005	13.5	91.9	36.5	173	1.80				34.8%	11.7%	18.3%
OXA 22	36.897024	-94.939357	14.0	87.5	37.5	250	2.45	5.08	37.2	158	38.9%	10.6%	21.2%
OXA 23	36.896769	-94.940759	13.1	95.6	32.6	170	1.77				37.3%	13.4%	20.2%
OXA 24	36.896813	-94.942001	16.7	87.4	20.6	198	2.00				36.3%	13.5%	18.6%
OXA 25	36.897164	-94.943086	11.0	54.2	24.3	149	1.59	4.16	30.3	122	42.6%	9.2%	21.7%
OXA 26	36.897142	-94.944534	23.1	89.0	24.8	118	1.33				17.6%	4.5%	5.9%
OXA 27	36.897373	-94.945714	14.5	74.0	21.9	75.8	0.979				10.8%	3.6%	5.7%
OXA 28	36.896942	-94.946733	16.9	79.3	16.4	83.6	1.04				16.6%	4.2%	5.4%

Table A.2 Continued page 10: Upland soil samples-coordinates, metals concentrations, moisture content, and organic content

Sample	Latitude	Longitude	<i>In Situ</i> XRFS		Lab XRFS		Eq. 2.3	ICP-OES			Moisture Content		Organic Content
			mg/kg		mg/kg		mg/kg	mg/kg			<i>In Situ</i> (Bulk sample)	<#60 Sieved Sample	<#60 Sieved Sample
			Pb	Zn	Pb	Zn	Est. Cd	Cd	Pb	Zn			
OXA 29	36.896797	-94.947923	15.5	65.4	22.2	93.9	1.13				10.7%	3.8%	4.7%
OXA 30	36.896854	-94.949412	13.2	48.5	21.2	73.2	0.956				20.1%	4.3%	5.2%
PTA 1	36.909497	-94.913799	27.8	202	30.9	184	1.89				14.6%	2.1%	6.6%
PTA 2	36.909465	-94.915042	< LOD	70.9	22.9	76.4	0.983				22.6%	2.2%	6.7%
PTA 3	36.909484	-94.916455	11.1	43.0	14.3	64.6	0.885				28.6%	2.0%	6.5%
PTA 4	36.909213	-94.917777	12.1	25.9	19.2	47.3	0.739				26.4%	1.7%	5.2%
PTA 5 - 16			16.0	137	21.0	48.1	0.746	1.20	22.7	50.8	27.1%	2.2%	5.8%
PTA 5 -26	36.909467	-94.918825	8.76	96.2	50.8	311	2.96				44.3%	7.2%	18.3%
PTA 6	36.909058	-94.919905	50.6	683	123	947	8.31	5.50	112	771	40.8%	4.9%	17.1%
PTA 7	36.908851	-94.921267	28.2	256	87.8	646	5.77				52.9%	8.8%	23.1%
PTA 8	36.908934	-94.922096	33.9	253	53.8	393	3.65				30.3%	4.9%	11.7%
PTA 9	36.908823	-94.923609	65.7	544	47.4	231	2.28	2.07	49.2	185	19.5%	2.1%	3.4%
PTA 10	36.907223	-94.923728	80.6	238	69.3	251	2.45				13.5%	3.2%	5.6%
PTA 11	36.907185	-94.924742	51.0	175	27.9	104	1.21				10.6%	3.3%	4.0%
PTA 12	36.907167	-94.925743	14.6	45.2	15.8	29.3	0.587				12.1%	2.1%	2.5%
PTA 13	36.907132	-94.927138	69.3	307	97.6	288	2.76				23.5%	4.4%	6.7%
PTA 14	36.907155	-94.928156	49.0	313	98.7	462	4.23	4.50	104	354	33.6%	6.6%	8.7%
PTA 15	36.907167	-94.928870	7.17	144	51.3	490	4.46				66.4%	5.2%	53.8%
PTA 16	36.907152	-94.930125	23.3	178	31.9	237	2.33				40.2%	5.4%	7.3%
PTA 17	36.907173	-94.932059	63.1	458	66.1	528	4.78	3.26	78.4	420	29.1%	5.7%	14.2%
PTA 18	36.907153	-94.933472	25.7	214	51.5	409	3.78				38.8%	6.8%	12.7%
PTA 19	36.907098	-94.935139	50.9	241	50.8	311	2.96				22.8%	6.1%	15.7%

Table A.2 Continued page 11: Upland soil samples-coordinates, metals concentrations, moisture content, and organic content

Sample	Latitude	Longitude	In Situ XRFS mg/kg		Lab XRFS mg/kg		Eq. 2.3 mg/kg Est. Cd	ICP-OES mg/kg			Moisture Content		Organic Content <#60 Sieved Sample
			Pb	Zn	Pb	Zn		Cd	Pb	Zn	In Situ (Bulk sample)	<#60 Sieved Sample	
PTA 20	36.907118	-94.936250	28.8	182	40.5	246	2.41				27.5%	6.0%	12.6%
PTA 21	36.907115	-94.937728	31.5	105	31.2	109	1.26				17.0%	3.6%	8.7%
PTA 22	36.907051	-94.938992	17.5	52.5	23.4	72.9	0.954				18.4%	2.8%	4.6%
PTA 23	36.907114	-94.940701	27.8	92.8	24.5	83.4	1.04				20.8%	3.8%	8.3%
PTA 24	36.908449	-94.941440	15.5	61.3	22.5	86.7	1.07				29.5%	3.3%	9.4%
PTA 25	36.907978	-94.942749	14.8	120	39.5	218	2.17				38.4%	5.3%	13.5%
PTA 26	36.908749	-94.944140	8.25	80.6	30.6	199	2.01				37.9%	4.5%	13.5%
PTA 27	36.908621	-94.945466	12.5	70.8	24.3	126	1.40				33.6%	4.7%	10.4%
PTA 28	36.908645	-94.946699	10.8	93.6	29.3	116	1.31				34.1%	5.3%	13.2%
PTA 29	36.908574	-94.947923	20.5	109	23.5	109	1.26				24.4%	4.5%	9.7%
PTA 30	36.908574	-94.948999	21.0	78.1	16.6	72.2	0.948				26.2%	3.3%	8.0%
PTA 31	36.908611	-94.949738	60.6	533	65.0	454	4.16				4.5%	3.6%	8.8%
SKA 1	36.921349	-94.945522	15.9	60.5	12.9	45.7	0.726				10.7%	2.5%	4.5%
SKA 2	36.921259	-94.946716	13.3	39.9	11.6	32.2	0.612	0.928	14.1	21.4	8.7%	0.9%	3.3%
SKA 3	36.921262	-94.947850	15.1	24.5	14.0	23.6	0.539				12.3%	2.5%	5.0%
SKA 4	36.921264	-94.949018	20.7	34.3	17.1	34.5	0.631				9.2%	7.4%	6.4%
SKA 5	36.921305	-94.949653	52.8	333	47.6	292	2.80	2.16	46.1	239	7.7%	7.2%	6.6%
STA 1	36.904934	-94.913930	8.46	45.7	24.5	75.7	0.978				34.9%	3.3%	7.9%
STA 2	36.905099	-94.915261	< LOD	44.8	21.2	30.9	0.601				30.5%	2.5%	6.1%
STA 3	36.904540	-94.915837	< LOD	34.9	19.2	31.9	0.609				23.8%	2.3%	4.1%
STA 6	36.904613	-94.919591	9.00	36.6	16.1	38.5	0.664				27.2%	4.1%	6.8%
STA 7	36.904987	-94.921088	36.2	817	151	2068	17.7	17.2	146	1628	52.5%	9.3%	43.2%

Table A.2 Continued page 12: Upland soil samples-coordinates, metals concentrations, moisture content, and organic content

Sample	Latitude	Longitude	<i>In Situ</i> XRFS		Lab XRFS		Eq. 2.3	ICP-OES			Moisture Content		Organic Content
			mg/kg		mg/kg		mg/kg	mg/kg			<i>In Situ</i> (Bulk sample)	<#60 Sieved Sample	<#60 Sieved Sample
			Pb	Zn	Pb	Zn	Est. Cd	Cd	Pb	Zn			
STA 8	36.905015	-94.922712	18.6	118	42.4	318	3.01				46.1%	4.6%	11.1%
TTA 1	36.895172	-94.931983	10.8	65.5	26.1	146	1.57				48.5%	7.2%	19.0%
TTA 2	36.895536	-94.933916	13.1	89.0	34.6	214	2.14				40.1%	2.9%	4.7%
TTA 3	36.895366	-94.935831	12.1	92.7	23.0	174	1.80				36.1%	4.1%	5.3%
TTA 4	36.895279	-94.937674	23.1	70.6	24.5	85.7	1.06				9.9%	3.8%	5.6%
TTA 5	36.895431	-94.939933	27.2	81.2	22.3	101	1.19	1.34	30.2	81.7	11.3%	4.8%	6.8%
UBA 1	36.917459	-94.943500	5.12	21.6	16.5	23.7	0.540	0.305	13.5	24.1	26.8%	1.6%	3.5%
UBA 2	36.917438	-94.944802	14.7	16.2	19.3	27.8	0.574				17.6%	1.7%	3.4%
UBA 3	36.917442	-94.945995	16.0	23.4	12.0	< LOD					26.6%	1.7%	4.7%
UBA 4	36.917419	-94.947244	11.7	27.3	24.3	25.2	0.553				20.2%	2.3%	5.6%
UBA 5	36.917488	-94.948532	8.62	12.7	13.0	< LOD					18.0%	1.5%	3.3%
UBA 6	36.917391	-94.949631	20.2	43.4	21.1	35.1	0.636				16.7%	1.4%	3.4%
XPA 1	36.902639	-94.913788	59.1	556	88.6	731	6.49	5.11	88.8	844	8.3%	4.6%	7.3%
XPA 2	36.902663	-94.915051	47.4	181	60.2	285	2.74				37.9%	4.6%	8.1%
XPA 3	36.902634	-94.916133	15.8	128	66.6	410	3.79				43.8%	8.6%	12.1%
XPA 4	36.903193	-94.917470	41.1	404	55.4	299	2.86	2.20	56.1	228	29.2%	9.8%	27.4%
XPA 5	36.902983	-94.918847	56.9	476	87.5	445	4.08				28.4%	7.0%	16.2%
XPA 6	36.902556	-94.919894	39.5	579	106	1285	11.15				46.7%	12.3%	25.5%
XPA 7	36.902619	-94.921451	82.2	786	160	1232	10.70	8.31	155	995	31.0%	13.5%	29.8%
XPA 8	36.902224	-94.922733	40.9	628	122	1277	11.09				36.4%	12.0%	17.7%
XPA 9	36.902153	-94.924187	39.3	478	77.8	938	8.23				42.1%	14.8%	19.1%
XPA 10	36.902636	-94.924826	36.1	334	133	671	5.99				44.5%	9.8%	15.1%

Table A.2 Continued page 13: Upland soil samples-coordinates, metals concentrations, moisture content, and organic content

Sample	Latitude	Longitude	<i>In Situ</i> XRFs		Lab XRFs		Eq. 2.3	ICP-OES			Moisture Content		Organic Content
			mg/kg		mg/kg		mg/kg	mg/kg			<i>In Situ</i> (Bulk sample)	<#60 Sieved Sample	<#60 Sieved Sample
			Pb	Zn	Pb	Zn	Est. Cd	Cd	Pb	Zn			
XPA 11	36.902940	-94.925921	30.9	380	115	783	6.93				34.3%	6.2%	8.9%
XPA 12	36.903438	-94.927616	53.9	373	103	481	4.39				27.2%	7.5%	12.1%
XPA 13	36.903425	-94.928248	18.6	123	33.5	242	2.38				35.0%	5.9%	37.8%
XPA 14	36.902818	-94.929670	36.6	302	61.2	398	3.69	4.57	75.5	345	30.3%	2.6%	6.7%
XPA 15	36.902398	-94.931374	11.3	113	18.5	203	2.05				54.9%	2.1%	5.7%
YDA 1	36.891706	-94.932131	15.8	68.1	12.3	69.5	0.926				35.5%	5.0%	4.8%
YDA 2	36.891849	-94.933240	12.8	42.9	20.2	72.2	0.948				23.2%	5.0%	4.9%
YDA 3	36.892084	-94.934589	14.4	51.7	14.8	56.8	0.819				19.5%	4.0%	4.0%
YDA 4	36.892226	-94.935616	12.1	33.4	20.5	53.0	0.787				19.0%	8.6%	5.1%
YDA 5	36.892364	-94.937138	10.1	40.7	25.0	87.9	1.08				22.4%	4.9%	4.1%
YDA 6	36.892104	-94.938266	< LOD	28.7	18.8	69.9	0.928				25.0%	3.8%	3.1%
YDA 7	36.892442	-94.939569	< LOD	23.1	14.1	61.0	0.854	1.45	17.9	38.7	29.1%	2.8%	2.4%
YDA 8	36.892406	-94.940756	11.8	25.0	11.8	57.7	0.826				22.2%	0.1%	0.2%
YDA 9	36.892408	-94.942090	< LOD	< LOD	10.1	24.9	0.550				35.2%	0.2%	0.2%

Table A.3: Elm Creek terrace soil samples-coordinates, metals concentrations, moisture content, and organic content

Sample	Latitude	Longitude	Terrace	<i>In Situ</i> XRFs		Lab XRFs		Eq. 2.3	ICP-OES			Moisture Content		Organic Content	
				mg/kg		mg/kg		mg/kg	mg/kg			<i>In Situ</i> (Bulk sample)	<#60 Sieved Sample	<#60 Sieved Sample	
				Pb	Zn	Pb	Zn	Est. Cd	Cd	Pb	Zn				
2.0 km ECA30	36.972367	-94.890508	Left	Top	144	1416	239	2140	18.3	36.2	406	5792	22.8%	4.2%	9.7%
				Primary	274	2372	394	4019	34.1				14.8%	1.4%	3.9%
				Lower	340	4322	88.9	1591	13.7				16.3%	1.9%	7.4%
			Right	Top	372	2577	801	5752	48.7	35.9	830	5529	16.2%	2.1%	7.2%
				Primary	361	3537	193	2324	19.9	63.4	503	8676	13.2%	2.4%	8.8%
				Lower	312	4283	591	7657	64.7				20.1%	2.3%	6.4%
4.0 km ECA40	36.957903	-94.892034	Left	Top	177	2968	347	3441	29.3				31.1	263	2722
				Primary	179	3221	334	3156	26.9	28.5%	3.8%	7.9%			
				Lower	116	1606	229	2494	21.3	30.9	220	2294			
			Right	Top	147	919	396	2113	18.1				20.4%	1.9%	5.5%
				Primary	101	783	287	2069	17.7				21.8%	1.6%	4.9%
				Lower	202	1899	277	2004	17.2				19.7%	2.0%	5.0%
7.0 km ECA50	36.943298	-94.904760	Left	Top	165	3039	75.7	937	8.22	7.94	66.8	703	17.1%	1.7%	5.6%
				Primary	117	2214	214	2808	24.0				22.0%	1.4%	3.9%
				Lower	58.7	1151	50.7	747	6.62				18.7%	2.0%	3.0%
			Right	Top	367	4115	618	5844	49.5						
				Primary	158	2477	169	1416	12.2	23.5%	1.8%	5.0%			
				Lower	279	1974	315	2384	20.4	20.6%	1.9%	5.0%			

Table A.3 Continued page 2: Elm Creek terrace soil samples-coordinates, metals concentrations, moisture content, and organic content

Sample	Latitude	Longitude	Terrace	<i>In Situ</i> XRFs		Lab XRFs		Eq. 2.3	ICP-OES			Moisture Content		Organic Content	
				mg/kg		mg/kg		mg/kg	mg/kg			<i>In Situ</i> (Bulk sample)	<#60 Sieved Sample	<#60 Sieved Sample	
				Pb	Zn	Pb	Zn	Est. Cd	Cd	Pb	Zn				
10.0 km ECA65	36.921508	-94.918451	Left	Top	26.5	449	48.3	676	6.03	6.10	36.3	503	11.3%	1.1%	3.3%
				Primary	33.4	676	40	580	5.22				15.5%	2.0%	4.2%
				Lower	30.5	510	183	1921	16.5				7.9%	2.0%	5.2%
			Right	Top	54.5	870	107	1730	14.9			26.1%			
				Primary	39.6	1210	84.1	1579	13.6			28.4%	2.8%	8.3%	
				Lower	46.7	1556	80.9	1166	10.1			20.8%	2.8%	4.8%	
11.0 km ECA67	36.917489	-94.919147	Left	Top	59.8	1216	62.1	1101	9.60	8.76	60.1	1029	21.0%	1.4%	4.1%
				Primary	35.5	725	64.3	1255	10.9				21.9%	3.3%	4.0%
				Lower	34.8	752	43.9	1117	9.74				21.3%	2.8%	4.4%
			Right	Top	74.5	513	67.6	333	3.14			17.7%	2.3%	6.1%	
				Primary	80.5	1036	153	857	7.55			18.6%	1.8%	4.8%	
				Lower	38.6	665	105	1072	9.35			30.1%	4.5%	7.8%	
11.5 km ECA70	36.915545	-94.921395	Left	Top	38.3	429	108	210	2.10				22.4%	2.5%	7.8%
				Primary	76.4	1033	154	425	3.92			21.2%	1.6%	5.6%	
				Lower	47.5	864	104	476	4.34			21.3%	2.5%	4.2%	
			Right	Top	29.1	1282	84.0	2593	22.1	16.8	78.4	1539	43.6%	6.0%	26.3%
11.6 km ECA72	36.914043	-94.921311	Left	Top	19.4	197	22.2	76.9	0.99				19.8%	2.0%	3.7%
				Primary	68.4	936	67.6	855	7.53			29.5%	4.4%	8.5%	
				Lower	42.1	1131	54.2	1162	10.1			27.1%	3.2%	5.7%	
			Right	Top	79.4	1255	115	1235	10.7			27.4%	5.0%	7.4%	
				Primary	47.3	1110	62.5	1444	12.5	10.9	65.8	1063	32.5%	2.2%	9.8%
				Lower	63.9	3731	30.8	603	5.41			11.9%	0.9%	2.1%	

Table A.3 Continued page 3: Elm Creek terrace soil samples-coordinates, metals concentrations, moisture content, and organic content

Sample	Latitude	Longitude	Terrace	<i>In Situ</i> XRFS		Lab XRFS		Eq. 2.3	ICP-OES			Moisture Content		Organic Content	
				mg/kg		mg/kg		mg/kg	mg/kg			<i>In Situ</i>	<#60	<#60	
				Pb	Zn	Pb	Zn	Est. Cd	Cd	Pb	Zn	(Bulk sample)	Sieved Sample	Sieved Sample	
13.0 km ECA75	36.906977	-94.918472	Left	Top	45.9	639	36.0	482	4.40				19.5%	2.4%	1.8%
				Primary	35.6	962	57.6	1003	8.78				19.1%	1.6%	3.3%
				Lower	59.3	619	76.8	1048	9.15				28.2%	2.2%	4.0%
			Right	Top	54.0	514	72.1	491	4.47	4.38	72.0	370	33.5%	3.2%	7.7%
				Primary	73.0	751	68.0	530	4.79				22.9%	2.4%	5.2%
				Lower	22.4	328	32.2	297	2.84				16.4%	2.6%	4.2%
14.0 km ECA80	36.902129	-94.926580	Left	Top	51.2	591	109	899	7.90				31.1%	10.4%	14.9%
				Primary	44.8	1043	61.3	955	8.38				24.6%	3.0%	5.1%
				Lower	55.7	1034	47.0	688	6.13				26.4%	2.7%	3.8%
			Right	Top	46.7	941	98.7	1196	10.4				35.0%	5.3%	9.8%
				Primary	47.9	1160	58.5	824	7.27				23.9%	2.3%	3.8%
				Lower	65.1	842	79.5	700	6.23	8.46	84.0	584	17.0%	1.7%	3.1%
15.0 km ECA85	36.898897	-94.931004	Left	Top	12.7	54.6	19.8	69.7	0.927				23.1%	3.8%	4.4%
				Primary	40.6	698	21.9	202	2.04				16.9%	2.3%	3.6%
				Lower	28.1	444	76.0	858	7.55				21.5%	4.4%	5.4%
			Right	Top	17.4	112	21.9	164	1.72				25.7%	4.1%	4.7%
				Primary	34.3	588	23.4	219	2.18				28.1%	3.0%	4.0%
				Lower	33.7	645	33.9	502	4.56				21.1%	4.0%	3.9%

Table A.3 Continued page 4: Elm Creek terrace soil samples-coordinates, metals concentrations, moisture content, and organic content

Sample	Latitude	Longitude	Terrace	<i>In Situ</i> XRFs		Lab XRFs		Eq. 2.3	ICP-OES			Moisture Content		Organic Content
				mg/kg		mg/kg		mg/kg	mg/kg			<i>In Situ</i> (Bulk sample)	<#60 Sieved Sample	<#60 Sieved Sample
				Pb	Zn	Pb	Zn	Est. Cd	Cd	Pb	Zn			
16.0 km ECA87	36.896259	-94.931520	Top	11.1	55.3	20.6	58.4	0.83				23.9%	4.2%	2.8%
			Left Primary	34.7	543	19.2	113	1.29	1.36	20.8	98.7	27.1%	2.5%	2.7%
			Lower	30.0	519	17.5	235	2.32				18.1%	2.2%	2.2%
			Right Top	13.9	59.1	20.2	79.8	1.01				25.5%	4.2%	5.1%
			Right Primary	25.9	314	24.6	216	2.15				14.4%	2.8%	3.7%
			Lower	32.5	675	31.6	430	3.95	3.75	29.5	365	16.6%	2.8%	4.2%
17.0 km ECA90	36.892576	-94.929353	Top	11.3	43.5	22.3	72.4	0.950				19.9%	3.7%	3.4%
			Left Primary	15.5	39.8	20.0	55.3	0.806				18.8%	2.1%	2.5%
			Lower	23.3	284	25.7	161	1.69	2.79	27.9	112	23.5%	3.7%	4.1%
			Right Top	16.4	48.1	13.3	50.7	0.767				18.2%	2.1%	2.5%
			Right Primary	26.4	353	26.3	132	1.45				19.2%	3.9%	3.5%
			Lower	27.4	387	23.5	149	1.59				24.5%	3.1%	3.4%

Table A.4: Elm Creek East Branch terrace soil samples-coordinates, metals concentrations, moisture content, and organic content

Sample	Latitude	Longitude	Terrace	<i>In Situ</i> XRFs		Lab XRFs		Eq. 2.3	ICP-OES			Moisture Content		Organic Content	
				mg/kg		mg/kg		mg/kg	mg/kg			<i>In Situ</i>	<#60	<#60	
				Pb	Zn	Pb	Zn	Est. Cd	Cd	Pb	Zn	(Bulk sample)	Sieved Sample	Sieved Sample	
East ECA30	36.972619	-94.890471	Left	Top	928	5088	271	2071	17.8	18.4	255	3135	13.6%	3.3%	8.9%
				Primary	319	3034	255	3213	27.4	22.5	306	3141	10.1%	3.4%	4.7%
				Lower	238	2347	210	3193	27.2				19.0%	2.6%	2.8%
			Right	Top	234	2069	926	5083	43.1				15.0%	3.6%	10.6%
				Primary	221	2701	465	4431	37.6	47.4	395	7574	10.5%	1.9%	3.8%
				Lower	127	3000	318	3544	30.1	31.6	305	5995	14.0%	2.1%	3.0%
East ECA40	36.958063	-94.891666	Left	Top	382	2488	503	2874	24.5				28.3%	2.1%	8.1%
				Primary	193	1042	296	2137	18.3				16.7%	4.0%	4.2%
				Lower	180	2206	358	2761	23.6				34.6%	2.5%	6.4%
			Right	Top	82.3	421	113	422	3.89				14.8%	3.7%	8.5%
				Primary	210	1497	287	1981	17.0				26.2%	2.4%	11.1%
				Lower	156	2633	201	2564	21.9	22.2	203	2480	37.0%	4.8%	5.4%
East ECA50t	36.943326	-94.904526	Left	Top	160	2316	155	1606	13.8				20.0%	3.3%	6.3%
				Primary	113	2343	150	1531	13.2				13.8%	2.7%	3.8%
				Lower	37.9	1387	38.1	611	5.48				21.1%	0.3%	3.2%
			Right	Top	110	2234	120	2011	17.3				22.9%	2.3%	3.5%
				Primary	167	2393	126	1406	12.2	9.95	107	1087	16.1%	2.1%	3.9%
				Lower	46.6	1899	37.6	1248	10.8	6.45	38.7	1123	20.7%	2.1%	2.7%

Table A.5: Elm Creek West Branch terrace soil samples-coordinates, metals concentrations, moisture content, and organic content

Sample	Latitude	Longitude	Terrace	<i>In Situ</i> XRFs		Lab XRFs		Eq. 2.3	ICP-OES			Moisture Content		Organic Content	
				mg/kg		mg/kg		mg/kg	mg/kg			<i>In Situ</i>	<#60	<#60	
				Pb	Zn	Pb	Zn	Est. Cd	Cd	Pb	Zn	(Bulk sample)	Sieved Sample	Sieved Sample	
West ECA30	36.972500	-94.926638	Top	38.7	657	56.4	445	4.08				20.3%	2.3%	5.7%	
			Left	Primary	29.5	82.8	19.6	95.2	1.14				10.4%	1.5%	2.2%
				Lower	17.5	198	12.8	129	1.42				35.9%	2.9%	2.3%
			Right	Top	16.3	231	15.5	171	1.78				21.0%	2.5%	5.5%
				Primary	16.4	334	23.1	320	3.03				23.2%	2.2%	9.6%
				Lower	14.1	173	15.5	125	1.39				13.4%	4.2%	5.3%
West ECA40	36.957962	-94.930005	Top	29.4	172	27.6	195	1.98	2.16	51.7	285	12.0%	2.2%	9.0%	
			Left	Primary	30.9	60.1	29.8	72.0	0.946				10.0%	3.2%	3.8%
				Lower	< LOD	< LOD	21.8	36.0	0.644				15.2%	2.6%	2.6%
			Right	Top	19.0	124	17.9	90.9	1.10				10.7%	3.4%	5.8%
				Primary	17.9	28.6	20.3	31.5	0.605				13.6%	2.6%	2.1%
				Lower	< LOD	< LOD	13.4	31.7	0.607				29.1%	2.2%	2.1%
West ECA50	36.943437	-94.924970	Top	59.2	741	94.0	866	7.63				15.1%	2.8%	6.7%	
			Left	Primary	45.3	601	43.3	717	6.37				6.3%	2.0%	3.3%
				Lower	29.7	671	40.5	567	5.11				17.7%	2.2%	1.8%
			Right	Top	35.3	449	49.7	522	4.73				11.0%	1.7%	2.6%
				Primary	26.4	408	36.8	1429	12.4				12.5%	2.5%	3.0%
				Lower	25.3	152	29.5	2375	20.3				8.5%	2.1%	1.8%